NASA TECHNICAL NOTE

NASA TN D-3375

NASA TN D-3375

AERODYNAMIC DATA ON A LARGE SEMISPAN TILTING WING WITH 0.5-DIAMETER CHORD, DOUBLE-SLOTTED FLAP, AND BOTH LEFT- AND RIGHT-HAND ROTATION OF A SINGLE PROPELLER

by Marvin P. Fink, Robert G. Mitchell, and Lucy C. White

Langley Research Center

Langley Station, Hampton, Va.

NATIONAL AERONAUTICS AND SPACE ADMINISTRATION • WASHINGTON, D. C. • APRIL 1966

AERODYNAMIC DATA ON A LARGE SEMISPAN TILTING WING WITH 0.5-DIAMETER CHORD, DOUBLE-SLOTTED FLAP, AND BOTH LEFT- AND RIGHT-HAND ROTATION OF A SINGLE PROPELLER

By Marvin P. Fink, Robert G. Mitchell, and Lucy C. White

Langley Research Center
Langley Station, Hampton, Va.

NATIONAL AERONAUTICS AND SPACE ADMINISTRATION

For sale by the Clearinghouse for Federal Scientific and Technical Information
Springfield, Virginia 22151 – Price $1.50

AERODYNAMIC DATA ON A LARGE SEMISPAN TILTING WING WITH 0.5-DIAMETER CHORD, DOUBLE-SLOTTED FLAP, AND BOTH LEFT- AND RIGHT-HAND ROTATION OF A SINGLE PROPELLER

By Marvin P. Fink, Robert G. Mitchell, and Lucy C. White
Langley Research Center

SUMMARY

An investigation has been made in the Langley full-scale tunnel to determine the longitudinal aerodynamic characteristics of a large-scale semispan V/STOL tilt-wing configuration having a single propeller which was tested for both right- and left-hand rotation. The wing had a chord-to-propeller-diameter ratio of 0.5, a double-slotted flap, an aspect ratio of 4.88 (2.44 for the semispan), a taper ratio of 1.0, and an NACA 4415 airfoil section.

The data have not been analyzed in detail but have been examined to observe the predominant trends. It was found that the direction of propeller rotation had no significant effect on the lift or descent capability attainable, although different types of flow-control devices were required to achieve the same results with different directions of rotation. The descent capability was determined from the values of attainable drag-to-lift ratios without stalling of any part of the wing within the propeller slipstream. The use of flaps was very effective in increasing the descent capability for either mode of rotation. For example, with the most favorable combination of flow-control devices tested, virtually no descent capability prior to wing stalling was achieved with 0° flap deflection, whereas, with 40°, 60°, or 70° flap deflection, a descent capability of about 20° was achieved.

INTRODUCTION

Most of the aerodynamic research done on the tilt-wing propeller-driven V/STOL configuration has been of an exploratory character and has been obtained with small-scale models. The interest in this type of airplane has become so substantial that there is a need for large-scale systematic aerodynamic design data for this type of airplane. A program has therefore been inaugurated at the Langley Research Center to provide such information by means of a large-scale semispan tilt-wing-and-propeller model in the Langley full-scale tunnel. References 1, 2, and 3 are concerned with this investigation, and the results of the fourth part of the investigation are reported herein. The present series of tests were made on a model having a single propeller on the semispan wing, a chord-to-propeller-diameter ratio of 0.50 (compared with a ratio of 0.60 for the three previous investigations), a 35-percent-chord double-slotted flap, and a leading-edge slat which could be located in either of two positions. The investigation covered a range of angles of attack from -20° to 90° and a range of power conditions from zero thrust to that required for hovering. Both modes of propeller rotation were tested in the present investigation. The results of previous investigations (refs. 2 and 3) show that the direction of propeller rotation has no appreciable effect, but it was believed that there might be some significant effect in the present investigation because of the shorter wing chord and increased loading due to the double-slotted flap. The lift, drag, and pitching moments of the model were measured over the range of test conditions and the flow was observed by means of tufts on the upper surface of the wing. The results of this investigation are presented herein without detailed analysis to expedite their dissemination.

SYMBOLS

The positive sense of forces, moments, and angles is shown in figure 1. The pitching-moment coefficients are referred to the wing quarter-chord line. The coefficients are based on the dynamic pressure in the propeller slipstream. Conventional lift, drag, and pitching-moment coefficients based on the free-stream dynamic pressure can be obtained by dividing the slipstream coefficients by $\left(1 - C_{T,s}\right)$; for example, $C_L = C_{L,s}/\left(1 - C_{T,s}\right)$. The thrust coefficient C_T' may be obtained from the equation $C_T' = \left[C_{T,s}\left(\frac{A}{S}\right)\right]/\left(1 - C_{T,s}\right)$.

Measurements for this investigation were made in the U.S. Customary System of Units. Equivalent values are indicated herein in the International System (SI) in the interest of promoting the use of this system in future NASA reports. Factors relating the two systems for units used in this paper may be found in the appendix.

C_L — lift coefficient based on free airstream, $\frac{L}{qS}$

$C_{L,s}$ — lift coefficient based on slipstream, $\frac{L}{q_sS}$

$C_{D,s}$ — drag coefficient based on slipstream, $\frac{D}{q_sS}$

$C_{m,s}$ — pitching-moment coefficient based on slipstream, $\frac{M_Y}{q_sSc}$

$C_{T,s}$ thrust coefficient based on slipstream, $\dfrac{T}{q_s \dfrac{\pi D^2}{4}}$

C_T' thrust coefficient based on free airstream, $\dfrac{T}{qS}$

A total area of propeller disk, ft^2 ($meters^2$)

b propeller-blade chord, in. (meters); or wing span, ft (meters)

c wing chord, ft (meters)

c_f flap chord, 11.90 in. (14.68 cm)

c_v vane chord, 5.78 in. (14.68 cm)

D propeller diameter, ft (meters) also, total model drag, lbf (newtons)

h width of slat or of flap-slot gap or thickness of propeller blade, ft (meters)

L total lift of model, lbf (newtons)

M_Y pitching moment, lbf-ft (newton-meters)

q free-stream dynamic pressure, $\dfrac{\rho V^2}{2}$, lbf/sq ft ($newtons/meter^2$)

q_s slipstream dynamic pressure, $q + \dfrac{T}{\dfrac{\pi D^2}{4}}$, lbf/sq ft ($newtons/meter^2$)

r radius to element on propeller blade, ft (meters)

R radius of propeller blade, 2.83 ft (0.86 meter)

S area of semispan wing, 19.60 ft^2 (1.82 $meters^2$)

T propeller thrust, lb (newtons)

x longitudinal distance along chord, ft (meters)

y vertical height above or below chord line, ft (meters)

α angle of attack, deg

δ_f flap deflection, deg

δ_s	leading-edge-slat deflection, deg
ρ	mass density of air, slugs/ft^3 (kilograms/meter^3)
V	free-stream velocity, ft/sec (meters/sec)

Subscript:

max	maximum

MODEL

The model used in this investigation was a semispan model which would represent the left panel of a full-span wing. The principal dimensions of the model are given in figure 2. The wing was mounted on the scale balance system in the tunnel so that the lift and drag measurements were read directly about the wind axis. Where the wing extended through the reflection plane, a circular end plate (with a diameter equal to twice the wing chord) was fitted around and attached to the wing to prevent air from leaking through the reflection plane at the wing root.

The model was constructed to allow numerous changes to be made in the test configuration, such as: leading-edge modification, and changes of airfoil, trailing-edge flap, direction of rotation of the propeller, and wing planform. The basic structure of the wing consists of a heavy steel box-beam spar to which a power train to drive the propellers through spanwise shafting is attached and around which various airfoil contours can be fitted.

The model configuration for the present tests had a 68-inch-diameter (1.73-meters) propeller having the characteristics shown in figure 3. The propeller location was such that the propeller tip extended to the wing tip. In the present investigation both directions of propeller rotation were tested. The propeller thrust was measured by a strain-gage balance which was a part of the propeller shaft. The output was fed through sliprings to an indicating instrument. The required values of thrust for each $C_{T,s}$ were set by the operator by changing the speed of the drive motor. The blade angle at the 0.75R station of the propeller was held constant at 17° throughout the investigation. The thrust axis was inclined upward 4° from the chord line on the wing to correspond approximately to the zero-lift line of the airfoil section.

The airfoil used was the NACA 4415 section with a 34-inch (0.864-meter) chord. This chord length gave a ratio of wing chord to propeller diameter of 0.50. The reference area of the wing based on a semispan of 83 inches (1.73 meters) was 19.60 square feet (1.82 meters^2) and did not include the area of the tip fairing.

The model had a 35-percent-chord double-slotted flap which was set at 0°, 40°, and 60° for most of the present tests. The flap was deflected to 70° for one set of tests. Figure 2(b) shows the flap deflected 60° relative to the vane. The flap bracket was constructed so that the nose of the flap positioned for each flap setting as shown in the detail in figure 2(b). This relationship was also true for the nose of the vane for flap deflections of 60° and greater. As the flap angle was decreased the nose of the vane moved forward under the skirt. Because of bracket limitations, the deflection angle of zero was not obtainable so the entire flap system was replaced with a solid trailing edge for this case. The ordinates for the vane and flap are given in table 1.

Two positions of a leading-edge slat were investigated in combination with the flap on this model. Some previous unpublished data have indicated that a higher than normal slat position gave better results for some test conditions. For this reason, some of the tests in the present investigation were conducted with the slat in a "high" position. The high and low positions of the slat with the angles and slot gaps used are shown in figure 2(b).

Fences having a height of 0.20c and extending from 0.13c on the lower surface of the wing around the leading edge to about 0.75c on the upper surface were installed at two spanwise locations on the wing in an attempt to confine the stall inboard of the propeller slipstream. The inboard fence was placed about where the side of a fuselage might be (20% of the semispan) and at 0.75r/R of the inboard propeller blade as indicated in figure 2(c). When tests were made with fences on, both fences were installed.

TESTS

The tests were made for various deflections of the double-slotted flap and for two different positions of a leading-edge slat. The specific configurations tested, together with a list of tables and figures in which the data for each may be found, are given in the following table:

Direction of rotation	Configuration	Flap deflection, δ_f, deg	Table	Figure
Down at tip	Basic leading edge	0	2	4
	Basic leading edge	40	3	5
	Basic leading edge	60	4	6
	Basic leading edge with fences on	0	5	7
	Basic leading edge with fences on	40	6	8
	Basic leading edge with fences on	60	7	9
	Inboard slat, $\delta_s = 30^{\circ}$	0	8	10
	Inboard slat, $\delta_s = 30^{\circ}$	40	9	11
	Inboard slat, $\delta_s = 30^{\circ}$	60	10	12

Direction of rotation	Configuration	Flap deflection, δ_f, deg	Table	Figure
Down at tip	Inboard slat, $\delta_s = 30^\circ$ with fences on	0	11	13
	Inboard slat, $\delta_s = 30^\circ$ with fences on	40	12	14
	Inboard slat, $\delta_s = 30^\circ$ with fences on	60	13	15
Up at tip	Inboard slat, $\delta_s = 30^\circ$	0	14	16
	Inboard slat, $\delta_s = 30^\circ$	40	15	17
	Inboard slat, $\delta_s = 30^\circ$	60	16	18
	Inboard slat, $\delta_s = 30^\circ$ with fences on	0	17	19
	Inboard slat, $\delta_s = 30^\circ$ with fences on	40	18	20
	Inboard slat, $\delta_s = 30^\circ$ with fences on	60	19	21
	Inboard slat, $\delta_s = 10^\circ$, high position	40	20	22
	Inboard slat, $\delta_s = 10^\circ$, high position	60	21	23
	Inboard slat, $\delta_s = 10^\circ$, high position	70	22	24

The tests were made over a range of thrust coefficients from 0 to 1.0 for the basic wing and for $C_{T,s} = 0.90$, 0.80, and 0.60 for the other configurations. For any given test the thrust coefficient was held constant over the angle-of-attack range by adjusting the propeller speed to give the required thrust at each angle of attack. The angle-of-attack range for the tests was approximately from the angle required for zero lift to that required to stall the wing or to develop a drag-lift ratio of about 0.30, whichever was lower, except for $C_{T,s} = 1.0$ (the static thrust case) where the angle-of-attack range was from 0° to 90°. The test Reynolds number, based on the wing chord length and the velocity of the propeller slipstream, was about 2.32×10^6 for thrust coefficients from 1.00 to 0.30. For the $C_{T,s} = 0$ condition, where the thrust was held at zero, the Reynolds number was about 1.91×10^6.

No tunnel-wall corrections have been applied to the data since surveys and analysis indicate that there would be no significant correction, as explained in reference 1.

DISCUSSION

The data presented have not been analyzed in detail but have been examined to observe general trends. A few such trends predominate. One very general observation was that the force-test data could not be used as an indication of the occurrence or extent of wing stalling. The results of the tuft tests show that the onset of stalling over significant areas of the part of the wing within the propeller slipstream frequently occurs at 20° to 30° angle of attack below or above the angle of attack for maximum lift coefficient.

Effect of Variables

Effect of direction of propeller rotation.- The results of the force tests show no consistent or very significant effects of the direction of propeller rotation on lift or drag. The tuft tests, however, show major effects of the direction of propeller rotation. Rotation of the propellers in the down-at-the-tip direction consistently causes stalling (of the part of the wing in the slipstream) to start inboard of the nacelle, that is, behind the upward-going blades. The up-at-the-tip rotation, on the other hand, may result in the onset of stalling occurring either inboard or outboard of the nacelle. In either case, however, up-at-the-tip rotation generally results in a strong outward spanwise flow of the boundary layer prior to the onset of stalling. As will be indicated in some detail in the subsequent discussion, however, results just as favorable with regard to wing stalling can be achieved with one mode of propeller rotation as with the other, but different types of flow-control devices are required to achieve these results.

Effect of fences.- The results of the tuft tests showed that the fences were quite effective in delaying the stall on the part of the wing inboard of the nacelles (and within the propeller slipstream) for the case of down-at-the-tip rotation where inboard stalling tends to occur. Evidently the fences prevented the spread of the early stall on the unblown center section of the wing from spreading outward and triggering the stall on the adjacent section of the wing in the slipstream. The fences had little or no effect on stalling for the case of up-at-the-tip propeller rotation - as might be expected on the basis of this reasoning.

The results of the force tests show much less consistent effects of the fences on lift and drag, but it was observed that the fences generally increased the maximum lift coefficient and increased the drag at maximum lift for the case of down-at-the-tip propeller rotation.

Effect of slat.- The inboard slat, used either alone or with the fences, was not effective in delaying the inboard stall for the case of down-at-the-tip propeller rotation where the stall onset (of the part of the wing in the slipstream) occurred inboard of the nacelle. In fact, in many cases the use of the slat caused a small reduction in $C_{L,max}$ and the drag-lift ratio at $C_{L,max}$. The slat did, however, consistently increase the maximum lift coefficient at the lower thrust coefficient $\left(C_{T,s} = 0.6\right)$. Neither the force tests nor the tuft tests showed any significant effect of slat position for the two positions tested, but the lower position (30° deflection) used in the majority of the tests seemed very slightly the better position.

Effect of flaps.- Deflecting the flaps greatly increased the drag-lift ratio achievable prior to stalling of any part of the wing within the propeller slipstream, as determined by tuft tests. There was no significant difference in this regard between the 40°, 60°, and 70° flap deflections. The 60° and 70° deflections, however, give higher lift coefficients than the 40° deflection.

Evaluation of Configurations

Many of the configurations tested do not produce a suitable positive value of the drag-lift ratio prior to the onset of stalling or violent flow disturbances (on the part of the wing immersed in the propeller slipstream), and the achievement of suitable positive values of D/L prior to the onset of serious flow separation is believed to be a necessary condition for the wing of a tilt-wing V/STOL aircraft to permit operation in descent and deceleration conditions, as explained in reference 4. Several of the configurations studied in the tests produced satisfactory characteristics: (1) the flap-down conditions with the up-at-the-tip propeller rotation and with slats (either with or without fences), and (2) the flap-down conditions with the down-at-the-tip mode of propeller rotation and with fences (either with or without slats). For example, figures 8 and 9 (down-at-tip rotation, fences only, and with 40° or 60° flap deflection) and figures 17 and 18 (up-at-tip rotation, slats only, and with 40° or 60° flap deflection) show the results for configurations which achieved values of D/L of the order of 0.3 to 0.4 prior to the onset of stall or violent flow disturbances as indicated by the tuft-test results. These values of D/L correspond to descent angles in flight of 17° to 22°. It should be noted that, in no case, were suitable values of D/L achieved for the flap-up conditions.

CONCLUSIONS

The following conclusions were drawn from the results of the investigation:

1. The direction of propeller rotation had no significant effect on the lift or descent capability attainable, although different types of flow-control devices were required to achieve the same results with the different directions of rotation. (The descent capability was determined from the attainable values of the drag-to-lift ratio without stalling of any part of the wing within the propeller slipstream.)

2. The use of flaps was very effective in increasing the descent capability for either right- or left-hand rotation. For example, with the most favorable

combination of flow-control devices tested, virtually no descent capability prior to wing stalling was achieved with 0° flap deflection; whereas, with 40°, 60°, or 70° flap deflection, a descent capability of about 20° was achieved.

Langley Research Center,
National Aeronautics and Space Administration,
Langley Station, Hampton, Va., January 5, 1966.

APPENDIX

CONVERSION FACTORS - U.S. UNITS TO SI UNITS

From NASA SP-7012, entitled "The International System of Units - Physical Constants and Conversion Factors" by E. A. Mechtly, the following conversion factors are included in this report for convenience:

Physical quantity	U.S. Customary Unit	Conversion factor (*)	SI Unit
Area	$feet^2$	0.0929	$meters^2$ (m^2)
Density	$slugs/ft^3$	5153.8	$kilograms/meter^3$ (kg/m^3)
Force	lbf	4.448	newtons (N)
Length	in.	0.0254	meters (m)
	ft	0.3048	meters (m)
Moment	lbf-ft	1.356	newton-meters (N-m)
Pressure	lbf/ft^2	47.88	$newtons/meter^2$ (N/m^2)
Velocity	ft/sec	0.3048	meters/second (m/sec)

*Multiply value given in U.S. Customary Unit by conversion factor to obtain equivalent value in SI Unit.

REFERENCES

1. Fink, Marvin P.; Mitchell, Robert G.; and White, Lucy C.: Aerodynamic Data on a Large Semispan Tilting Wing With 0.6-Diameter Chord, Fowler Flap, and Single Propeller Rotating Up at Tip. NASA TN D-2180, 1964.

2. Fink, Marvin P.; Mitchell, Robert G.; and White, Lucy C.: Aerodynamic Data on a Large Semispan Tilting Wing With 0.6-Diameter Chord, Single-Slotted Flap, and Single Propeller Rotating Down at Tip. NASA TN D-2412, 1964.

3. Fink, Marvin P.; Mitchell, Robert G.; and White, Lucy C.: Aerodynamic Data on Large Semispan Tilting Wing With 0.6-Diameter Chord, Single Slotted Flap, and Single Propeller Rotating Up at Tip. NASA TN D-1586, 1964.

4. McKinney, M. O.; Kirby, Robert H.; and Newsom, W. A.: Aerodynamic Factors To be Considered in the Design of Tilt-Wing V/STOL Airplanes. Vertical Take-Off and Landing (VTOL) Aircraft. Ann. N.Y. Acad. Sci., vol. 107, art. 1, Mar. 25, 1963, pp. 221-248.

TABLE 1.- VANE AND FLAP ORDINATES

Vane ordinates			Flap ordinates		
x/c_v	y/c_v upper	y/c_v lower	x/c_f	y/c_f upper	y/c_f lower
0	0	0	0	0	0
.0125	.0381	-.0268	.0125	.0456	-.0200
.0249	.0522	-.0343	.0250	.0609	-.0276
.0500	.0739	-.0408	.0500	.0853	-.0365
.0751	.0905	-.0446	.0750	.1027	-.0413
.1000	.1040	-.0448	.1000	.1165	-.0431
.1500	.1270	-.0408	.1500	.1377	-.0466
.2000	.1439	-.0299	.2000	.1532	
.3000	.1630	-.0140	.2500	.1623	
.4000	.1661	.0010	.3000	.1671	
.5000	.1600	.0180	.3500	.1678	
.6000	.1439	.0299	.4286	.1586	-.0339
.7000	.1170	.0300	.7143	.0880	-.0192
.8000	.0830	.0299	1.0000	.0045	-.0045
.9000	.0450	.0180			
.9500	.0260	.0107			
1.0000	0	0			

TABLE 2.- TABULATED AERODYNAMIC DATA FOR BASIC LEADING EDGE, $\delta_f = 0^{\circ}$, AND DOWN-AT-TIP ROTATION

α, deg	$C_{L,s}$	$C_{D,s}$	$C_{m,s}$
$C_{T,s}$ = 1.00			
-20	-----	------	-----
-15	-----	------	-----
-10	-----	------	-----
-5	-----	------	-----
0	0.128	-1.289	0.011
5	.252	-1.279	.021
10	.380	-1.253	.022
15	.501	-1.215	.026
20	.606	-1.164	.028
25	-----	------	-----
30	.786	-1.043	.005
35	-----	------	-----
40	.938	-.895	-.010
45	-----	------	-----
50	1.055	-.725	-.036
55	-----	------	-----
60	1.164	-.541	-.050
65	-----	------	-----
70	1.242	-.330	-.062
75	-----	------	-----
80	1.273	-.108	-.072
90	1.284	.121	-.071
$C_{T,s}$ = 0.95			
-20	-0.445	-1.160	-0.055
-15	-.297	-1.190	-.038
-10	-.151	-1.220	-.017
-5	.004	-1.211	-.006
0	.149	-1.212	.011
5	.299	-1.189	.024
10	.441	-1.153	.026
15	.570	-1.105	.040
20	.697	-1.043	.052
25	.831	-.954	.051
30	.951	-.849	.058
35	1.039	-.795	.062
40	1.114	-.659	.067
45	1.179	-.533	.063
50	1.239	-.420	.050
55	1.292	-.290	.055
60	1.311	-.151	.049
65	1.320	-.050	.050
70	1.329	.072	.062
75	1.313	.189	.069
80	1.289	.300	.081
90	------	------	------
$C_{T,s}$ = 0.90			
-20	-0.515	-1.050	-0.077
-15	-.345	-1.111	-.053
-10	-.182	-1.138	-.026
-5	.005	-1.154	-.005
0	.183	-1.151	.016
5	.365	-1.128	.039
10	.533	-1.084	.050
15	.670	-1.018	.063
20	.802	-.942	.066
25	.921	-.846	.070
30	1.042	-.739	.078
35	1.144	-.618	.081
40	1.233	-.483	.078
45	1.294	-.354	.072
50	1.333	-.223	.075
55	1.369	-.067	.076
60	1.373	.044	.086
65	1.360	.157	.086
70	1.333	.264	.098
75	1.314	.412	.095
$C_{T,s}$ = 0.80			
-20	-0.570	-0.932	-0.089
-15	-.400	-.964	-.084
-10	-.199	-1.007	-.041
-5	.002	-1.030	.014
0	.209	-1.027	.019
5	.405	-1.066	.043
10	.595	-.938	.067
15	.768	-.880	.080
20	.917	-.767	.074
25	1.051	-.660	.092
30	1.176	-.536	.084
35	1.266	-.399	.082
40	1.346	-.255	.080
45	1.387	-.093	.075
50	1.413	.062	.081
55	1.406	.197	.080
60	1.380	.308	.084
65	1.344	.418	.091
$C_{T,s}$ = 0.60			
-20	-0.706	-0.562	-0.120
-15	-.514	-.689	-.112
-10	-.276	-.733	-.077
-5	-.024	-.749	-.038
0	.236	-.747	.003
5	.473	-.724	.033
10	.708	-.668	.066
15	.931	-.594	.091
20	1.062	-.482	.091
25	1.186	-.354	.078
30	1.283	-.199	.079
35	1.354	-.018	.074
40	1.379	.121	.059
45	1.372	.257	.054
50	1.361	.374	.056
55	1.296	.462	.058
$C_{T,s}$ = 0.30			
-20	-0.834	-0.176	-0.149
-15	-.667	-.305	-.167
-10	-.387	-.355	-.129
-5	-.068	-.391	-.064
0	.251	-.384	-.015
5	.555	-.348	.026
10	.857	-.292	.060
15	1.147	-.202	.099
20	1.301	-.091	.085
25	1.420	.070	.071
30	1.376	.247	.036
35	1.388	.400	.025
40	1.362	.526	.024
$C_{T,s}$ = 0			
-20	-0.878	0.233	-0.137
-15	-.757	.066	-.200
-10	-.484	-.014	-.164
-5	-.129	-.018	-.097
0	.232	-.013	-.041
5	.584	.014	.024
10	.931	.074	.066
15	1.264	.168	.101
20	1.419	.296	.085
25	1.312	.448	.032
30	1.276	.584	-.003

TABLE 3.- TABULATED AERODYNAMIC DATA FOR BASIC LEADING EDGE, $\delta_f = 40^\circ$, AND DOWN-AT-TIP ROTATION

α, deg	$C_{L,s}$	$C_{D,s}$	$C_{m,s}$
	$C_{T,s} = 0.90$		
-20	0.045	-1.064	-0.285
-15	.262	-1.078	-.307
-10	.452	-1.059	-.301
-5	.640	-1.024	-.294
0	.812	-.961	-.292
5	.978	-.875	-.292
10	1.135	-.772	-.300
15	1.249	-.645	-.295
20	1.344	-.513	-.294
25	1.428	-.367	-.300
30	1.486	-.211	-.309
35	1.536	-.059	-.311
40	1.538	.070	-.304
45	1.527	.187	-.276
50	1.478	.278	-.246
55	1.429	.359	-.223
60	1.359	.415	-.174
65	1.299	.468	-.144
	$C_{T,s} = 0.80$		
-20	0.067	-0.928	-0.348
-15	.336	-.953	-.368
-10	.545	-.929	-.356
-5	.786	-.877	-.354
0	1.024	-.803	-.361
5	1.254	-.702	-.368
10	1.449	-.577	-.366
15	1.543	-.431	-.374
20	1.557	-.273	-.367
25	1.591	-.108	-.374
30	1.619	.031	-.369
35	1.622	.162	-.343
40	1.577	.272	-.310
45	1.508	.361	-.263
50	1.444	.434	-.219
55	1.371	.495	-.172
	$C_{T,s} = 0.60$		
-20	0.036	-0.621	-0.386
-15	.423	-.661	-.444
-10	.700	-.635	-.424
-5	1.014	-.565	-.421
0	1.351	-.489	-.449
5	1.662	-.375	-.464
10	1.939	-.221	-.470
15	2.046	-.052	-.454
20	1.867	.138	-.457
25	1.807	.287	-.460
30	1.711	.401	-.402
35	1.619	.482	-.350
40	1.545	.596	-.328

TABLE 4.- TABULATED AERODYNAMIC DATA FOR BASIC LEADING EDGE, $\delta_f = 60^\circ$, AND DOWN-AT-TIP ROTATION

α, deg	$C_{L,s}$	$C_{D,s}$	$C_{m,s}$
	$C_{T,s} = 0.90$		
-20	0.403	-0.990	-0.406
-15	.592	-.963	-.403
-10	.764	-.911	-.398
-5	.934	-.837	-.393
0	1.096	-.752	-.392
5	1.241	-.643	-.398
10	1.357	-.517	-.398
15	1.445	-.379	-.393
20	1.487	-.248	-.384
25	1.532	-.105	-.380
30	1.553	.030	-.369
35	1.554	.161	-.350
40	1.533	.277	-.331
45	1.468	.354	-.298
50	1.409	.417	-.265
55	1.337	.473	-.230
	$C_{T,s} = 0.80$		
-20	0.508	-0.834	-0.472
-15	.720	-.802	-.465
-10	.963	-.746	-.461
-5	1.201	-.667	-.464
0	1.413	-.557	-.471
5	1.598	-.413	-.495
10	1.681	-.284	-.478
15	1.649	-.136	-.453
20	1.638	.008	-.432
25	1.619	.131	-.417
30	1.600	.241	-.387
35	1.536	.329	-.341
40	1.455	.397	-.291
45	1.375	.461	-.261
50	1.311	.507	-.208
	$C_{T,s} = 0.60$		
-20	0.687	-0.535	-0.565
-15	.958	-.508	-.560
-10	1.238	-.452	-.562
-5	1.553	-.352	-.571
0	1.891	-.202	-.597
5	2.179	-.044	-.628
10	2.350	.132	-.616
15	2.056	.260	-.560
20	1.845	.392	-.493
25	1.718	.487	-.445
30	1.573	.551	-.387

TABLE 5.- TABULATED AERODYNAMIC DATA FOR BASIC LEADING EDGE WITH FENCES ON, $\delta_f = 0^{\circ}$, AND DOWN-AT-TIP ROTATION

α, deg	$C_{L,s}$	$C_{D,s}$	$C_{m,s}$
	$C_{T,s} = 0.90$		
-20	-0.483	-1.051	-0.073
-15	-.327	-1.115	-.058
-10	-.164	-1.148	-.025
-5	.013	-1.155	-.005
0	.199	-1.147	.016
5	.371	-1.120	.032
10	.524	-1.074	.040
15	.671	-1.006	.055
20	.811	-.934	.055
25	.935	-.842	.060
30	1.043	-.735	.074
35	1.158	-.603	.074
40	1.246	-.471	.071
45	1.310	-.330	.062
50	1.355	-.198	.068
55	1.388	-.062	.074
60	1.388	.056	.078
65	1.378	.180	.085
70	1.353	.294	.094
75	1.325	.401	.107
80	1.275	.500	.113
	$C_{T,s} = 0.80$		
-20	-0.563	-0.894	-0.096
-15	-.372	-.937	-.078
-10	-.183	-1.001	-.044
-5	.015	-1.011	-.022
0	.215	-1.011	.016
5	.414	-.984	.031
10	.594	-.931	.056
15	.768	-.870	.066
20	.932	-.764	.069
25	1.091	-.657	.087
30	1.212	-.508	.076
35	1.335	-.363	.073
40	1.419	-.201	.077
45	1.471	-.053	.078
50	1.504	.099	.079
55	1.491	.240	.078
60	1.398	.315	.095
65	1.335	.401	.101
70	1.287	.493	.109
	$C_{T,s} = 0.60$		
-20	-0.717	-0.559	-0.134
-15	-.509	-.680	-.117
-10	-.277	-.724	-.086
-5	-.025	-.738	-.038
0	.223	-.742	.001
5	.461	-.711	.031
10	.701	-.658	.053
15	.937	-.585	.085
20	1.113	-.469	.083
25	1.308	-.335	.087
30	1.428	-.161	.083
35	1.532	.012	.076
40	1.420	.170	.040
45	1.414	.300	.041
50	1.381	.398	.049
55	1.337	.490	.053

TABLE 6.- TABULATED AERODYNAMIC DATA FOR BASIC LEADING EDGE WITH FENCES ON, $\delta_f = 40^{\circ}$, AND DOWN-AT-TIP ROTATION

α, deg	$C_{L,s}$	$C_{D,s}$	$C_{m,s}$
	$C_{T,s} = 0.90$		
-20	0.066	-1.071	-0.302
-15	.285	-1.075	-.311
-10	.461	-1.062	-.300
-5	.648	-1.009	-.303
0	.828	-.948	-.294
5	.995	-.858	-.294
10	1.141	-.750	-.298
15	1.287	-.613	-.307
20	1.392	-.474	-.311
25	1.460	-.329	-.311
30	1.530	-.164	-.325
35	1.580	-.011	-.330
40	1.590	.126	-.321
45	1.556	.265	-.303
50	1.548	.377	-.268
55	1.495	.476	-.230
60	1.437	.545	-.194
	$C_{T,s} = 0.80$		
-20	0.063	-0.918	-0.345
-15	.349	-.942	-.365
-10	.556	-.914	-.349
-5	.793	-.859	-.348
0	1.038	-.793	-.353
5	1.265	-.688	-.359
10	1.458	-.570	-.364
15	1.554	-.380	-.388
20	1.671	-.211	-.400
25	1.693	-.049	-.396
30	1.742	.130	-.398
35	1.731	.273	-.365
40	1.696	.384	-.350
45	1.636	.478	-.300
50	1.562	.559	-.248
55	1.442	.578	-.174
	$C_{T,s} = 0.60$		
-20	0.038	-0.612	-0.389
-15	.414	-.653	-.451
-10	.699	-.626	-.423
-5	.995	-.556	-.420
0	1.318	-.477	-.438
5	1.641	-.361	-.454
10	1.926	-.219	-.462
15	1.986	-.008	-.478
20	2.087	.230	-.515
25	2.149	.420	-.510
30	1.995	.571	-.475
35	1.806	.641	-.391
40	1.616	.656	-.340

TABLE 7.- TABULATED AERODYNAMIC DATA FOR BASIC LEADING EDGE WITH FENCES ON, $\delta_f = 60^\circ$, AND DOWN-AT-TIP ROTATION

α, deg	$C_{L,s}$	$C_{D,s}$	$C_{m,s}$
	$C_{T,s} = 0.90$		
-20	0.427	-0.985	-0.416
-15	.626	-.955	-.412
-10	.790	-.903	-.405
-5	.961	-.832	-.397
0	1.116	-.737	-.401
5	1.257	-.626	-.398
10	1.378	-.493	-.403
15	1.476	-.338	-.412
20	1.526	-.196	-.407
25	1.581	-.040	-.413
30	1.613	.122	-.409
35	1.615	.258	-.400
40	1.606	.383	-.379
45	1.562	.492	-.350
50	1.498	.584	-.310
55	1.427	.648	-.266
	$C_{T,s} = 0.80$		
-20	0.531	-0.831	-0.482
-15	.768	-.798	-.471
-10	.994	-.743	-.469
-5	1.217	-.663	-.472
0	1.430	-.548	-.479
5	1.614	-.415	-.488
10	1.646	-.240	-.486
15	1.754	-.050	-.494
20	1.744	.090	-.476
25	1.757	.252	-.461
30	1.738	.385	-.442
35	1.672	.483	-.408
40	1.607	.557	-.371
45	1.527	.621	-.305
	$C_{T,s} = 0.60$		
-20	0.677	-0.536	-0.568
-15	.949	-.499	-.554
-10	1.234	-.442	-.555
-5	1.543	-.345	-.568
0	1.886	-.202	-.597
5	2.156	-.035	-.612
10	2.312	.134	-.596
15	2.210	.394	-.616
20	2.217	.568	-.590
25	2.049	.708	-.535
30	1.879	.764	-.487
35	1.680	.768	-.374

TABLE 8.- TABULATED AERODYNAMIC DATA FOR $\delta_f = 0^\circ$; $\delta_s = 30^\circ$; AND DOWN-AT-TIP ROTATION

α, deg	$C_{L,s}$	$C_{D,s}$	$C_{m,s}$
	$C_{T,s} = 0.90$		
-20	-0.501	-1.018	-0.078
-15	-.348	-1.075	-.063
-10	-.181	-1.121	-.037
-5	-.001	-1.131	-.027
0	.172	-1.137	-.005
5	.341	-1.112	.013
10	.503	-1.073	.032
15	.660	-1.022	.050
20	.795	-.943	.055
25	.922	-.861	.057
30	1.044	-.759	.060
35	1.130	-.639	.058
40	1.194	-.527	.048
45	1.251	-.400	.051
50	1.293	-.274	.051
55	1.330	-.119	.060
60	1.350	.015	.068
65	1.340	.121	.080
70	1.320	.220	.090
75	1.295	.331	.105
80	1.270	.440	.102
	$C_{T,s} = 0.80$		
-20	-0.545	-0.856	-0.100
-15	-.382	-.932	-.082
-10	-.217	-.969	-.059
-5	-.014	-1.006	-.040
0	.194	-1.009	-.014
5	.393	-.987	.012
10	.564	-.942	.039
15	.761	-.879	.049
20	.932	-.794	.073
25	1.079	-.693	.085
30	1.209	-.574	.096
35	1.322	-.430	.077
40	1.418	-.286	.084
45	1.410	-.142	.059
50	1.440	.015	.076
55	1.446	.163	.091
60	1.430	.292	.092
65	1.401	.408	.108
70	1.357	.507	.123
	$C_{T,s} = 0.60$		
-20	-0.586	-0.515	-0.127
-15	-.407	-.599	-.099
-10	-.236	-.655	-.070
-5	-.049	-.698	-.041
0	.184	-.723	-.028
5	.417	-.704	.007
10	.661	-.656	.045
15	.860	-.559	.038
20	1.043	-.462	.054
25	1.234	-.355	.080
30	1.405	-.220	.094
35	1.507	-.071	.095
40	1.563	.088	.073
45	1.594	.229	.071
50	1.605	.361	.086
55	1.445	.474	.081
60	1.372	.568	.080

TABLE 9.- TABULATED AERODYNAMIC DATA

FOR $\delta_f = 40^\circ$, $\delta_s = 30^\circ$, AND

DOWN-AT-TIP ROTATION

α, deg	$C_{L,s}$	$C_{D,s}$	$C_{m,s}$
	$C_{T,s} = 0.90$		
-20	0.010	-1.045	-0.290
-15	.223	-1.064	-.306
-10	.426	-1.052	-.300
-5	.624	-1.016	-.303
0	.809	-.956	-.303
5	.981	-.879	-.304
10	1.143	-.784	-.308
15	1.306	-.656	-.311
20	1.411	-.525	-.306
25	1.490	-.391	-.308
30	1.520	-.257	-.305
35	1.531	-.111	-.299
40	1.502	.005	-.286
45	1.487	.108	-.258
50	1.444	.196	-.229
55	1.392	.272	-.192
60	1.356	.345	-.163
65	1.310	.403	-.128
	$C_{T,s} = 0.80$		
-20	-0.030	-0.893	-0.303
-15	.227	-.907	-.328
-10	.481	-.915	-.341
-5	.724	-.873	-.338
0	.989	-.803	-.349
5	1.233	-.706	-.367
10	1.440	-.580	-.361
15	1.634	-.437	-.382
20	1.743	-.286	-.368
25	1.761	-.136	-.351
30	1.794	.014	-.339
35	1.717	.119	-.319
40	1.553	.199	-.285
45	1.498	.294	-.239
50	1.445	.369	-.209
55	1.411	.474	-.150
60	1.351	.554	-.112
65	1.296	.614	-.084
	$C_{T,s} = 0.60$		
-20	-0.153	-0.562	-0.298
-15	.115	-.595	-.314
-10	.425	-.612	-.343
-5	.797	-.587	-.370
0	1.207	-.495	-.413
5	1.578	-.383	-.452
10	1.900	-.225	-.465
15	2.142	-.041	-.464
20	2.306	.145	-.454
25	2.327	.305	-.428
30	1.917	.350	-.405
35	1.816	.434	-.339
40	1.764	.534	-.286

TABLE 10.- TABULATED AERODYNAMIC DATA

FOR $\delta_f = 60^\circ$, $\delta_s = 30^\circ$ AND

DOWN-AT-TIP ROTATION

α, deg	$C_{L,s}$	$C_{D,s}$	$C_{m,s}$
	$C_{T,s} = 0.90$		
-20	0.349	-0.956	-0.401
-15	.541	-.944	-.401
-10	.717	-.902	-.397
-5	.897	-.838	-.386
0	1.080	-.762	-.403
5	1.242	-.643	-.405
10	1.382	-.508	-.414
15	1.502	-.376	-.419
20	1.608	-.222	-.422
25	1.648	-.082	-.410
30	1.628	.026	-.384
35	1.510	.095	-.343
40	1.452	.181	-.312
45	1.394	.246	-.296
50	1.345	.304	-.255
55	1.274	.356	-.221
60	1.223	.397	-.171
65	1.181	.443	-.136
	$C_{T,s} = 80$		
-20	0.350	-0.726	-0.387
-15	.564	-.702	-.386
-10	.773	-.669	-.390
-5	1.004	-.601	-.396
0	1.210	-.505	-.407
5	1.424	-.378	-.437
10	1.572	-.239	-.438
15	1.678	-.091	-.437
20	1.635	.018	-.402
25	1.620	.124	-.364
30	1.553	.205	-.329
35	1.340	.223	-.302
40	1.274	.291	-.241
45	1.215	.346	-.208
50	1.184	.411	-.173
55	1.147	.479	-.135
60	1.099	.536	-.099
65	1.042	.566	-.046
	$C_{T,s} = 0.60$		
-20	0.291	-0.501	-0.450
-15	.639	-.497	-.467
-10	1.015	-.455	-.498
-5	1.376	-.383	-.529
0	1.768	-.229	-.572
5	2.114	-.061	-.604
10	2.350	.136	-.607
15	2.509	.319	-.579
20	2.565	.498	-.547
25	1.936	.418	-.427
30	1.747	.452	-.358
35	1.653	.522	-.305
40	1.611	.611	-.255

TABLE 11.- TABULATED AERODYNAMIC DATA FOR

$\delta_f = 0^\circ$, $\delta_s = 30^\circ$ WITH FENCES ON,

AND DOWN-AT-TIP ROTATION

α, deg	$C_{L,s}$	$C_{D,s}$	$C_{m,s}$
	$C_{T,s} = 0.90$		
-20	-0.485	-1.015	-0.071
-15	-.325	-1.077	-.049
-10	-.161	-1.166	-.026
-5	.018	-1.137	-.015
0	.195	-1.130	.012
5	.367	-1.112	.025
10	.529	-1.073	.041
15	.676	-1.011	.061
20	.814	-.942	.068
25	.943	-.851	.075
30	1.050	-.745	.081
35	1.128	-.619	.071
40	1.208	-.499	.077
45	1.331	-.340	.077
50	1.376	-.193	.081
55	1.391	-.059	.088
60	1.391	.064	.096
65	1.376	.181	.102
70	1.350	.278	.111
75	1.318	.391	.122
80	1.273	.479	.130
	$C_{T,s} = 0.80$		
-20	-0.539	-0.844	-0.094
-15	-.365	-.921	-.076
-10	-.201	-.969	-.055
-5	-.005	-.988	-.031
0	.209	-.994	-.005
5	.403	-.981	.017
10	.576	-.928	.045
15	.760	-.860	.062
20	.923	-.758	.060
25	1.070	-.667	.080
30	1.195	-.551	.076
35	1.265	-.426	.074
40	1.349	-.298	.072
45	1.401	-.147	.078
50	1.490	.068	.089
55	1.514	.223	.101
60	1.481	.342	.111
65	1.421	.432	.125
70	1.372	.517	.135
75	1.311	.603	.147
	$C_{T,s} = 0.60$		
-20	-0.582	-0.528	-0.121
-15	-.409	-.612	-.098
-10	-.243	-.672	-.073
-5	-.051	-.707	-.048
0	.194	-.728	-.021
5	.424	-.720	0
10	.645	-.649	.031
15	.855	-.567	.049
20	1.024	-.470	.064
25	1.154	-.354	.061
30	1.327	-.221	.081
35	1.371	-.105	.074
40	1.468	.042	.072
45	1.531	.206	.062
50	1.526	.320	.069
55	1.461	.488	.068

TABLE 12.- TABULATED AERODYNAMIC DATA FOR

$\delta_f = 40^\circ$, $\delta_s = 30^\circ$ WITH FENCES ON,

AND DOWN-AT-TIP ROTATION

α, deg	$C_{L,s}$	$C_{D,s}$	$C_{m,s}$
	$C_{T,s} = 0.90$		
-20	0.026	-1.032	-0.308
-15	.239	-1.049	-.318
-10	.442	-1.043	-.312
-5	.633	-1.005	-.313
0	.807	-.951	-.314
5	.985	-.864	-.308
10	1.143	-.753	-.315
15	1.283	-.633	-.312
20	1.413	-.503	-.315
25	1.493	-.356	-.325
30	1.550	-.199	-.325
35	1.574	-.041	-.328
40	1.590	.104	-.314
45	1.560	.244	-.363
50	1.564	.358	-.263
55	1.519	.452	-.232
60	1.399	.437	-.169
65	1.337	.479	-.130
	$C_{T,s} = 0.80$		
-20	-0.030	-0.875	-0.314
-15	.234	-.906	-.339
-10	.479	-.902	-.341
-5	.732	-.855	-.347
0	.987	-.788	-.348
5	1.223	-.689	-.366
10	1.433	-.564	-.371
15	1.626	-.420	-.379
20	1.733	-.248	-.390
25	1.813	-.066	-.389
30	1.841	.094	-.384
35	1.808	.256	-.368
40	1.753	.392	-.334
45	1.685	.492	-.305
50	1.610	.573	-.249
55	1.529	.636	-.187
60	1.438	.662	-.126
	$C_{T,s} = 0.60$		
-20	-0.153	-0.553	-0.299
-15	.143	-.593	-.602
-10	.446	-.602	-.348
-5	.795	-.572	-.367
0	1.189	-.493	-.411
5	1.586	-.370	-.453
10	1.879	-.215	-.457
15	2.119	-.039	-.455
20	2.230	.167	-.468
25	2.200	.348	-.464
30	2.220	.542	-.447
35	2.165	.672	-.396
40	1.703	.527	-.282

TABLE 13.- TABULATED AERODYNAMIC DATA FOR

$\delta_f = 60^\circ$, $\delta_s = 30^\circ$ WITH FENCES ON,

AND DOWN-AT-TIP ROTATION

α, deg	$C_{L,s}$	$C_{D,s}$	$C_{m,s}$
	$C_{T,s} = 0.90$		
-20	0.370	-0.954	-0.403
-15	.552	-.940	-.399
-10	.728	-.886	-.397
-5	.915	-.821	-.400
0	1.090	-.734	-.402
5	1.255	-.617	-.413
10	1.377	-.492	-.411
15	1.507	-.356	-.424
20	1.579	-.207	-.424
25	1.615	-.059	-.417
30	1.629	.088	-.406
35	1.633	.239	-.393
40	1.610	.359	-.366
45	1.556	.452	-.326
50	1.513	.541	-.288
55	1.438	.603	-.251
60	1.271	.503	-.177
65	1.215	.529	-.140
	$C_{T,s} = 0.80$		
-20	0.385	-0.788	-0.437
-15	.624	-.772	-.441
-10	.900	-.737	-.452
-5	1.142	-.658	-.452
0	1.367	-.554	-.469
5	1.584	-.410	-.490
10	1.756	-.254	-.489
15	1.883	-.084	-.488
20	1.883	.084	-.488
25	1.898	.253	-.477
30	1.805	.378	-.436
35	1.744	.488	-.391
40	1.660	.558	-.353
45	1.562	.614	-.289
50	1.479	.667	-.238
55	1.399	.709	-.176
60	1.308	.715	-.120
	$C_{T,s} = 0.60$		
-20	0.290	-0.488	-0.441
-15	.628	-.486	-.479
-10	.999	-.445	-.494
-5	1.379	-.374	-.536
0	1.765	-.223	-.567
5	2.094	-.046	-.597
10	2.306	.140	-.603
15	2.469	.337	-.581
20	2.426	.543	-.581
25	2.407	.709	-.548
30	2.185	.789	-.462
35	2.075	.860	-.385
40	1.604	.639	-.276

TABLE 14.- TABULATED AERODYNAMIC DATA

FOR $\delta_f = 0^\circ$, $\delta_s = 30^\circ$, AND

UP-AT-TIP ROTATION

α, deg	$C_{L,s}$	$C_{D,s}$	$C_{m,s}$
	$C_{T,s} = 0.90$		
-20	-0.477	-0.981	-0.051
-15	-.331	-1.039	-.040
-10	-.177	-1.068	-.014
-5	-.002	-1.097	-.003
0	.171	-1.089	.009
5	.341	-1.070	.037
10	.500	-1.032	.048
15	.661	-.989	.064
20	.812	-.914	.072
25	.954	-.823	.074
30	1.077	-.710	.079
35	1.171	-.596	.077
40	1.242	-.473	.077
45	1.307	-.341	.076
50	1.353	-.215	.072
55	1.372	-.085	.074
60	1.390	.038	.077
65	1.385	.168	.086
70	1.358	.272	.080
75	1.327	.377	.099
	$C_{T,s} = 0.80$		
-20	-0.517	-0.809	-0.069
-15	-.373	-.870	-.045
-10	-.217	-.913	-.015
-5	-.024	-.942	-.005
0	.187	-.953	.012
5	.375	-.931	.034
10	.567	-.897	.047
15	.763	-.843	.066
20	.914	-.758	.070
25	1.082	-.654	.082
30	1.232	-.537	.084
35	1.375	-.391	.089
40	1.488	-.241	.098
45	1.493	-.089	.094
50	1.514	.061	.096
55	1.510	.260	.095
60	1.495	.310	.092
65	1.425	.422	.092
70	1.381	.532	.099
	$C_{T,s} = 0.60$		
-20	-0.541	-0.490	-0.097
-15	-.379	-.567	-.065
-10	-.232	-.614	-.039
-5	-.068	-.655	-.008
0	.159	-.685	.002
5	.411	-.682	.018
10	.662	-.639	.042
15	.900	-.570	.066
20	1.098	-.485	.085
25	1.229	-.358	.092
30	1.420	-.228	.106
35	1.564	-.080	.107
40	1.643	.110	.093
45	1.695	.275	.104
50	1.677	.429	.093
55	1.480	.549	.064
60	1.351	.611	.068

TABLE 15.- TABULATED AERODYNAMIC DATA

FOR $\delta_f = 40^\circ$, $\delta_s = 30^\circ$, AND

UP-AT-TIP ROTATION

α, deg	$C_{L,s}$	$C_{D,s}$	$C_{m,s}$
	$C_{T,s} = 0.90$		
-20	-0.128	-0.984	-0.216
-15	.040	-1.006	-.204
-10	.232	-1.011	-.197
-5	.415	-.994	-.190
0	.597	-.950	-.193
5	.775	-.883	-.193
10	.937	-.801	-.197
15	1.097	-.686	-.211
20	1.268	-.542	-.245
25	1.350	-.401	-.263
30	1.424	-.251	-.273
35	1.458	-.116	-.268
40	1.472	.006	-.257
45	1.457	.117	-.245
50	1.438	.214	-.216
55	1.403	.309	-.194
60	1.380	.382	-.153
65	1.340	.457	-.126
	$C_{T,s} = 0.80$		
-20	-0.134	-0.824	-0.232
-15	.018	-.854	-.204
-10	.203	-.865	-.195
-5	.470	-.847	-.218
0	.733	-.795	-.237
5	.986	-.717	-.259
10	1.227	-.597	-.284
15	1.457	-.444	-.312
20	1.657	-.263	-.352
25	1.691	-.112	-.358
30	1.743	.051	-.343
35	1.746	.211	-.333
40	1.695	.329	-.301
45	1.664	.435	-.268
50	1.601	.507	-.219
55	1.544	.574	-.172
60	1.492	.640	-.137
	$C_{T,s} = 0.60$		
-20	-0.105	-0.526	-0.291
-15	.054	-.556	-.255
-10	.233	-.588	-.244
-5	.486	-.570	-.251
0	.926	-.494	-.303
5	1.358	-.378	-.374
10	1.749	-.219	-.443
15	2.065	-.014	-.472
20	2.263	.173	-.470
25	2.323	.350	-.443
30	2.107	.425	-.376
35	2.087	.542	-.315
40	2.013	.620	-.254

TABLE 16.- TABULATED AERODYNAMIC DATA

FOR $\delta_f = 60^\circ$, $\delta_s = 30^\circ$, AND

UP-AT-TIP ROTATION

α, deg	$C_{L,s}$	$C_{D,s}$	$C_{m,s}$
	$C_{T,s} = 0.90$		
-20	0.050	-0.938	-0.265
-15	.242	-.943	-.264
-10	.454	-.920	-.279
-5	.660	-.871	-.294
0	.854	-.791	-.313
5	1.004	-.690	-.320
10	1.192	-.567	-.354
15	1.366	-.383	-.389
20	1.413	-.251	-.383
25	1.461	-.113	-.378
30	1.505	.008	-.358
35	1.491	.112	-.328
40	1.457	.200	-.305
45	1.419	.282	-.282
50	1.388	.355	-.252
55	1.336	.408	-.207
60	1.314	.464	-.165
65	1.273	.532	-.148
	$C_{T,s} = 0.80$		
-20	0.020	-0.776	-0.291
-15	.268	-.789	-.305
-10	.493	-.777	-.313
-5	.779	-.714	-.344
0	1.076	-.613	-.378
5	1.320	-.476	-.403
10	1.555	-.303	-.455
15	1.745	-.131	-.460
20	1.858	.054	-.469
25	1.761	.156	-.428
30	1.741	.277	-.390
35	1.678	.392	-.368
40	1.634	.469	-.314
45	1.574	.538	-.258
50	1.524	.580	-.202
55	1.459	.626	-.163
60	1.414	.696	-.127
65	1.350	.714	-.069
	$C_{T,s} = 0.60$		
-20	0.090	-0.456	-0.361
-15	.320	-.472	-.375
-10	.610	-.455	-.381
-5	.986	-.408	-.417
0	1.429	-.283	-.477
5	1.833	-.105	-.527
10	2.196	.130	-.590
15	2.442	.358	-.609
20	2.531	.553	-.572
25	2.230	.562	-.444
30	2.055	.575	-.346
35	1.980	.633	-.299
40	1.870	.708	-.220

TABLE 17.- TABULATED AERODYNAMIC DATA FOR

$\delta_f = 0^\circ$, $\delta_s = 30^\circ$ WITH FENCES ON,

AND UP-AT-TIP ROTATION

α, deg	$C_{L,s}$	$C_{D,s}$	$C_{m,s}$
	$C_{T,s}$ = 0.90		
-20	-0.487	-0.965	-0.044
-15	-.340	-1.031	-.036
-10	-.186	-1.061	-.016
-5	-.015	-1.087	.007
0	.148	-1.088	.015
5	.324	-1.073	.036
10	.490	-1.035	.042
15	.653	-.980	.059
20	.793	-.909	.063
25	.939	-.816	.063
30	1.073	-.711	.073
35	1.171	-.591	.067
40	1.260	-.455	.067
45	1.323	-.327	.066
50	1.364	-.196	.067
55	1.384	-.069	.068
60	1.389	.048	.074
65	1.379	.164	.075
70	1.359	.279	.083
	$C_{T,s}$ = 0.80		
-20	-0.506	-0.802	-0.063
-15	-.366	-.856	-.038
-10	-.230	-.906	-.010
-5	-.046	-.934	.004
0	.156	-.949	.005
5	.357	-.934	.037
10	.551	-.887	.049
15	.752	-.825	.069
20	.939	-.740	.078
25	1.109	-.638	.095
30	1.258	-.513	.095
35	1.391	-.376	.103
40	1.491	-.230	.106
45	1.528	-.065	.101
50	1.558	.095	.100
55	1.549	.228	.097
60	1.521	.349	.095
65	1.437	.440	.100
70	1.349	.529	.109
	$C_{T,s}$ = 0.60		
-20	-0.514	-0.503	-0.093
-15	-.363	-.561	-.069
-10	-.230	-.622	-.039
-5	-.071	-.652	-.004
0	.144	-.673	-.003
5	.398	-.672	.021
10	.642	-.625	.033
15	.884	-.550	.048
20	1.109	-.456	.071
25	1.279	-.332	.086
30	1.457	-.197	.104
35	1.557	-.027	.078
40	1.608	.124	.083
45	1.656	.307	.076
50	1.643	.470	.069
55	1.567	.599	.070

TABLE 18.- TABULATED AERODYNAMIC DATA FOR

$\delta_f = 40^\circ$, $\delta_s = 30^\circ$ WITH FENCES ON,

AND UP-AT-TIP ROTATION

α, deg	$C_{L,s}$	$C_{D,s}$	$C_{m,s}$
	$C_{T,s}$ = 0.90		
-20	-0.154	-0.982	-0.190
-15	-.009	-1.003	-.177
-10	.187	-1.009	-.175
-5	.380	-.998	-.178
0	.552	-.958	-.173
5	.729	-.899	-.174
10	.895	-.814	-.180
15	1.057	-.699	-.203
20	1.209	-.569	-.234
25	1.330	-.409	-.255
30	1.396	-.250	-.265
35	1.454	-.099	-.273
40	1.479	.031	-.267
45	1.464	.136	-.249
50	1.438	.237	-.232
55	1.417	.333	-.204
60	1.368	.382	-.162
65	1.330	.450	-.124
	$C_{T,s}$ = 0.80		
-20	-0.156	-0.822	-0.221
-15	-.014	-.860	-.201
-10	.175	-.866	-.189
-5	.446	-.844	-.212
0	.696	-.805	-.224
5	.940	-.712	-.234
10	1.186	-.606	-.259
15	1.418	-.449	-.297
20	1.594	-.272	-.347
25	1.734	-.069	-.375
30	1.786	.095	-.368
35	1.788	.271	-.355
40	1.774	.400	-.324
45	1.719	.493	-.301
50	1.658	.579	-.258
55	1.593	.653	-.200
60	1.514	.688	-.152
	$C_{T,s}$ = 0.60		
-20	-0.116	-0.510	-0.277
-15	.041	-.556	-.254
-10	.218	-.573	-.239
-5	.484	-.566	-.241
0	.899	-.502	-.290
5	1.317	-.382	-.353
10	1.729	-.216	-.429
15	2.048	-.013	-.467
20	2.235	.179	-.455
25	2.271	.391	-.469
30	2.293	.558	-.437
35	2.283	.694	-.383
40	2.177	.798	-.316

TABLE 19.- TABULATED AERODYNAMIC DATA FOR

$\delta_f = 60^\circ$, $\delta_s = 30^\circ$ WITH FENCES ON,

AND UP-AT-TIP ROTATION

α, deg	$C_{L,s}$	$C_{D,s}$	$C_{m,s}$
$C_{T,s}$ = 0.90			
-20	0.026	-0.931	-0.254
-15	.205	-.940	-.251
-10	.417	-.923	-.261
-5	.625	-.877	-.273
0	.823	-.795	-.303
5	.978	-.698	-.310
10	1.155	-.554	-.342
15	1.271	-.418	-.357
20	1.383	-.263	-.367
25	1.422	-.119	-.364
30	1.474	.019	-.363
35	1.491	.153	-.350
40	1.487	.260	-.320
45	1.439	.339	-.292
50	1.373	.375	-.256
55	1.324	.430	-.218
60	1.289	.481	-.183
65	1.258	.531	-.148
70	1.215	.566	-.099
$C_{T,s}$ = 0.80			
-20	0.018	-0.766	-0.276
-15	.224	-.788	-.281
-10	.478	-.764	-.294
-5	.762	-.718	-.320
0	1.045	-.613	-.354
5	1.304	-.471	-.401
10	1.535	-.312	-.437
15	1.731	-.128	-.448
20	1.787	.055	-.462
25	1.817	.238	-.468
30	1.774	.375	-.435
35	1.746	.487	-.401
40	1.692	.569	-.358
45	1.635	.642	-.308
50	1.569	.687	-.252
55	1.492	.730	-.201
60	1.410	.732	-.148
$C_{T,s}$ = 0.60			
-20	0.084	-0.438	-0.350
-15	.341	-.459	-.368
-10	.622	-.439	-.379
-5	.991	-.404	-.414
0	1.394	-.285	-.460
5	1.806	-.109	-.516
10	2.184	.125	-.566
15	2.402	.359	-.590
20	2.441	.537	-.562
25	2.342	.702	-.539
30	2.276	.805	-.469
35	2.206	.871	-.385
40	1.995	.932	-.311

TABLE 20.- TABULATED AERODYNAMIC DATA FOR

$\delta_f = 40^\circ$, $\delta_s = 10^\circ$ IN HIGH POSITION,

AND UP-AT-TIP ROTATION

α, deg	$C_{L,s}$	$C_{D,s}$	$C_{m,s}$
$C_{T,s}$ = 0.90			
-20	-0.107	-1.004	-0.223
-15	.058	-1.031	-.209
-10	.251	-1.032	-.207
-5	.450	-1.010	-.209
0	.629	-.961	-.205
5	.815	-.879	-.226
10	1.007	-.780	-.244
15	1.179	-.650	-.265
20	1.275	-.515	-.278
25	1.384	-.362	-.290
30	1.467	-.222	-.286
35	1.488	-.093	-.278
40	1.483	.019	-.254
45	1.469	.128	-.237
50	1.436	.220	-.223
55	1.408	.324	-.207
60	1.379	.399	-.163
65	1.335	.447	-.127
$C_{T,s}$ = 0.80			
-20	-0.106	-0.859	-0.256
-15	.053	-.886	-.238
-10	.260	-.892	-.237
-5	.539	-.868	-.255
0	.787	-.807	-.274
5	1.067	-.710	-.307
10	1.329	-.570	-.348
15	1.546	-.411	-.368
20	1.685	-.247	-.383
25	1.663	-.114	-.355
30	1.685	.043	-.355
35	1.697	.186	-.319
40	1.664	.291	-.289
45	1.627	.395	-.247
50	1.582	.481	-.206
55	1.528	.549	-.168
60	1.474	.629	-.146
$C_{T,s}$ = 0.60			
-20	-0.097	-0.541	-0.311
-15	.073	-.578	-.291
-10	.277	-.592	-.286
-5	.638	-.571	-.319
0	1.071	-.491	-.370
5	1.478	-.363	-.431
10	1.835	-.183	-.471
15	2.104	.007	-.477
20	2.276	.194	-.467
25	2.178	.332	-.423
30	2.069	.446	-.388
35	1.896	.538	-.313
40	1.764	.624	-.246

TABLE 21.- TABULATED AERODYNAMIC DATA FOR

$\delta_f = 60^\circ$, $\delta_s = 10^\circ$ IN HIGH POSITION,

AND UP-AT-TIP ROTATION

α, deg	$C_{L,s}$	$C_{D,s}$	$C_{m,s}$
	$C_{T,s} = 0.90$		
-20	0.117	-0.958	-0.297
-15	.308	-.958	-.304
-10	.520	-.928	-.311
-5	.719	-.864	-.318
0	.903	-.777	-.330
5	1.096	-.660	-.362
10	1.269	-.514	-.384
15	1.385	-.373	-.386
20	1.457	-.228	-.386
25	1.540	-.066	-.395
30	1.548	.043	-.366
35	1.517	.135	-.328
40	1.477	.206	-.291
45	1.431	.298	-.268
50	1.362	.350	-.243
55	1.323	.409	-.205
60	1.288	.469	-.182
65	1.271	.524	-.141
70	1.227	.554	-.085
	$C_{T,s} = 0.80$		
-20	0.102	-0.795	-0.333
-15	.325	-.798	-.336
-10	.560	-.768	-.348
-5	.867	-.707	-.366
0	1.144	-.594	-.397
5	1.408	-.441	-.437
10	1.652	-.252	-.482
15	1.822	-.074	-.485
20	1.771	.041	-.443
25	1.725	.153	-.418
30	1.684	.249	-.368
35	1.604	.332	-.324
40	1.564	.412	-.273
45	1.529	.489	-.225
50	1.487	.549	-.189
55	1.442	.614	-.144
60	1.378	.650	-.119
	$C_{T,s} = 0.60$		
-20	0.171	-0.470	-0.410
-15	.409	-.485	-.403
-10	.713	-.471	-.413
-5	1.152	-.388	-.451
0	1.610	-.245	-.534
5	1.965	-.052	-.580
10	2.286	.194	-.618
15	2.469	.392	-.601
20	2.482	.558	-.542
25	2.165	.574	-.443
30	1.909	.597	-.361
35	1.741	.628	-.287

TABLE 22.- TABULATED AERODYNAMIC DATA FOR

$\delta_f = 70^\circ$, $\delta_s = 10^\circ$ IN HIGH POSITION,

AND UP-AT-TIP ROTATION

α, deg	$C_{L,s}$	$C_{D,s}$	$C_{m,s}$
	$C_{T,s} = 0.90$		
-20	0.184	-0.919	-0.319
-15	.392	-.900	-.329
-10	.607	-.855	-.343
-5	.807	-.780	-.350
0	1.014	-.673	-.377
5	1.168	-.555	-.392
10	1.331	-.397	-.415
15	1.444	-.243	-.411
20	1.497	-.115	-.406
25	1.552	.031	-.403
30	1.528	.116	-.355
35	1.491	.185	-.306
40	1.447	.254	-.277
45	1.384	.326	-.252
50	1.316	.376	-.232
55	1.292	.430	-.192
60	1.256	.474	-.161
65	1.230	.527	-.113
	$C_{T,s} = 0.80$		
-20	0.175	-0.758	-0.355
-15	.428	-.752	-.360
-10	.676	-.702	-.384
-5	.979	-.618	-.411
0	1.257	-.483	-.441
5	1.520	-.311	-.477
10	1.749	-.125	-.510
15	1.840	.037	-.489
20	1.716	.104	-.443
25	1.692	.220	-.398
30	1.623	.303	-.348
35	1.558	.373	-.290
40	1.510	.443	-.255
45	1.468	.484	-.204
50	1.426	.559	-.166
55	1.390	.614	-.120
60	1.344	.649	-.093
65	1.274	.668	-.051
	$C_{T,s} = 0.60$		
-20	0.218	-0.429	-0.428
-15	.504	-.429	-.416
-10	.813	-.394	-.426
-5	1.253	-.311	-.447
0	1.736	-.139	-.556
5	2.081	.088	-.597
10	2.378	.321	-.628
15	2.476	.503	-.590
20	2.398	.620	-.522
25	2.096	.622	-.442
30	1.783	.619	-.394
35	1.632	.637	-.234
40	1.516	.651	-.194

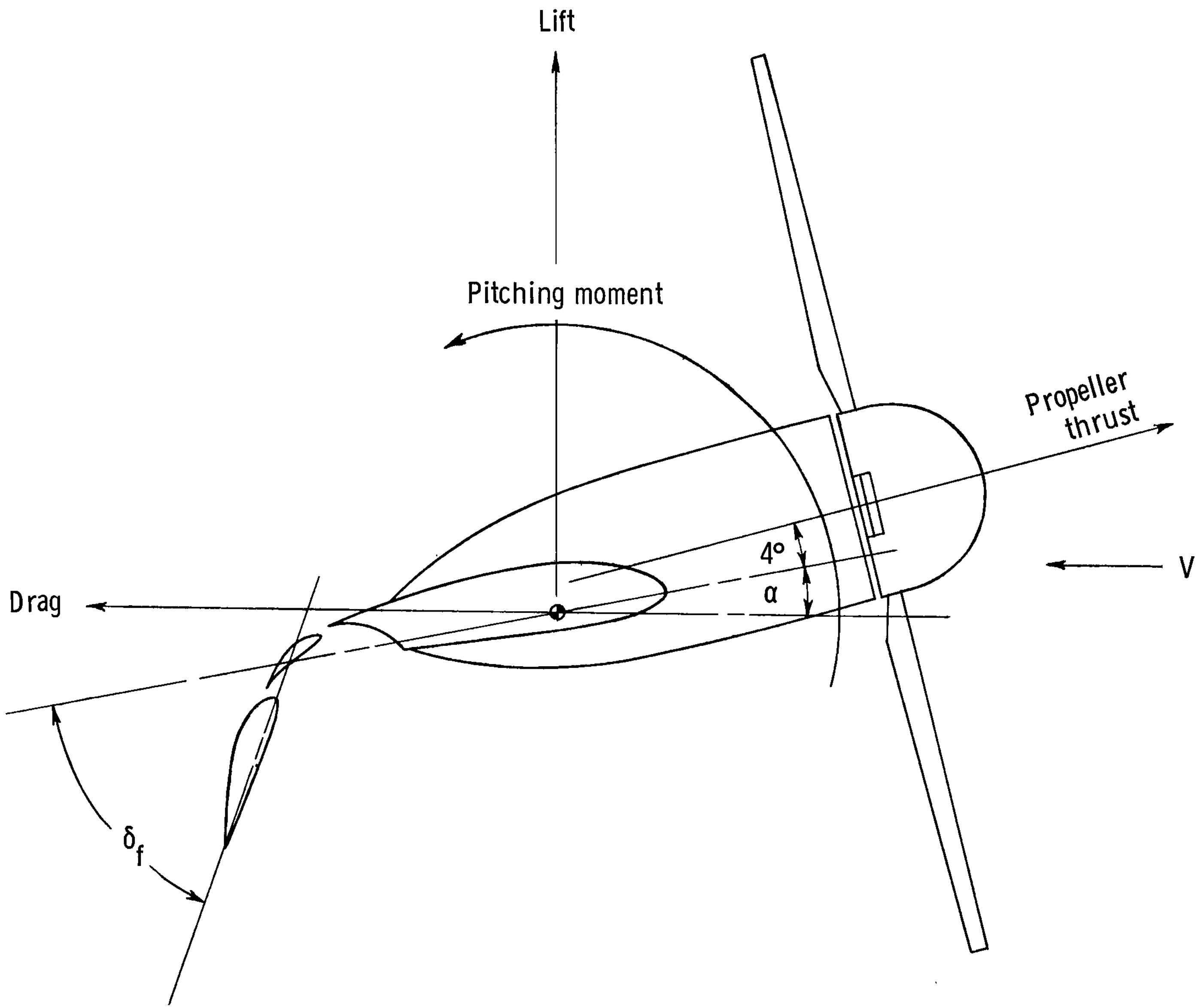

Figure 1.- The positive sense of forces, moments, and angles.

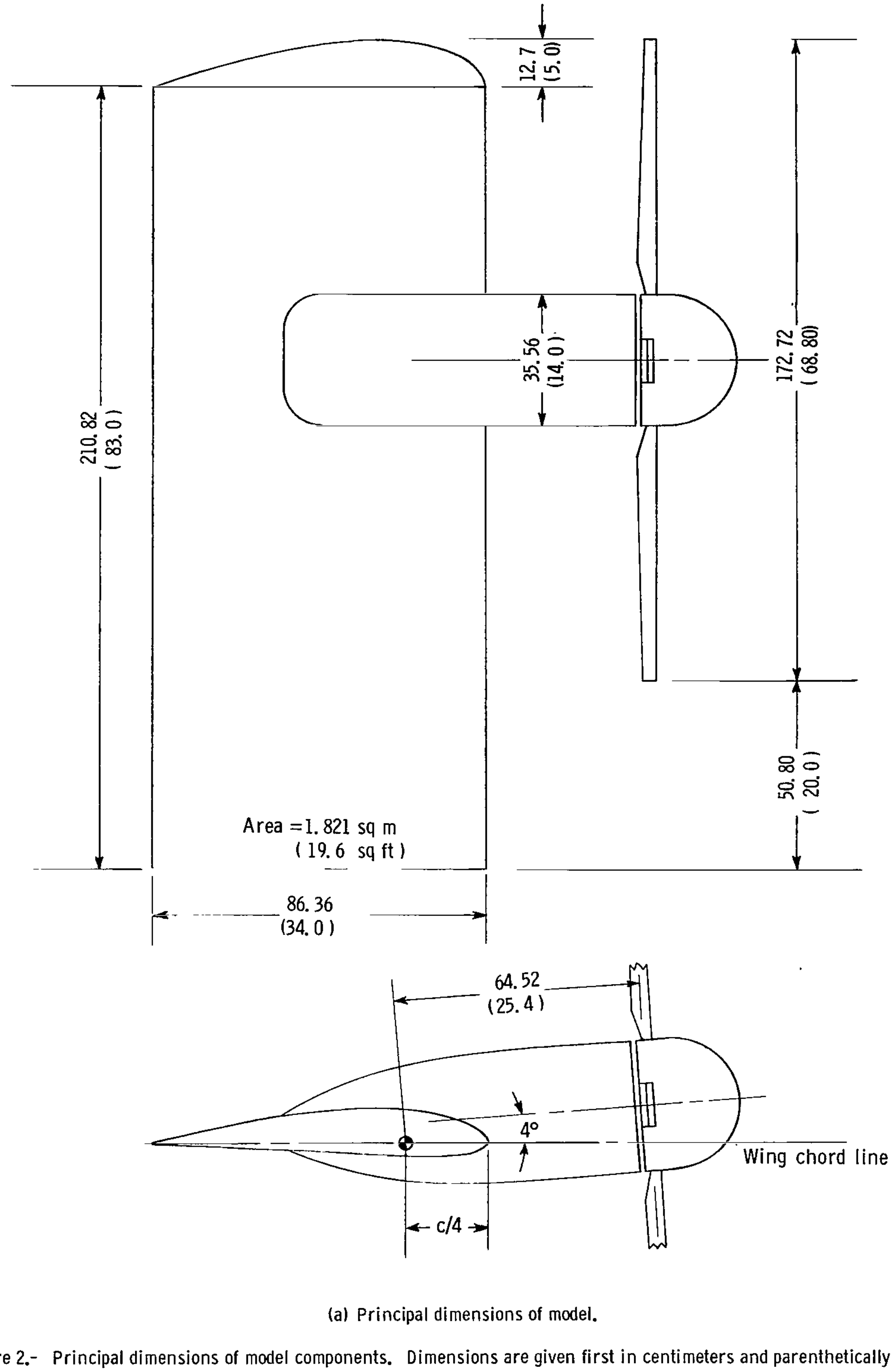

(a) Principal dimensions of model.

Figure 2.- Principal dimensions of model components. Dimensions are given first in centimeters and parenthetically in inches.

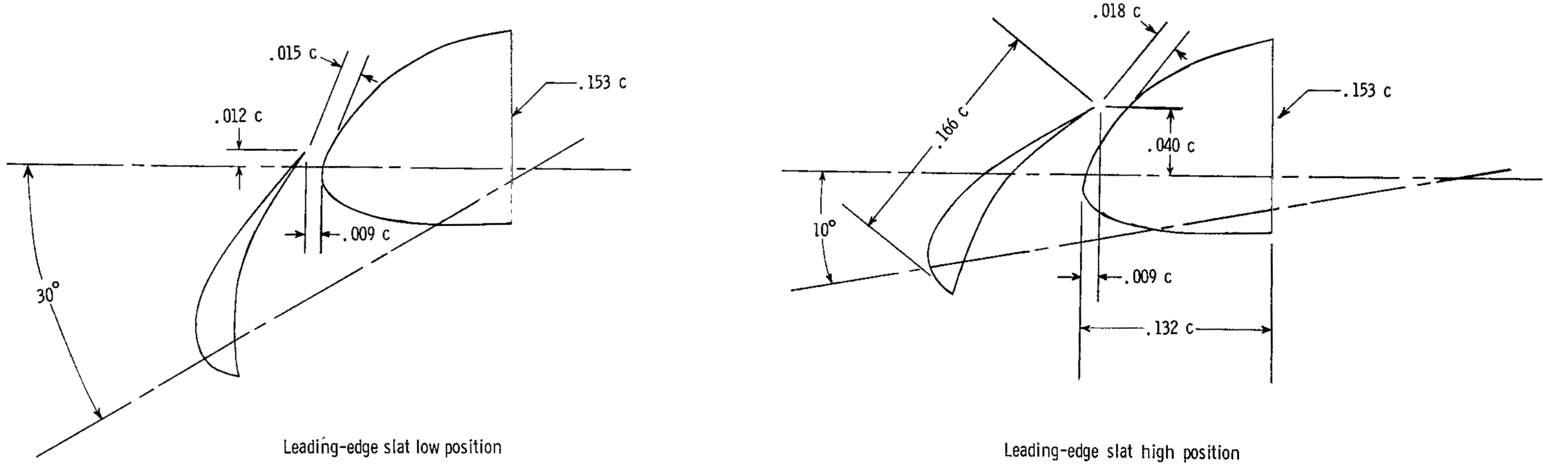

Leading-edge slat low position

Leading-edge slat high position

(b) Sectional views of leading-edge slat configuration.

Figure 2.- Continued.

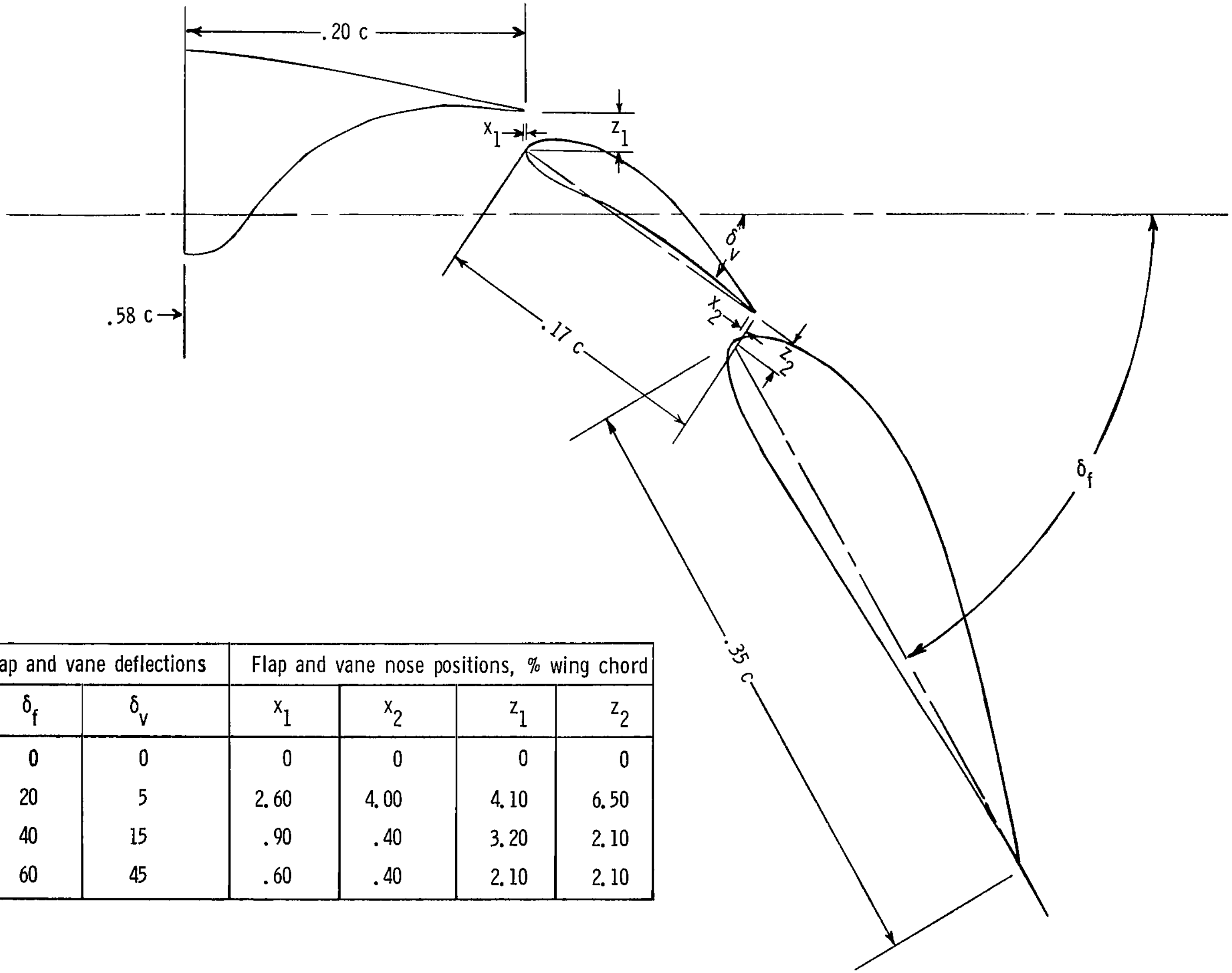

Flap and vane deflections		Flap and vane nose positions, % wing chord			
δ_f	δ_v	x_1	x_2	z_1	z_2
0	0	0	0	0	0
20	5	2.60	4.00	4.10	6.50
40	15	.90	.40	3.20	2.10
60	45	.60	.40	2.10	2.10

(c) Sectional view of trailing-edge flap.

Figure 2.- Continued.

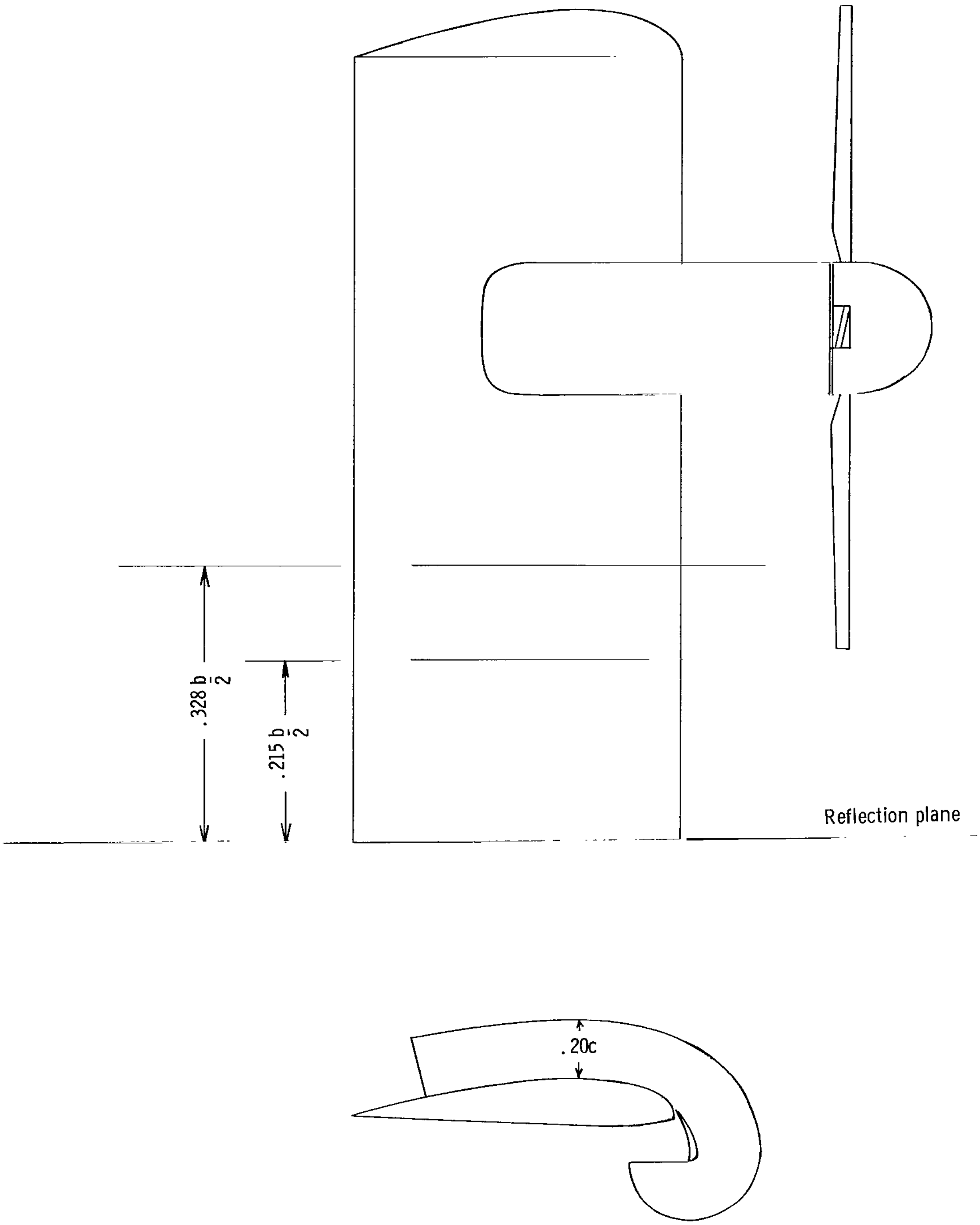

(d) Sectional view of fences.

Figure 2.- Concluded.

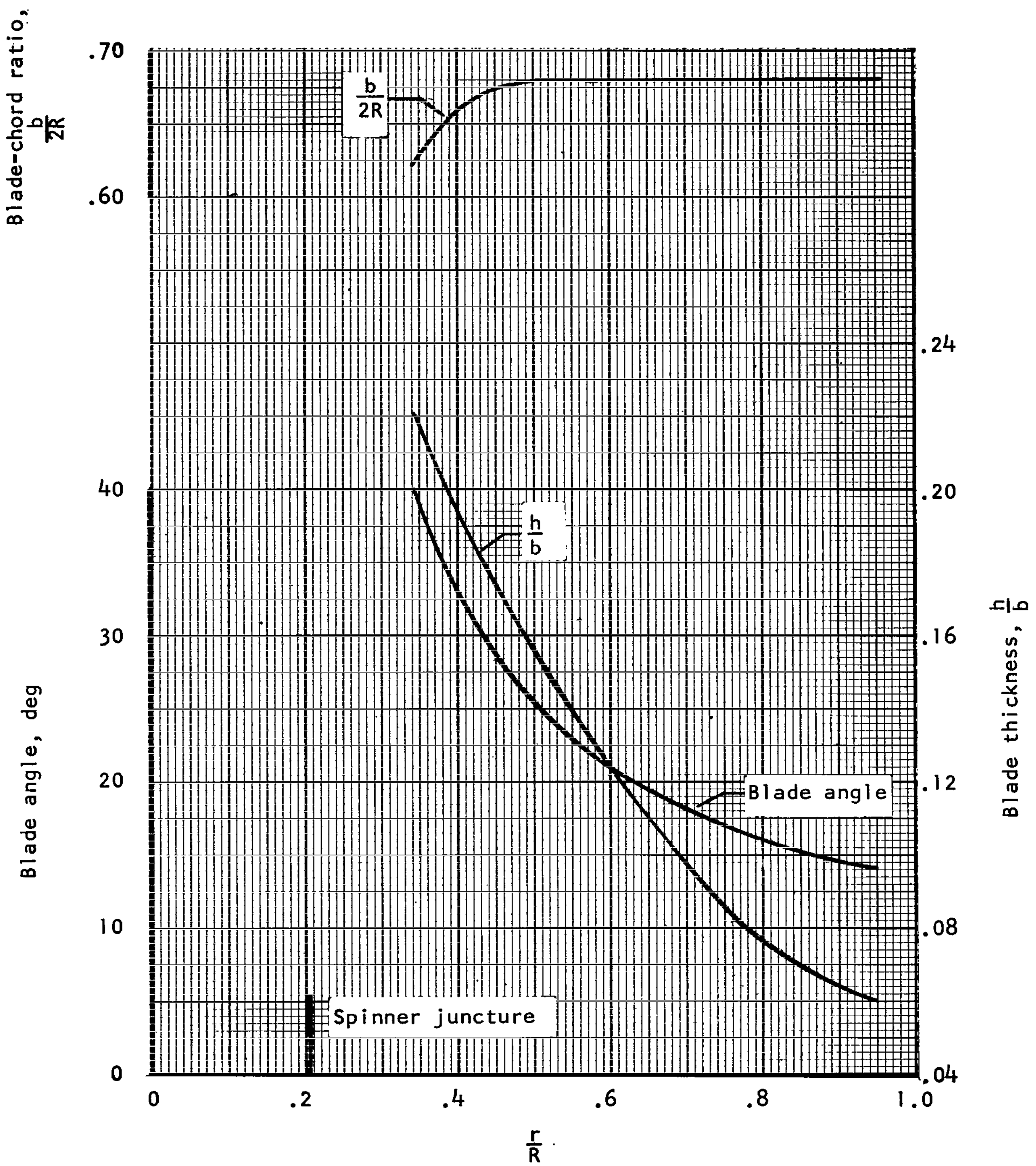

Figure 3.- Propeller-blade form curves.

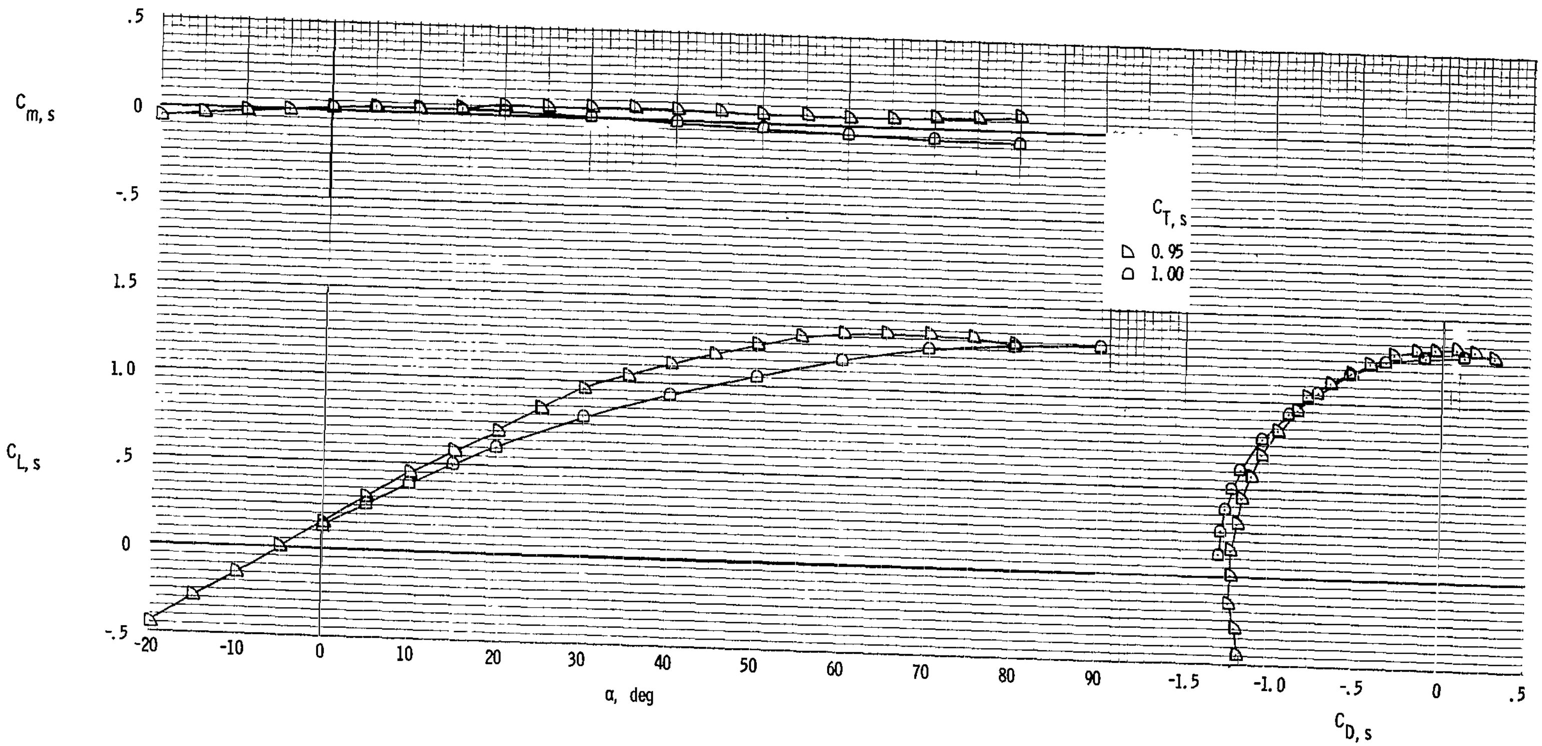

(a) Aerodynamic characteristics.

Figure 4.- Aerodynamic and flow characteristics of the model with basic leading edge and with trailing-edge flap undeflected. $\delta_f = 0^0$. Down-at-tip rotation.

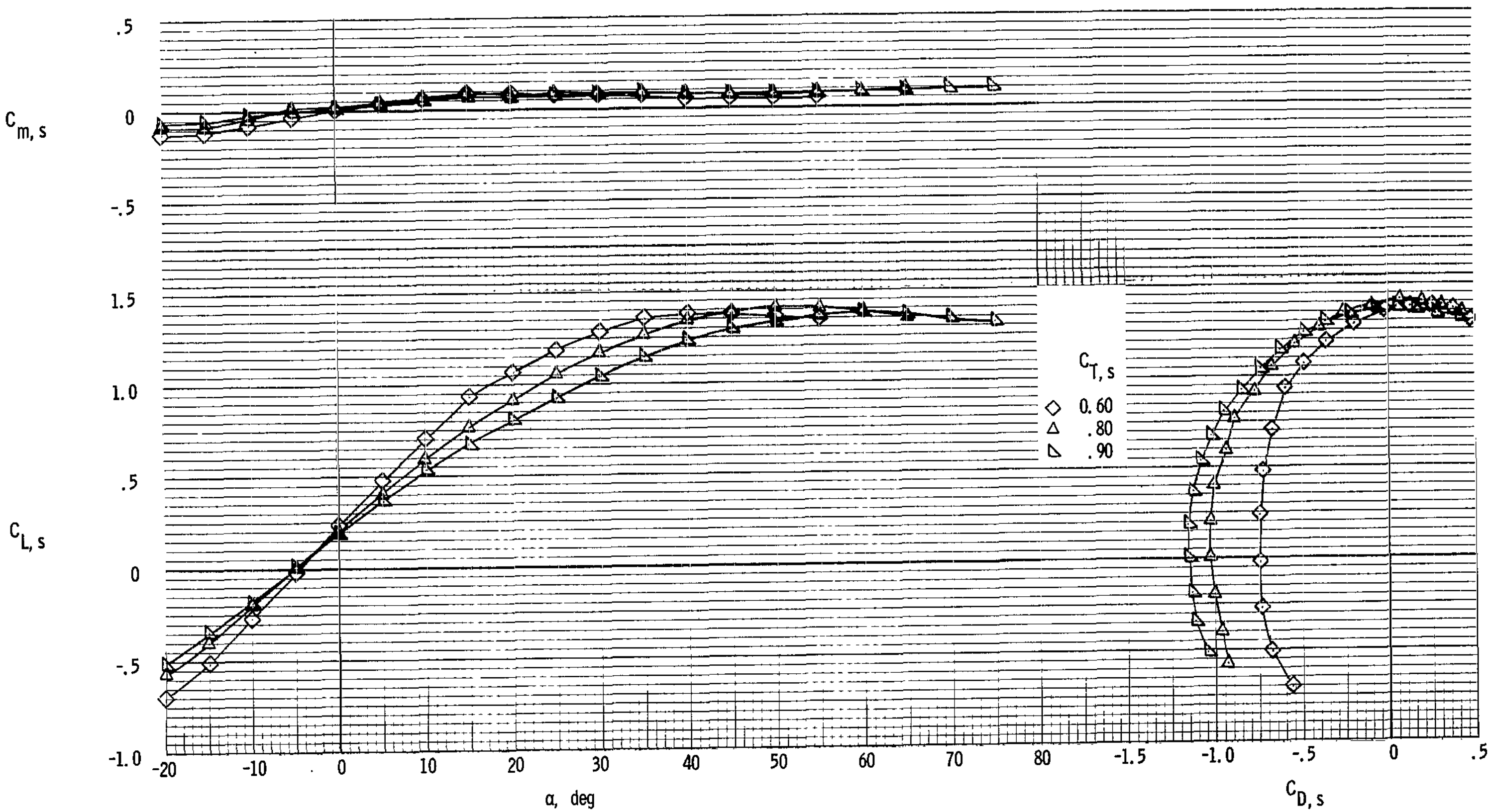

(a) Continued.

Figure 4.- Continued.

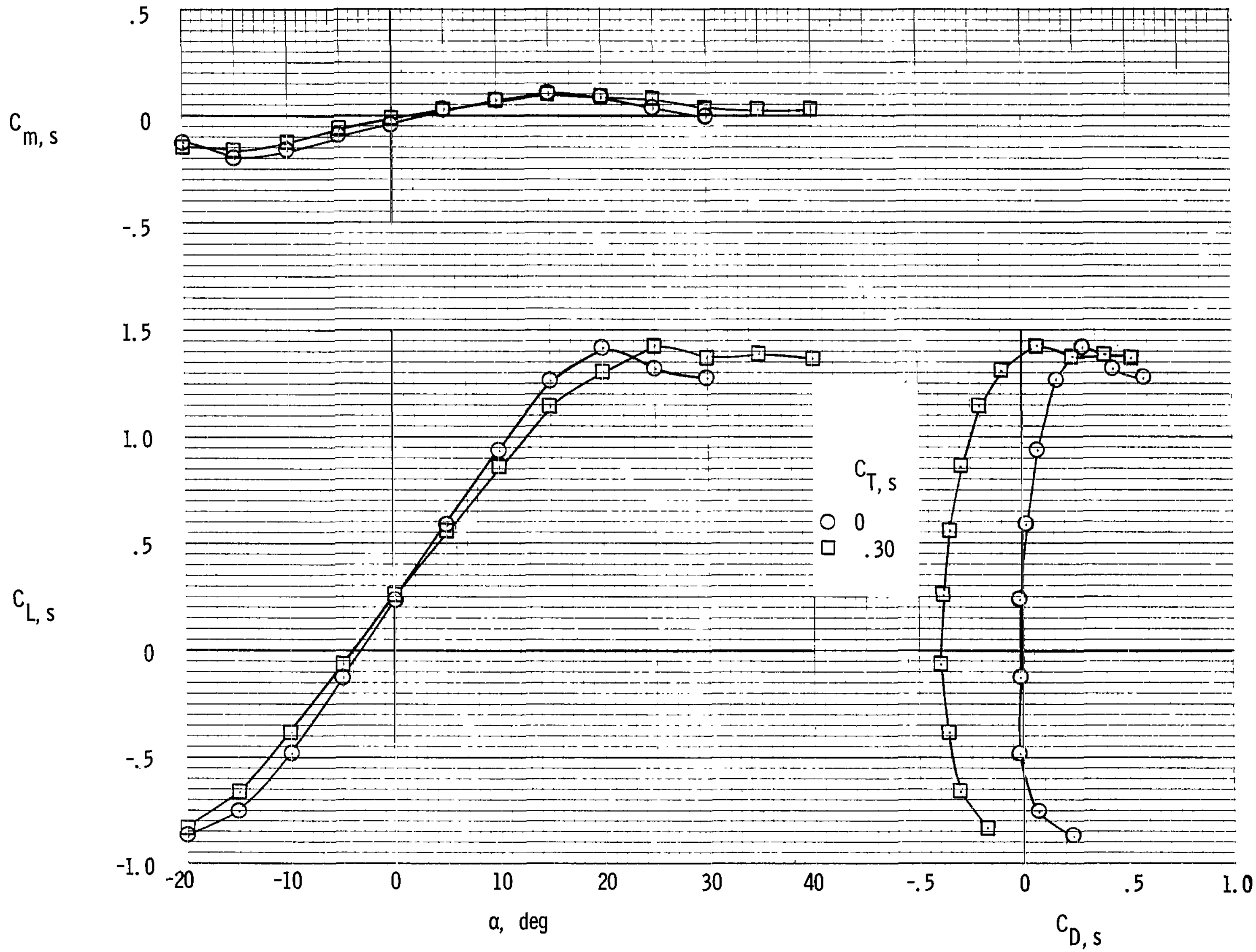

(a) Concluded.

Figure 4.- Continued.

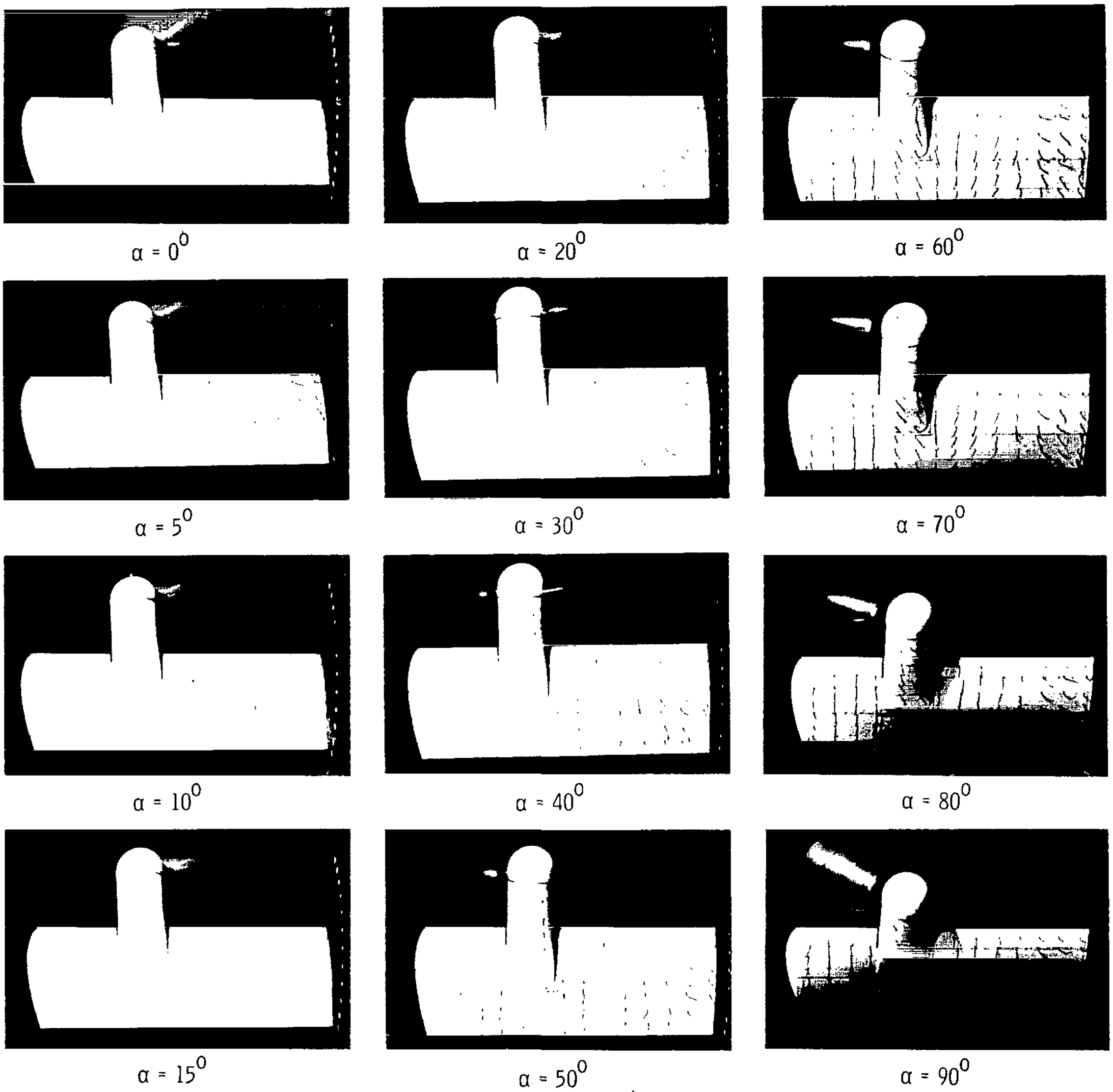

(b) Flow characteristics; $C_{T,s} = 1.00$.

L-66-1023

Figure 4.- Continued.

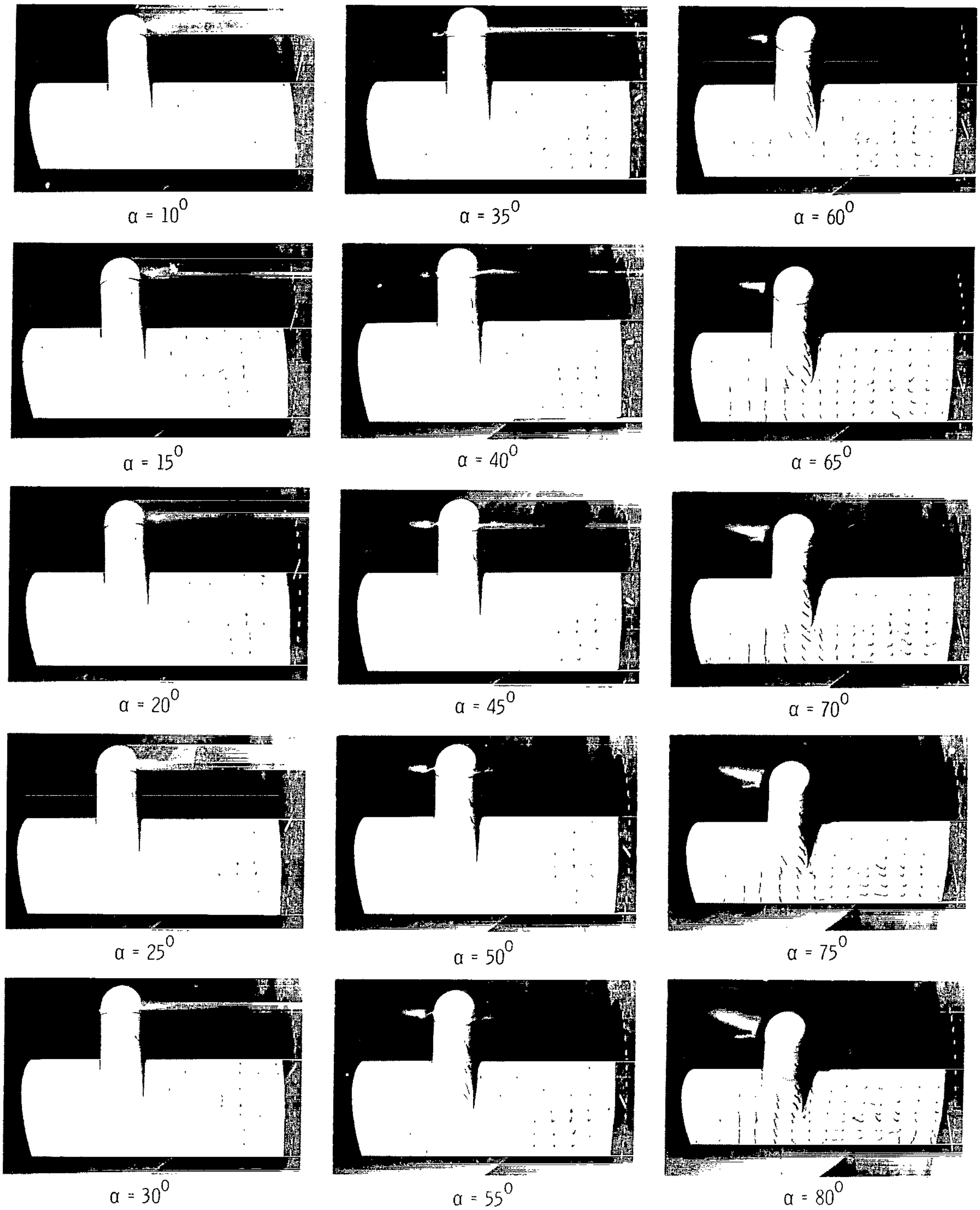

(c) Flow characteristics; $C_{T,s} = 0.95$. L-66-1024

Figure 4.- Continued.

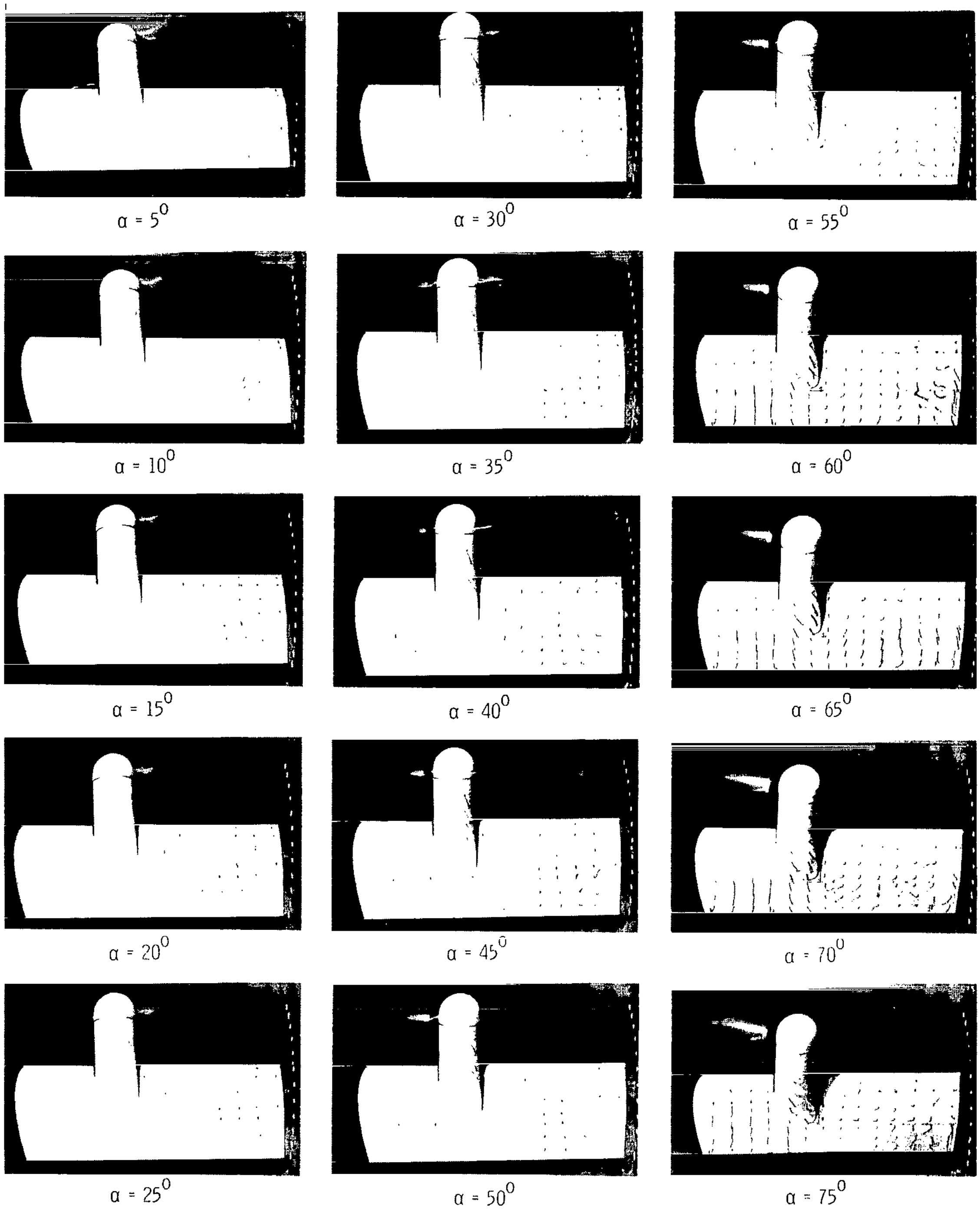

(d) Flow characteristics; $C_{T,s} = 0.90$. L-66-1025

Figure 4.- Continued.

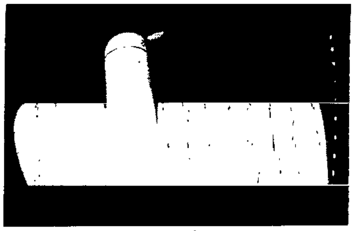

$\alpha = -5^0$

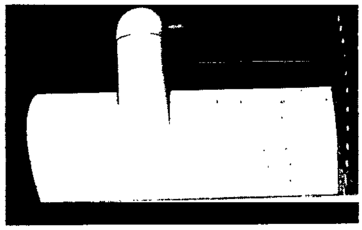

$\alpha = 20^0$

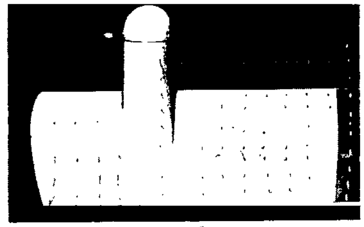

$\alpha = 45^0$

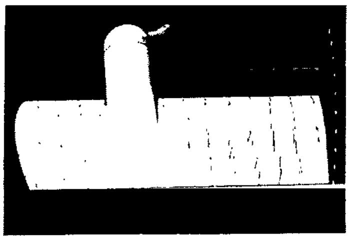

$\alpha = 0^0$

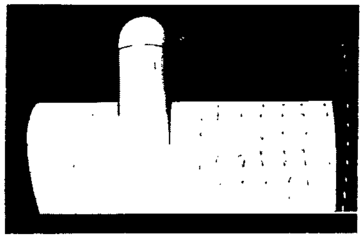

$\alpha = 25^0$

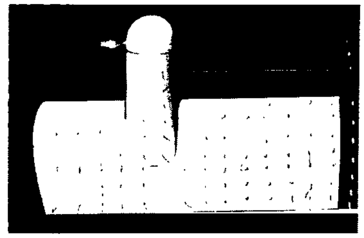

$\alpha = 50^0$

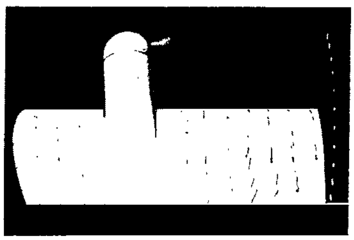

$\alpha = 5^0$

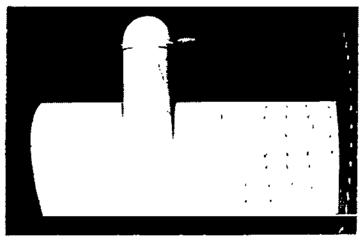

$\alpha = 30^0$

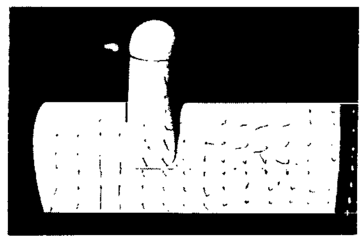

$\alpha = 55^0$

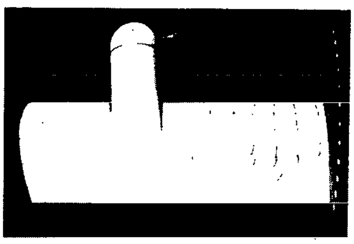

$\alpha = 10^0$

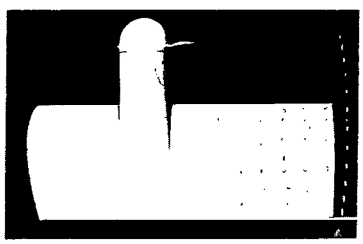

$\alpha = 35^0$

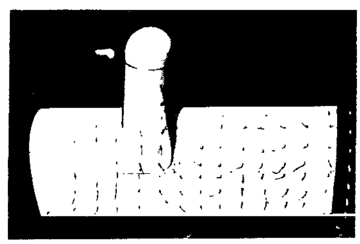

$\alpha = 60^0$

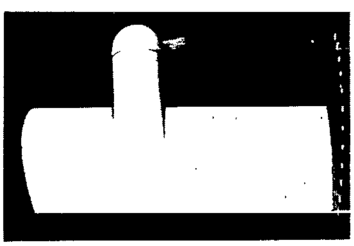

$\alpha = 15^0$

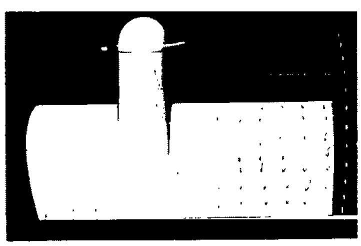

$\alpha = 40^0$

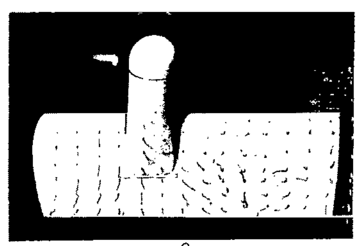

$\alpha = 65^0$

(e) Flow characteristics; $C_{T,s} = 0.80$. L-66-1026

Figure 4.- Continued.

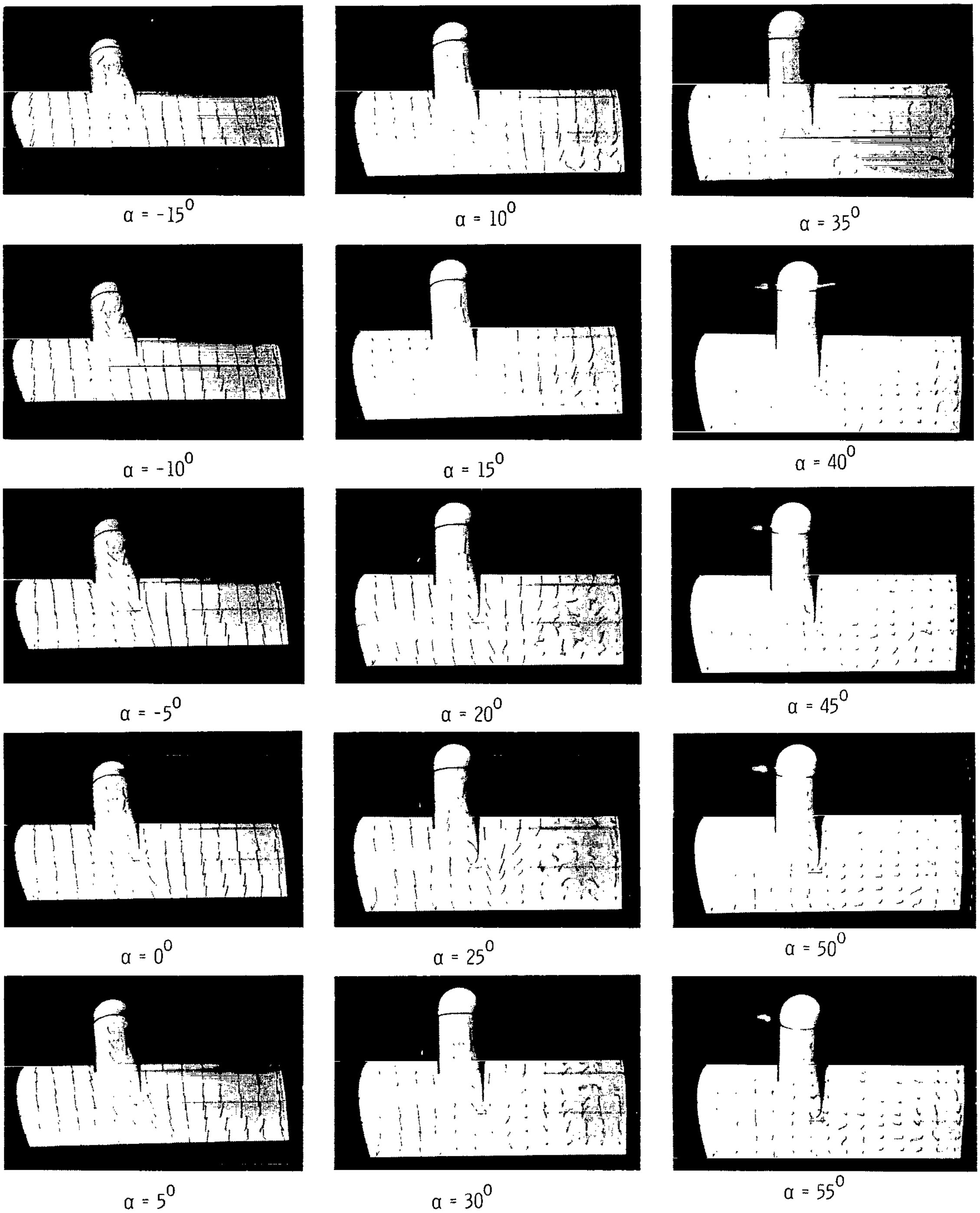

(f) Flow characteristics; $C_{T,s} = 0.60$. L-66-1027

Figure 4.- Continued.

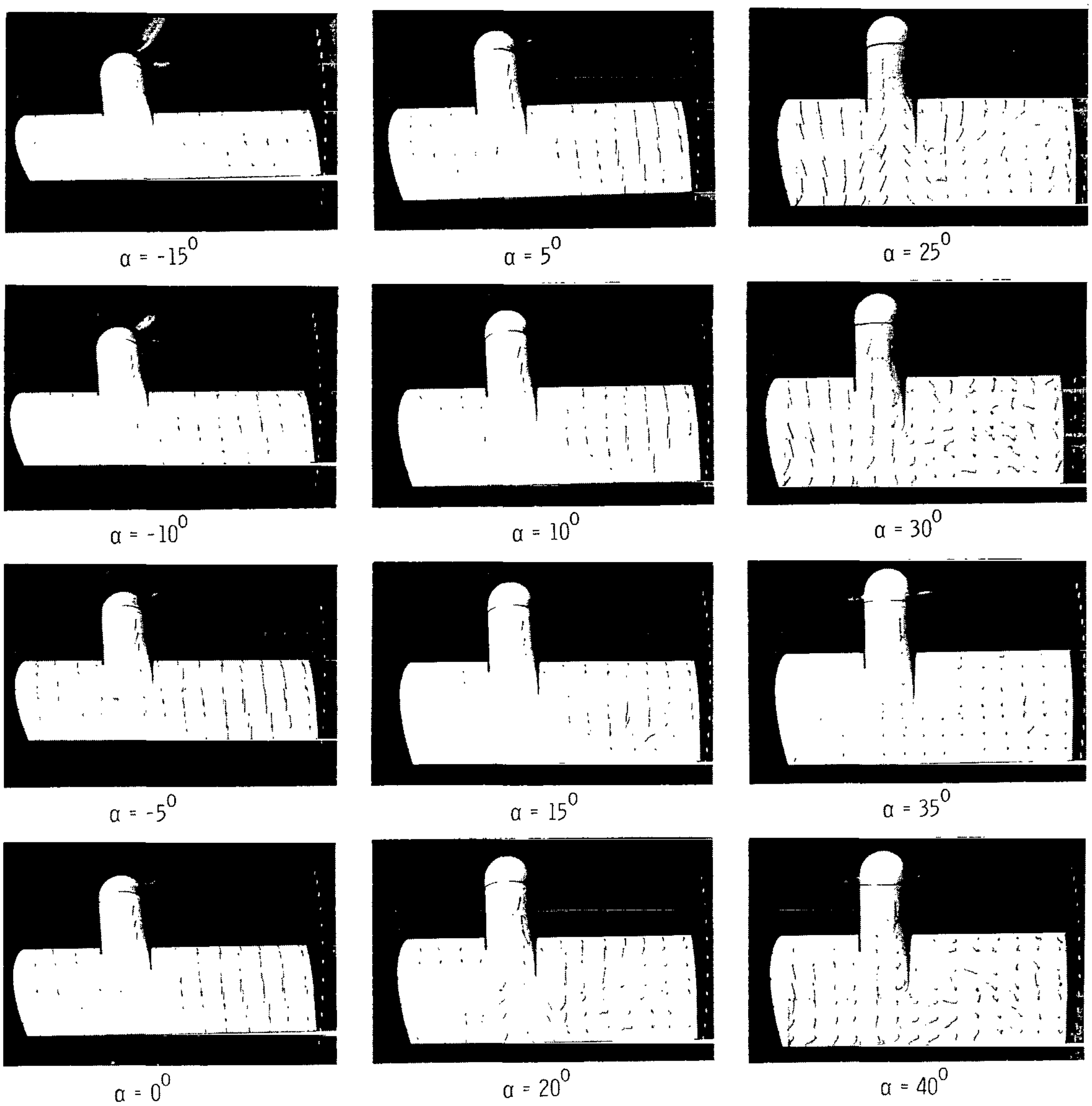

(g) Flow characteristics; $C_{T,s} = 0.30$. L-66-1028

Figure 4.- Continued.

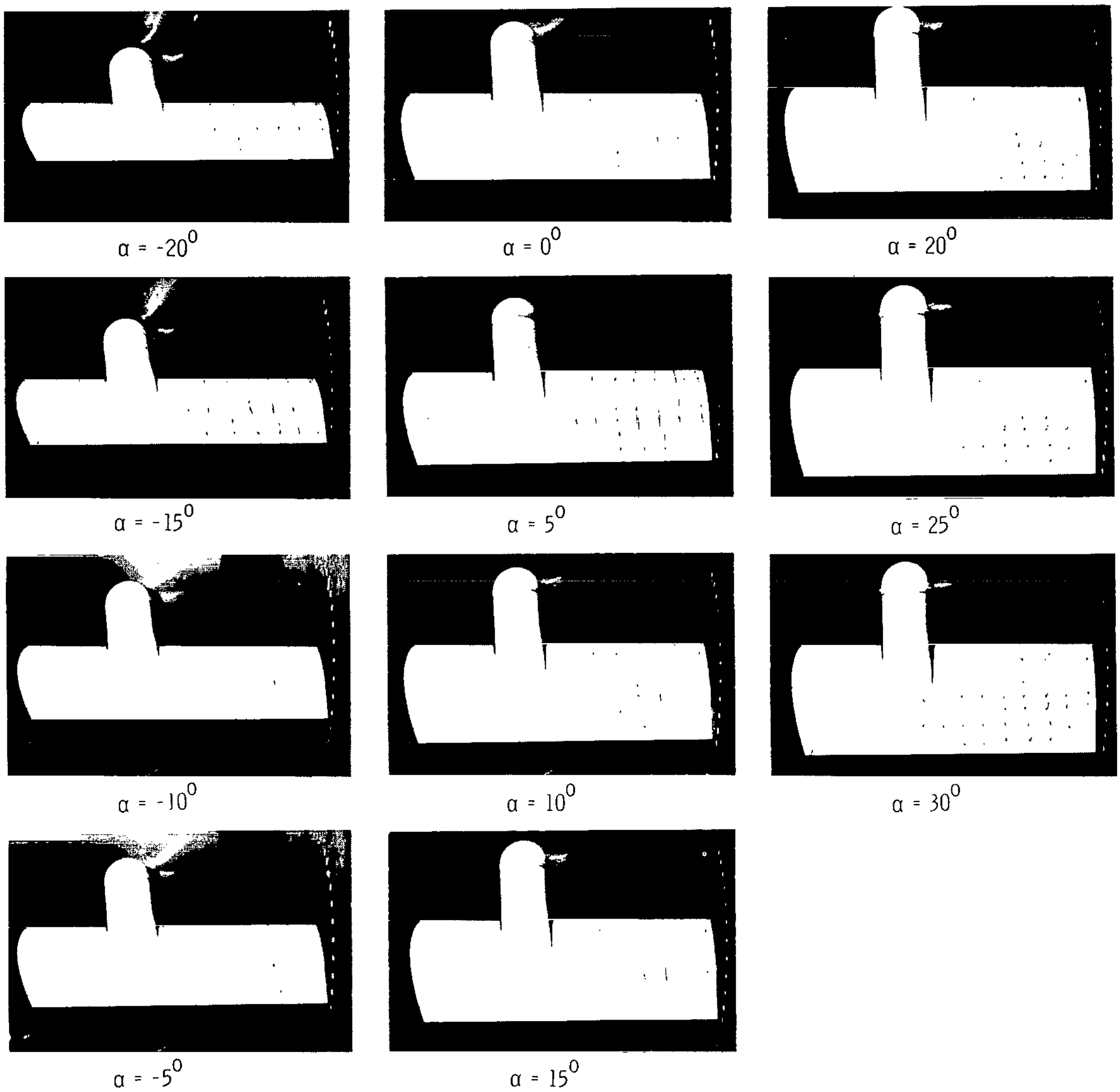

(h) Flow characteristics; $C_{T,s} = 0$. L-66-1029

Figure 4.- Concluded.

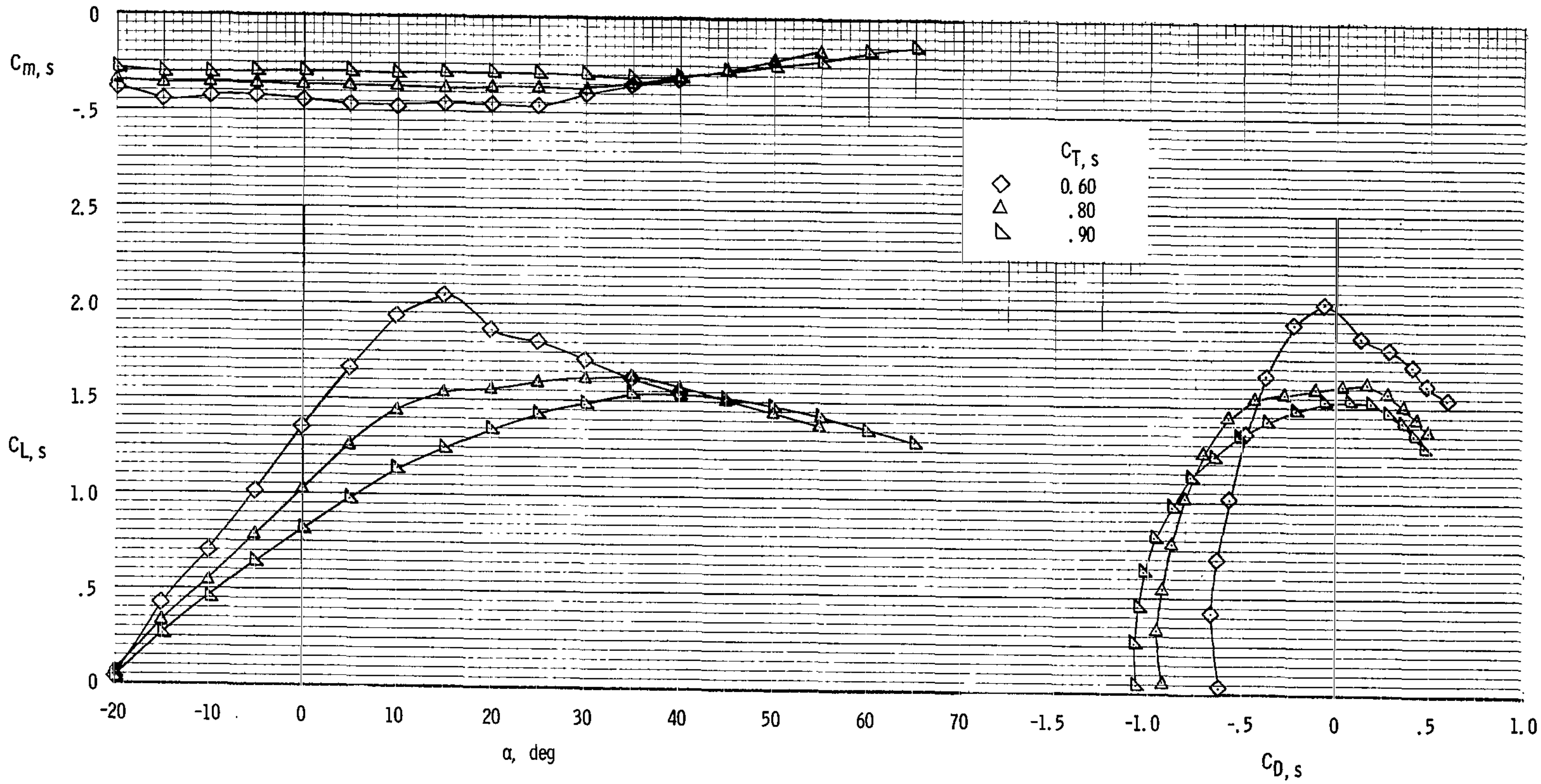

(a) Aerodynamic characteristics.

Figure 5.- Aerodynamic and flow characteristics of model with basic leading edge and with trailing-edge flap deflected 40°. Down-at-tip rotation.

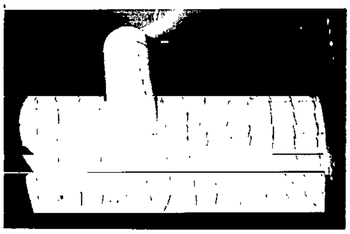

$\alpha = -5^0$

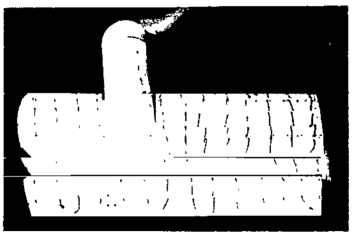

$\alpha = 0^0$

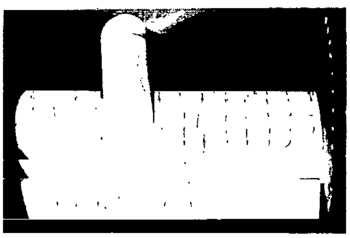

$\alpha = 5^0$

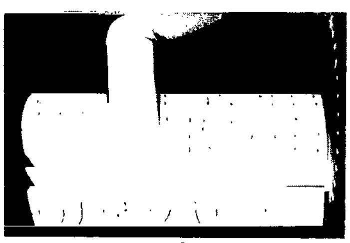

$\alpha = 10^0$

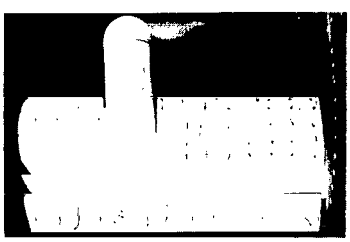

$\alpha = 15^0$

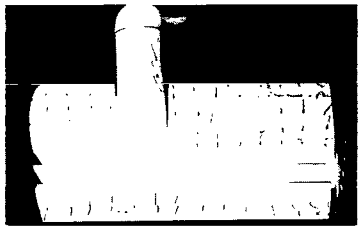

$\alpha = 20^0$

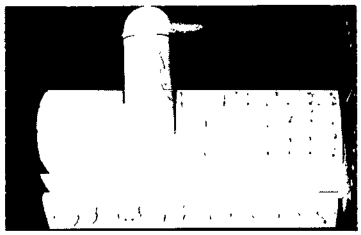

$\alpha = 25^0$

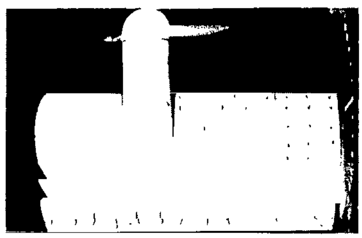

$\alpha = 30^0$

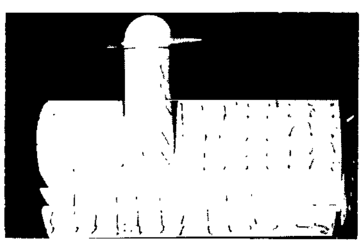

$\alpha = 35^0$

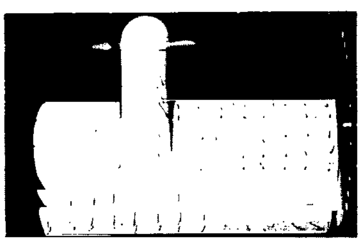

$\alpha = 40^0$

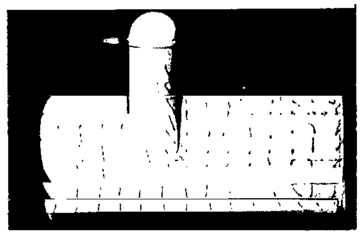

$\alpha = 45^0$

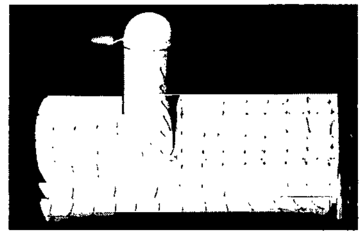

$\alpha = 50^0$

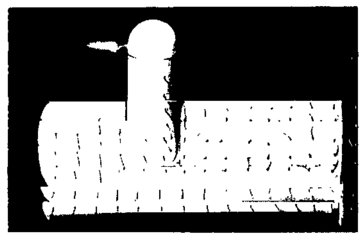

$\alpha = 55^0$

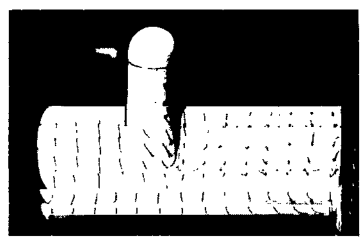

$\alpha = 60^0$

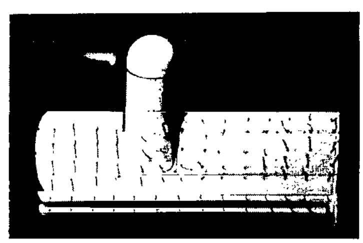

$\alpha = 65^0$

(b) Flow characteristics; $C_{T,s} = 0.90$. L-66-1030

Figure 5.- Continued.

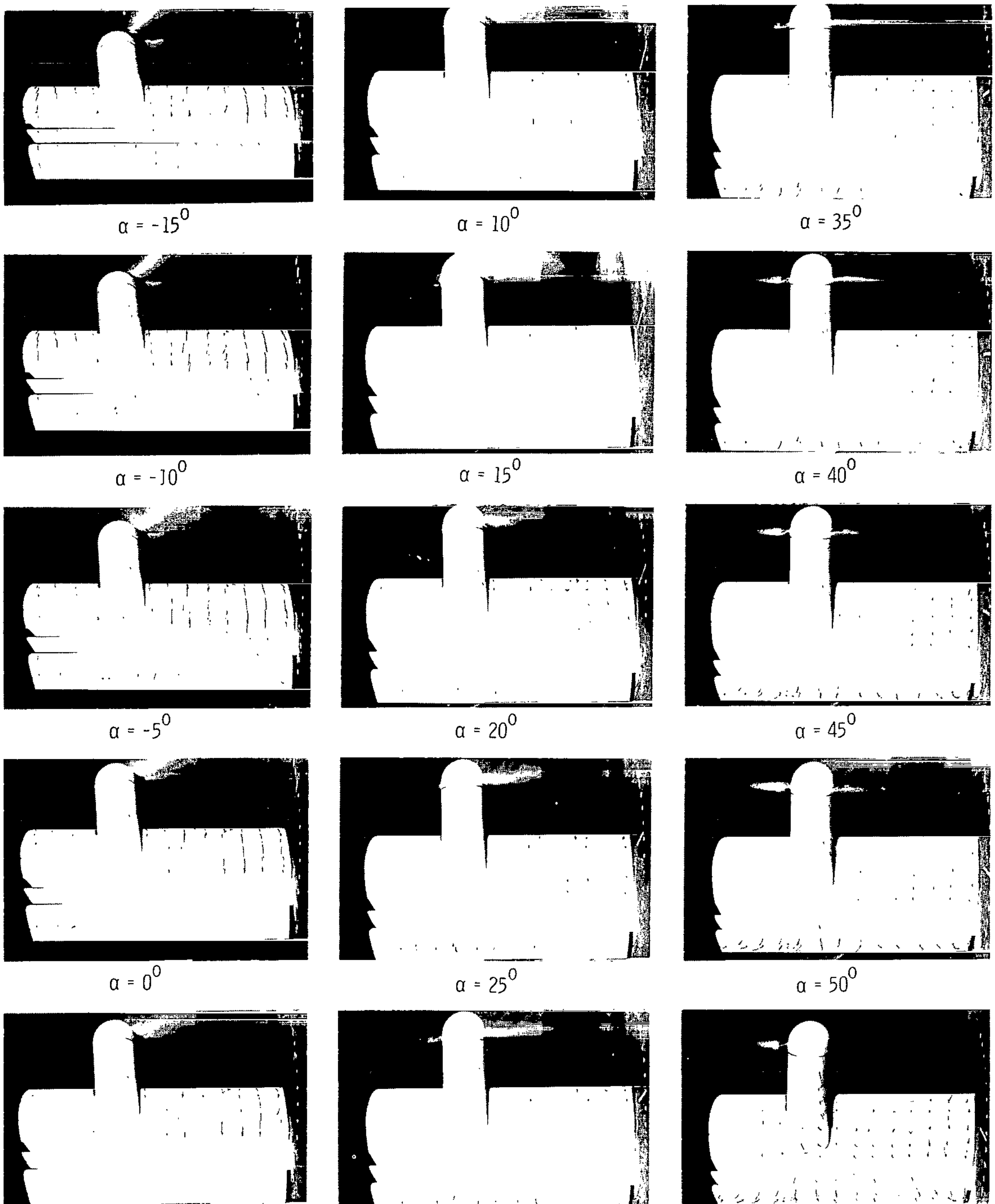

$\alpha = -15^0$ $\alpha = 10^0$ $\alpha = 35^0$

$\alpha = -10^0$ $\alpha = 15^0$ $\alpha = 40^0$

$\alpha = -5^0$ $\alpha = 20^0$ $\alpha = 45^0$

$\alpha = 0^0$ $\alpha = 25^0$ $\alpha = 50^0$

$\alpha = 5^0$ $\alpha = 30^0$ $\alpha = 55^0$

(c) Flow characteristics; $C_{T,s} = 0.80$. L-66-1031

Figure 5.- Continued.

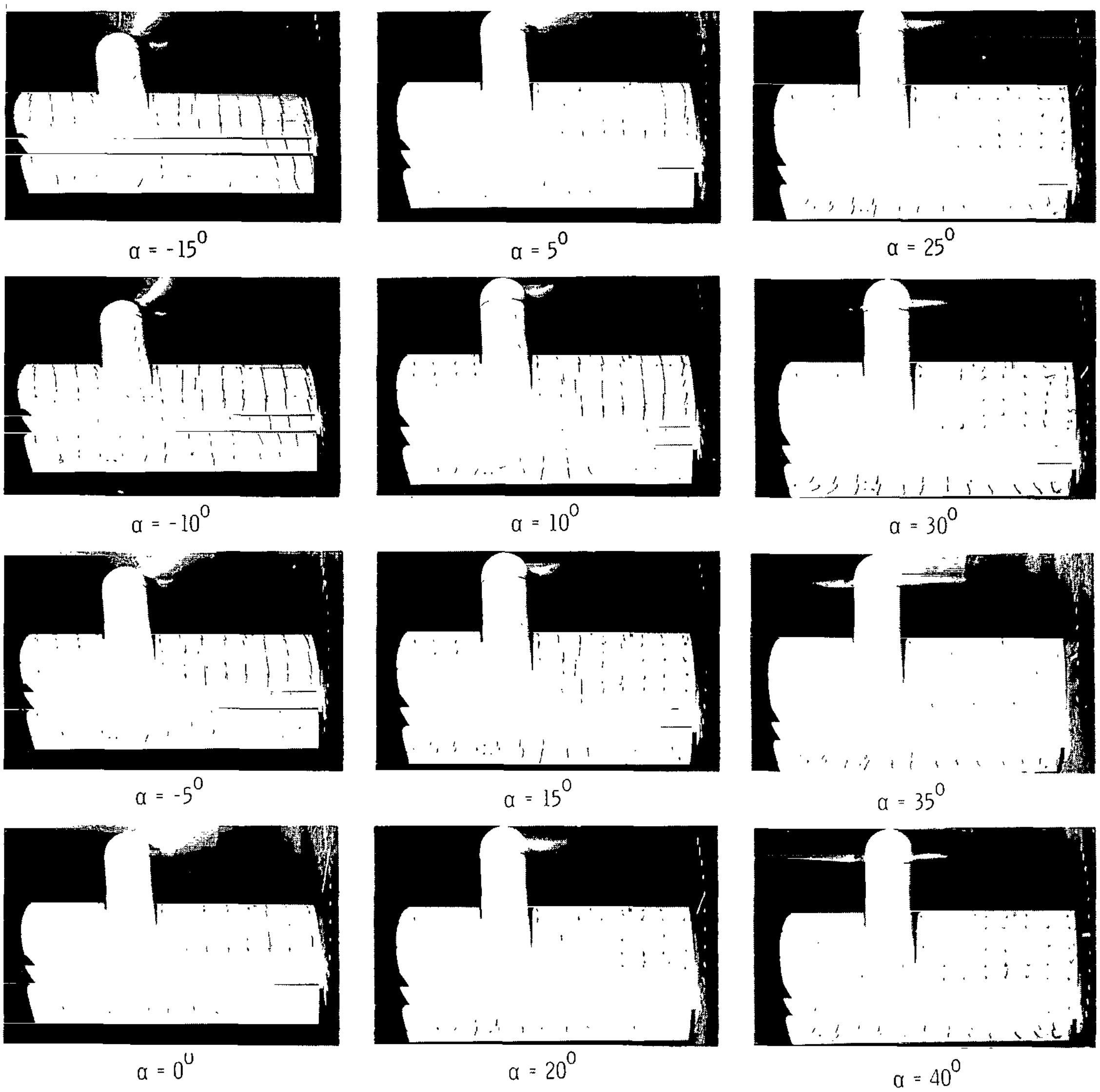

(d) Flow characteristics; $C_{T,s} = 0.60$. L-66-1032

Figure 5.- Concluded.

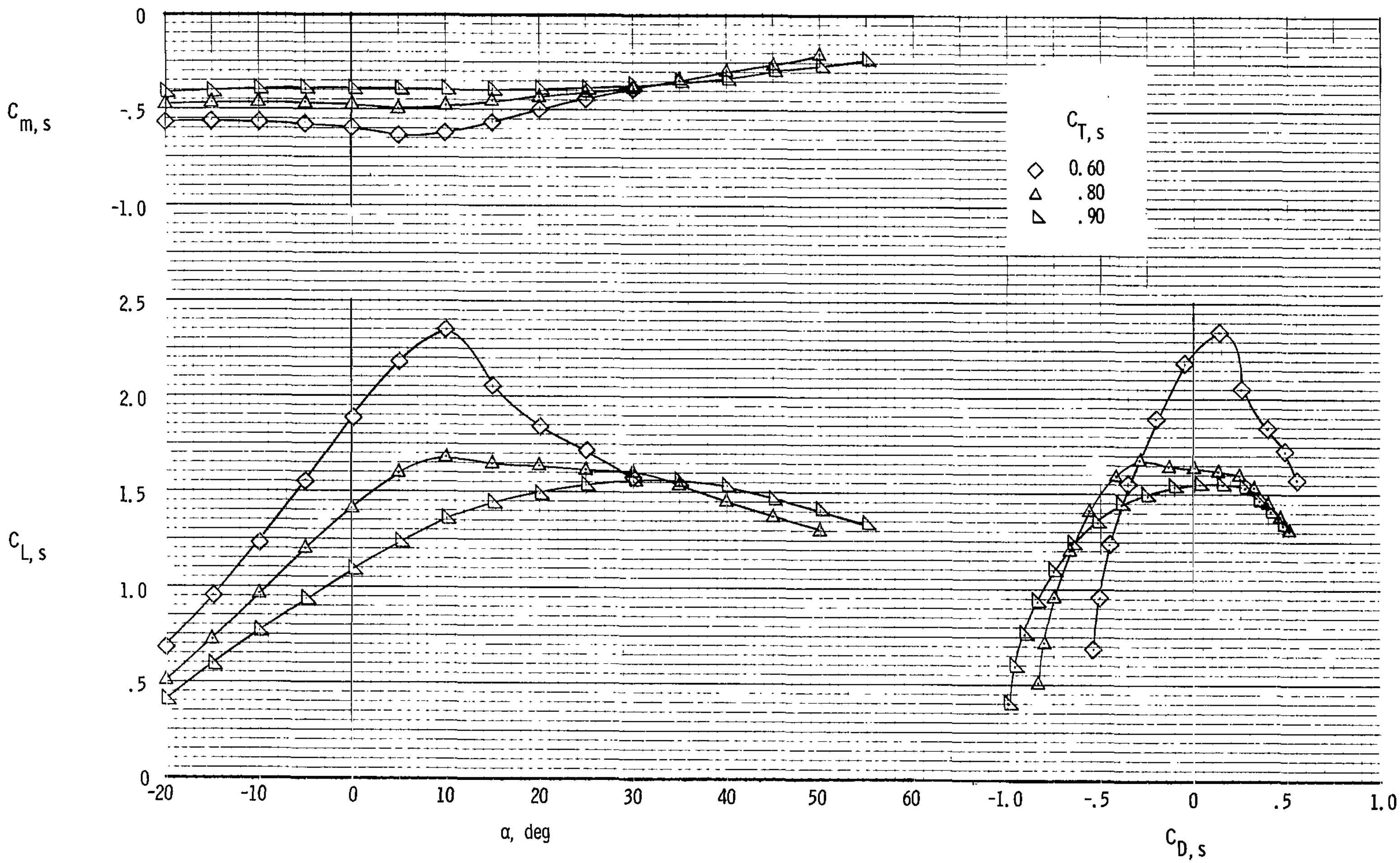

(a) Aerodynamic characteristics.

Figure 6.- Aerodynamic and flow characteristics of the model with basic leading edge and with trailing-edge flap deflected 60°. Down-at-tip rotation.

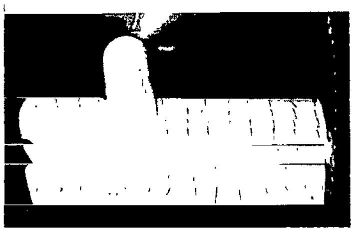

$\alpha = -15^0$

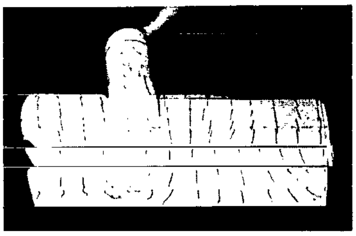

$\alpha = -10^0$

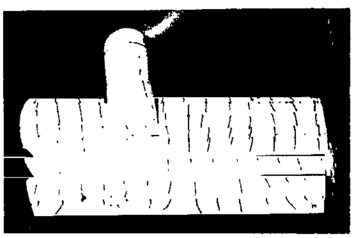

$\alpha = -5^0$

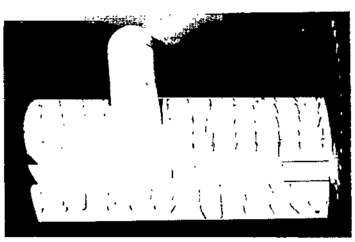

$\alpha = 0^0$

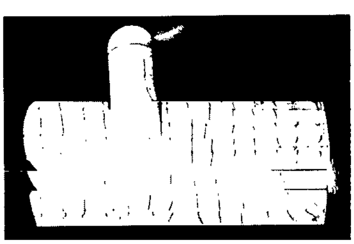

$\alpha = 5^0$

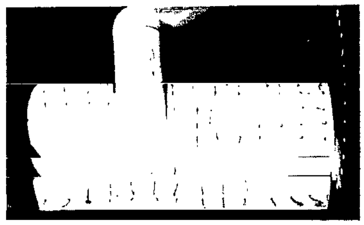

$\alpha = 10^0$

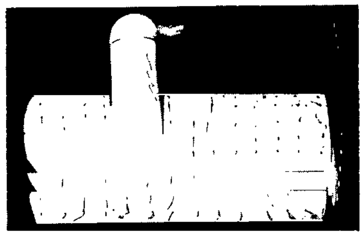

$\alpha = 15^0$

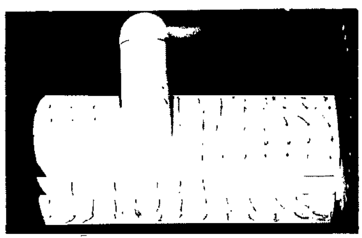

$\alpha = 20^0$

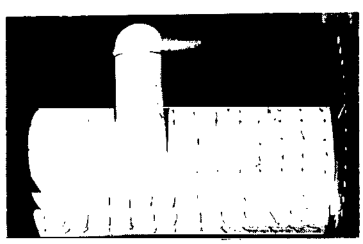

$\alpha = 25^0$

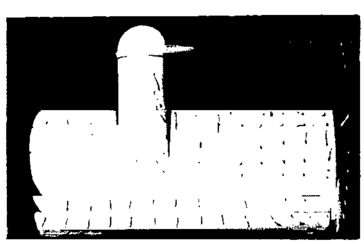

$\alpha = 30^0$

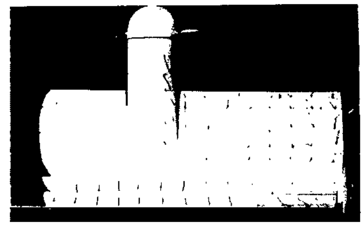

$\alpha = 35^0$

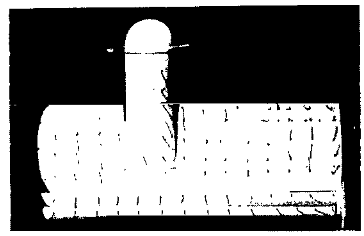

$\alpha = 40^0$

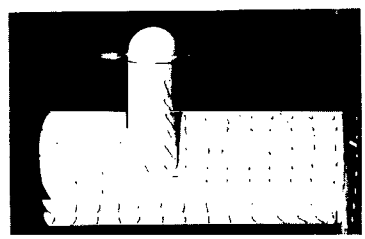

$\alpha = 45^0$

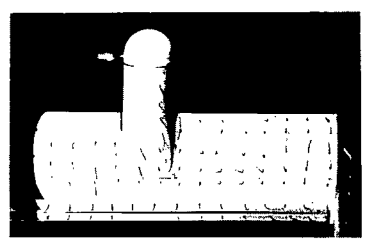

$\alpha = 50^0$

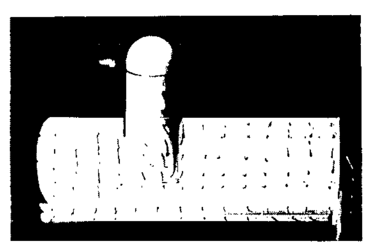

$\alpha = 55^0$

(b) Flow characteristics; $C_{T,s} = 0.90$. L-66-1033

Figure 6.- Continued.

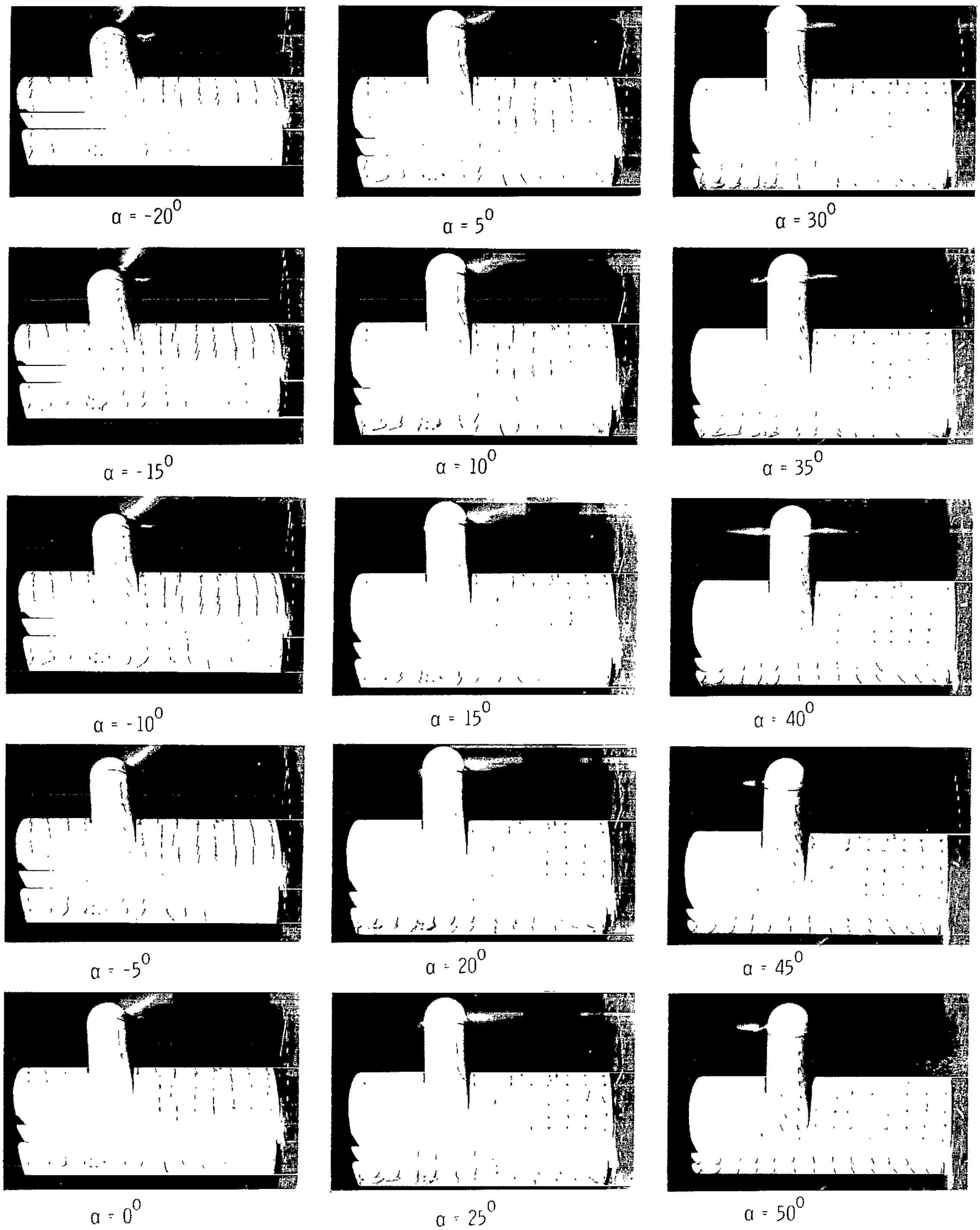

(c) Flow characteristics; $C_{T,s} = 0.80$. L-66-1034

Figure 6.- Continued.

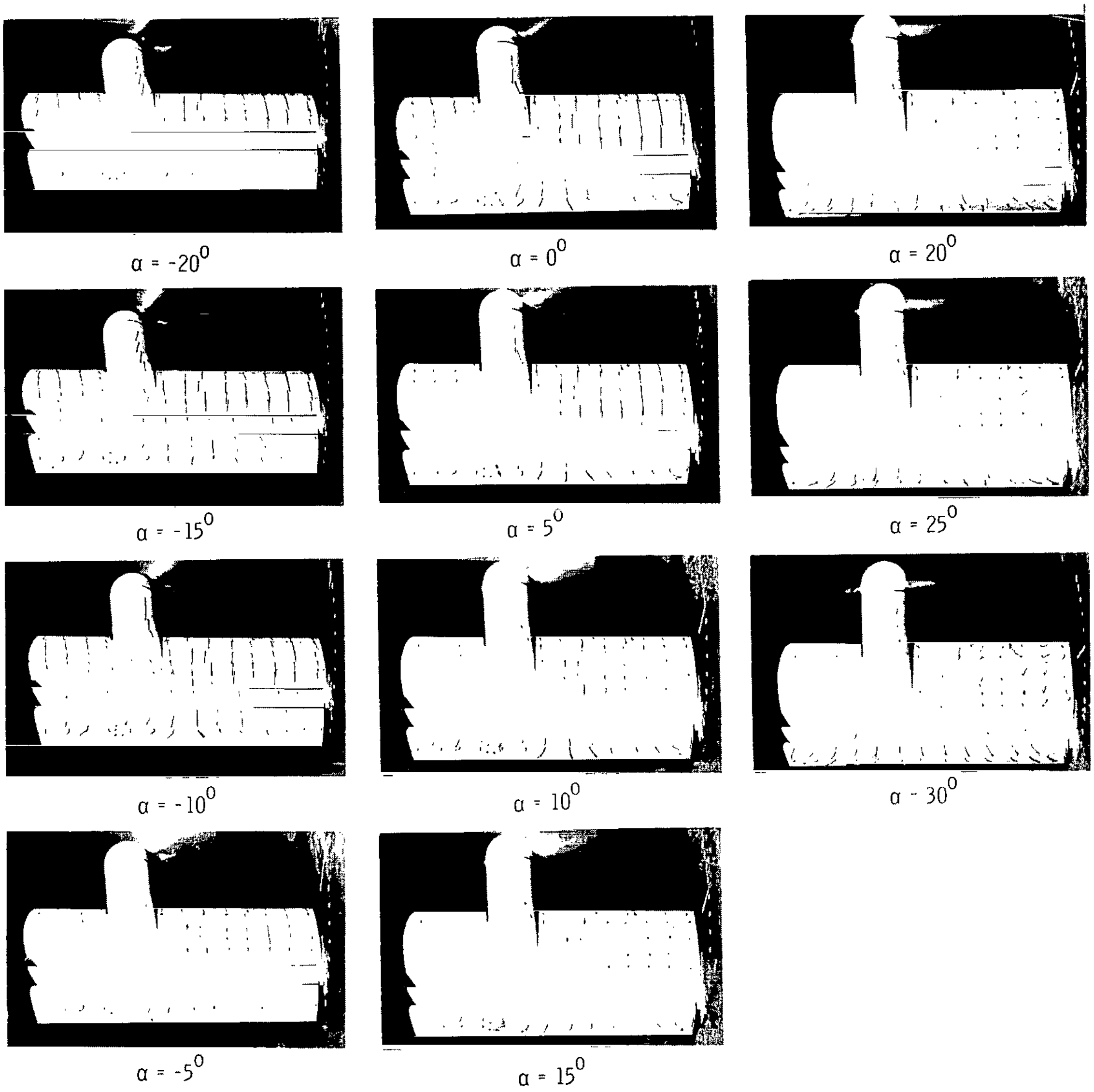

(d) Flow characteristics; $C_{T,s} = 0.60$. L-66-1035

Figure 6.- Concluded.

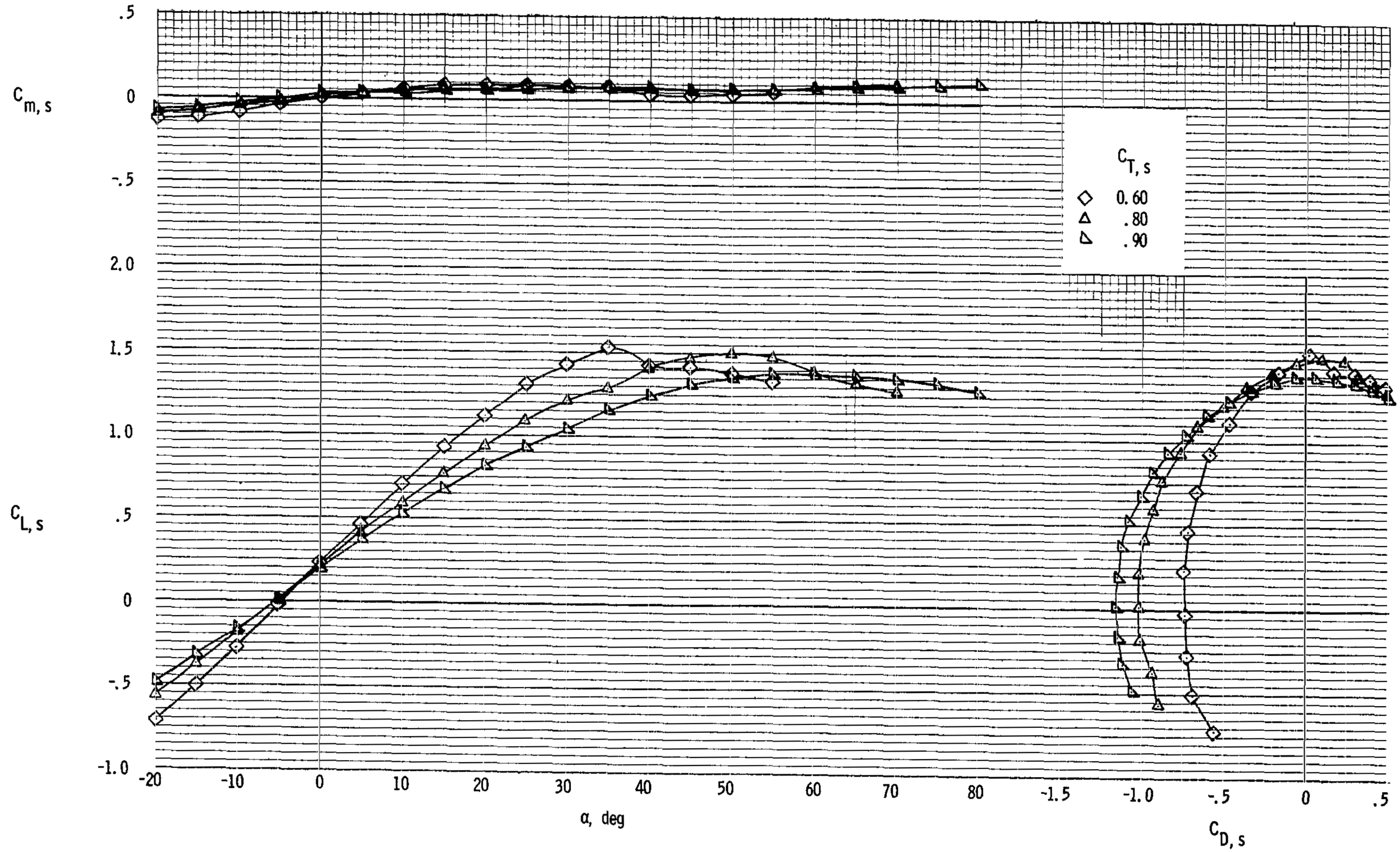

(a) Aerodynamic characteristics.

Figure 7.- Aerodynamic and flow characteristics of model with basic leading edge and with trailing-edge flap undeflected. $\delta_f = 0^o$. Fences on. Down-at-tip rotation.

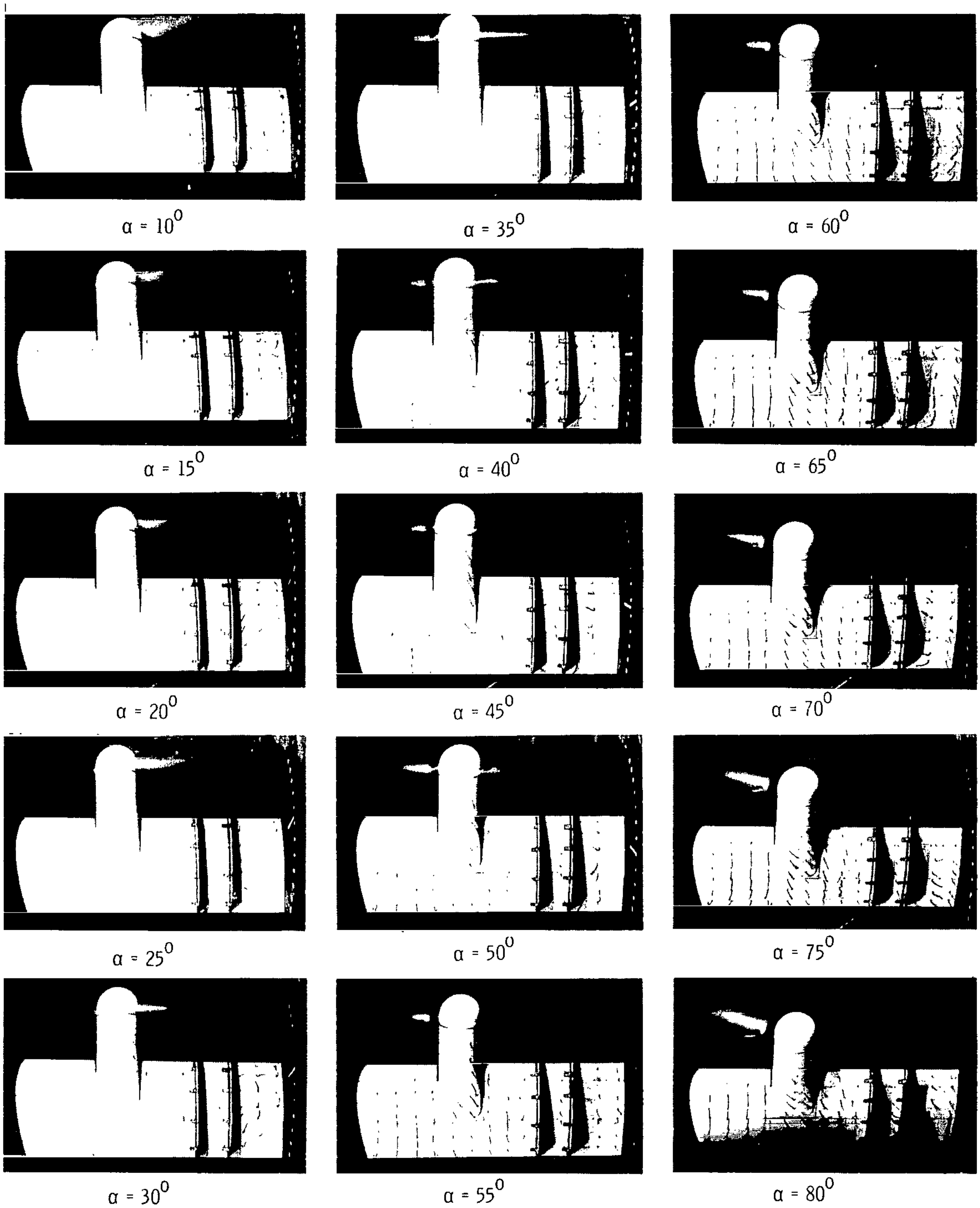

(b) Flow characteristics; $C_{T,s} = 0.90$.

L-66-1036

Figure 7.- Continued.

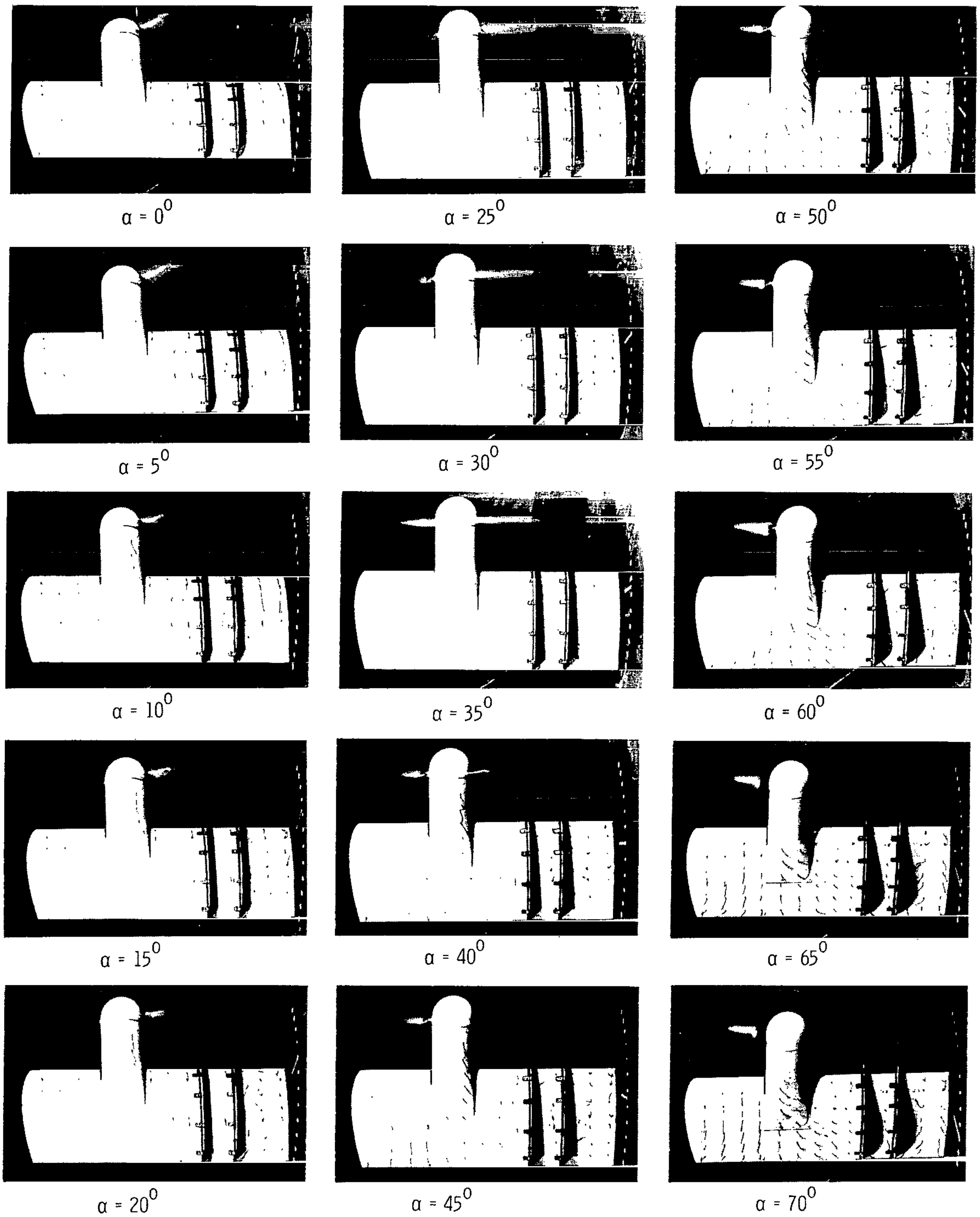

(c) Flow characteristics; $C_{T,s} = 0.80$.

L-66-1037

Figure 7.- Continued.

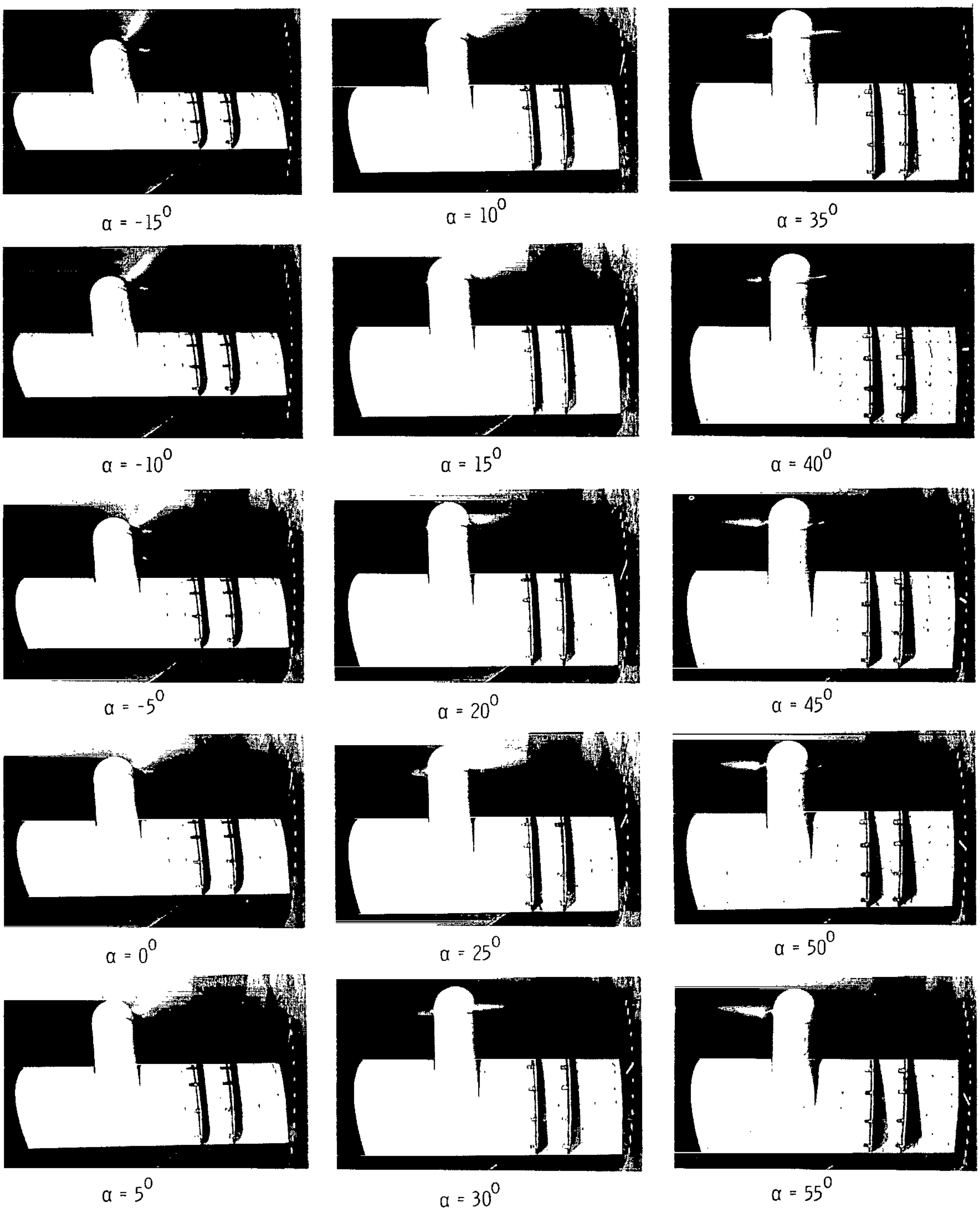

(d) Flow characteristics; $C_{T,s} = 0.60$. L-66-1038

Figure 7.- Concluded.

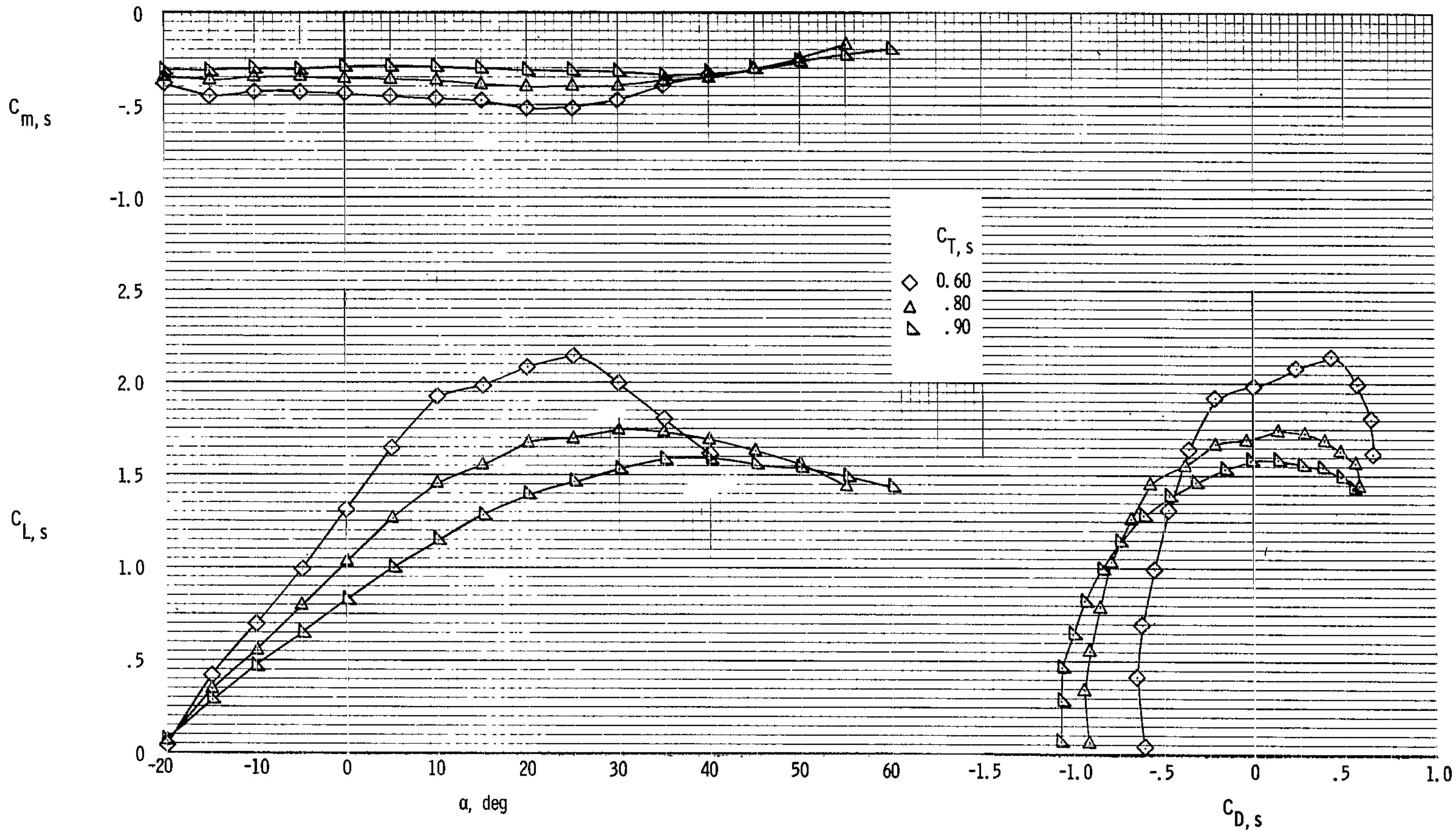

(a) Aerodynamic characteristics.

Figure 8.- Aerodynamic and flow characteristics of model with basic leading edge and with trailing-edge flap deflected 40°. Fences on. Down-at-tip rotation.

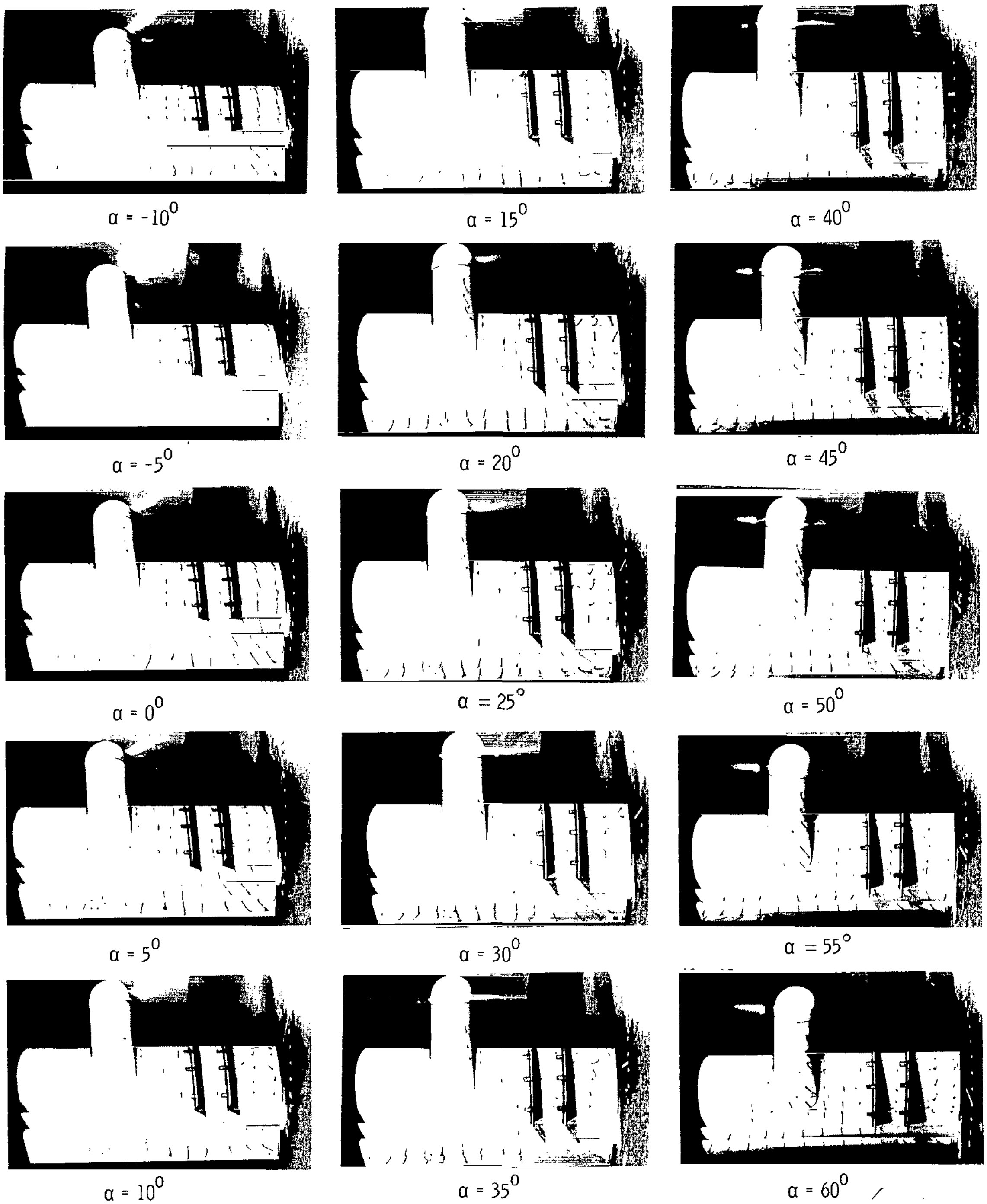

(b) Flow characteristics; $C_{T,s} = 0.90$. L-66-1039

Figure 8.- Continued.

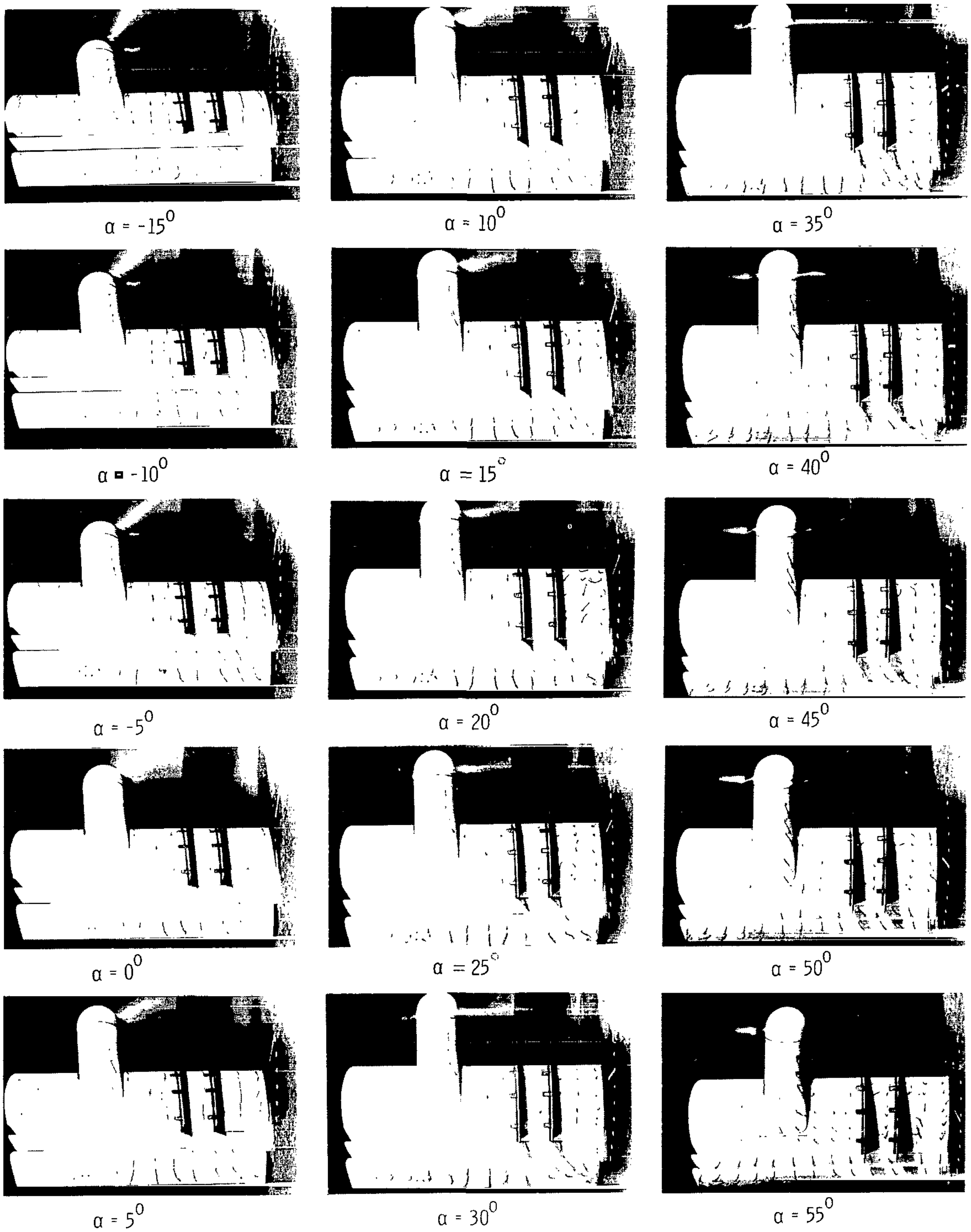

(c) Flow characteristics; $C_{T,s} = 0.80$.

L-66-1040

Figure 8.- Continued.

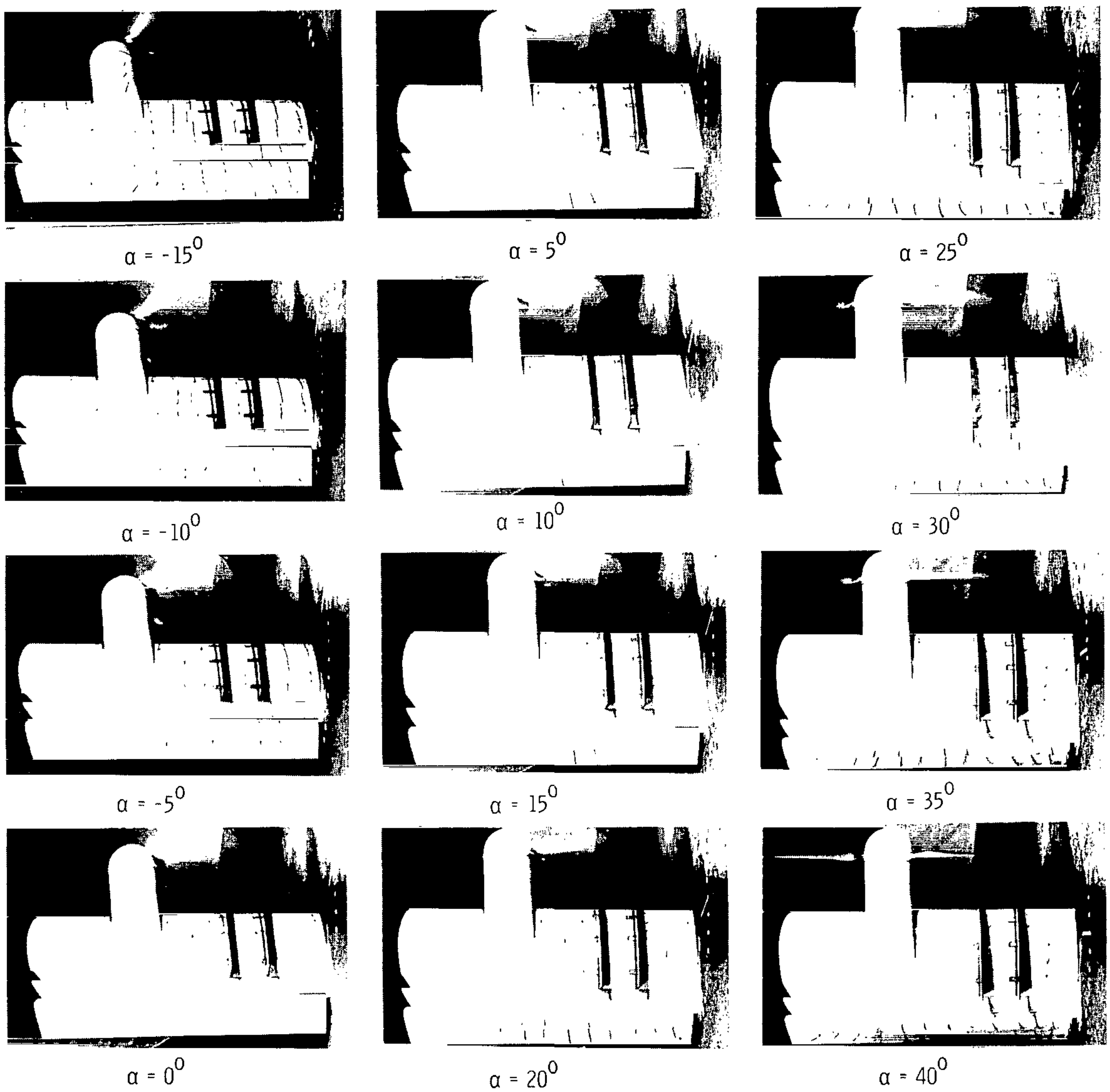

(d) Flow characteristics; $C_{T,s} = 0.60$.

L-66-1041

Figure 8.- Concluded.

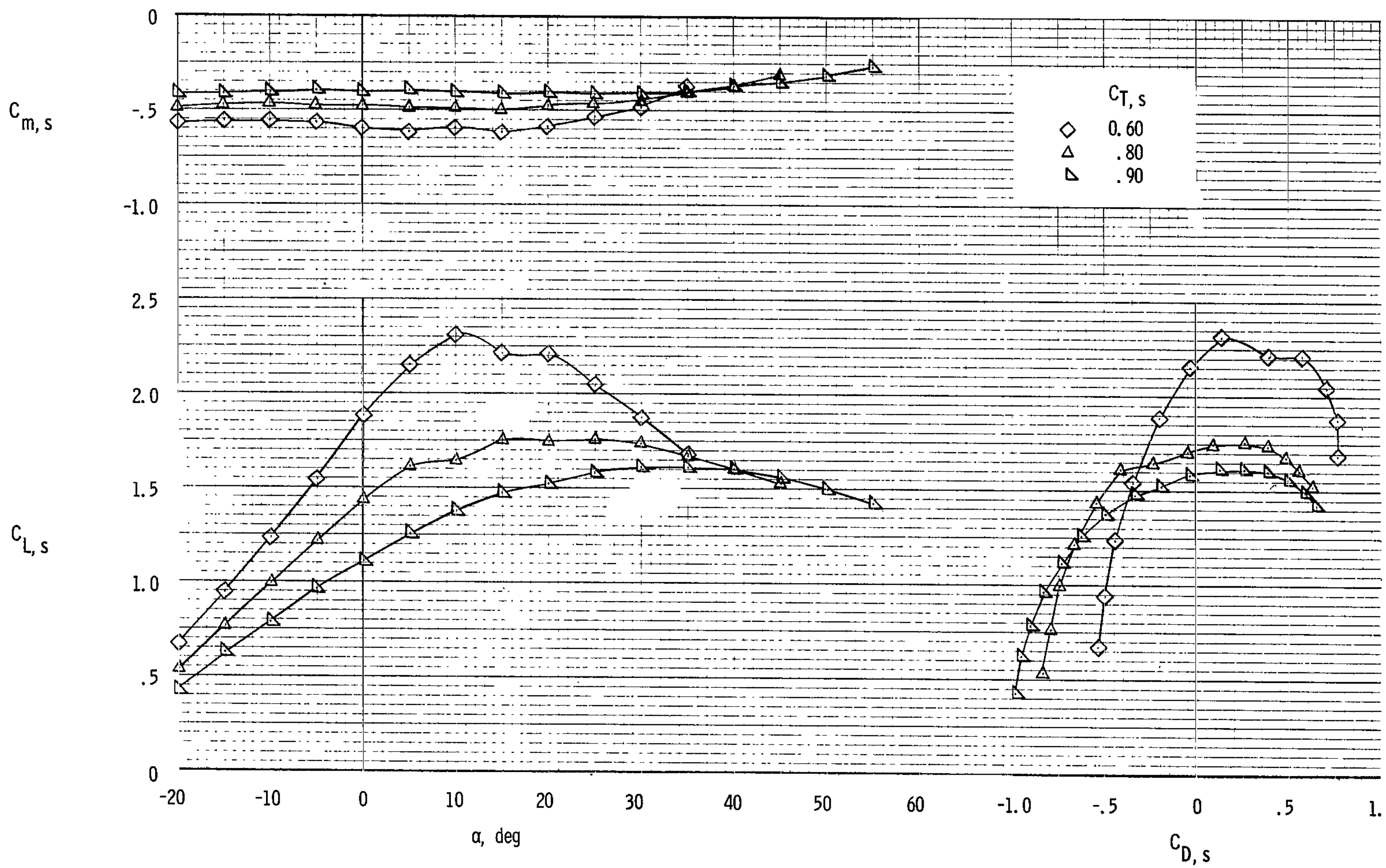

(a) Aerodynamic characteristics.

Figure 9.- Aerodynamic and flow characteristics of model with basic leading edge and with trailing-edge flap deflected 60°. Fences on. Down-at-tip rotation.

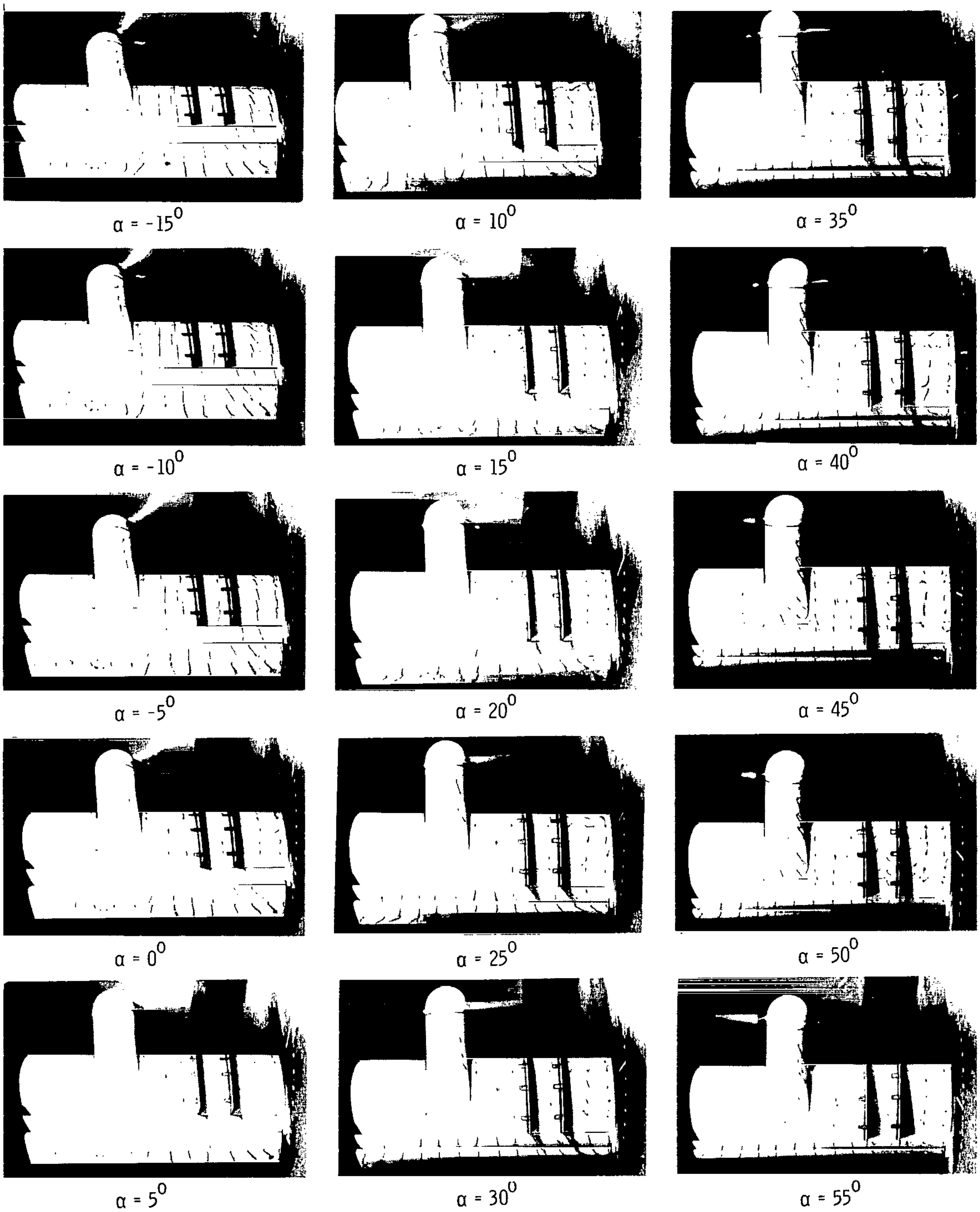

(b) Flow characteristics; $C_{T,s} = 0.90$.

L-66-1042

Figure 9.- Continued.

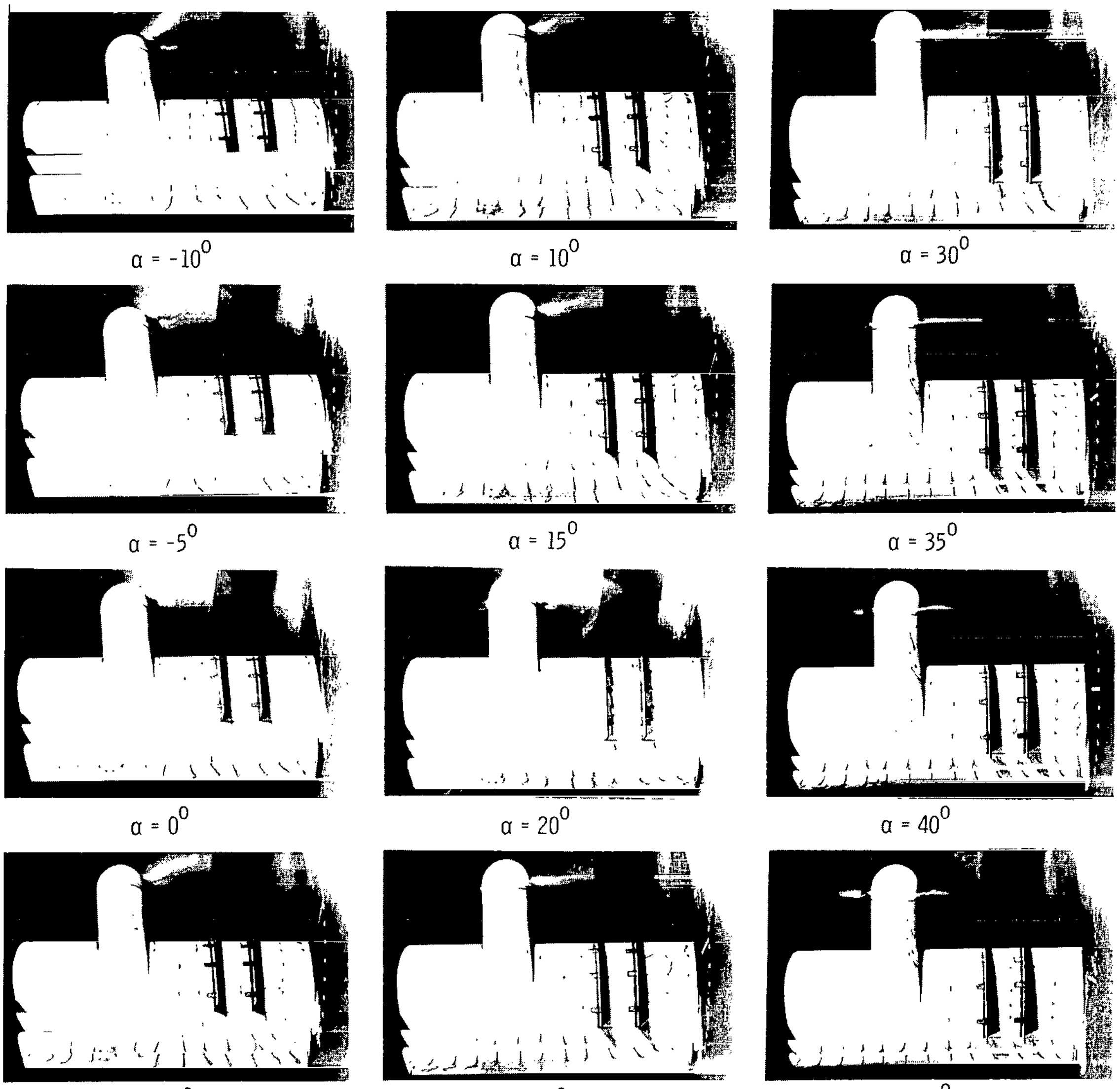

(c) Flow characteristics; $C_{T,s} = 0.80$. L-66-1043

Figure 9.- Continued.

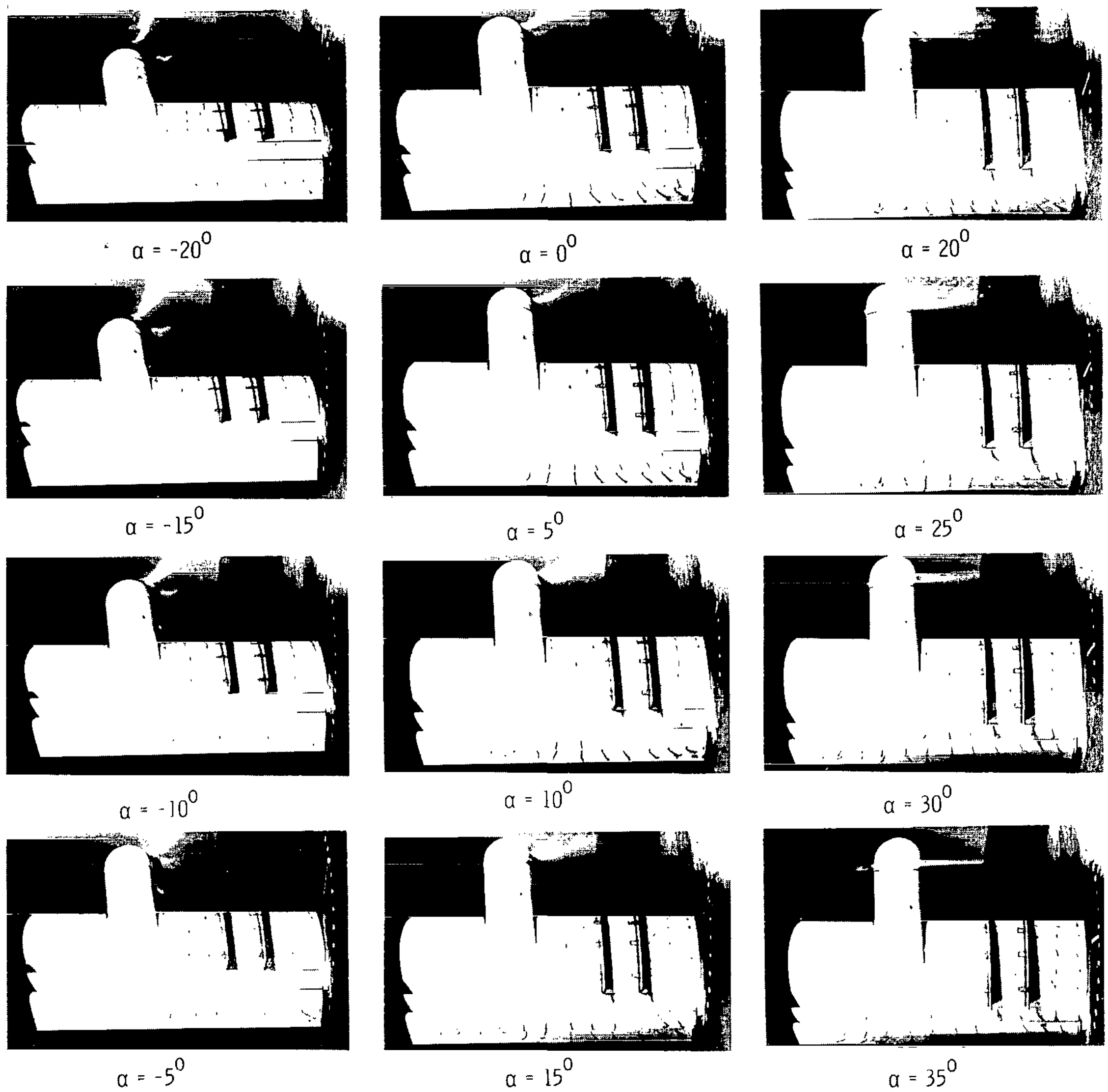

(d) Flow characteristics; $C_{T,s} = 0.60$. L-66-1044

Figure 9.- Concluded.

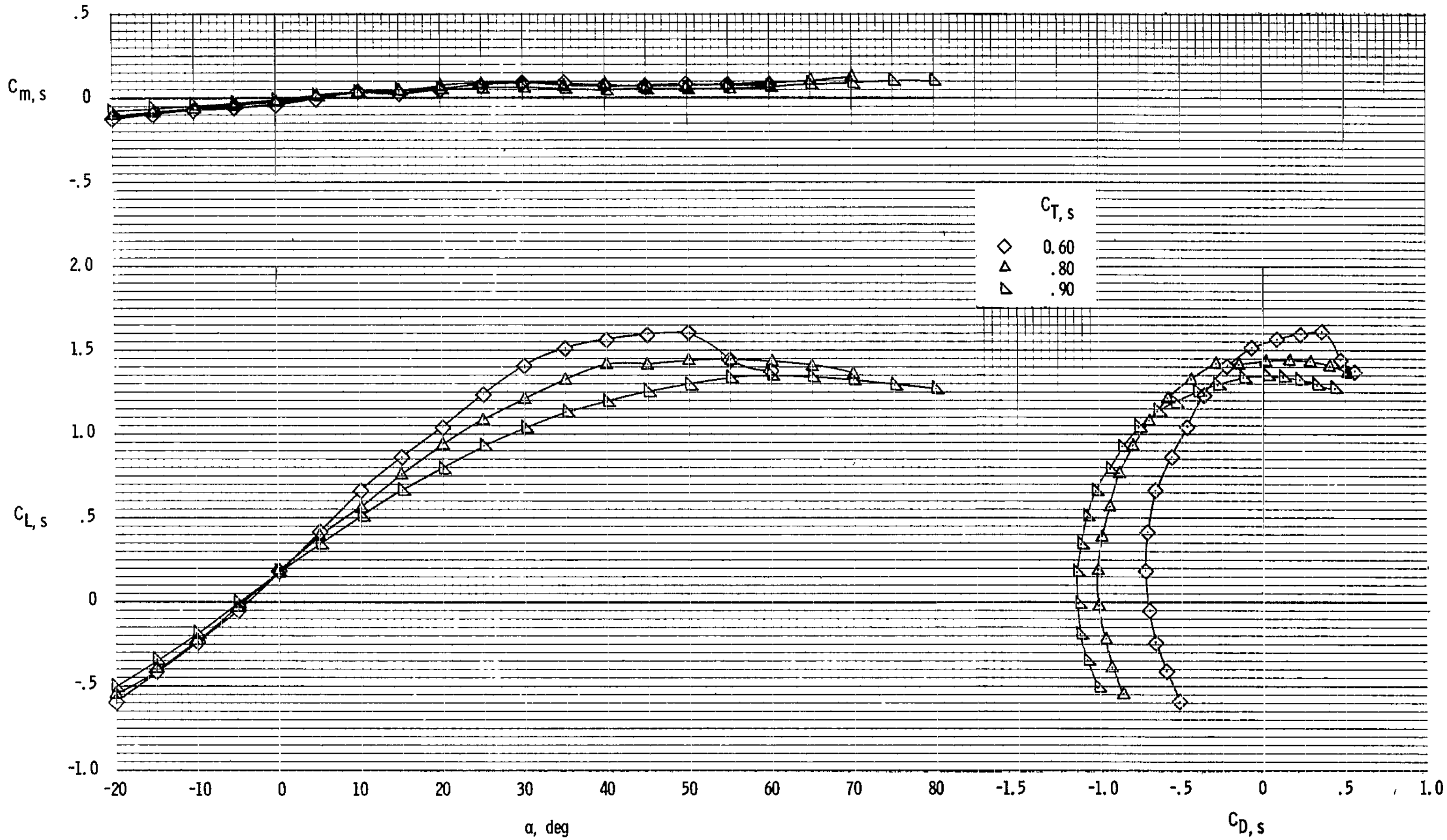

(a) Aerodynamic characteristics.

Figure 10.- Aerodynamic and flow characteristics of model with inboard section of slat deflected 30^{0} and with trailing-edge flap undeflected. $\delta_f = 0^{0}$. Down-at-tip rotation.

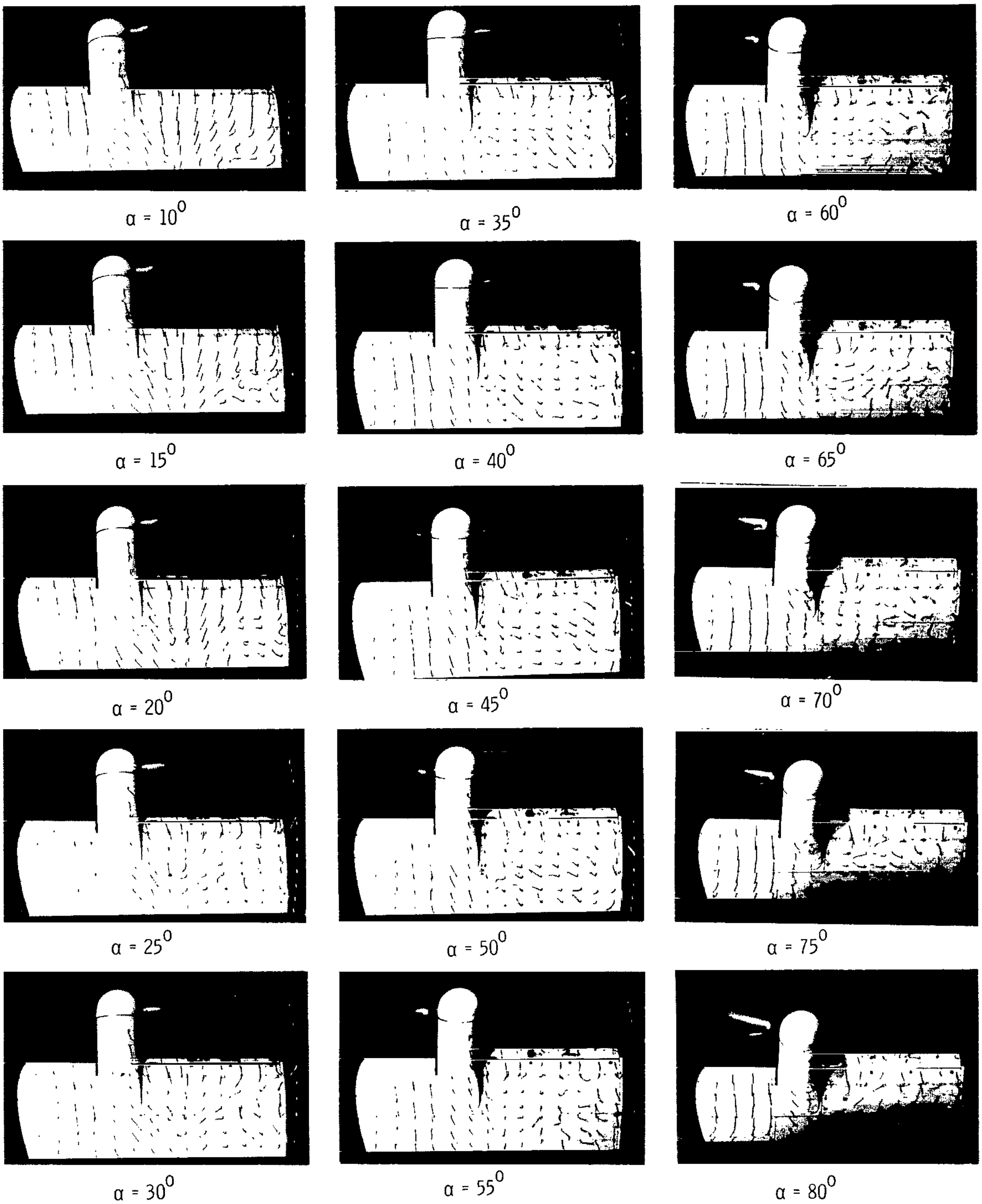

(b) Flow characteristics; $C_{T,s} = 0.90$. L-66-1045

Figure 10.- Continued.

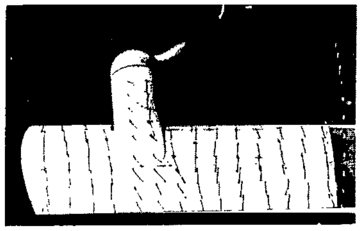

$\alpha = 0^0$

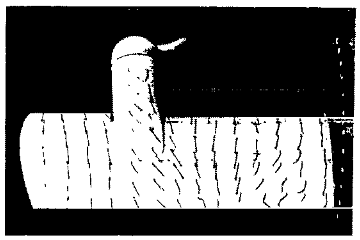

$\alpha = 5^0$

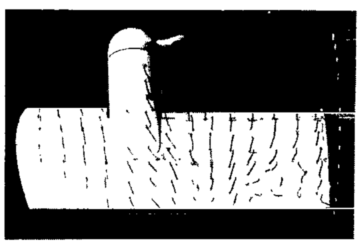

$\alpha = 10^0$

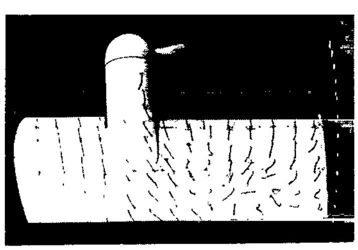

$\alpha = 15^0$

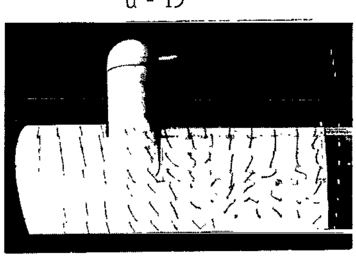

$\alpha = 20^0$

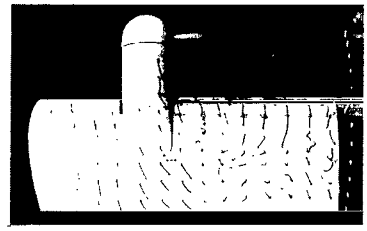

$\alpha = 25^\circ$

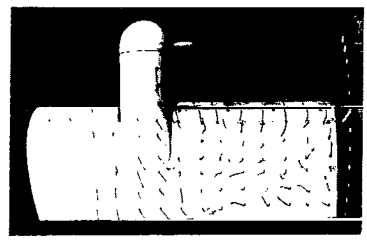

$\alpha = 30^0$

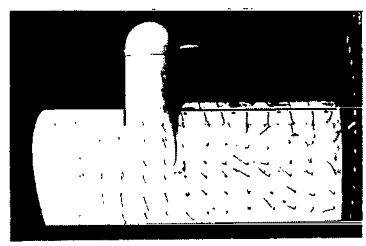

$\alpha = 35^0$

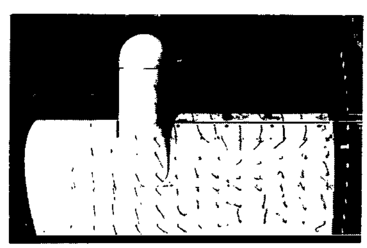

$\alpha = 40^0$

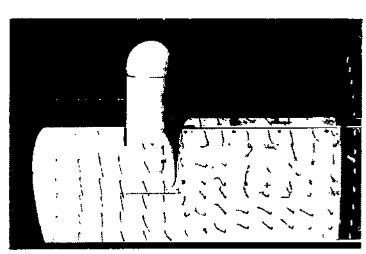

$\alpha = 45^0$

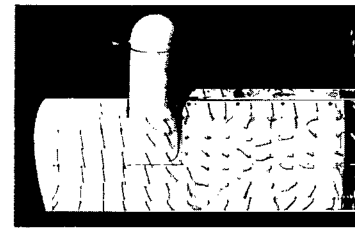

$\alpha = 50^0$

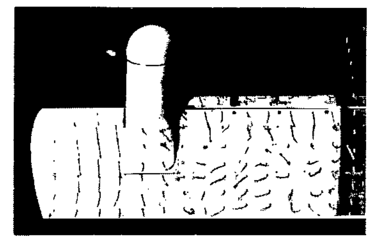

$\alpha = 55^0$

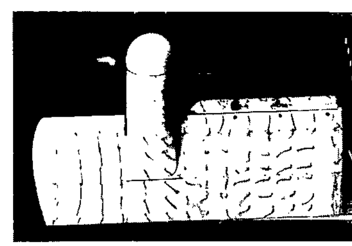

$\alpha = 60^0$

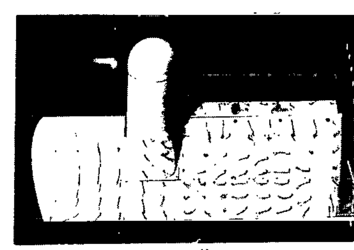

$\alpha = 65^0$

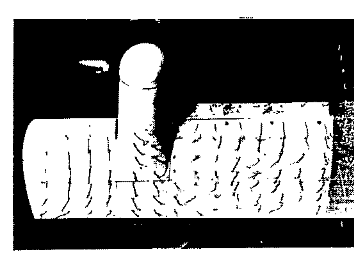

$\alpha = 70^0$

(c) Flow characteristics; $C_{T,s} = 0.80$. L-66-1046

Figure 10.- Continued.

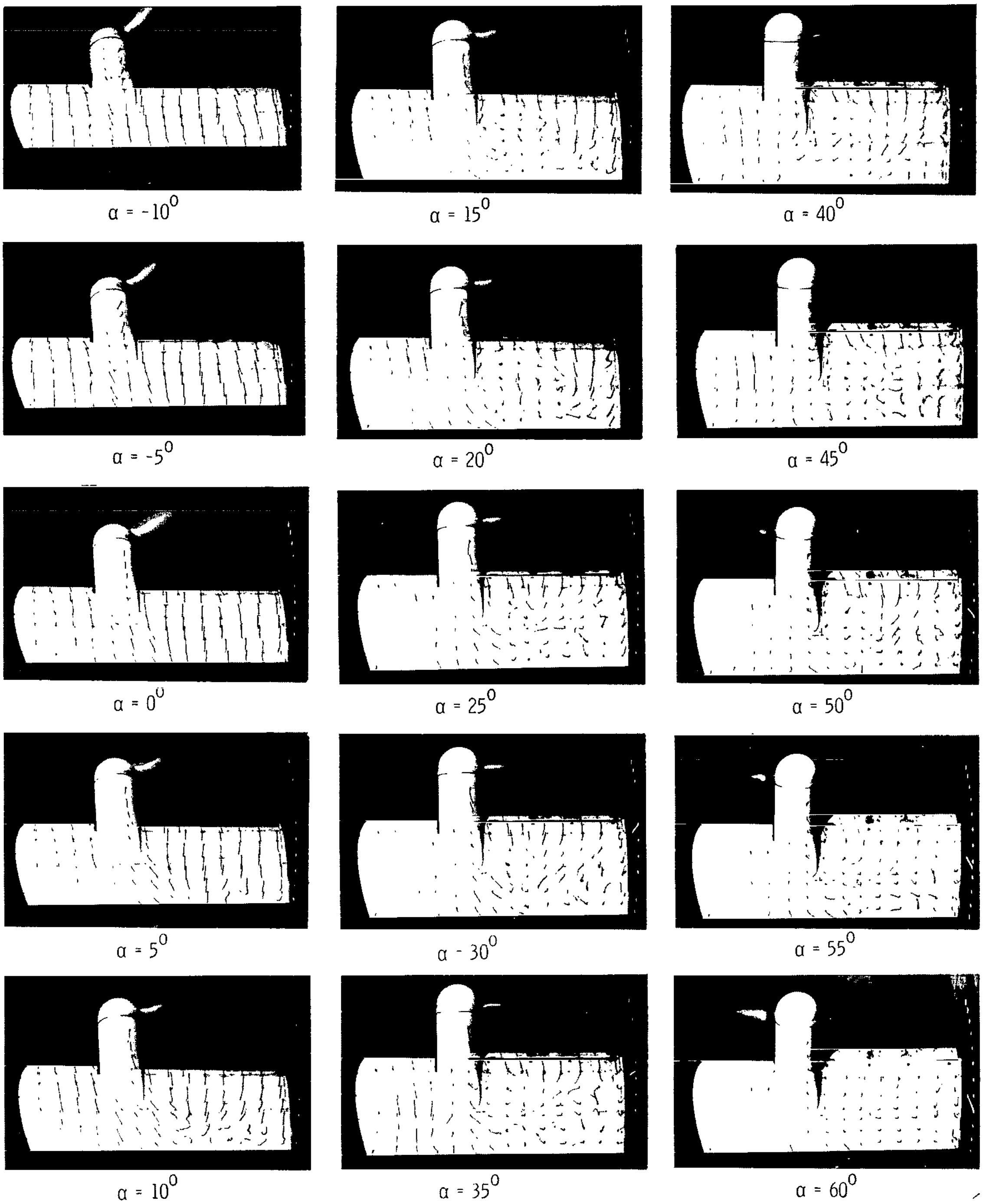

(d) Flow characteristics; $C_{T,s} = 0.60$.

L-66-1047

Figure 10.- Concluded.

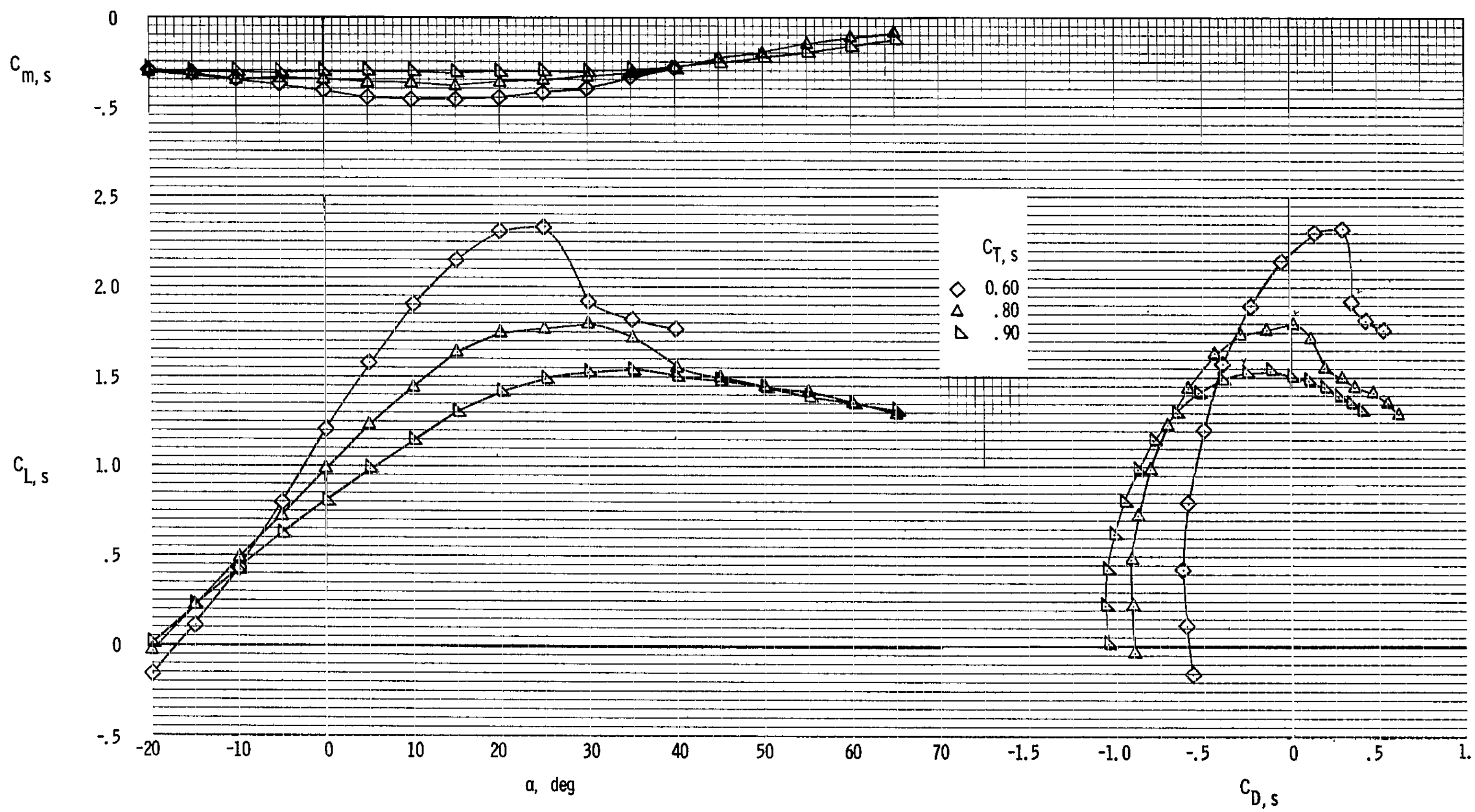

(a) Aerodynamic characteristics.

Figure 11.- Aerodynamic and flow characteristics of model with inboard section of slat deflected 30° and with trailing-edge flap deflected 40°. Down-at-tip rotation.

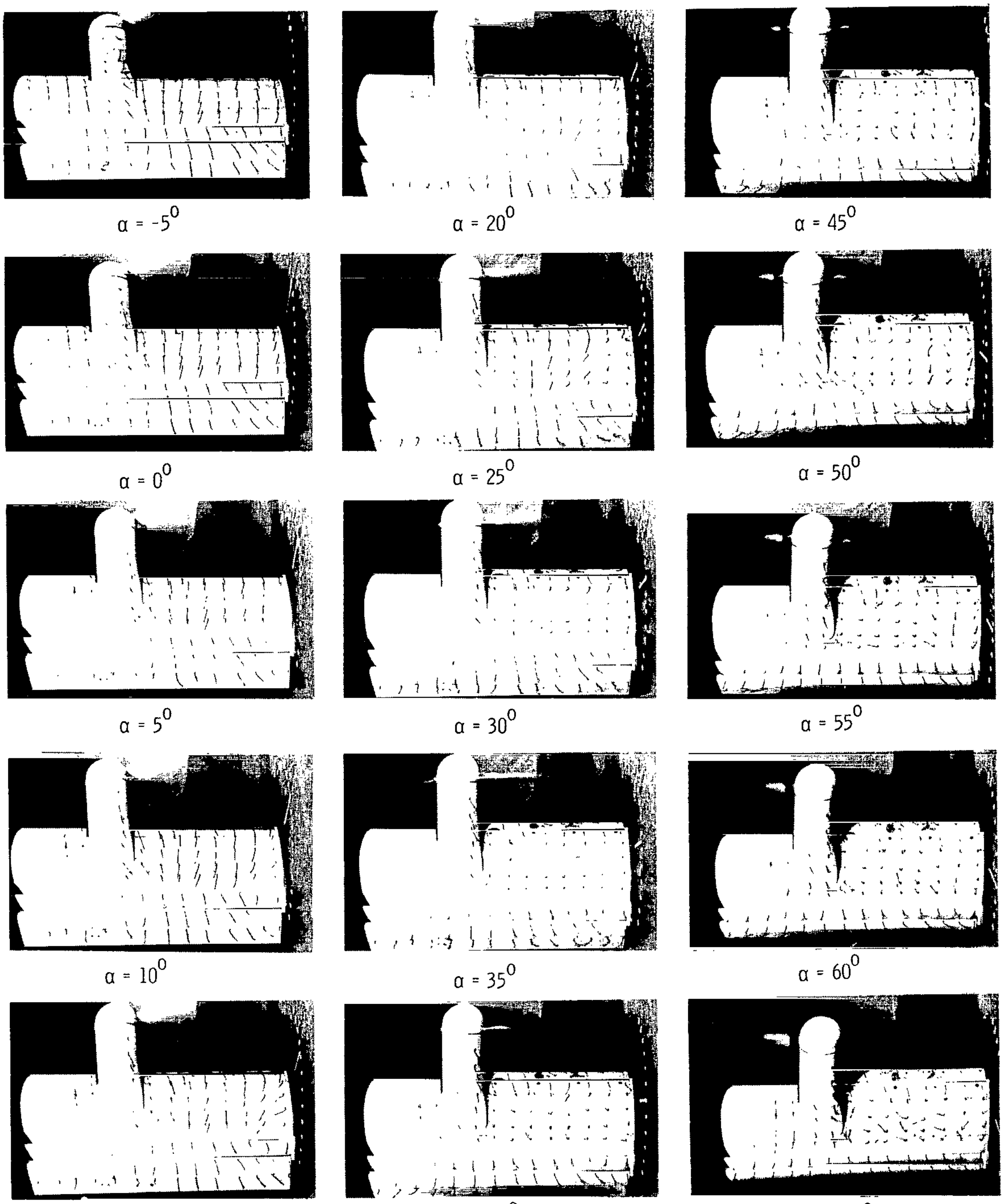

$\alpha = -5^0$ $\alpha = 20^0$ $\alpha = 45^0$

$\alpha = 0^0$ $\alpha = 25^0$ $\alpha = 50^0$

$\alpha = 5^0$ $\alpha = 30^0$ $\alpha = 55^0$

$\alpha = 10^0$ $\alpha = 35^0$ $\alpha = 60^0$

$\alpha = 15^0$ $\alpha = 40^0$ $\alpha = 65^0$

(b) Flow characteristics; $C_{T,s} = 0.90$. L-66-1048

Figure 11.- Continued.

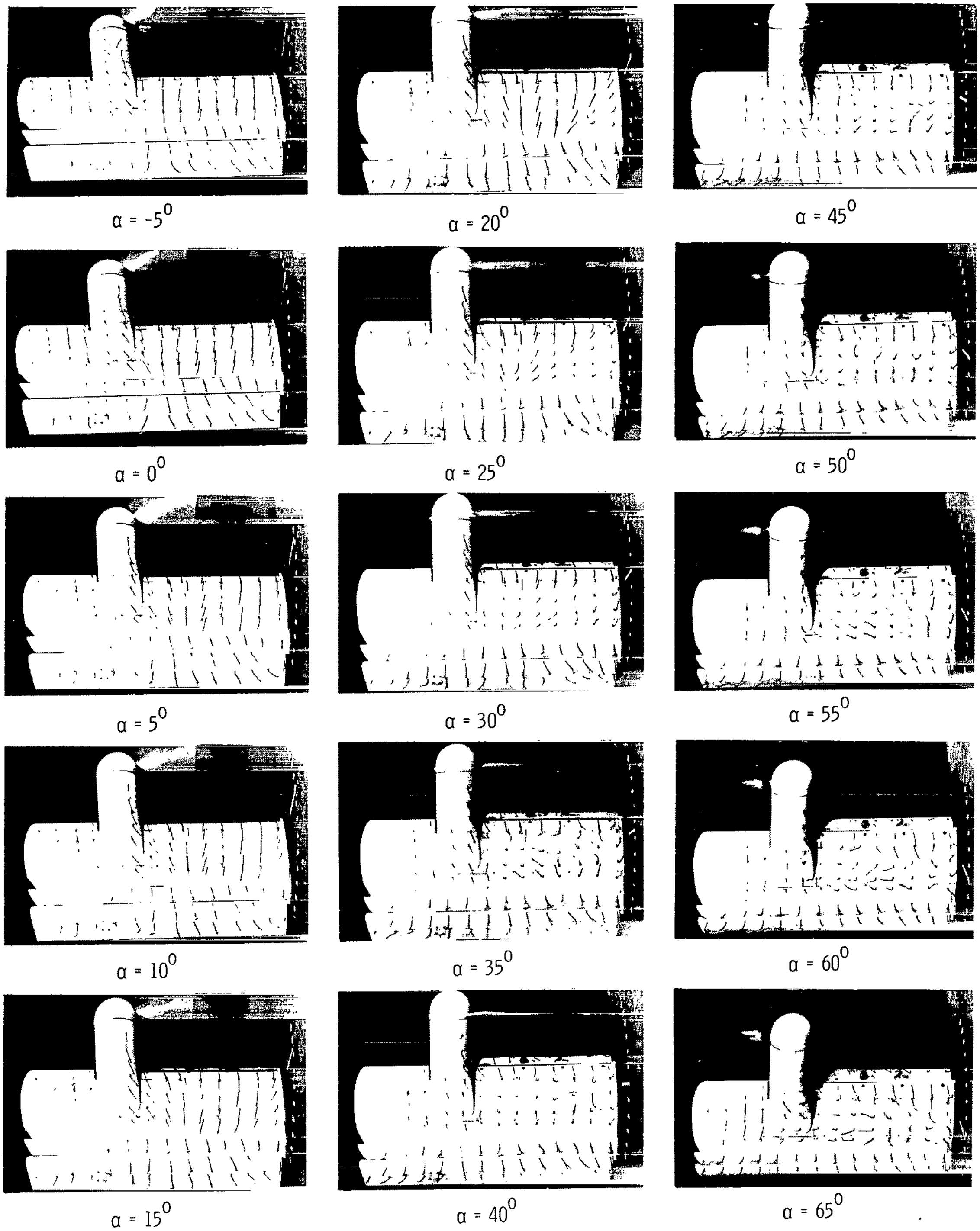

(c) Flow characteristics; $C_{T,s} = 0.80$. L-66-1049

Figure 11.- Continued.

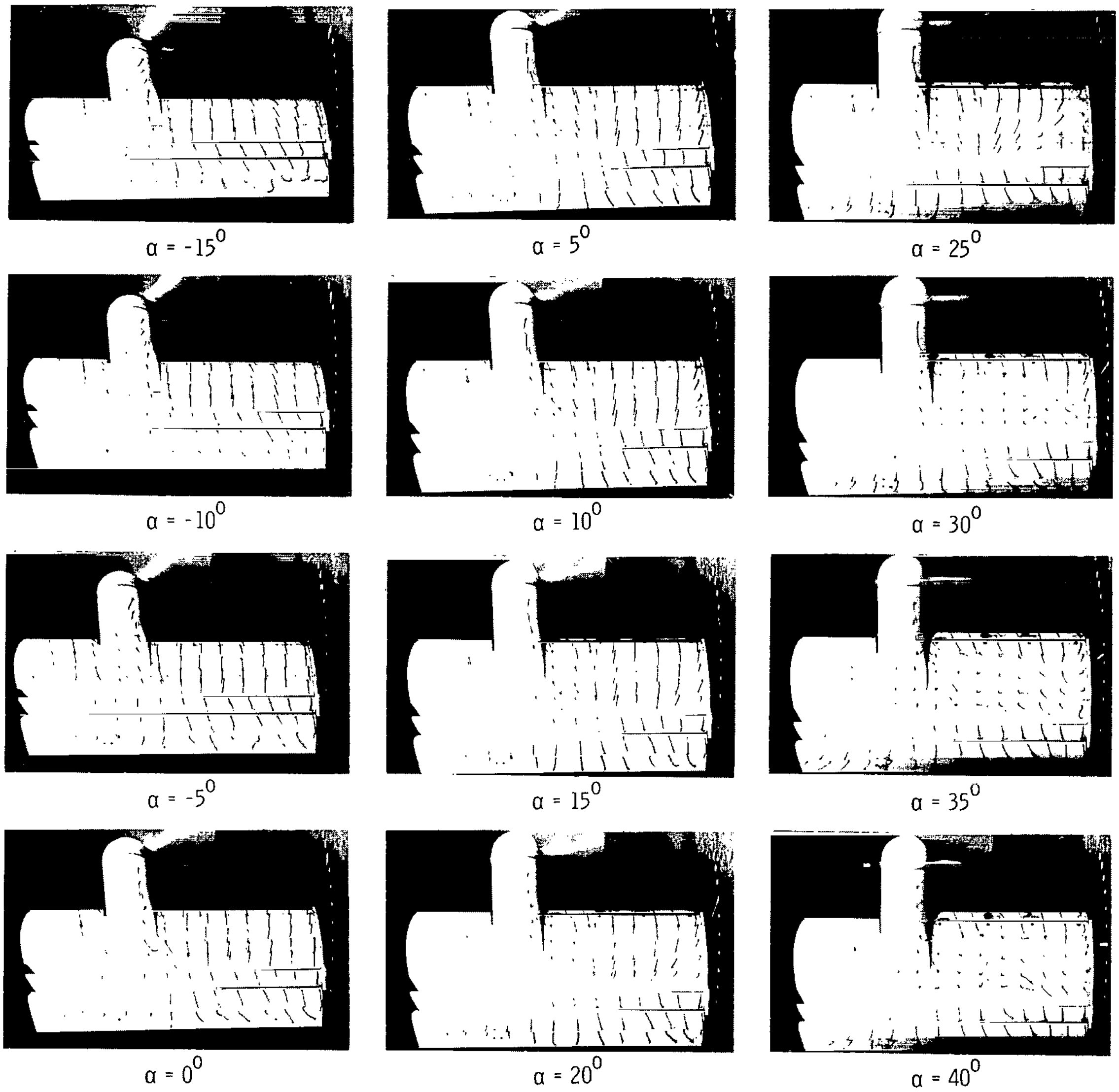

(d) Flow characteristics; $C_{T,s} = 0.60$.

L-66-1050

Figure 11.- Concluded.

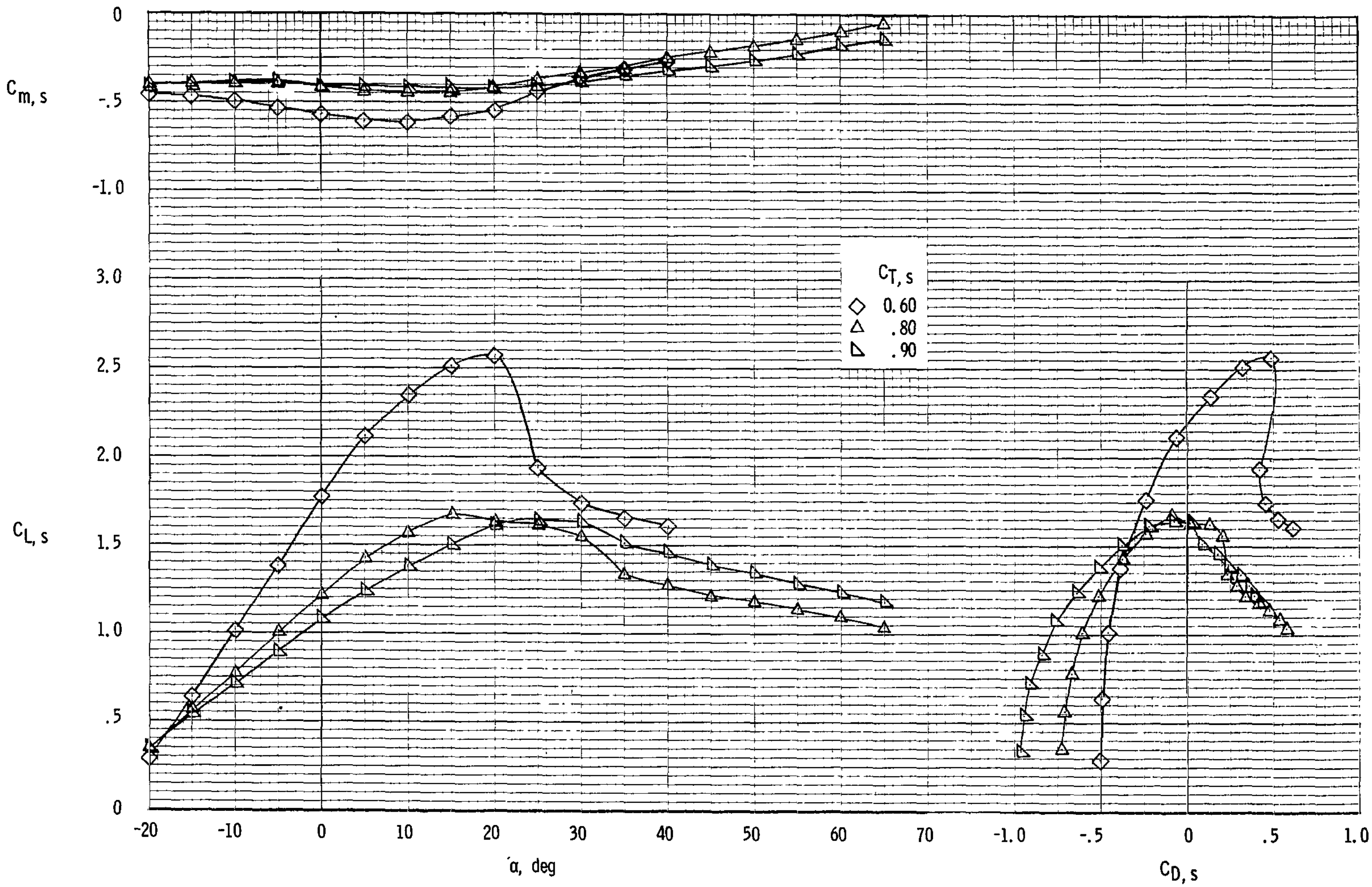

(a) Aerodynamic characteristics.

Figure 12.- Aerodynamic and flow characteristics of model with inboard section of slat deflected 30° and with trailing-edge flap deflected 60°. Down-at-tip rotation.

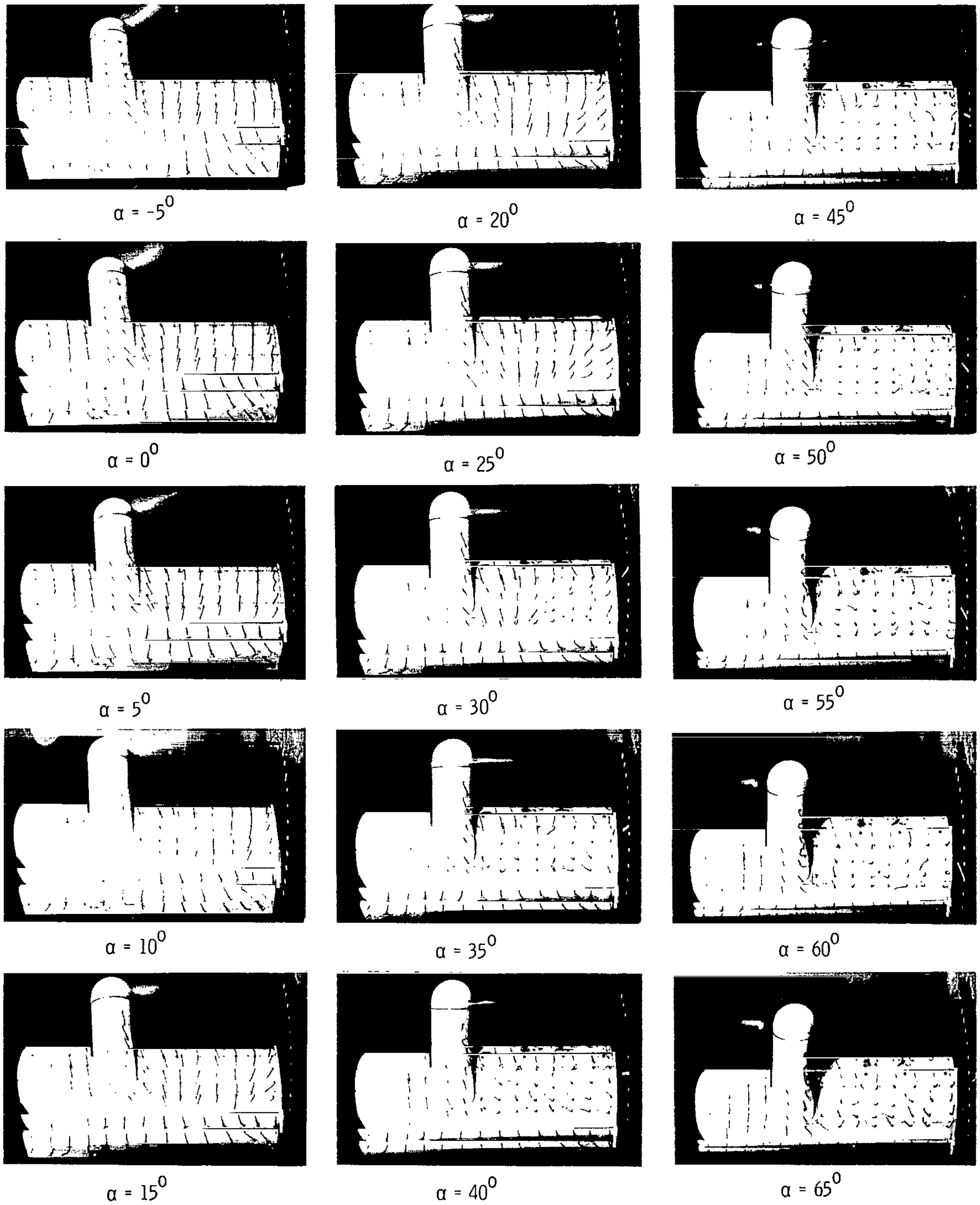

(b) Flow characteristics; $C_{T,s} = 0.90$. L-66-1051

Figure 12.- Continued.

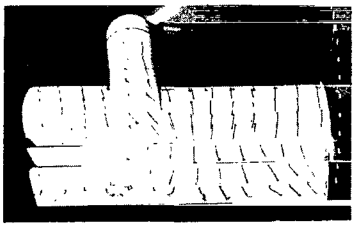
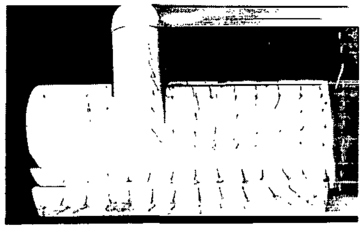
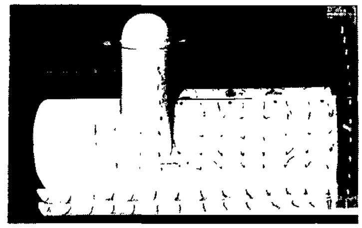

$\alpha = -5^0$ $\alpha = 20^0$ $\alpha = 45^0$

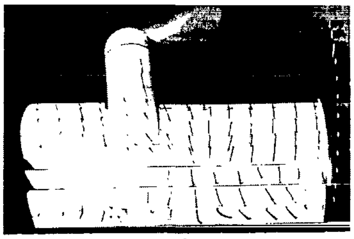
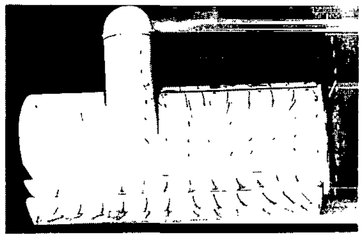
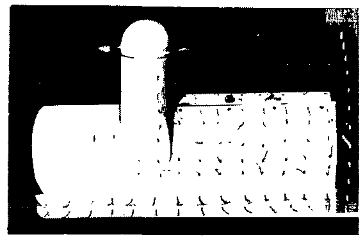

$\alpha = 0^0$ $\alpha = 25^0$ $\alpha = 50^0$

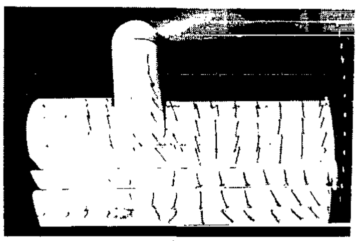
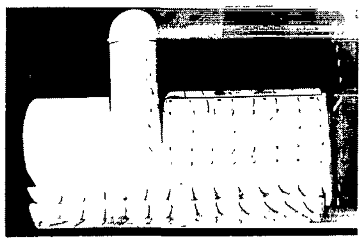
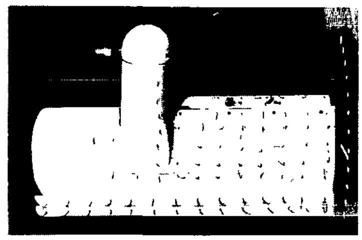

$\alpha = 5^0$ $\alpha = 30^0$ $\alpha = 55^0$

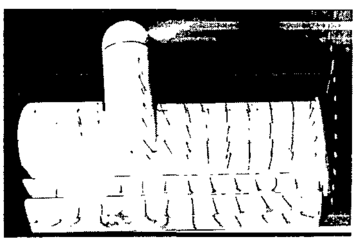
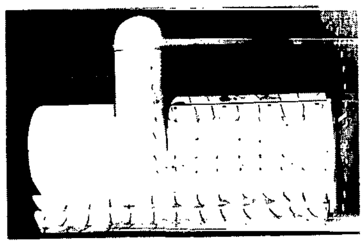
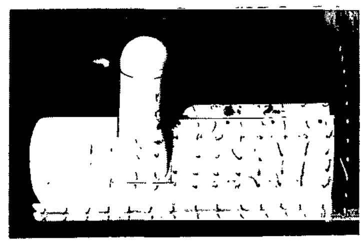

$\alpha = 10^0$ $\alpha = 35^0$ $\alpha = 60^0$

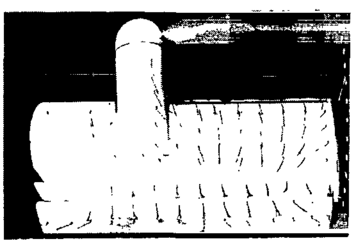
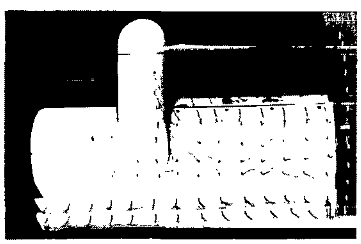
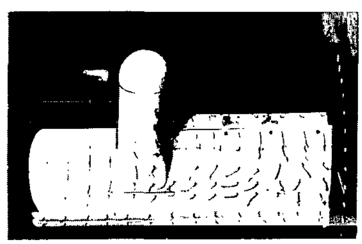

$\alpha = 15^0$ $\alpha = 40^0$ $\alpha = 65^0$

(c) Flow characteristics; $C_{T,s} = 0.80$. L-66-1052

Figure 12.- Continued.

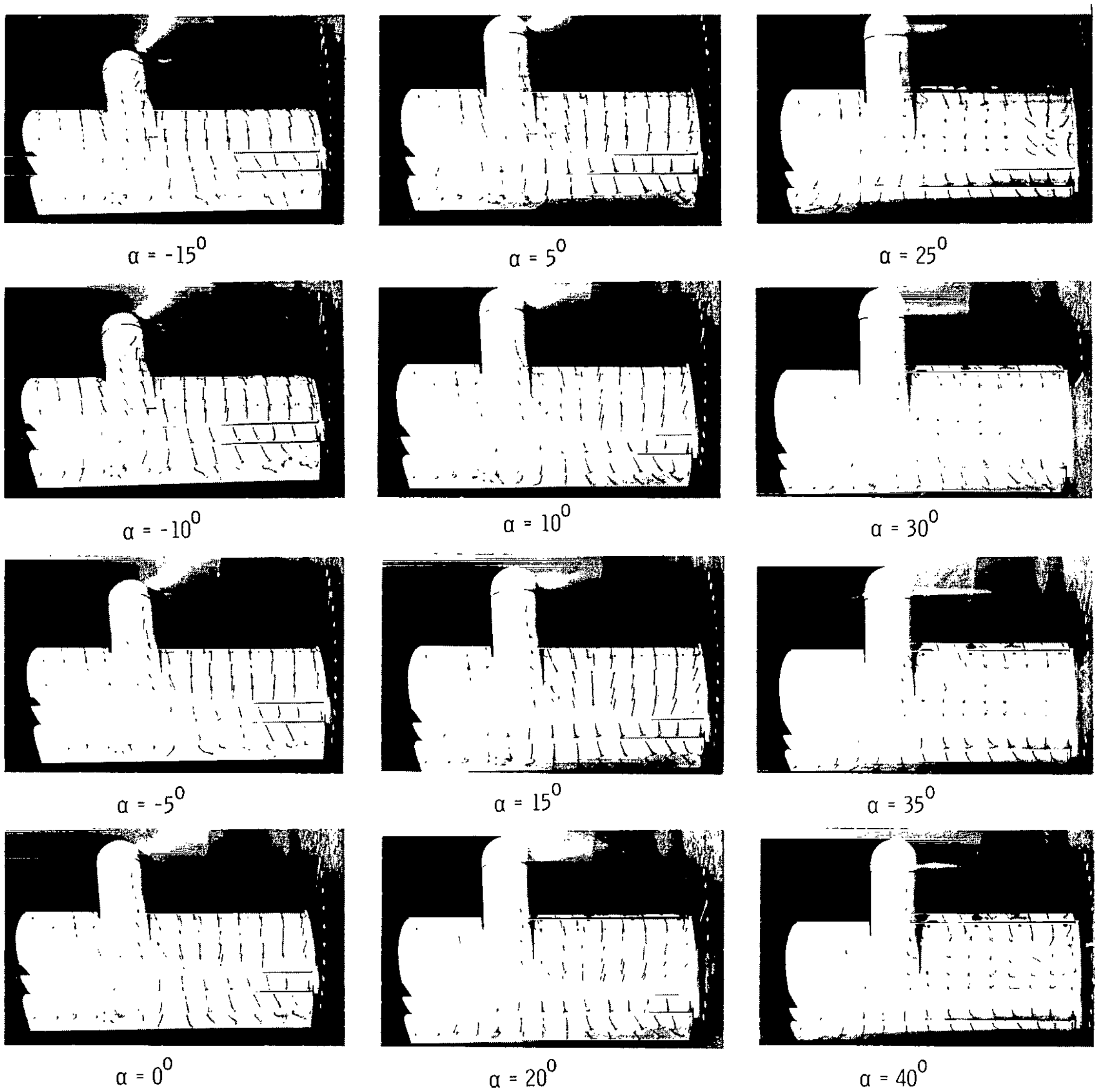

(d) Flow characteristics; $C_{T,s} = 0.60$. L-66-1053

Figure 12.- Concluded.

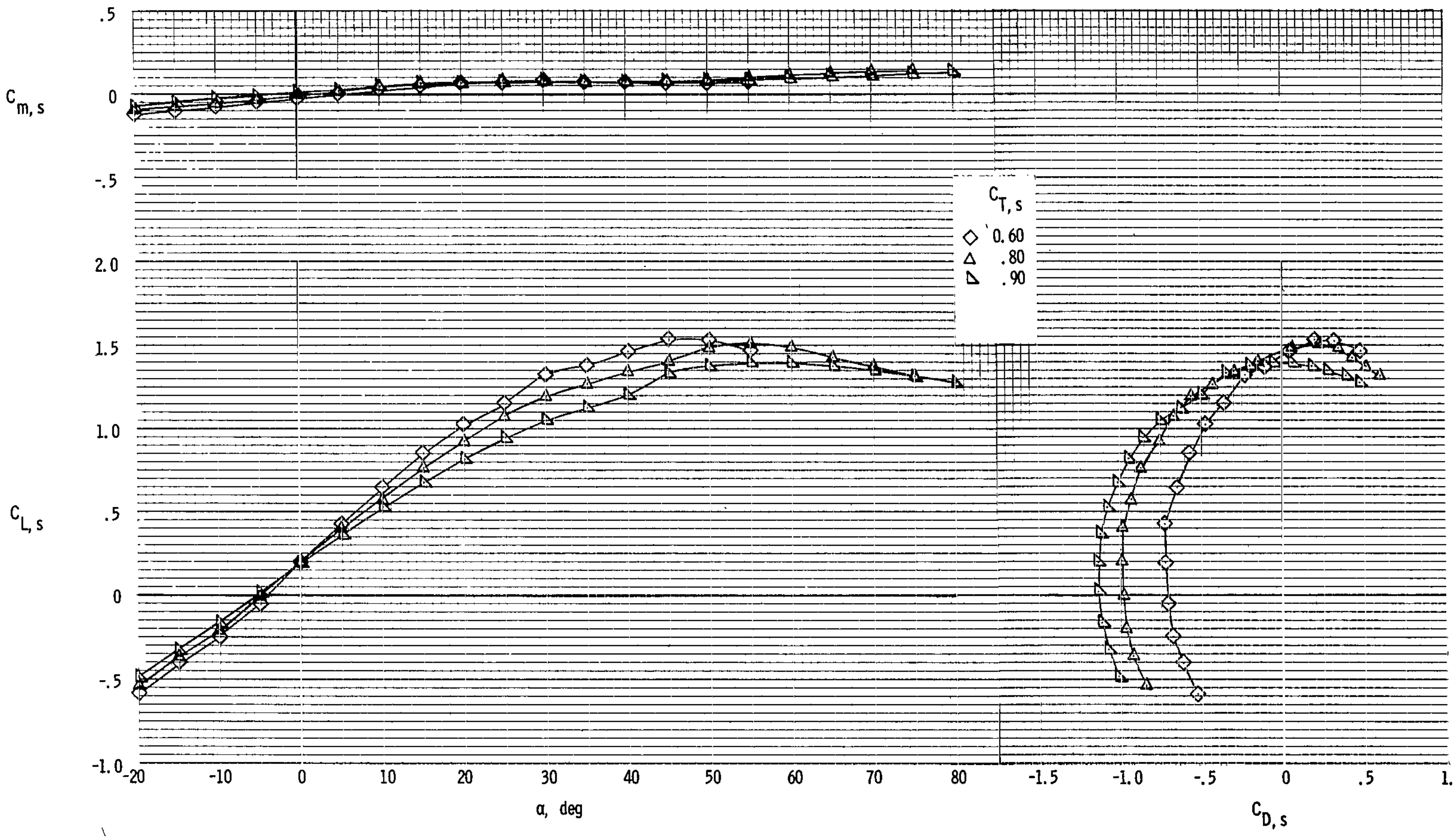

(a) Aerodynamic characteristics.

Figure 13.- Aerodynamic and flow characteristics of model with inboard section of slat deflected 30^{0} and with trailing-edge flap undeflected. $\delta_f = 0^{0}$. Fences on. Down-at-tip rotation.

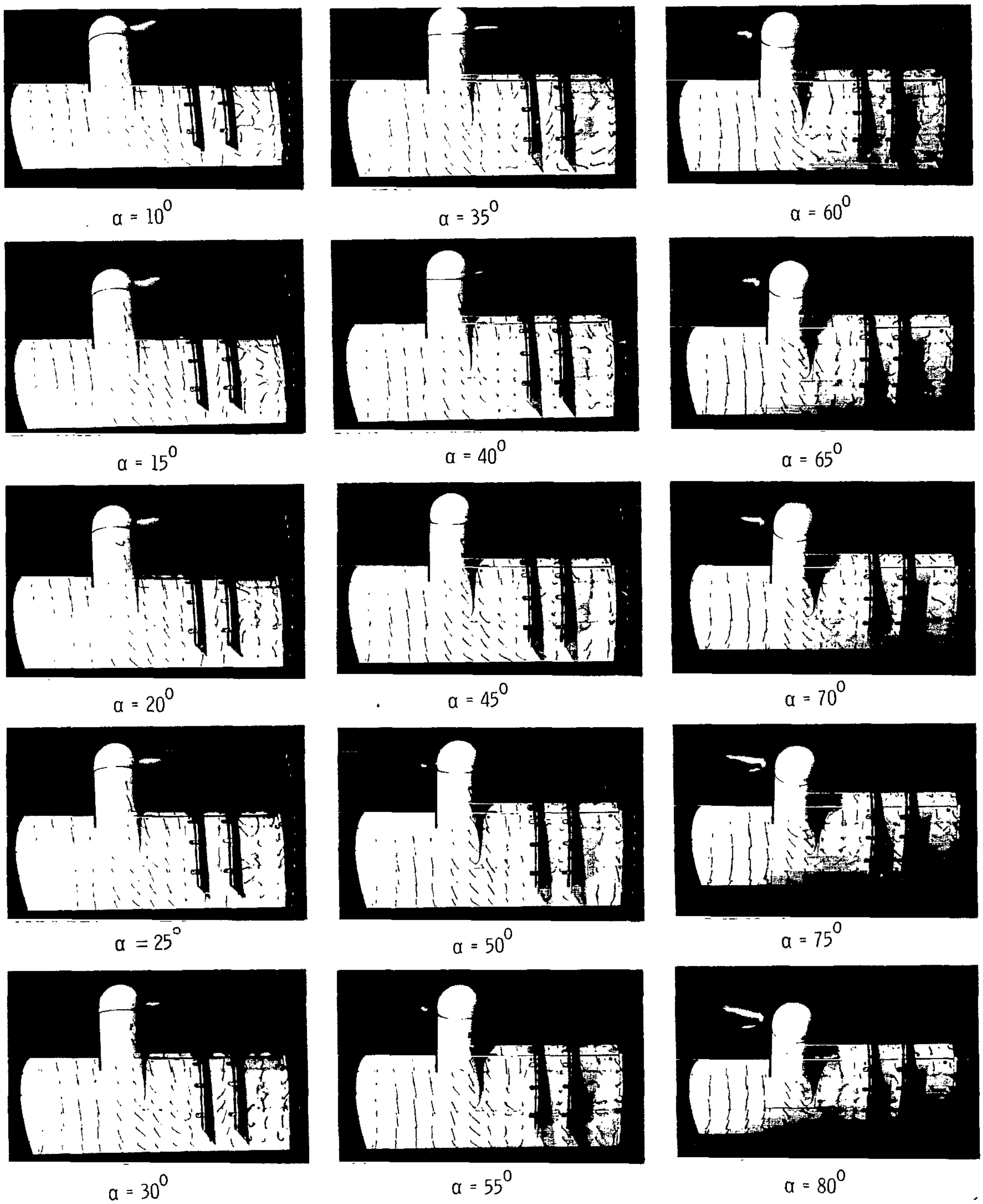

(b) Flow characteristics; $C_{T,s} = 0.90$. L-66-1054

Figure 13.- Continued.

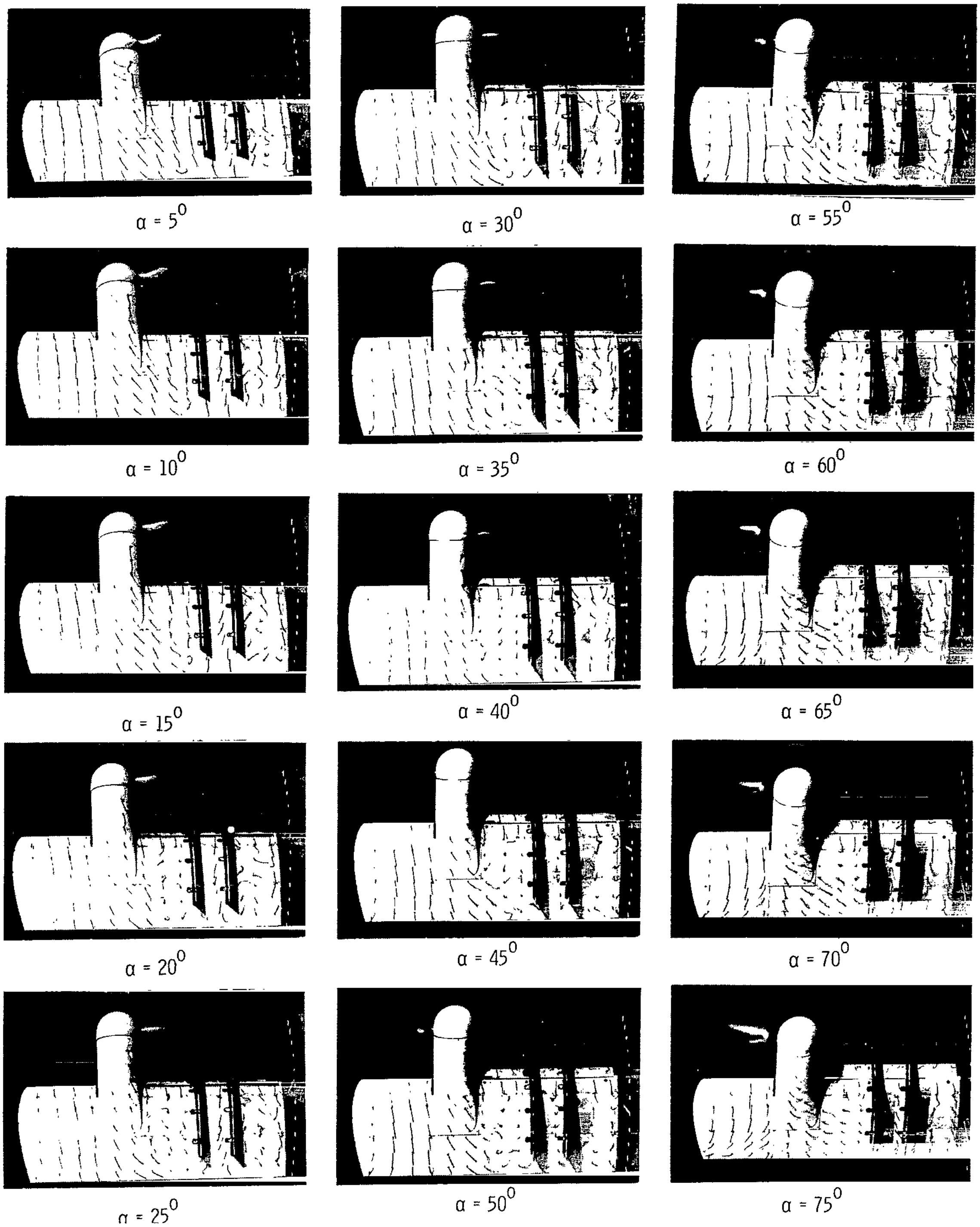

(c) Flow characteristics; $C_{T,s} = 0.80$. L-66-1055

Figure 13.- Continued.

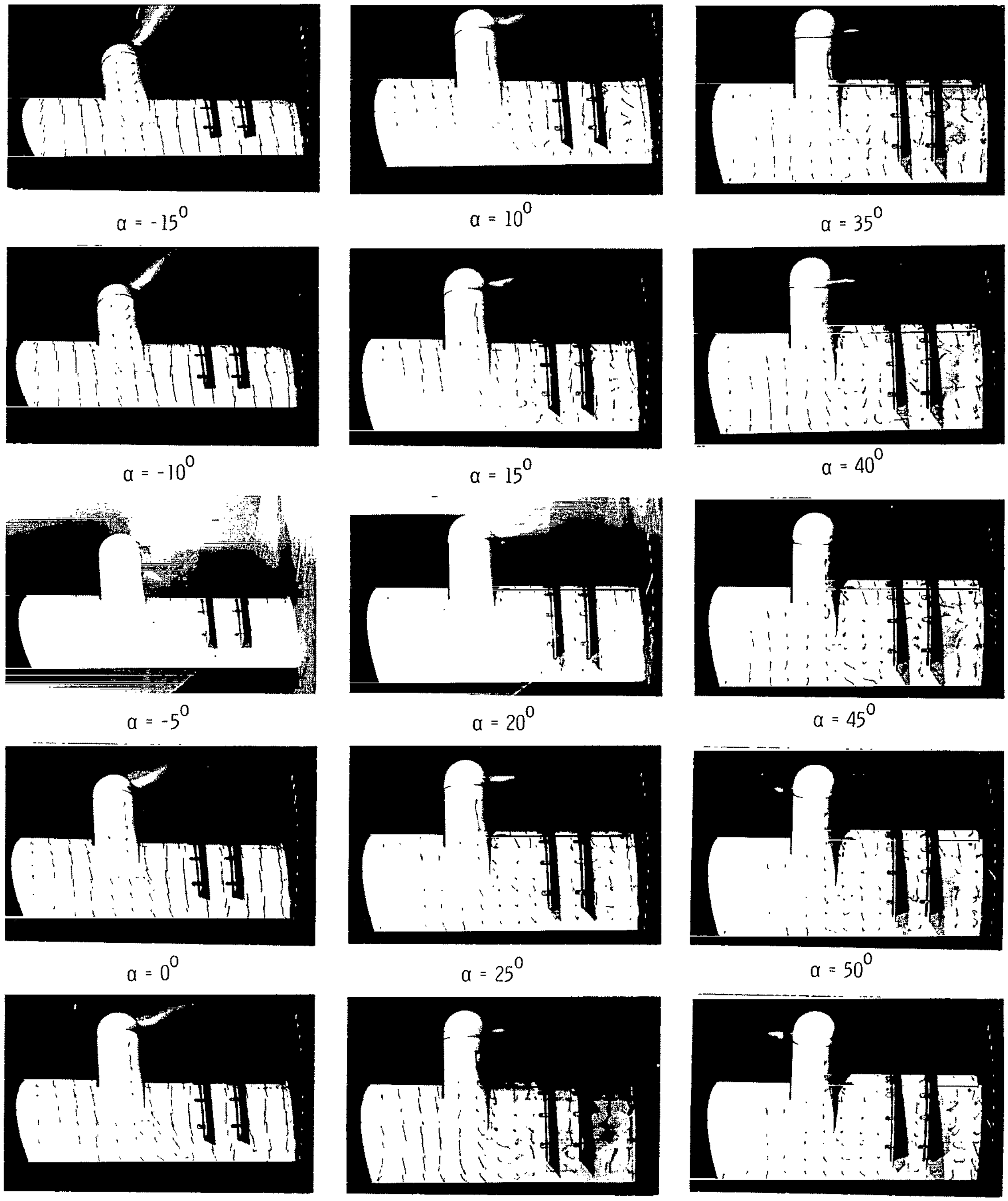

(d) Flow characteristics; $C_{T,s} = 0.60$. L-66-1056

Figure 13.- Concluded.

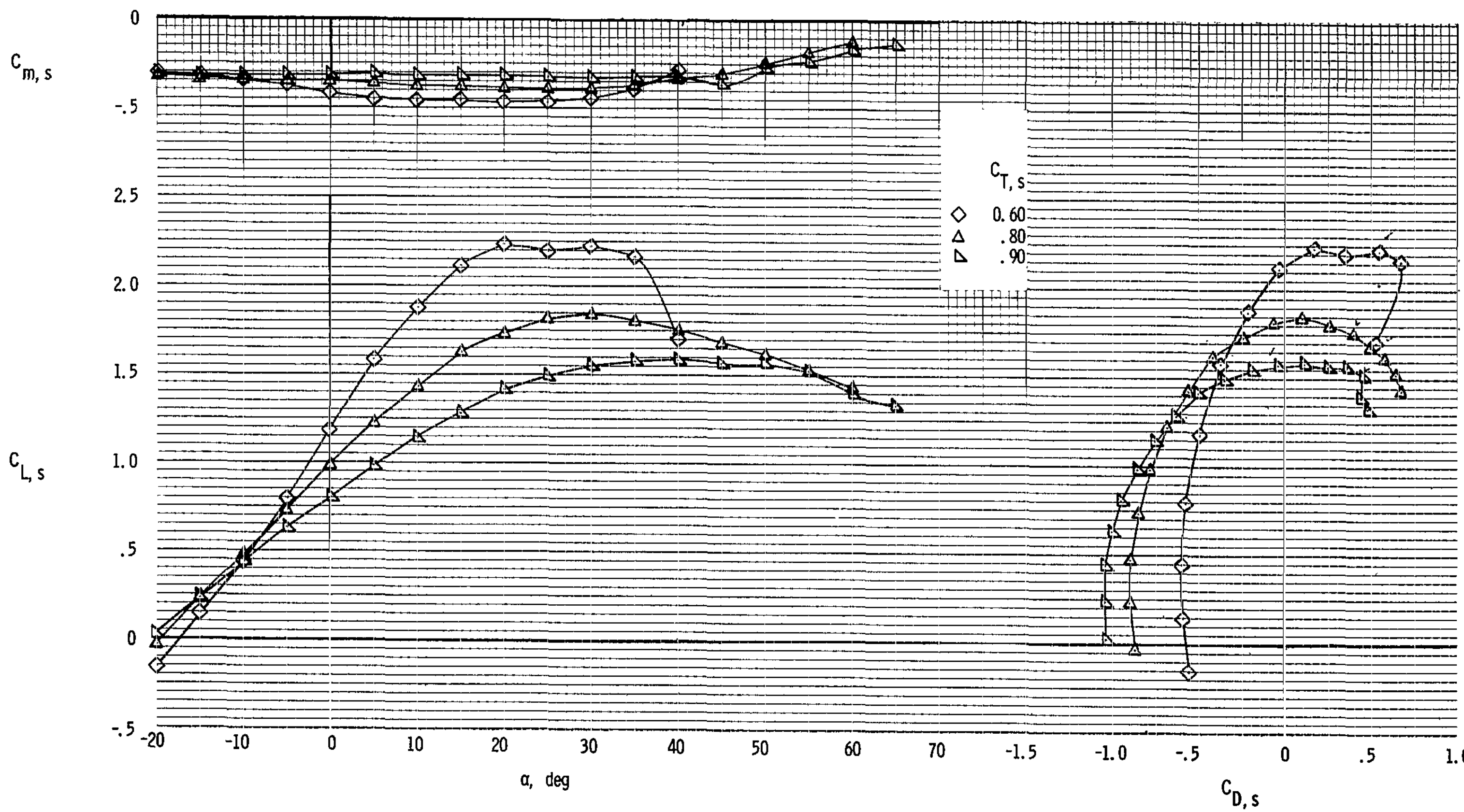

(a) Aerodynamic characteristics.

Figure 14.- Aerodynamic and flow characteristics of model with inboard section of slat deflected 30° and with trailing-edge flap deflected 40°. Fences on. Down-at-tip rotation.

$\alpha = -5^0$

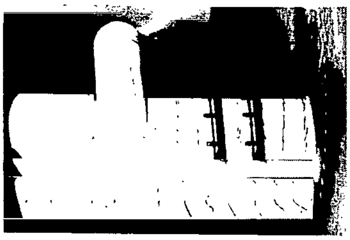

$\alpha = 0^0$

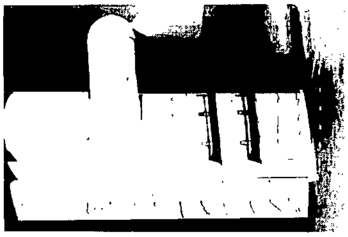

$\alpha = 5^0$

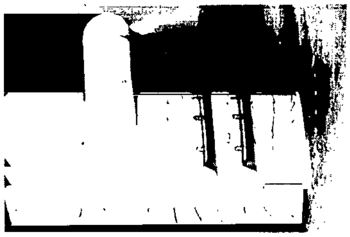

$\alpha = 10^0$

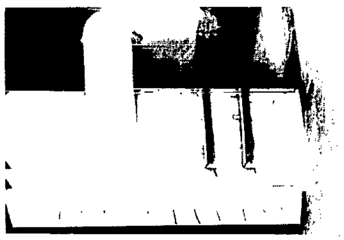

$\alpha = 15^0$

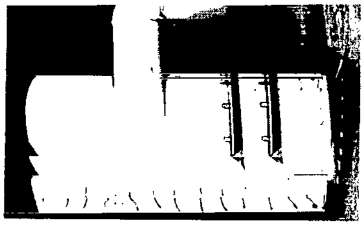

$\alpha = 20^0$

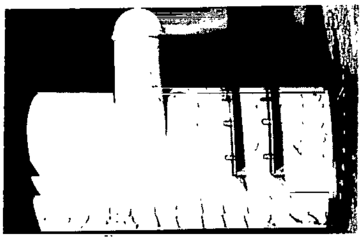

$\alpha = 25^0$

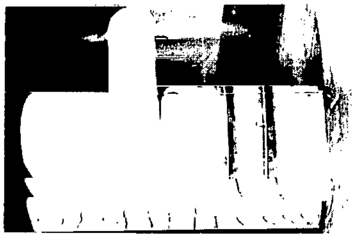

$\alpha = 30^0$

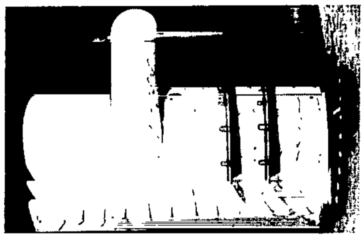

$\alpha = 35^0$

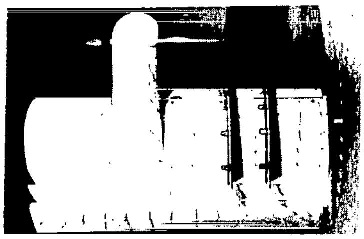

$\alpha = 40^0$

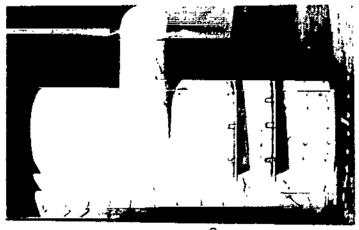

$\alpha = 45^0$

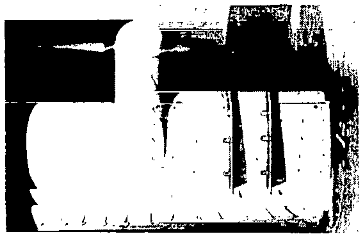

$\alpha = 50^0$

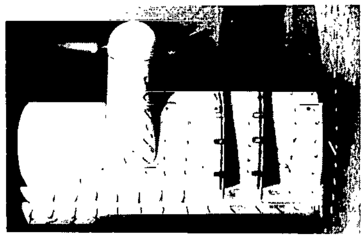

$\alpha = 55^0$

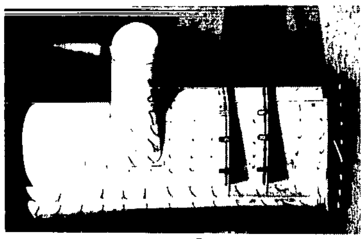

$\alpha = 60^0$

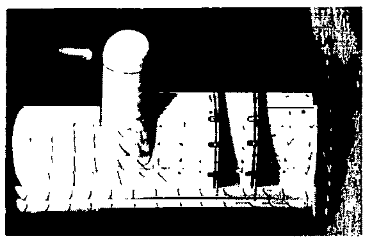

$\alpha = 65^0$

(b) Flow characteristics; $C_{T,s} = 0.90$.

L-66-1057

Figure 14.- Continued.

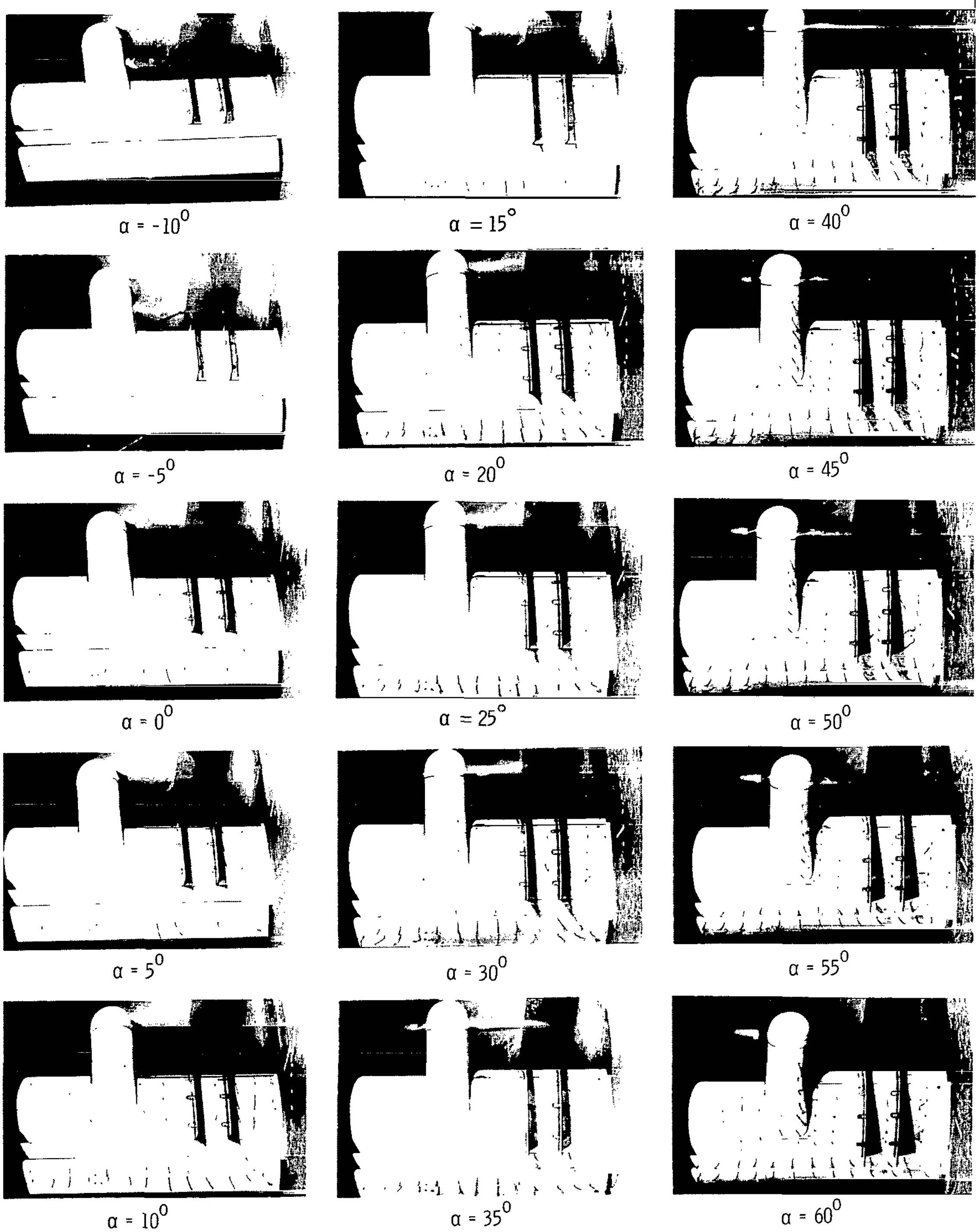

(c) Flow characteristics; $C_{T,s} = 0.80$.

L-66-1058

Figure 14.- Continued.

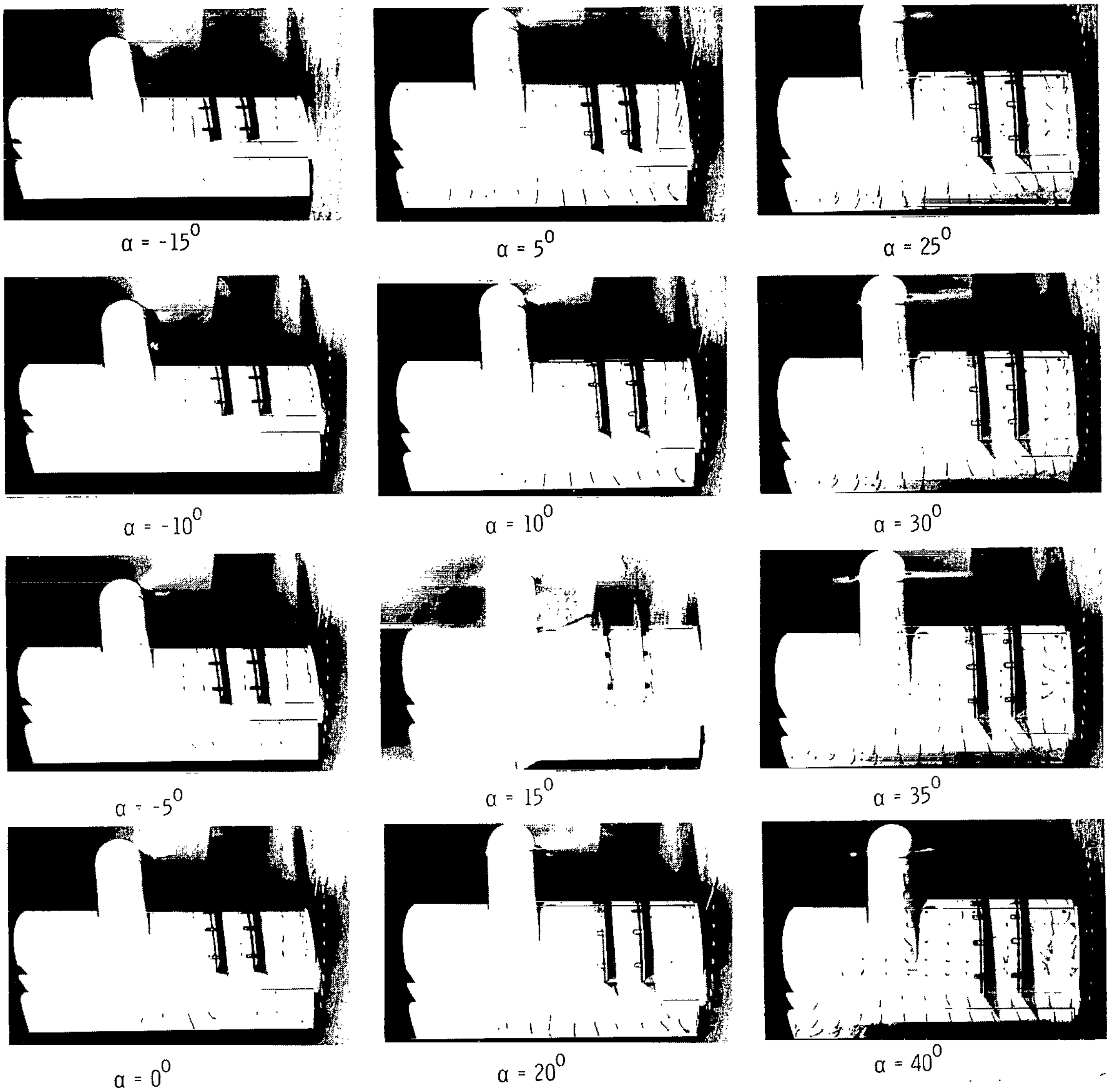

(d) Flow characteristics; $C_{T,s} = 0.60$.

L-66-1059

Figure 14.- Concluded.

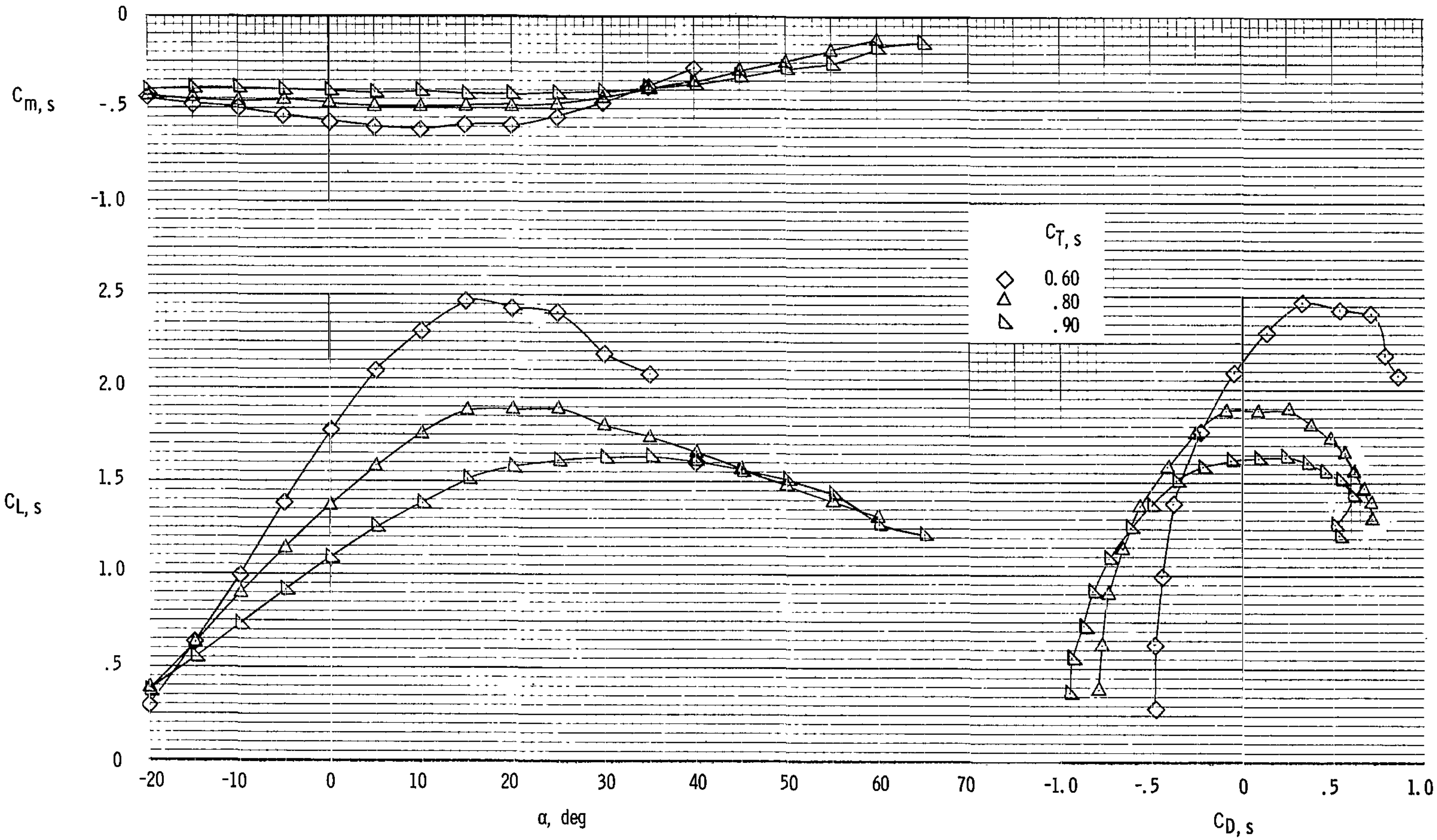

(a) Aerodynamic characteristics.

Figure 15.- Aerodynamic and flow characteristics of model with inboard section of slat deflected 30° and with trailing-edge flap deflected 60°. Fences on. Down-at-tip rotation.

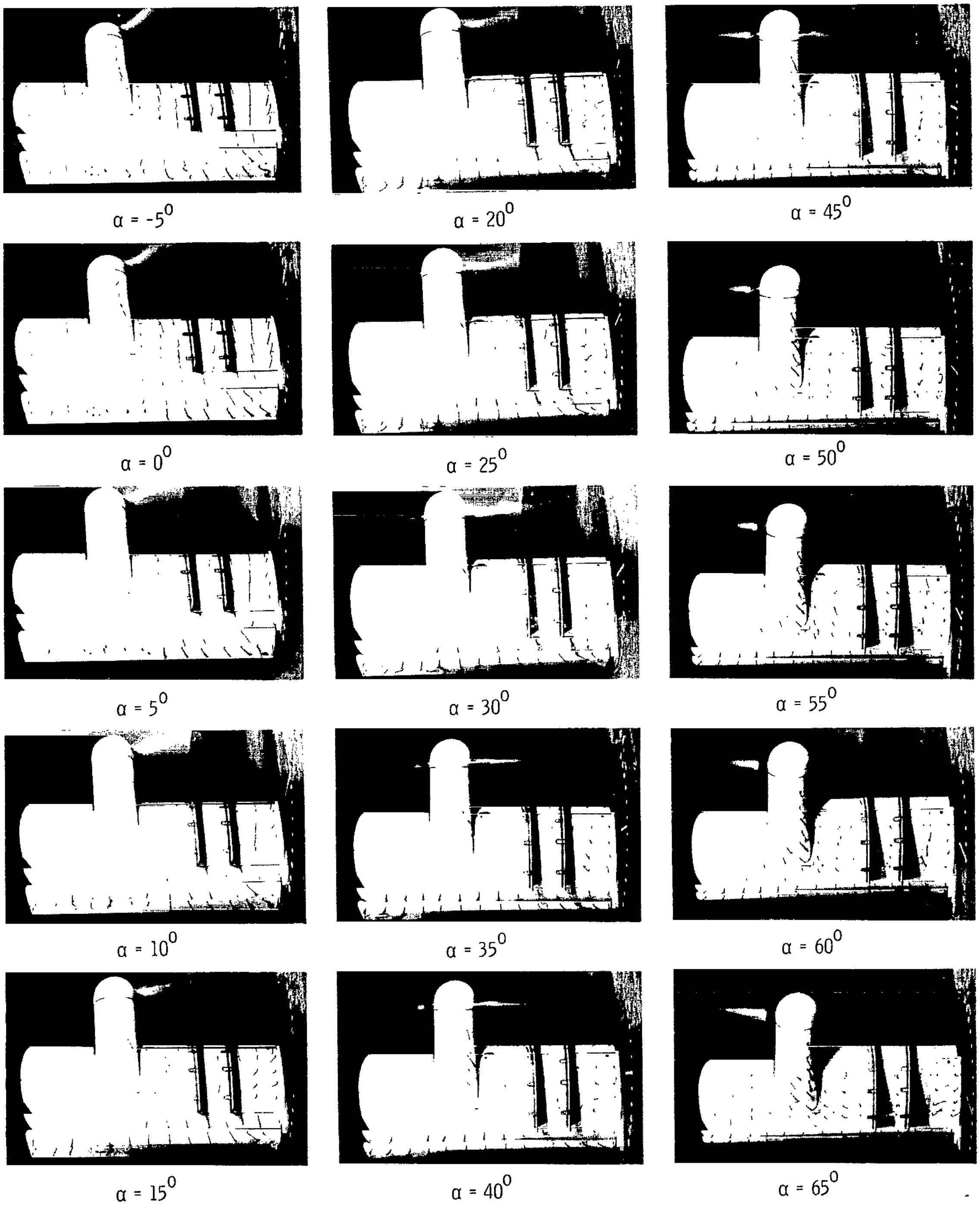

(b) Flow characteristics; $C_{T,s} = 0.90$.

L-66-1060

Figure 15.- Continued.

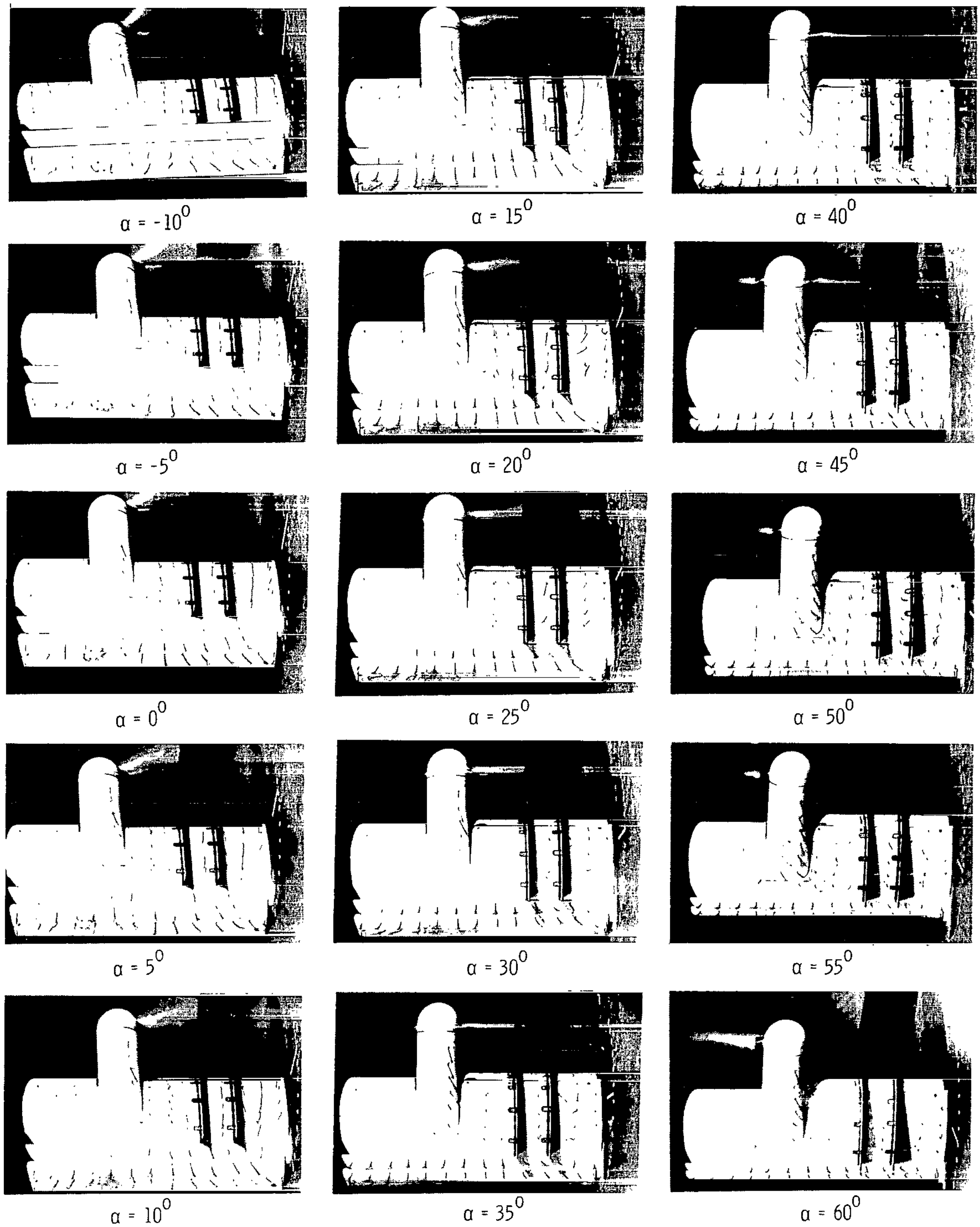

(c) Flow characteristics; $C_{T,s} = 0.80$. L-66-1061

Figure 15.- Continued.

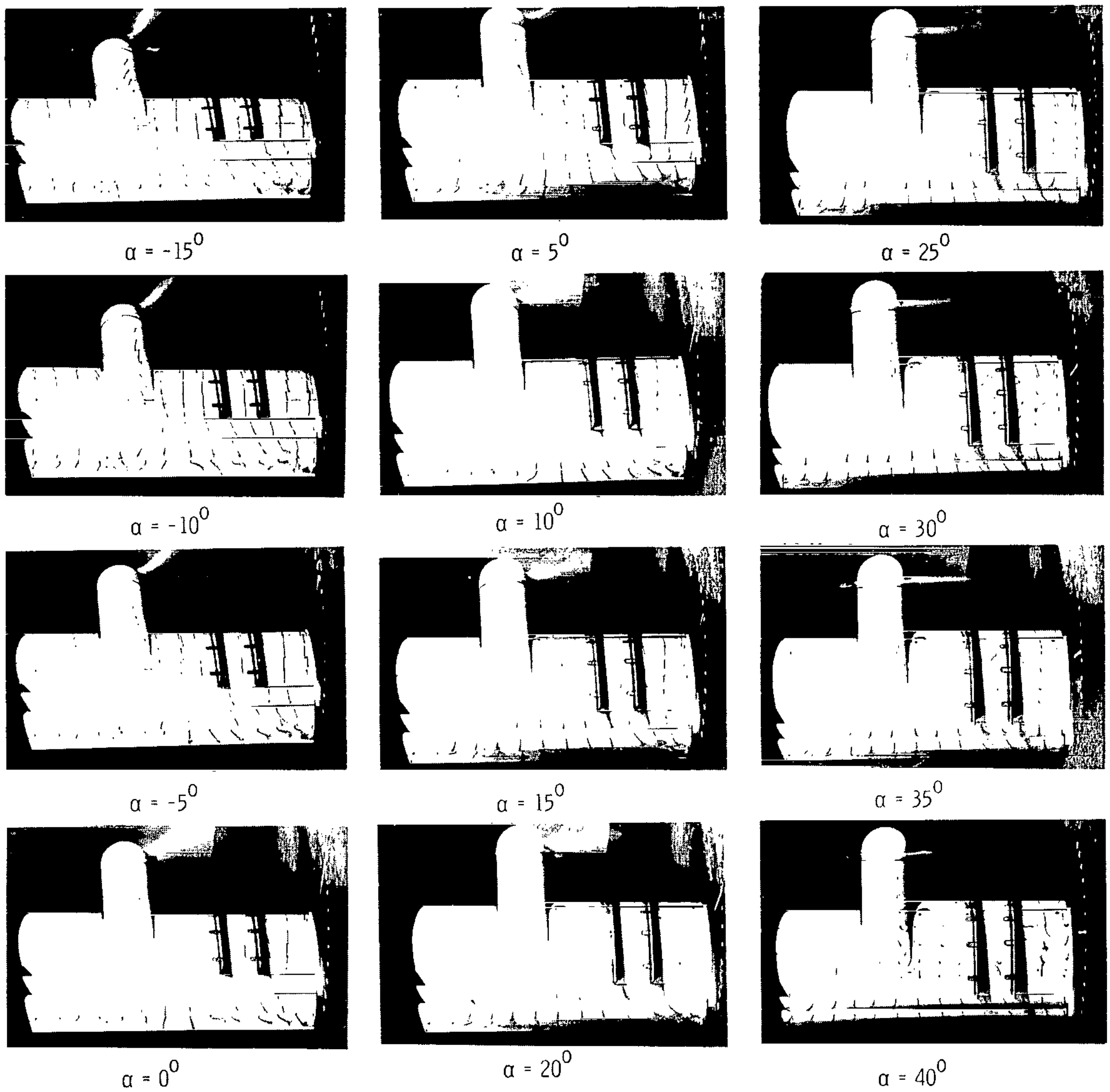

(d) Flow characteristics; $C_{T,s} = 0.60$.

L-66-1062

Figure 15.- Concluded.

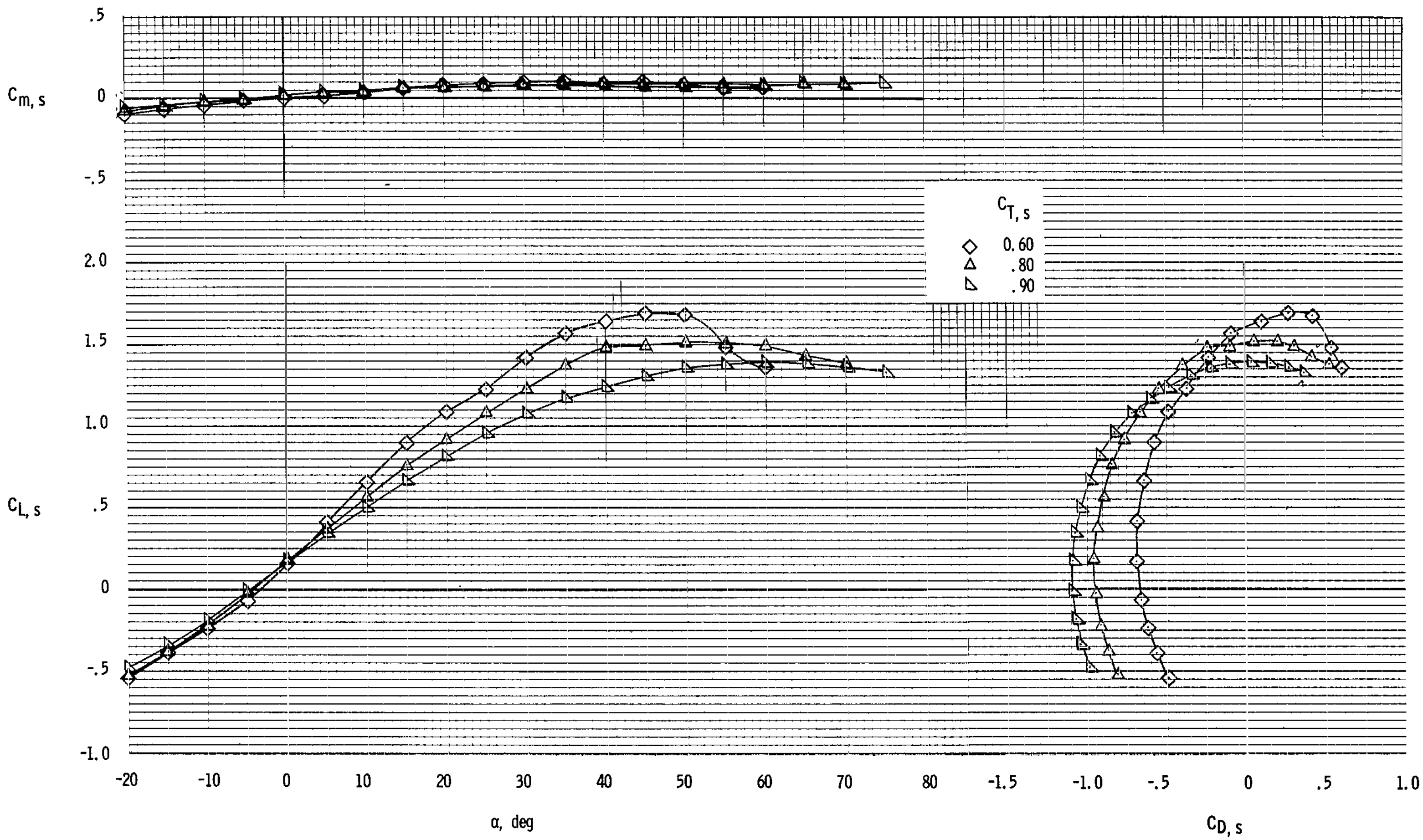

(a) Aerodynamic characteristics.

Figure 16.- Aerodynamic and flow characteristics of model with inboard section of slat deflected 30° and with trailing-edge flap undeflected. $\delta_f = 0^\circ$. Up-at-tip rotation.

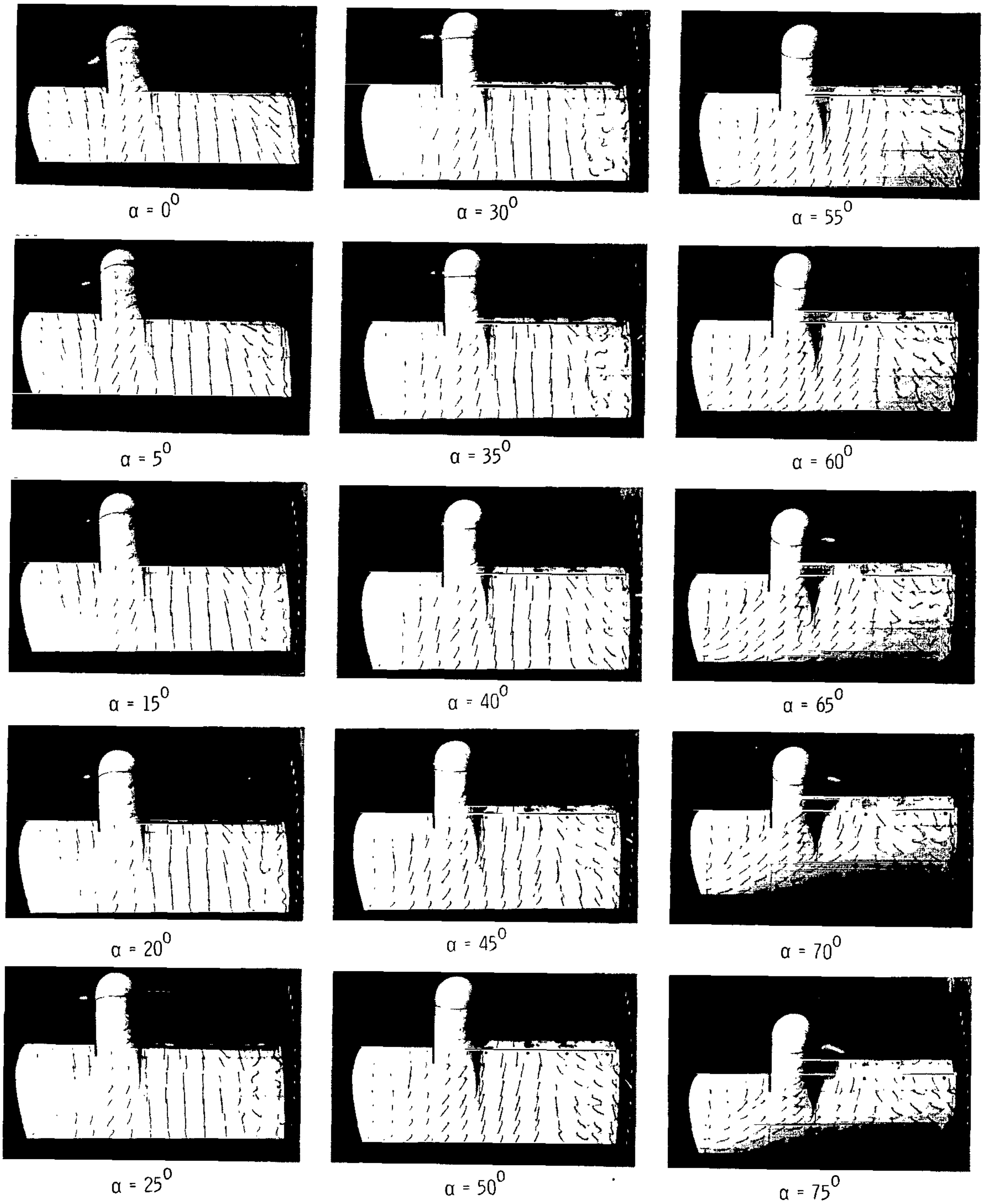

(b) Flow characteristics; $C_{T,s} = 0.90$.

L-66-1063

Figure 16.- Continued.

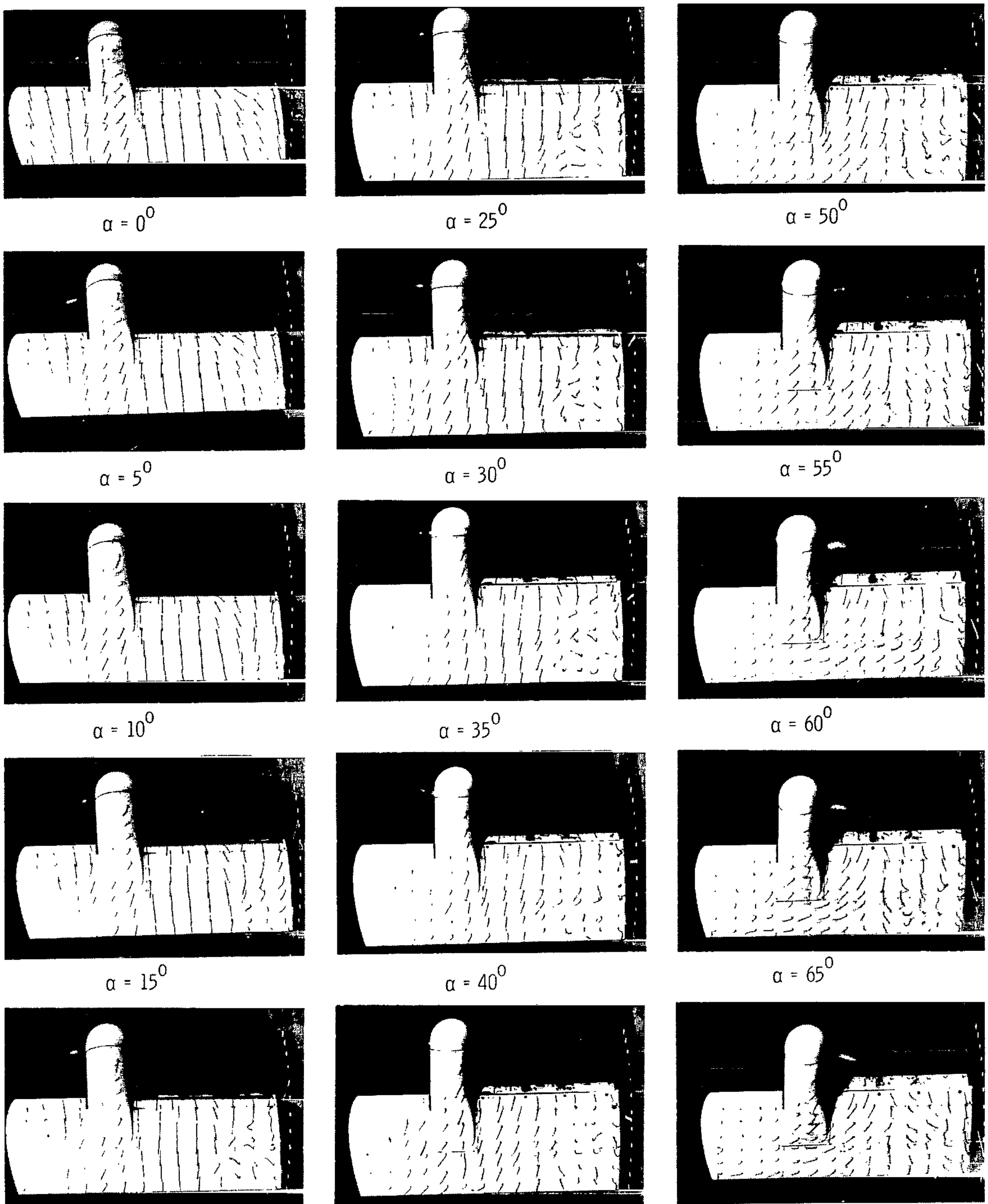

$\alpha = 0^0$ $\alpha = 25^0$ $\alpha = 50^0$

$\alpha = 5^0$ $\alpha = 30^0$ $\alpha = 55^0$

$\alpha = 10^0$ $\alpha = 35^0$ $\alpha = 60^0$

$\alpha = 15^0$ $\alpha = 40^0$ $\alpha = 65^0$

$\alpha = 20^0$ $\alpha = 45^0$ $\alpha = 70^0$

(c) Flow characteristics; $C_{T,s} = 0.80$. L-66-1064

Figure 16.- Continued.

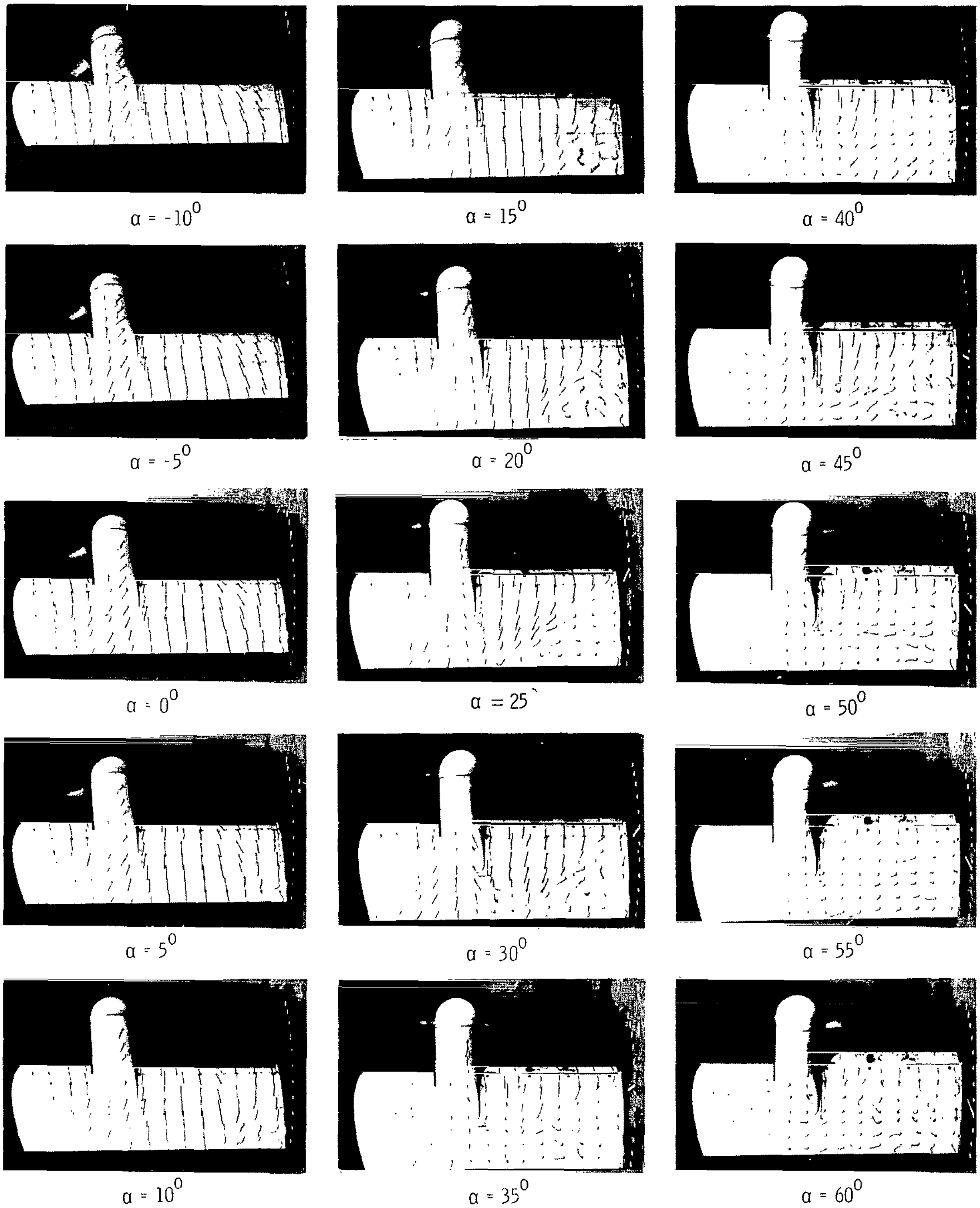

(d) Flow characteristics; $C_{T,s} = 0.60$.

L-66-1065

Figure 16.- Concluded.

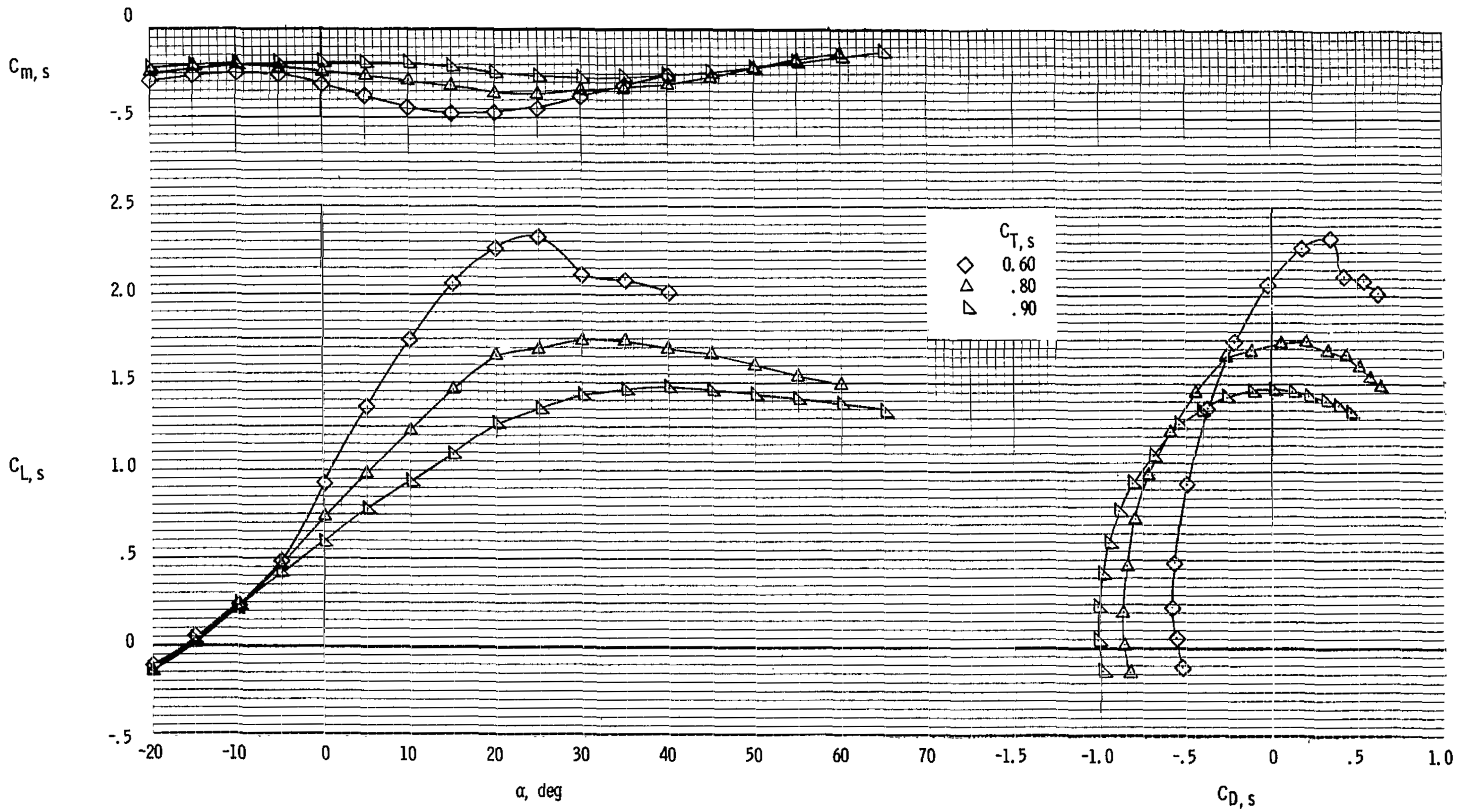

(a) Aerodynamic characteristics.

Figure 17.- Aerodynamic and flow characteristics of model with inboard section of slat deflected 30° and with trailing-edge flap deflected 40°. Up-at-tip rotation.

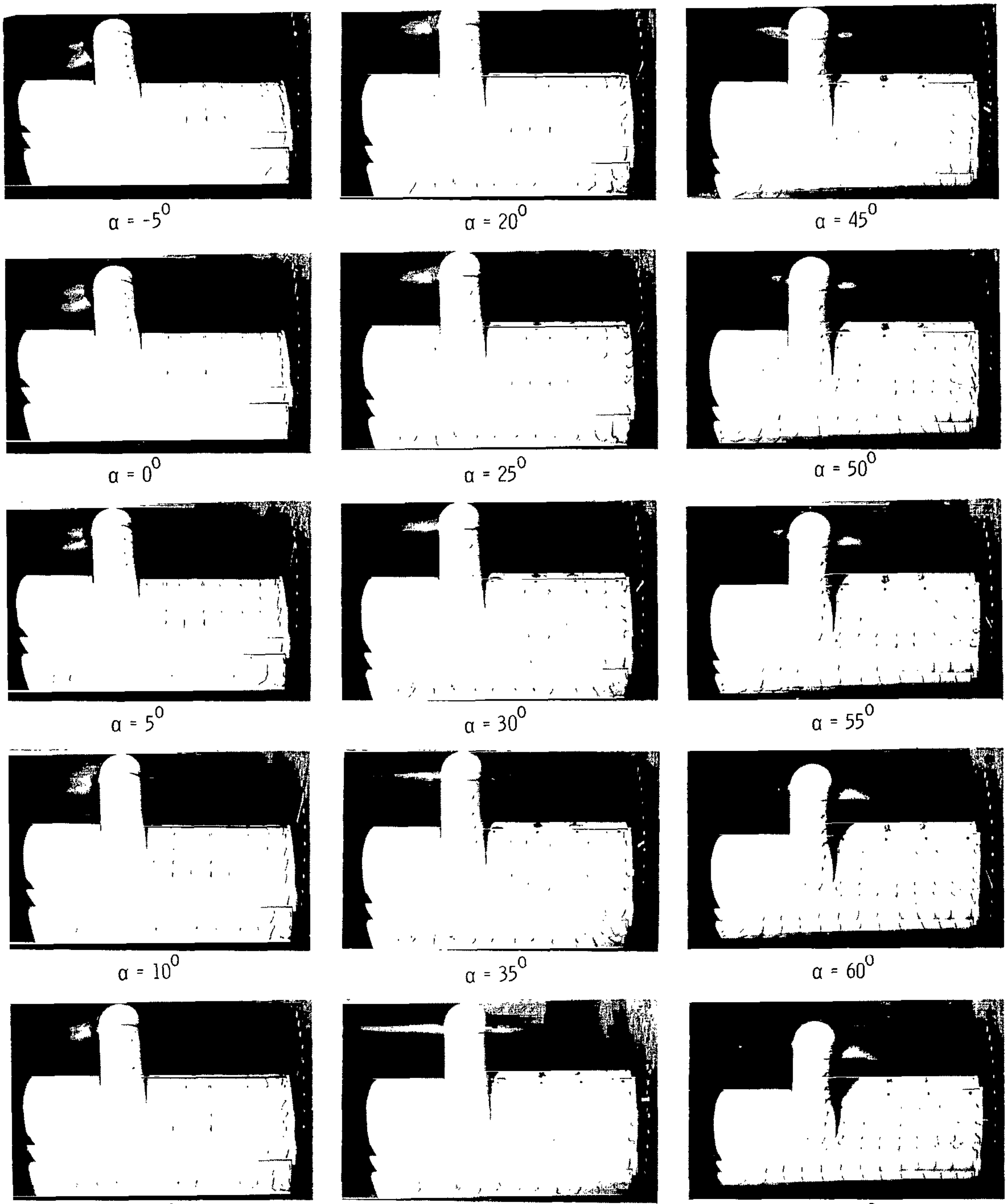

$\alpha = -5^0$ $\alpha = 0^0$ $\alpha = 5^0$ $\alpha = 10^0$ $\alpha = 15^0$

$\alpha = 20^0$ $\alpha = 25^0$ $\alpha = 30^0$ $\alpha = 35^0$ $\alpha = 40^0$

$\alpha = 45^0$ $\alpha = 50^0$ $\alpha = 55^0$ $\alpha = 60^0$ $\alpha = 65^0$

(b) Flow characteristics; $C_{T,s} = 0.90$. L-66-1066

Figure 17.- Continued.

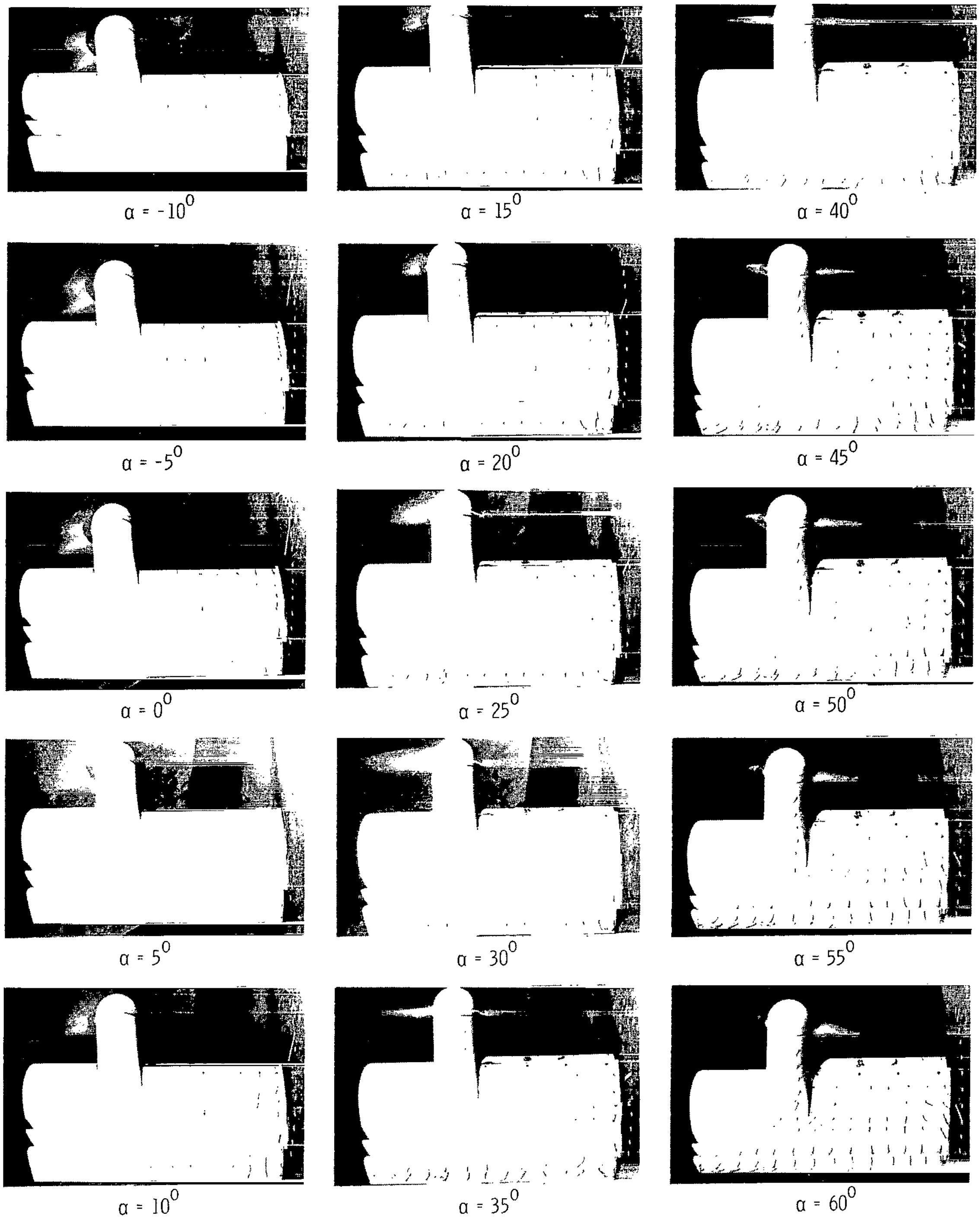

(c) Flow characteristics; $C_{T,s} = 0.80$. L-66-1067

Figure 17.- Continued.

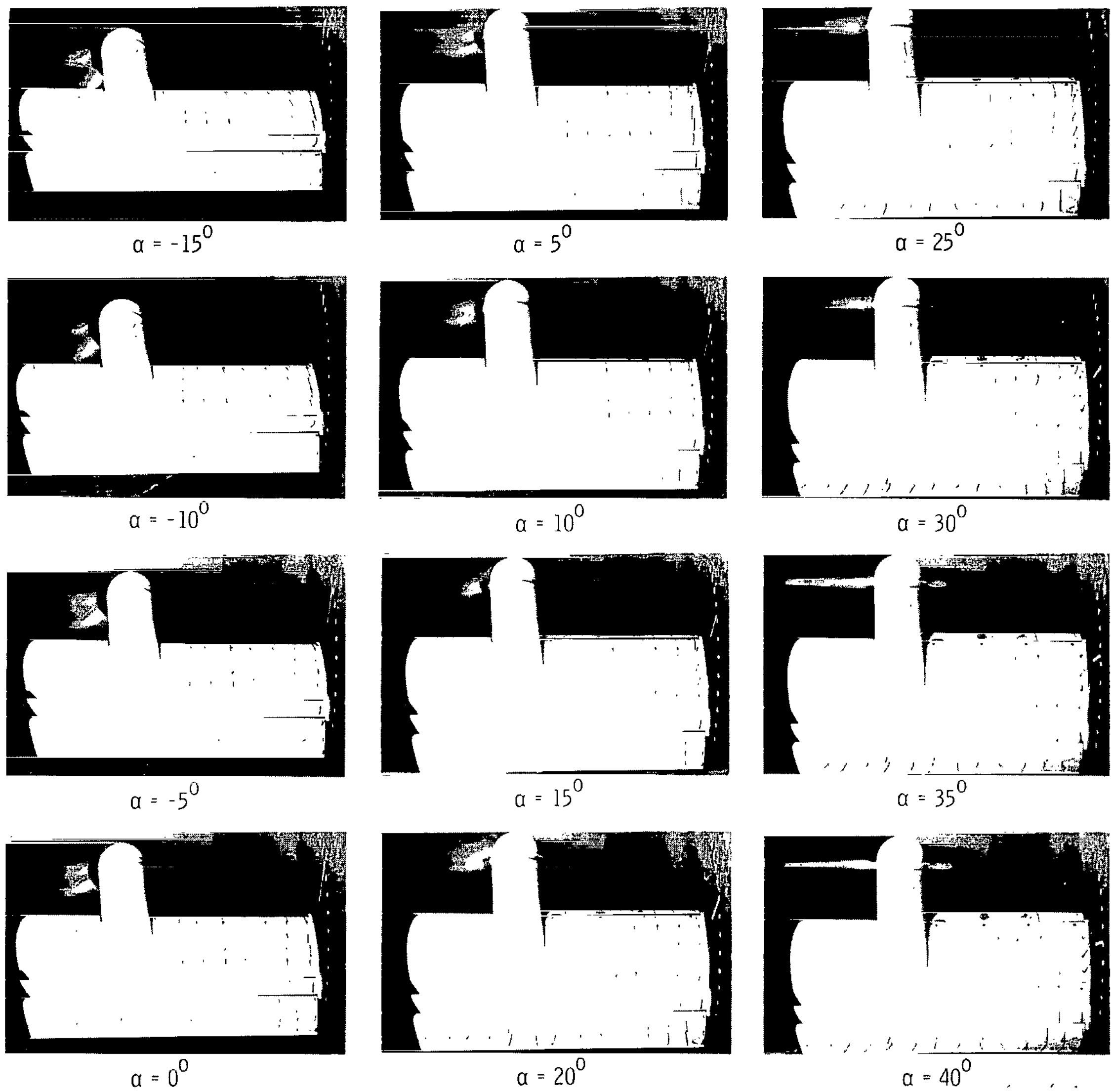

(d) Flow characteristics; $C_{T,s} = 0.60$. L-66-1068

Figure 17.- Concluded.

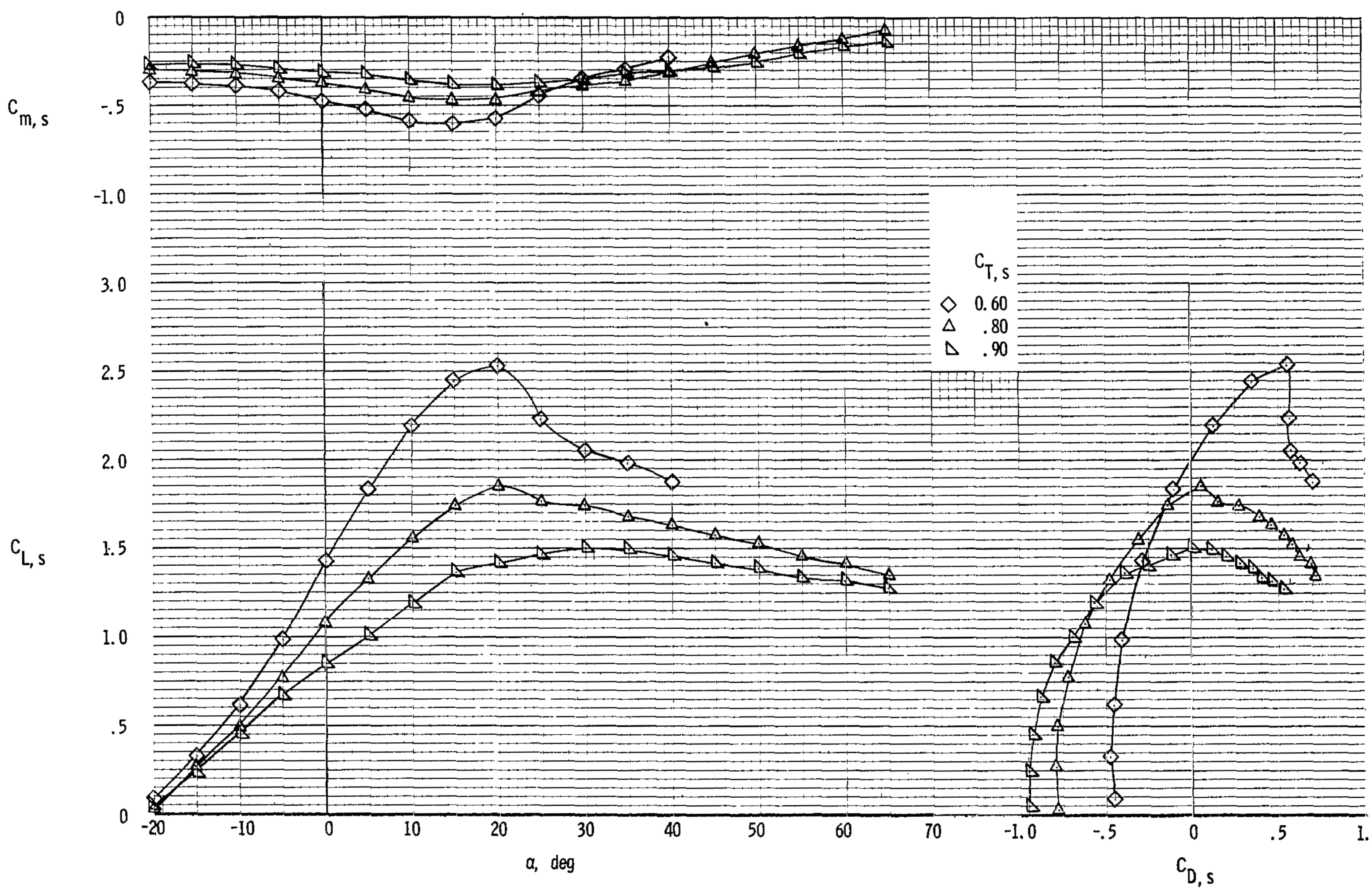

(a) Aerodynamic characteristics.

Figure 18.- Aerodynamic and flow characteristics of model with inboard section of slat deflected 30° and with trailing-edge flap deflected 60°. Up-at-tip rotation.

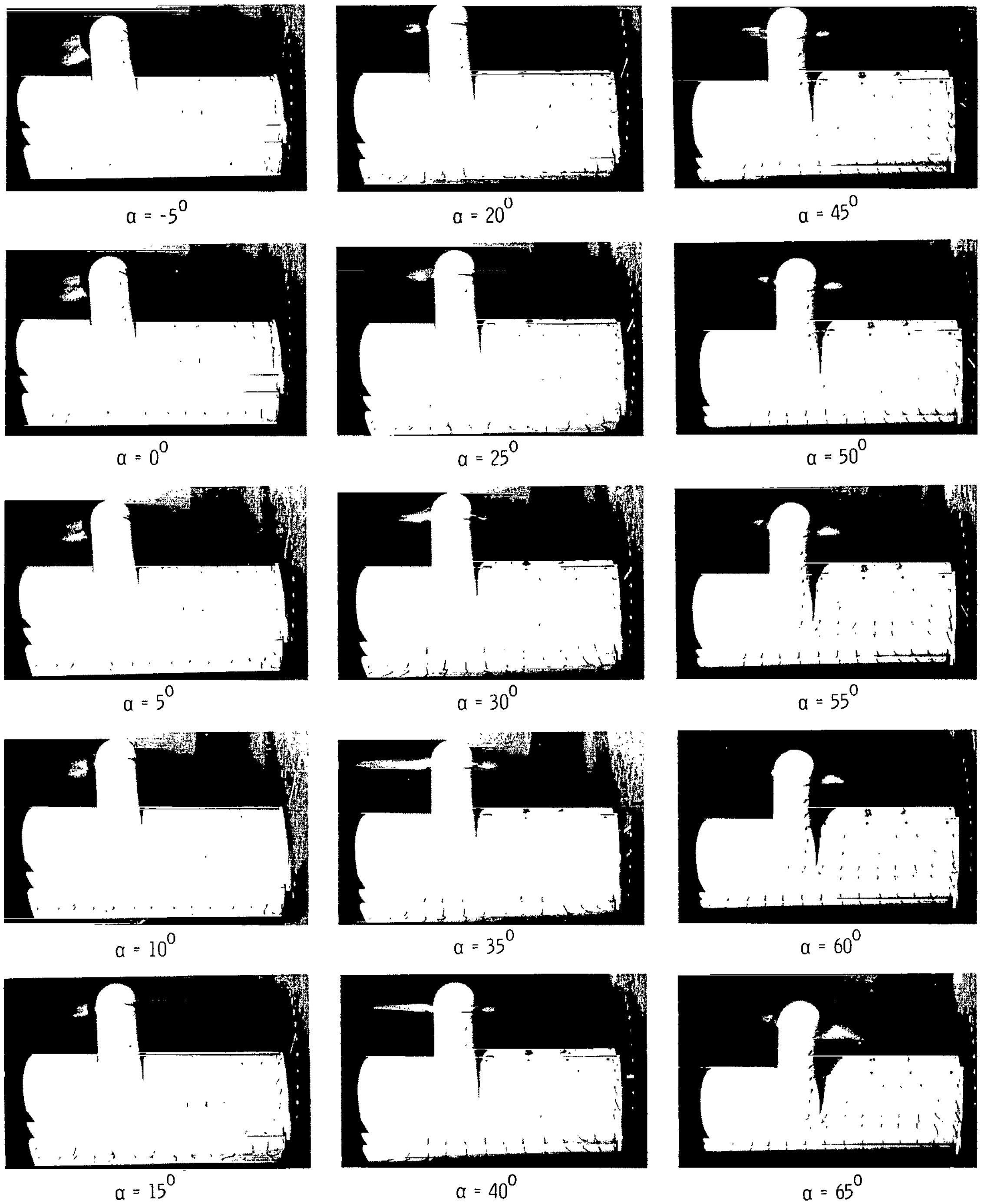

(b) Flow characteristics; $C_{T,s} = 0.90$. L-66-1069

Figure 18.- Continued.

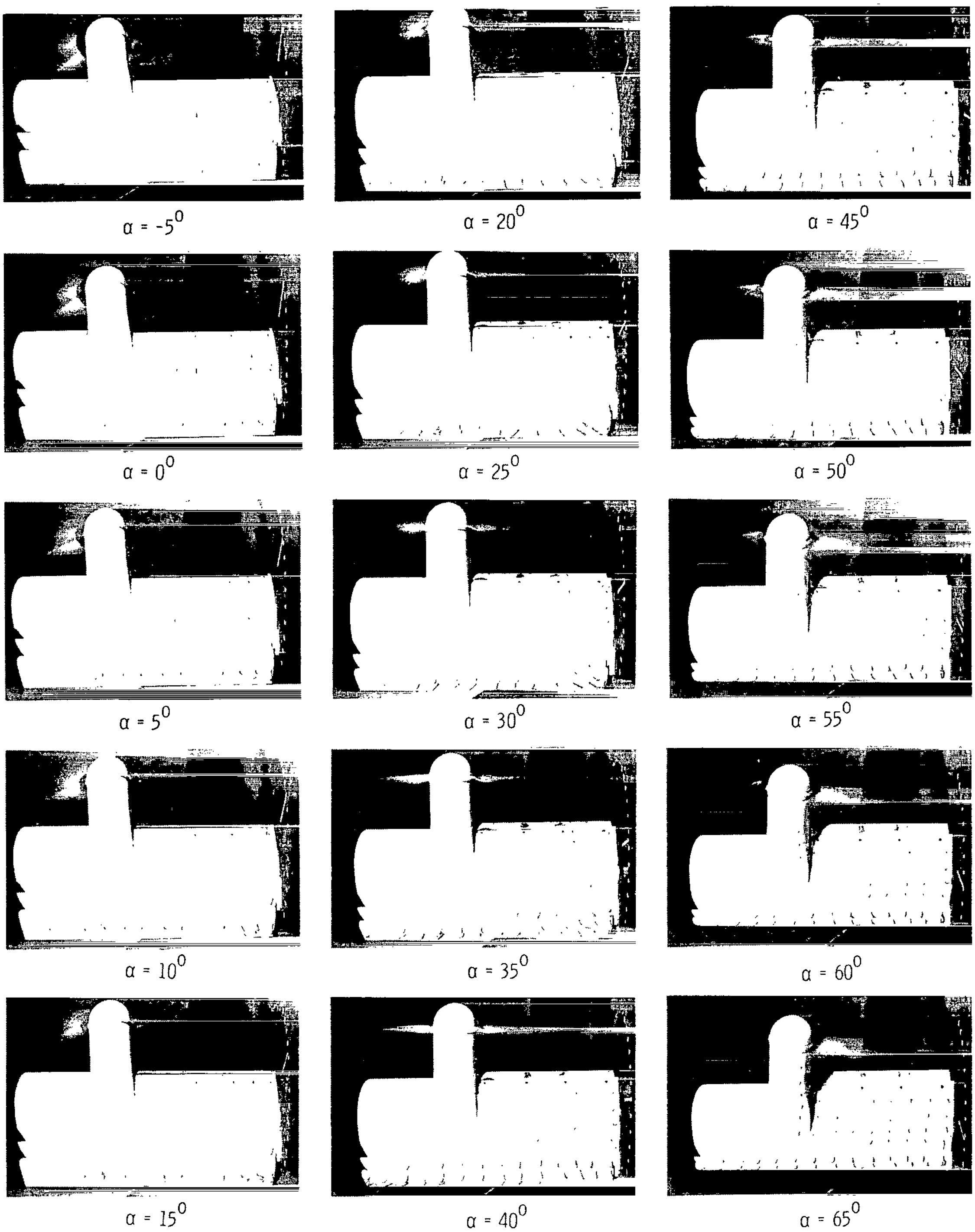

(c) Flow characteristics; $C_{T,s} = 0.80$. L-66-1070

Figure 18.- Continued.

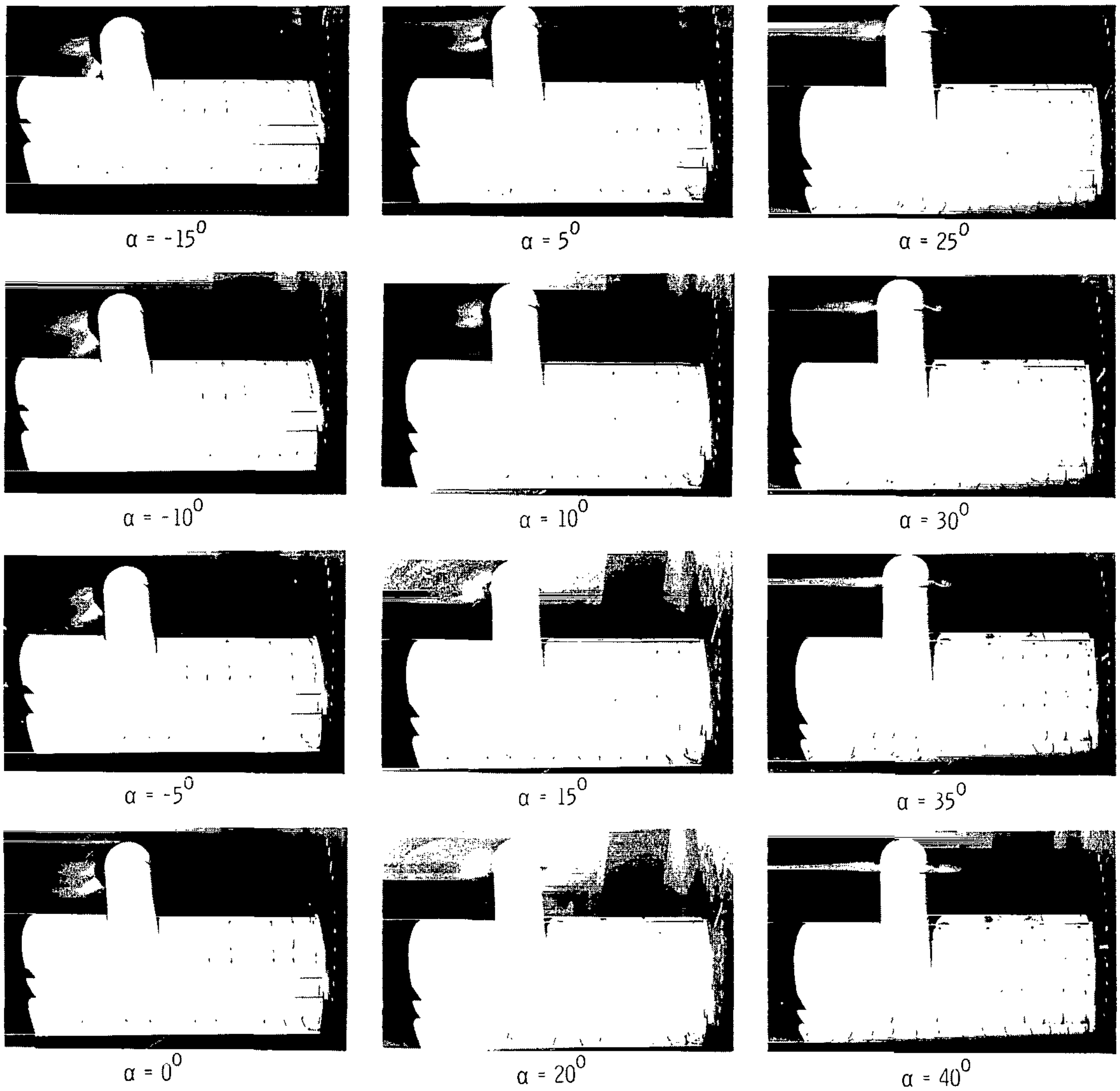

(d) Flow characteristics; $C_{T,s} = 0.60$. L-66-1071

Figure 18.- Concluded.

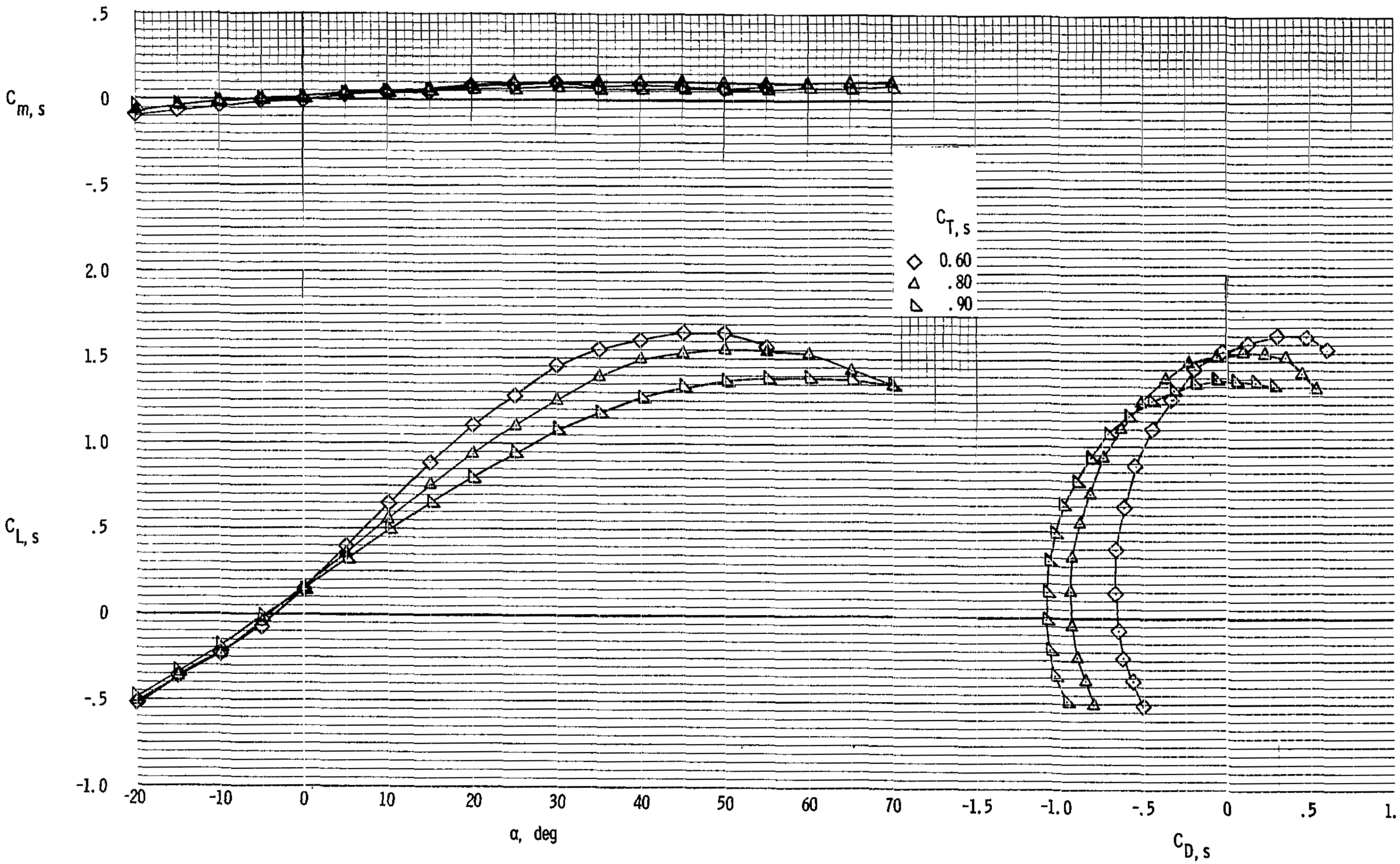

(a) Aerodynamic characteristics.

Figure 19.- Aerodynamic and flow characteristics of model with inboard section of slat deflected 30° and with trailing-edge flap undeflected. $\delta_f = 0^\circ$. Fences on. Up-at-tip rotation.

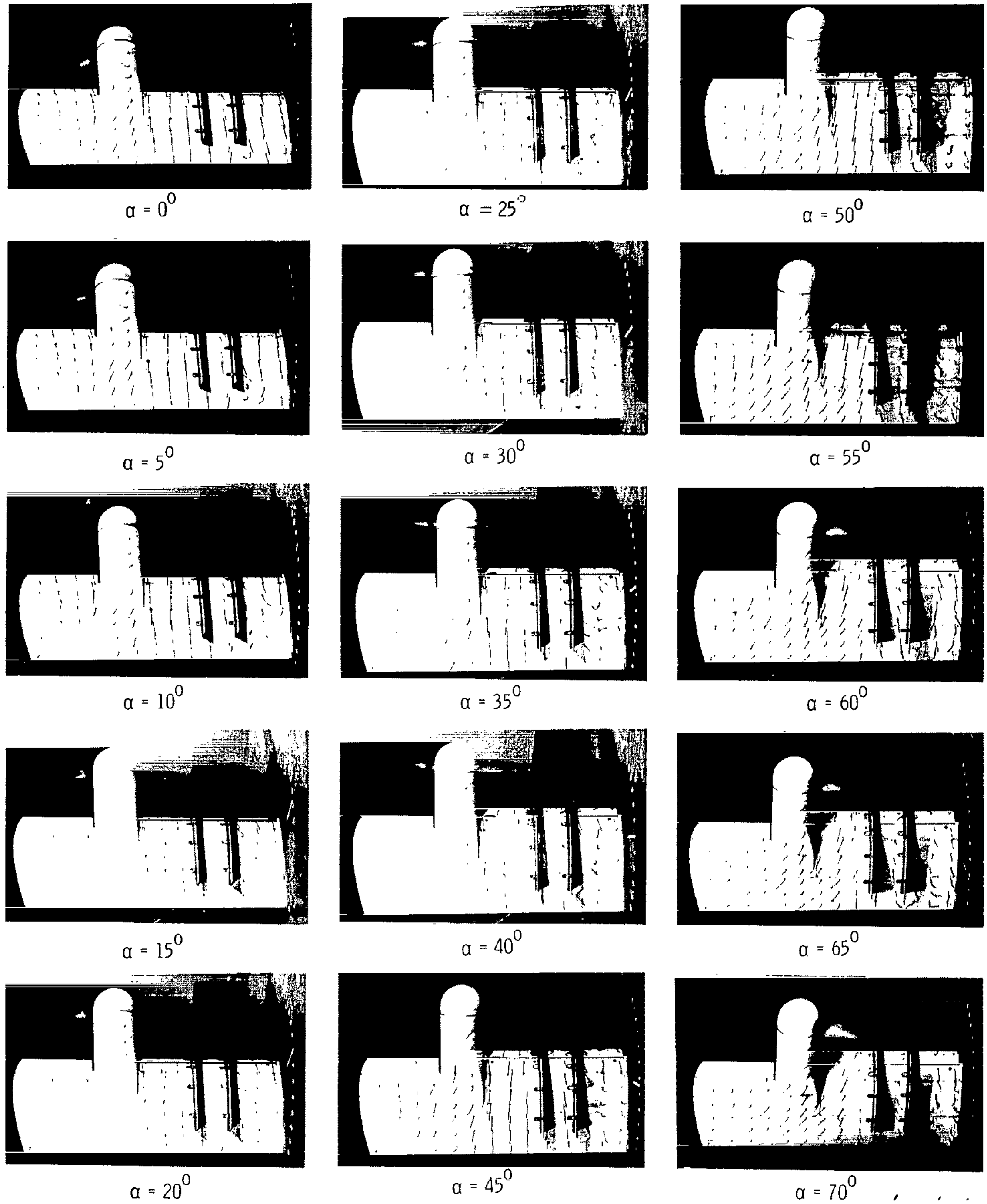

(b) Flow characteristics; $C_{T,s} = 0.90$. L-66-1072

Figure 19.- Continued.

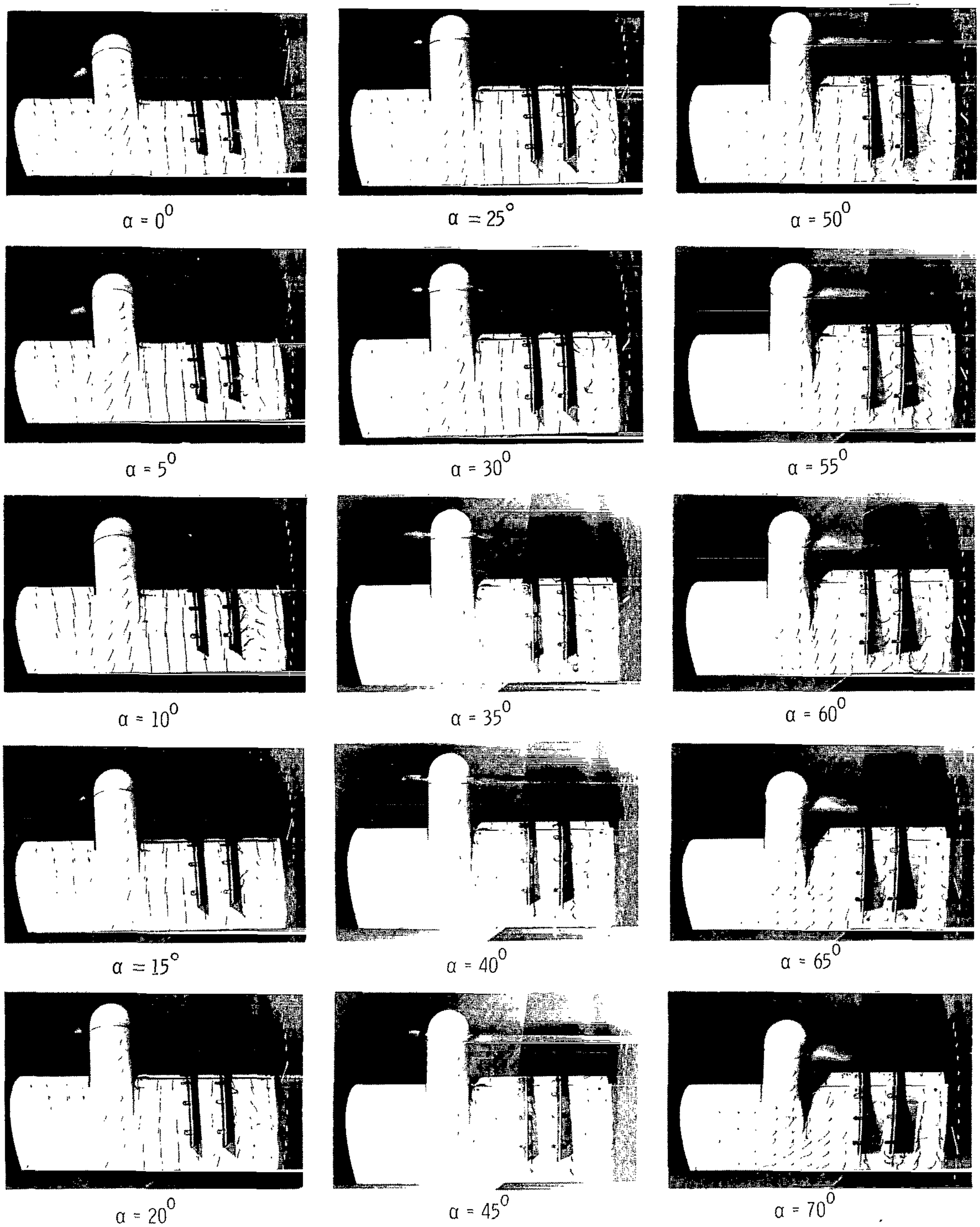

(c) Flow characteristics; $C_{T,s} = 0.80$. L-66-1073

Figure 19.- Continued.

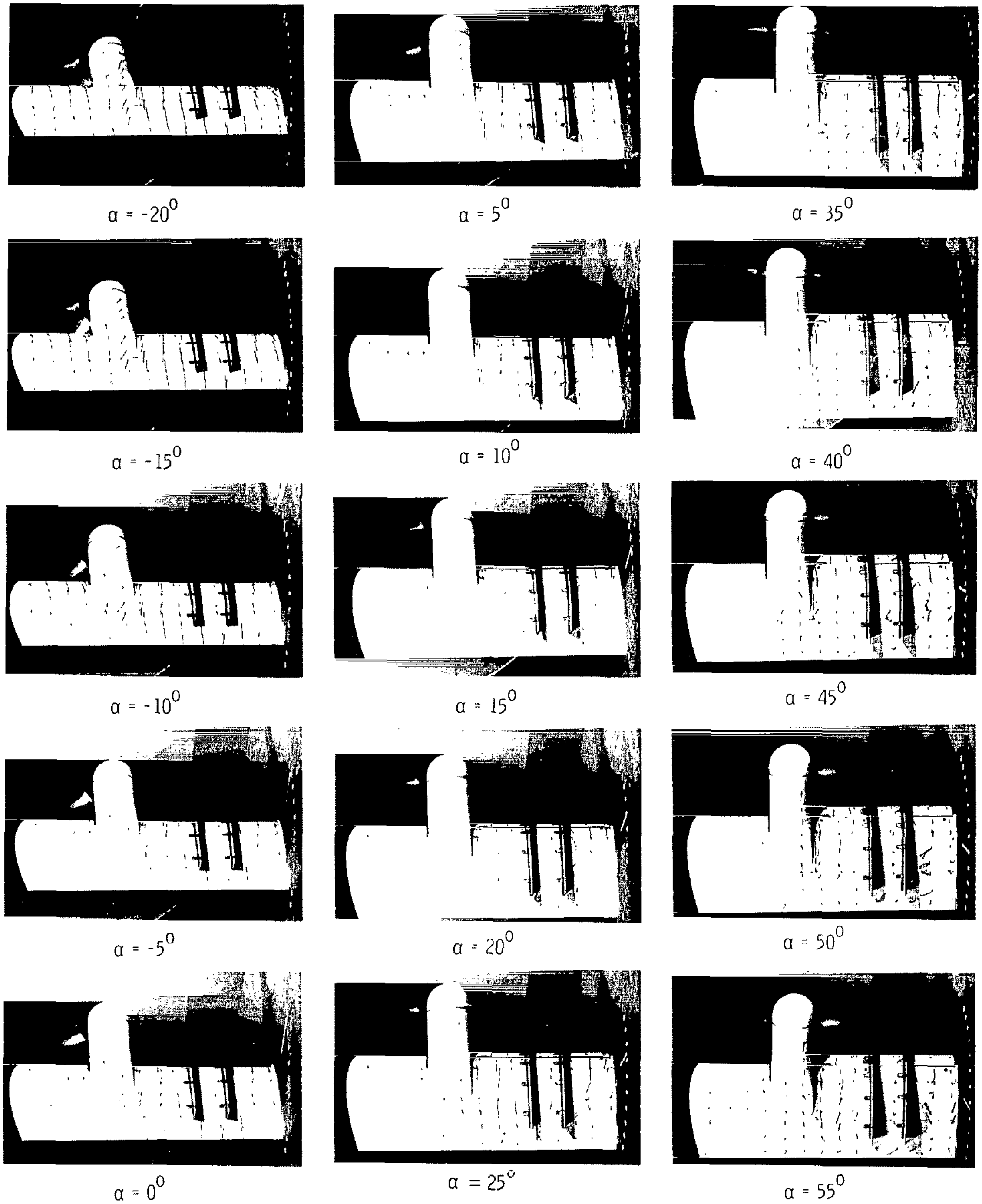

(d) Flow characteristics; $C_{T,s} = 0.60$.

L-66-1074

Figure 19.- Concluded.

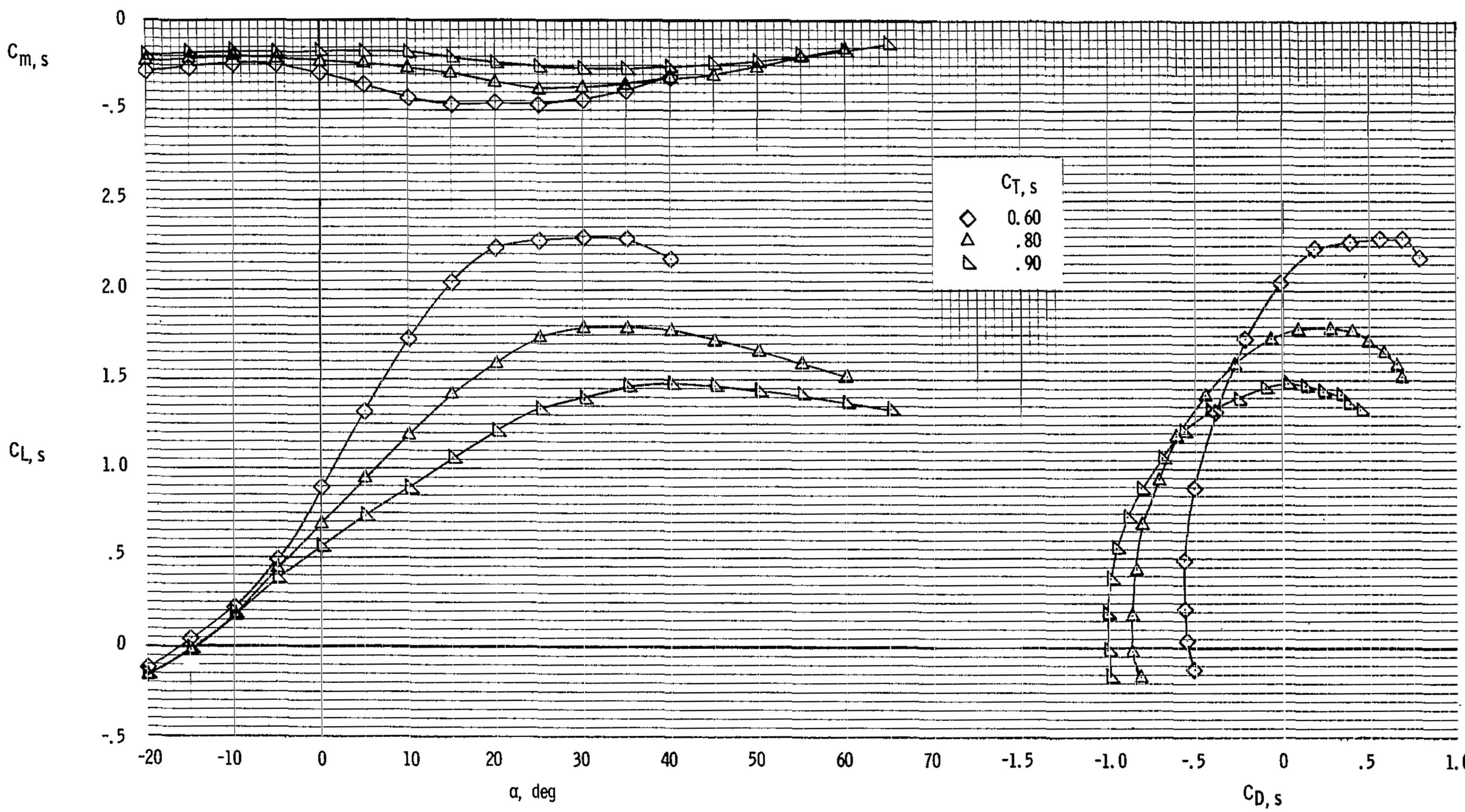

(a) Aerodynamic characteristics.

Figure 20.- Aerodynamic and flow characteristics of model with inboard section of slat deflected 30° and with trailing-edge flap deflected 40°. Fences on. Up-at-tip rotation.

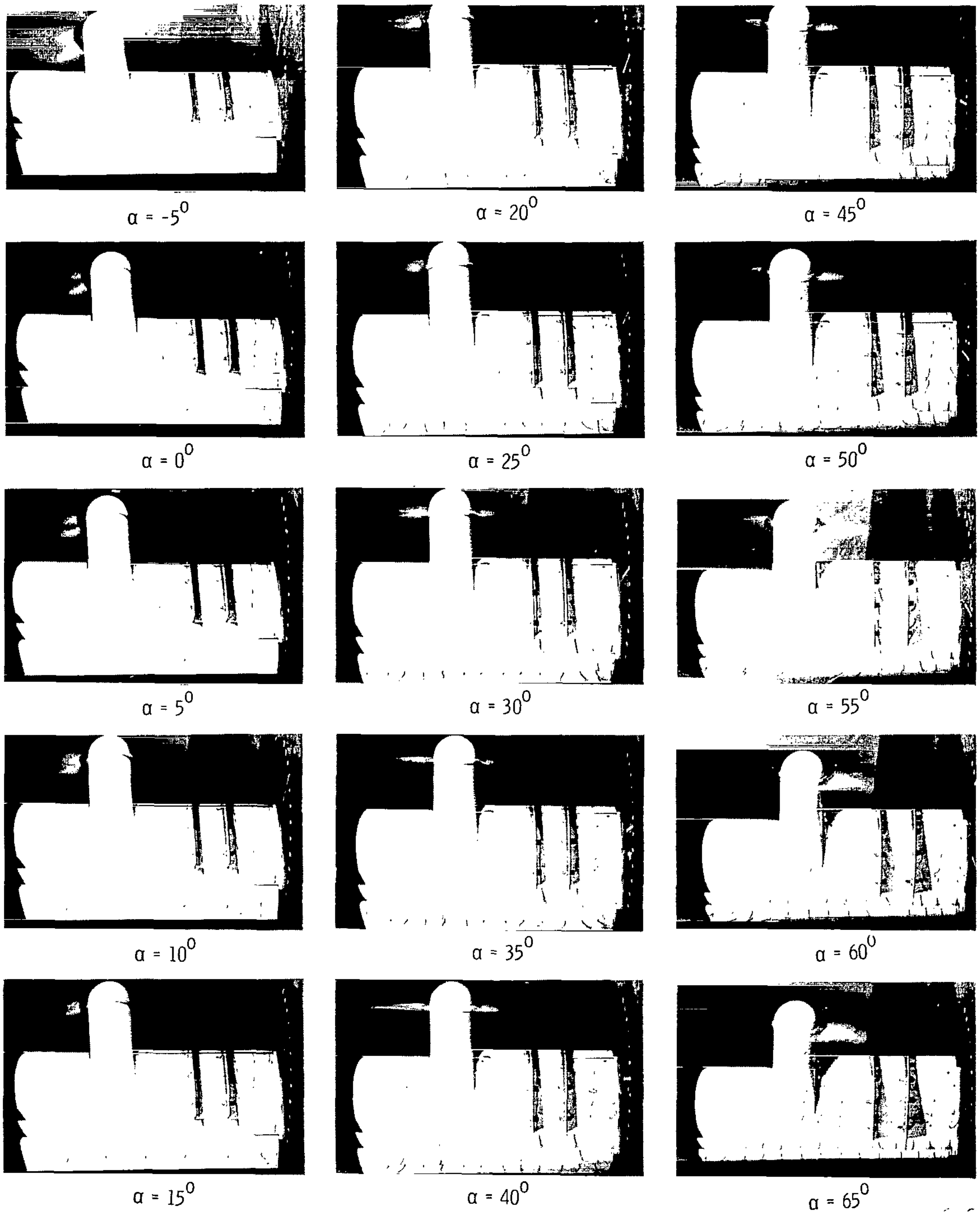

(b) Flow characteristics; $C_{T,s} = 0.90$. L-66-1075

Figure 20.- Continued.

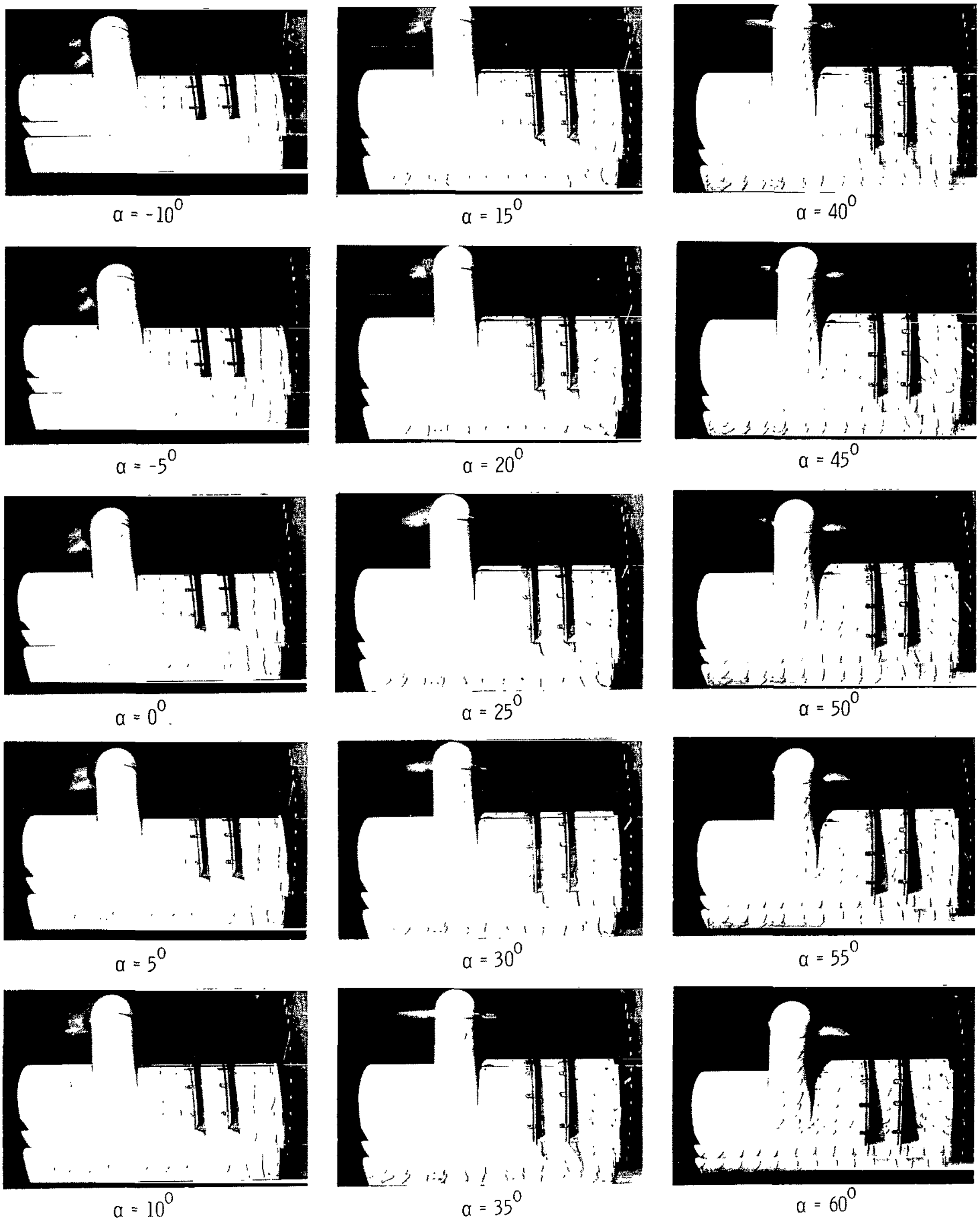

(c) Flow characteristics; $C_{T,s} = 0.80$.

L-66-1076

Figure 20.- Continued.

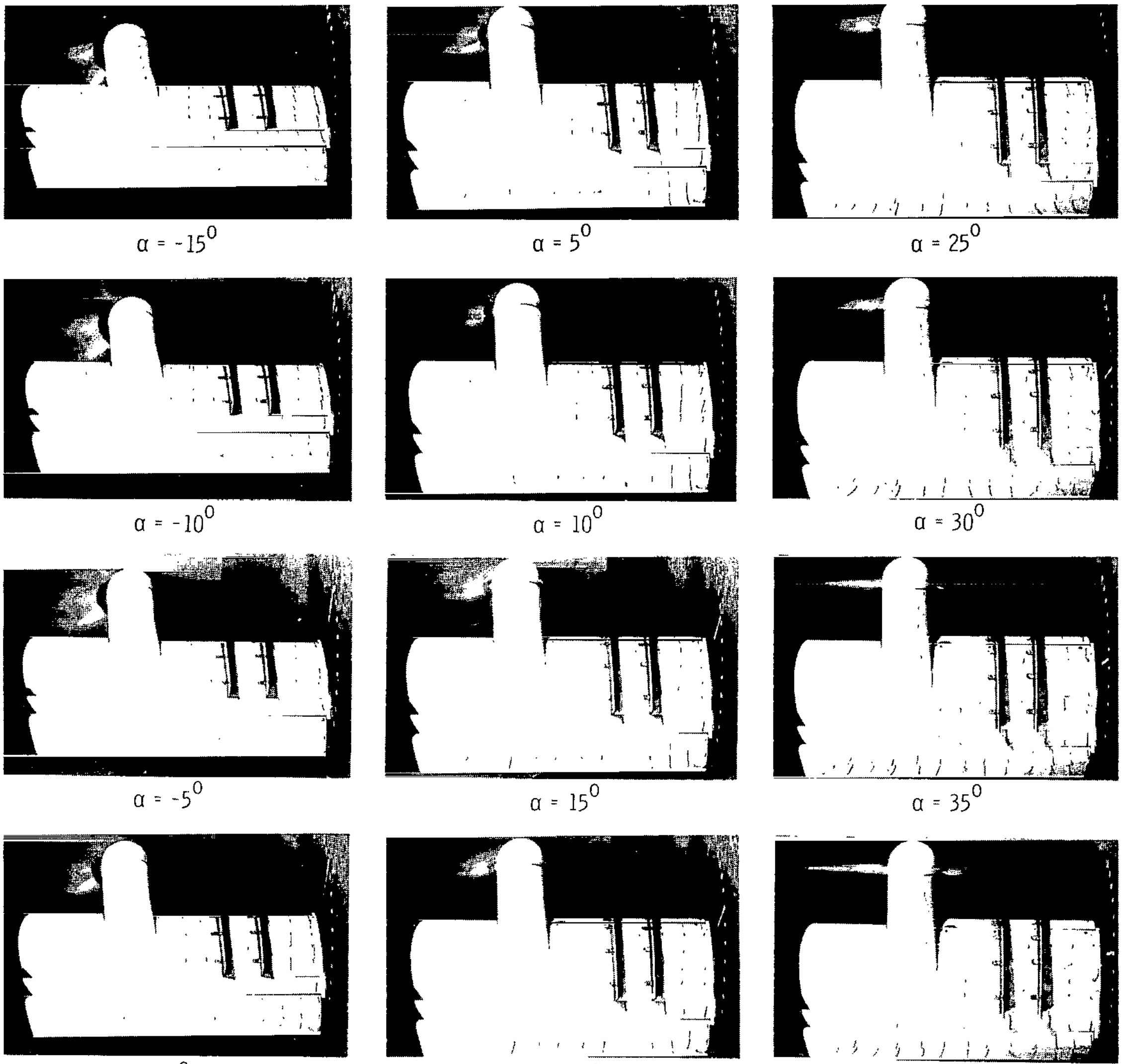

(d) Flow characteristics; $C_{T,s} = 0.60$.

L-66-1077

Figure 20.- Concluded.

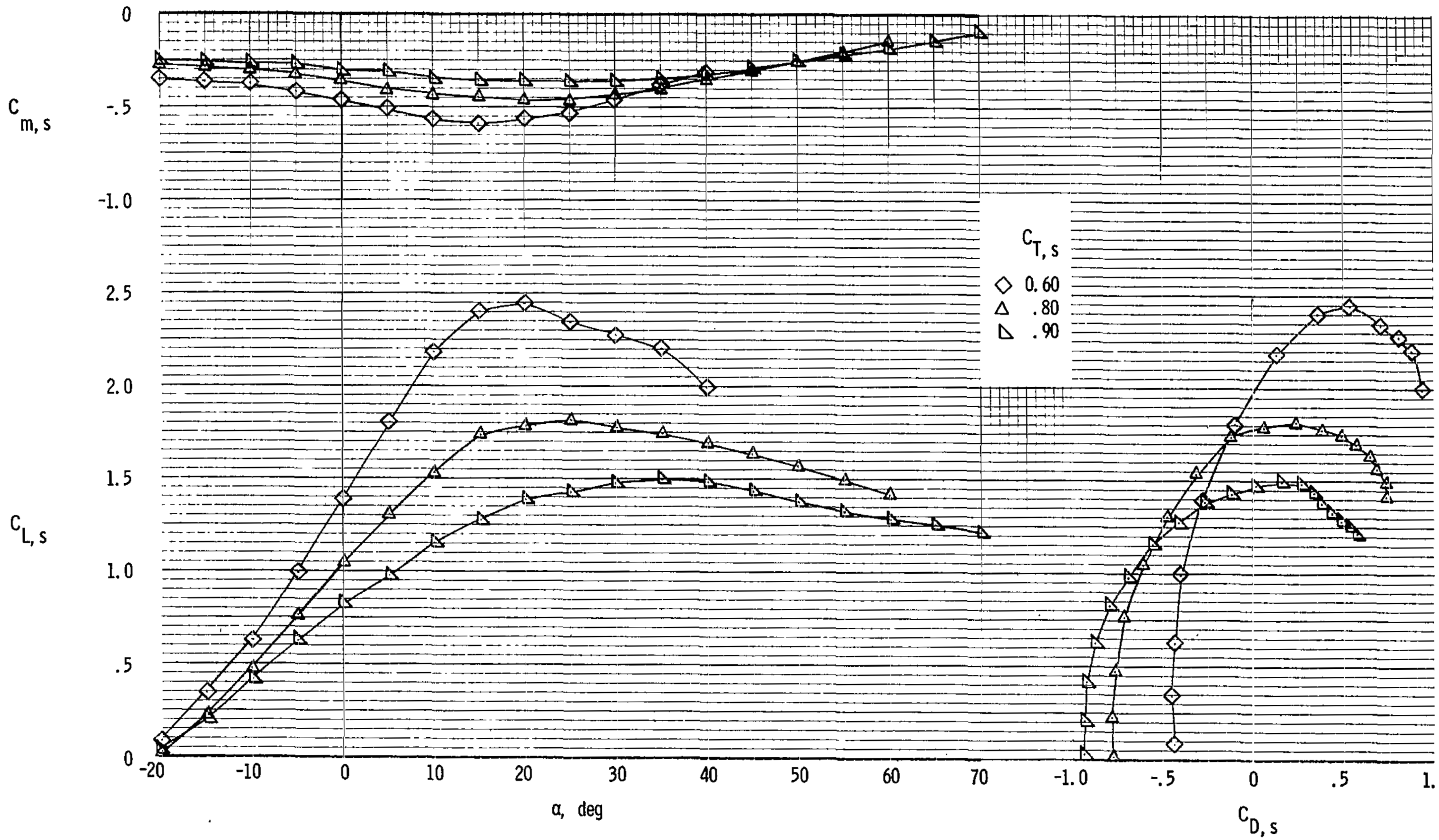

(a) Aerodynamic characteristics.

Figure 21.- Aerodynamic and flow characteristics of model with inboard section of slat deflected 30° and with trailing-edge flap deflected 60°. Fences on. Up-at-tip rotation.

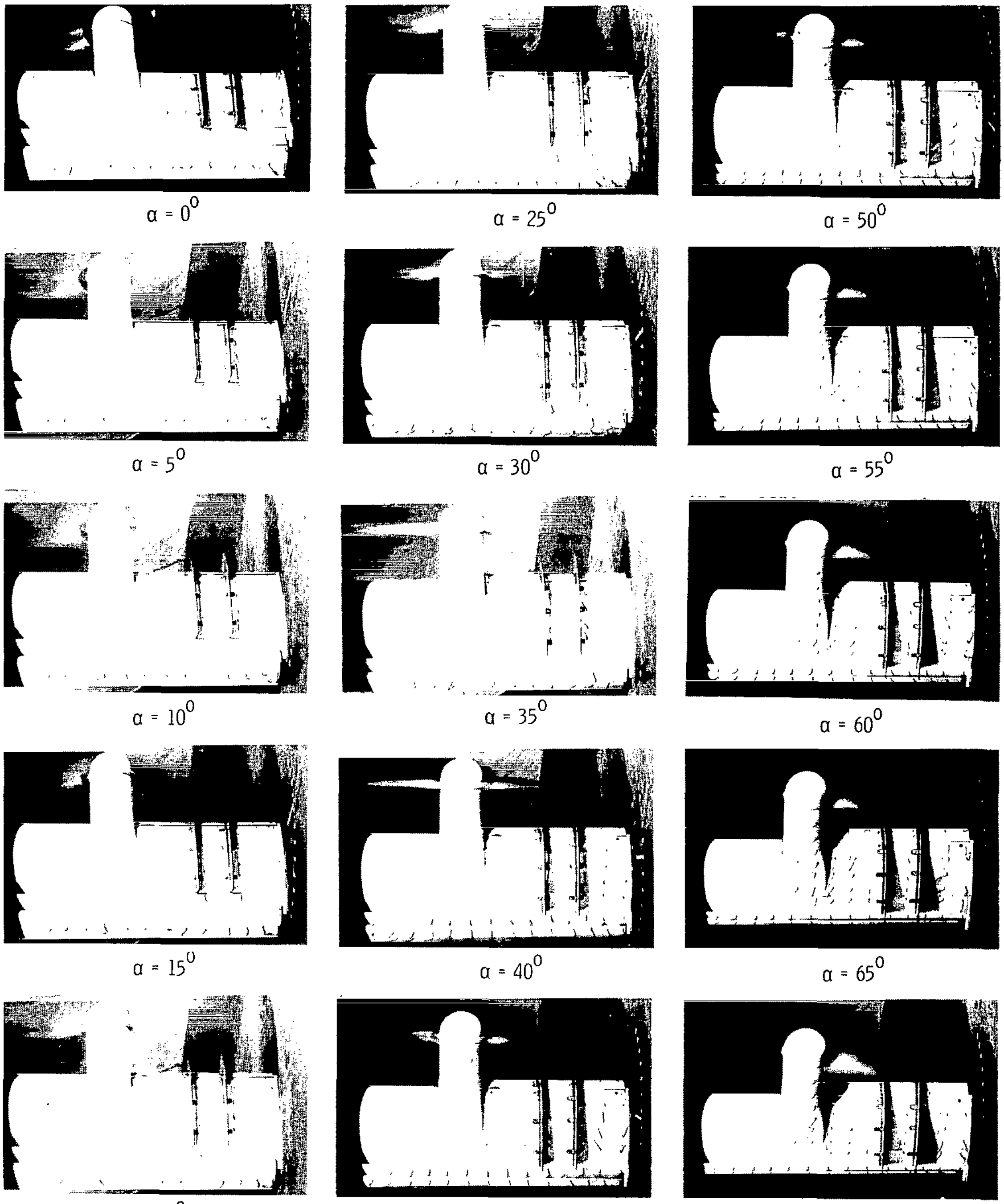

$\alpha = 0^0$ $\alpha = 25^0$ $\alpha = 50^0$

$\alpha = 5^0$ $\alpha = 30^0$ $\alpha = 55^0$

$\alpha = 10^0$ $\alpha = 35^0$ $\alpha = 60^0$

$\alpha = 15^0$ $\alpha = 40^0$ $\alpha = 65^0$

$\alpha = 20^0$ $\alpha = 45^0$ $\alpha = 70^0$

(b) Flow characteristics; $C_{T,s} = 0.90$. L-66-1078

Figure 21.- Continued.

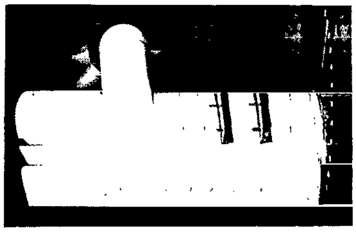

$\alpha = -10^0$

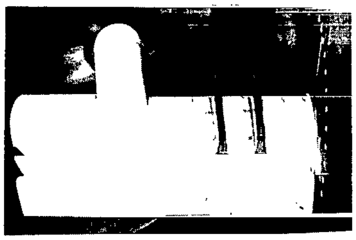

$\alpha = -5^0$

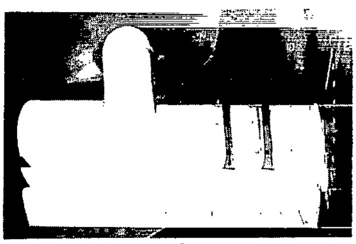

$\alpha = 0^0$

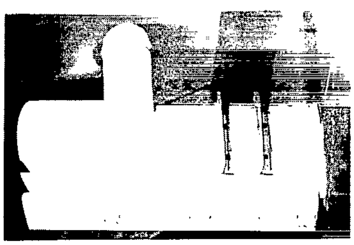

$\alpha = 5^0$

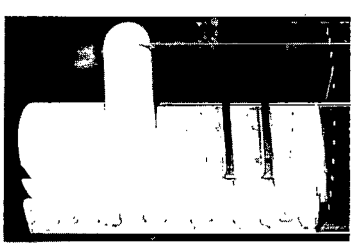

$\alpha = 10^0$

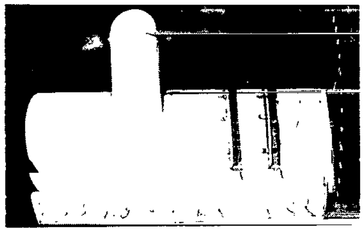

$\alpha = 15^0$

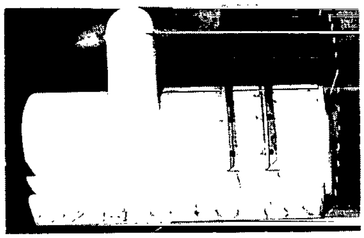

$\alpha = 20^0$

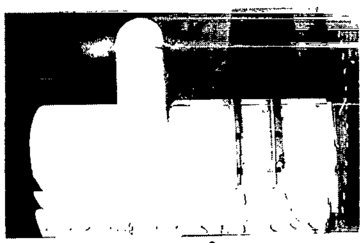

$\alpha = 25^0$

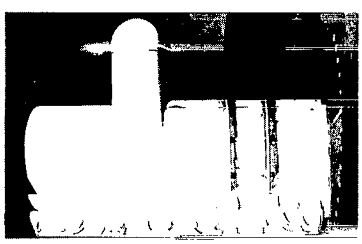

$\alpha = 30^0$

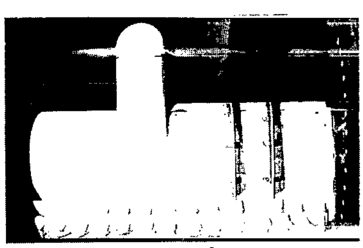

$\alpha = 35^0$

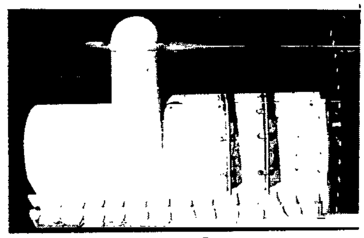

$\alpha = 40^0$

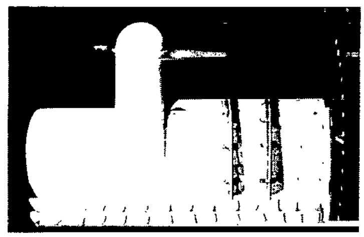

$\alpha = 45^0$

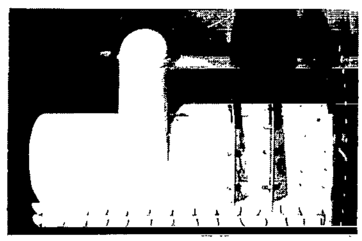

$\alpha = 50^0$

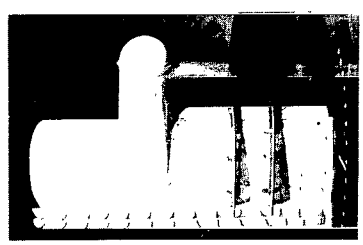

$\alpha = 55^0$

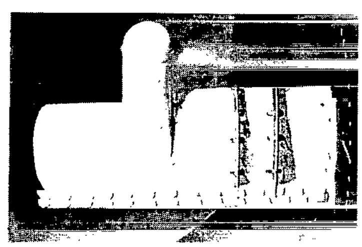

$\alpha = 60^0$

(c) Flow characteristics; $C_{T,s} = 0.80$. L-66-1079

Figure 21.- Continued.

(d) Flow characteristics; $C_{T,s} = 0.60$. L-66-1080

Figure 21.- Concluded.

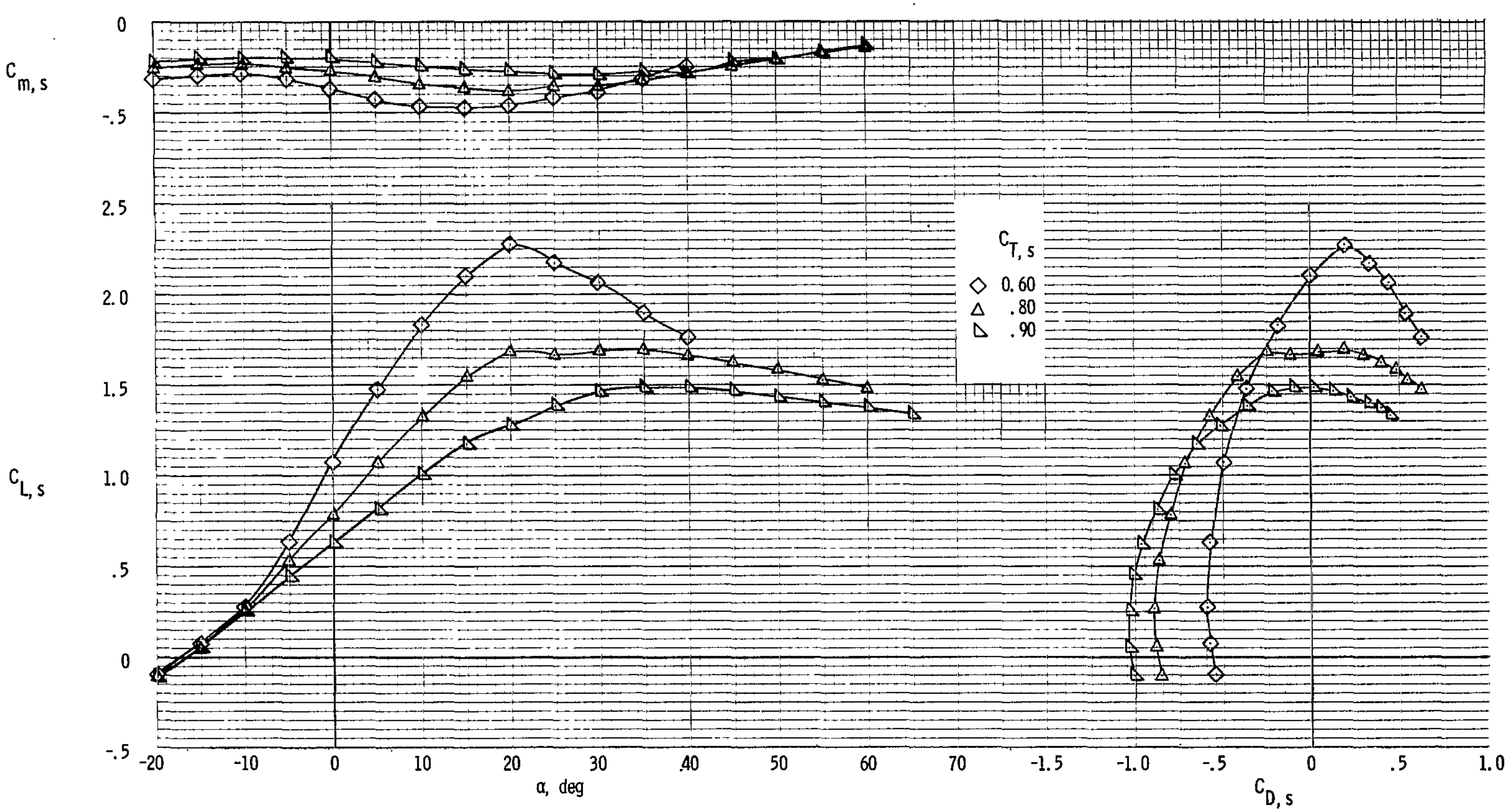

(a) Aerodynamic characteristics.

Figure 22.- Aerodynamic and flow characteristics of model with inboard section of slat deflected 10° (high position) and with trailing-edge flap deflected 40°. Up-at-tip rotation.

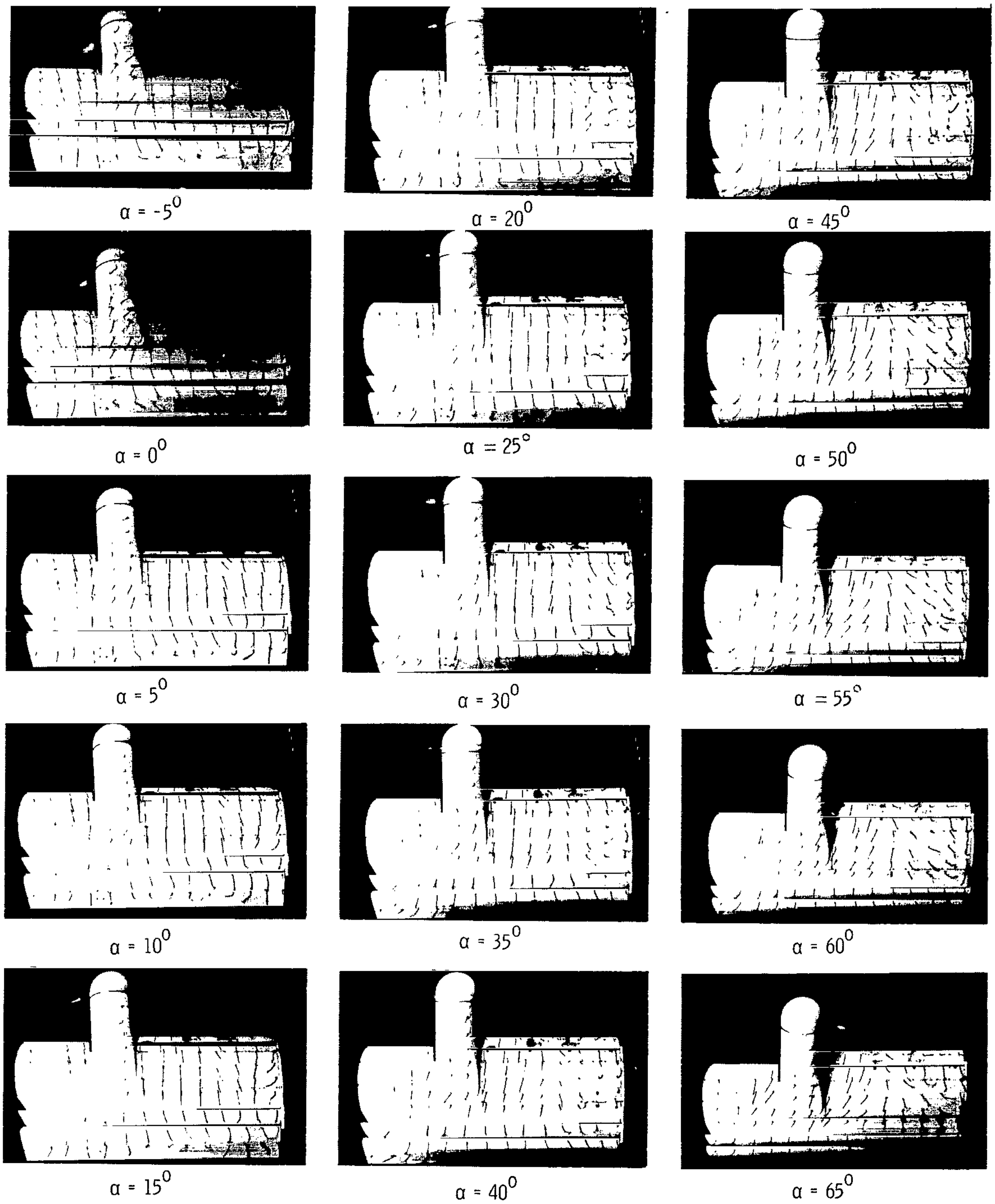

(b) Flow characteristics; $C_{T,s} = 0.90$. L-66-1081

Figure 22.- Continued.

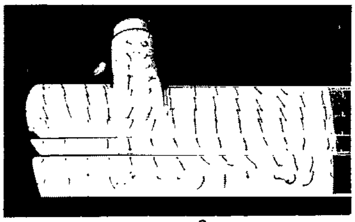

$\alpha = -10^{\circ}$

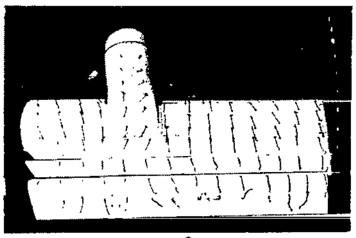

$\alpha = -5^{\circ}$

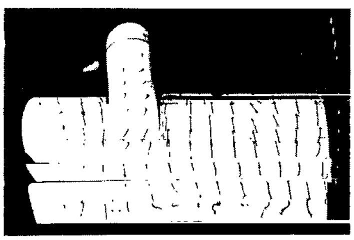

$\alpha = 0^{\circ}$

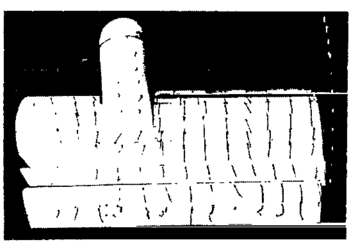

$\alpha = 5^{\circ}$

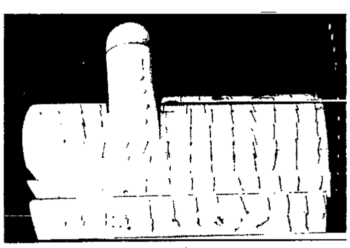

$\alpha = 10^{\circ}$

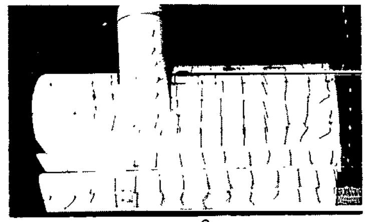

$\alpha = 15^{\circ}$

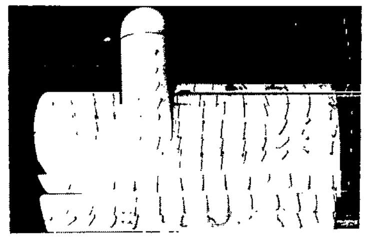

$\alpha = 20^{\circ}$

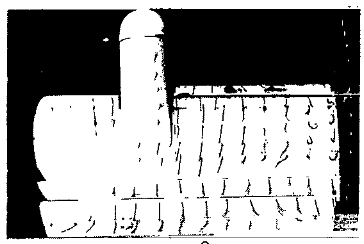

$\alpha = 25^{\circ}$

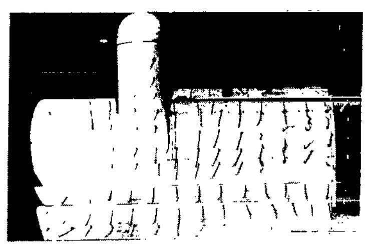

$\alpha = 30^{\circ}$

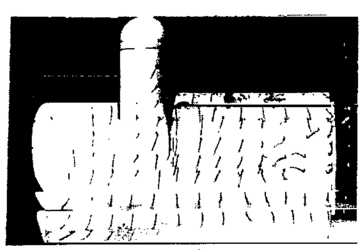

$\alpha = 35^{\circ}$

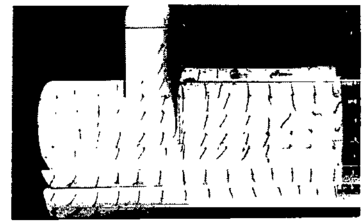

$\alpha = 40^{\circ}$

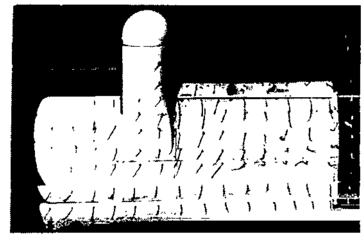

$\alpha = 45^{\circ}$

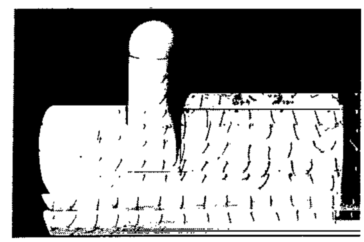

$\alpha = 50^{\circ}$

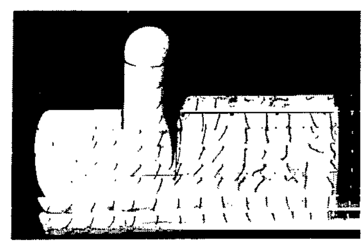

$\alpha = 55^{\circ}$

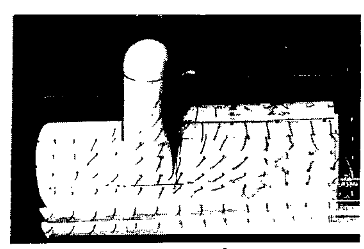

$\alpha = 60^{\circ}$

(c) Flow characteristics; $C_{T,s} = 0.80$. L-66-1082

Figure 22.- Continued.

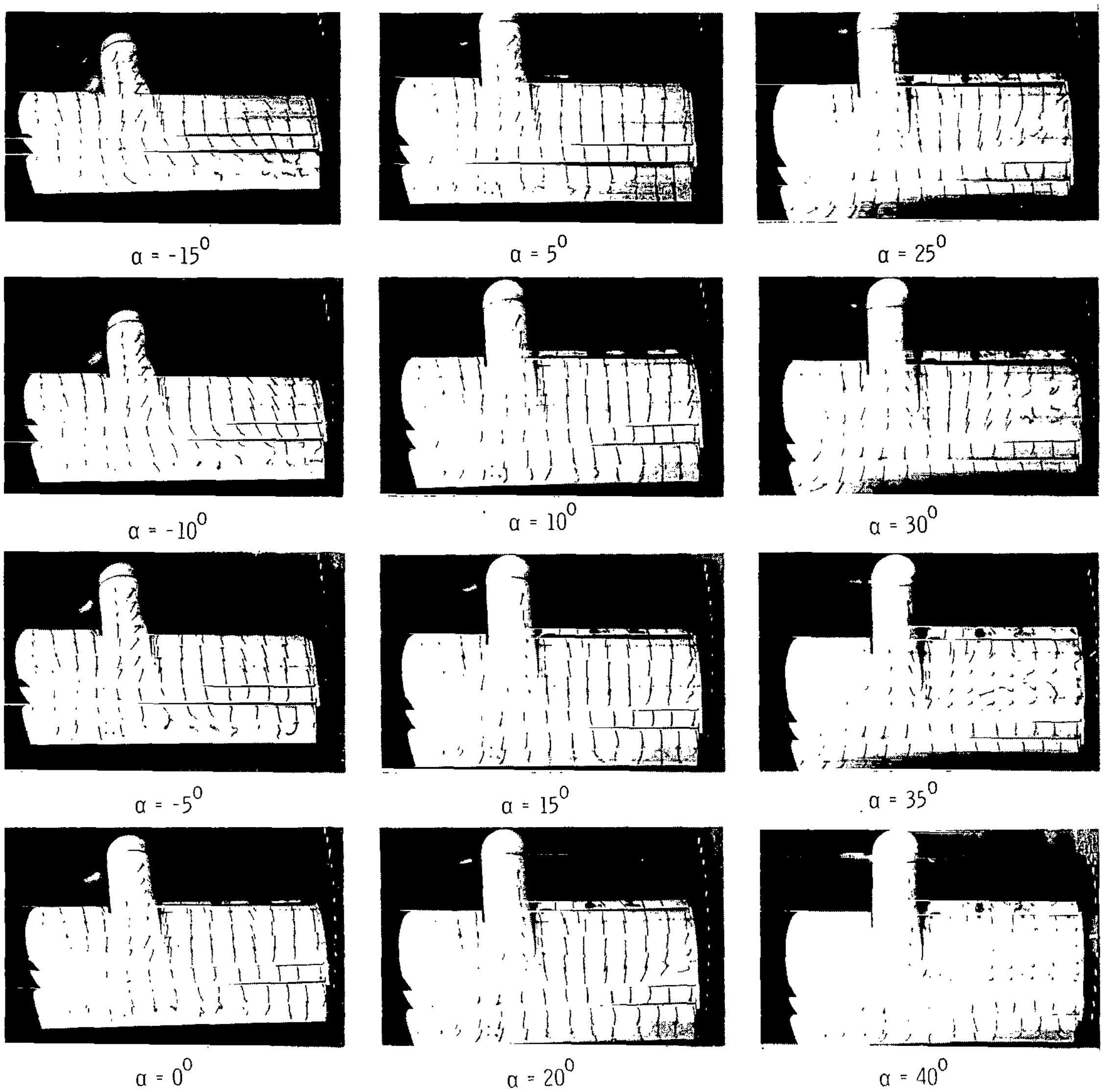

(d) Flow characteristics; $C_{T,s} = 0.60$.

L-66-1083

Figure 22.- Concluded.

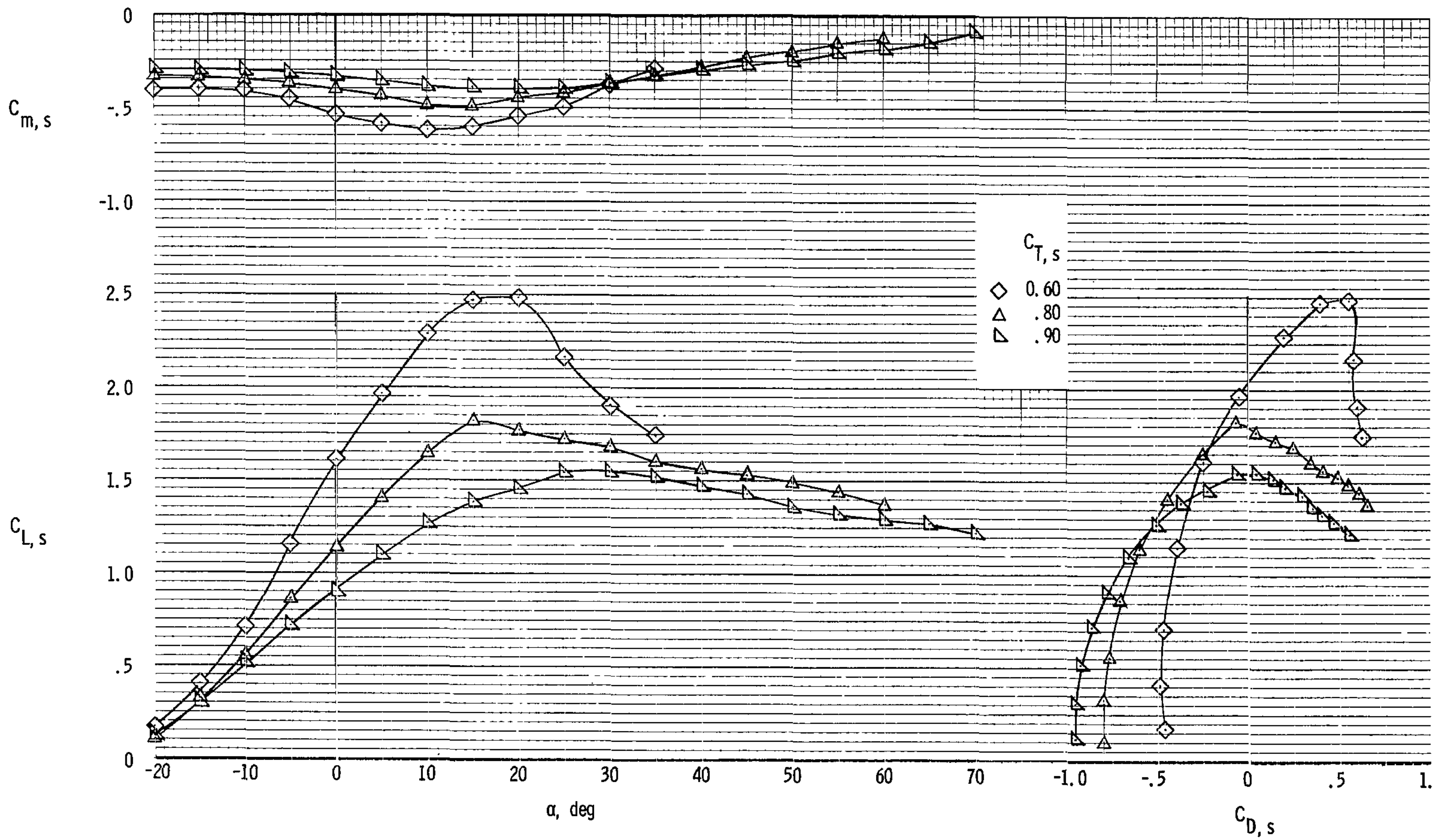

(a) Aerodynamic characteristics.

Figure 23.- Aerodynamic and flow characteristics of model with inboard section of slat deflected 10° (high position) and with trailing-edge flap deflected 60°. Up-at-tip rotation.

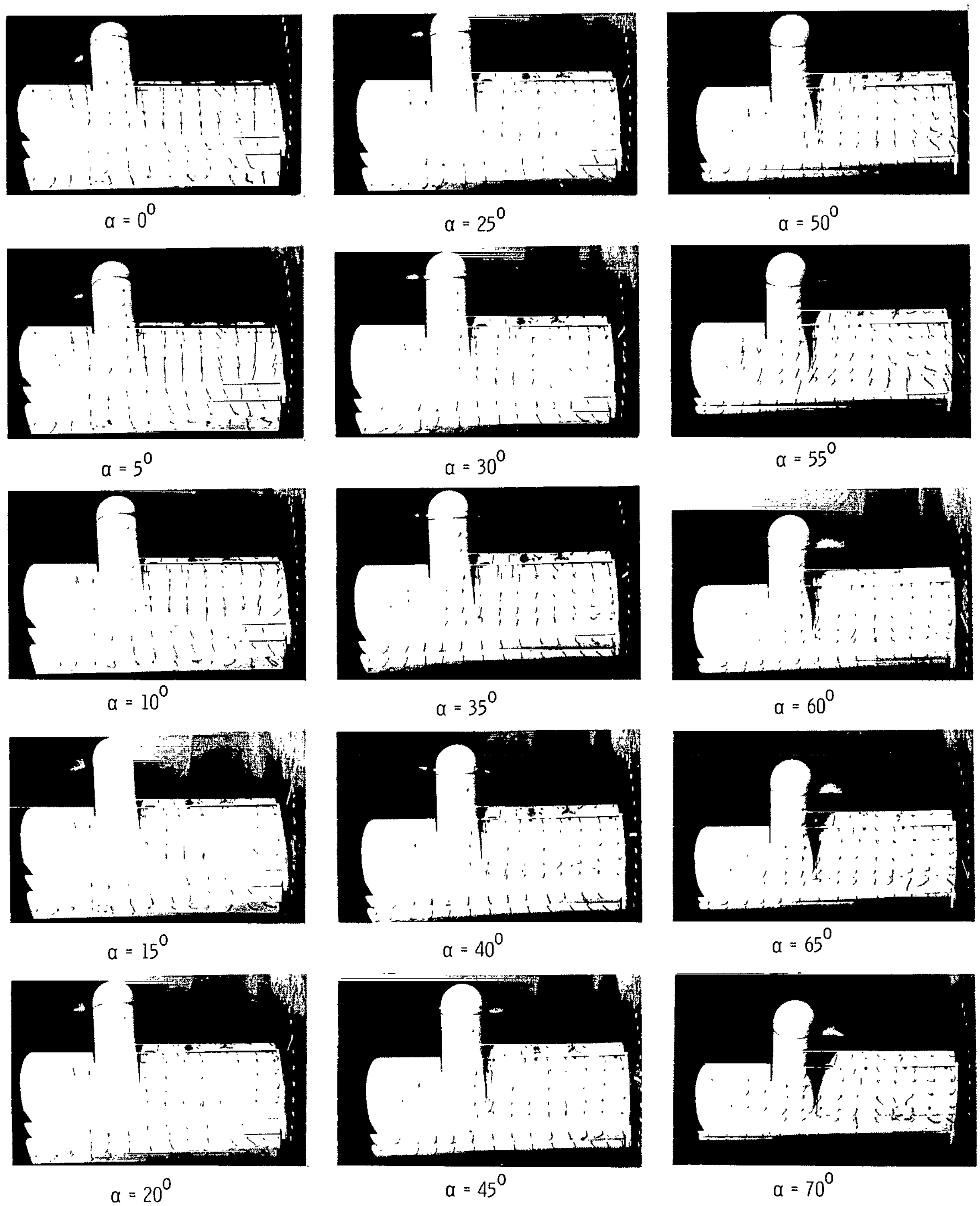

(b) Flow characteristics; $C_{T,s} = 0.90$. L-66-1084

Figure 23.- Continued.

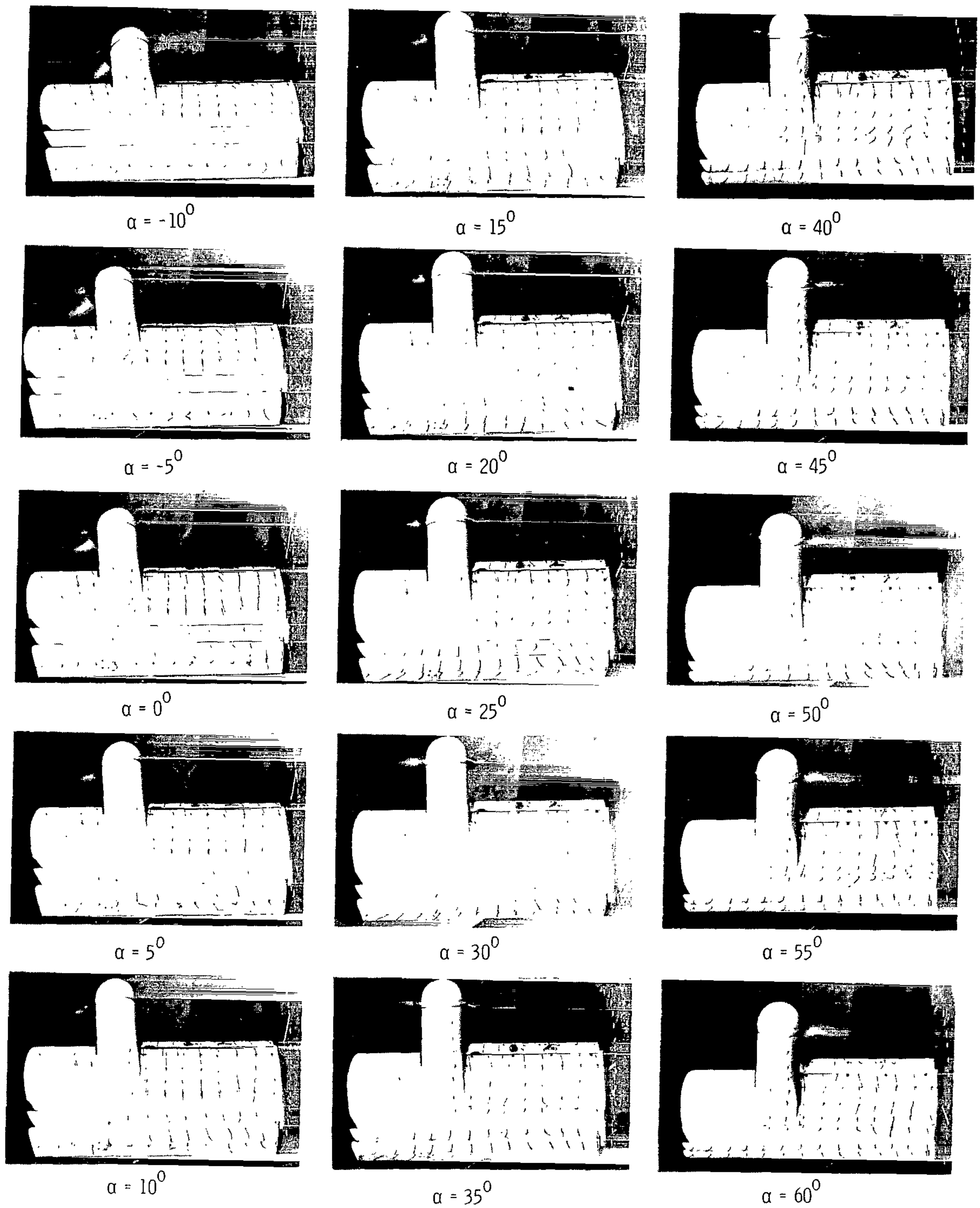

(c) Flow characteristics; $C_{T,s} = 0.80$. L-66-1085

Figure 23.- Continued.

$\alpha = -20^0$

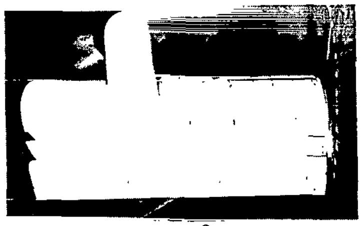

$\alpha = -5^0$

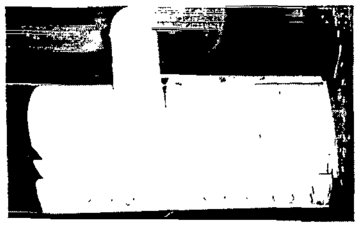

$\alpha = 10^0$

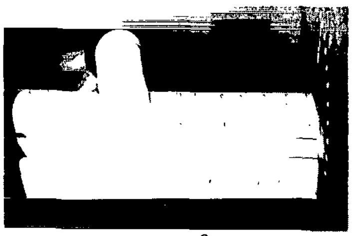

$\alpha = -15^0$

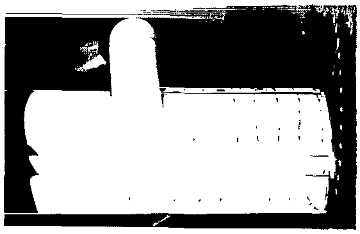

$\alpha = 0^0$

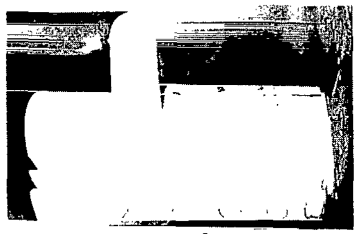

$\alpha = 15^0$

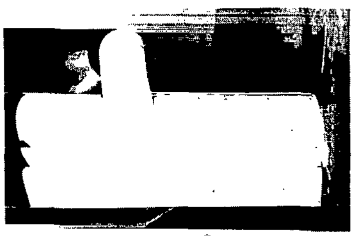

$\alpha = -10^0$

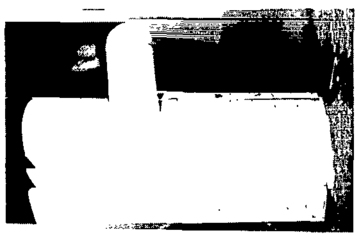

$\alpha = 5^0$

(d) Flow characteristics; $C_{T,s} = 0.60$.

L-66-1086

Figure 23.- Concluded.

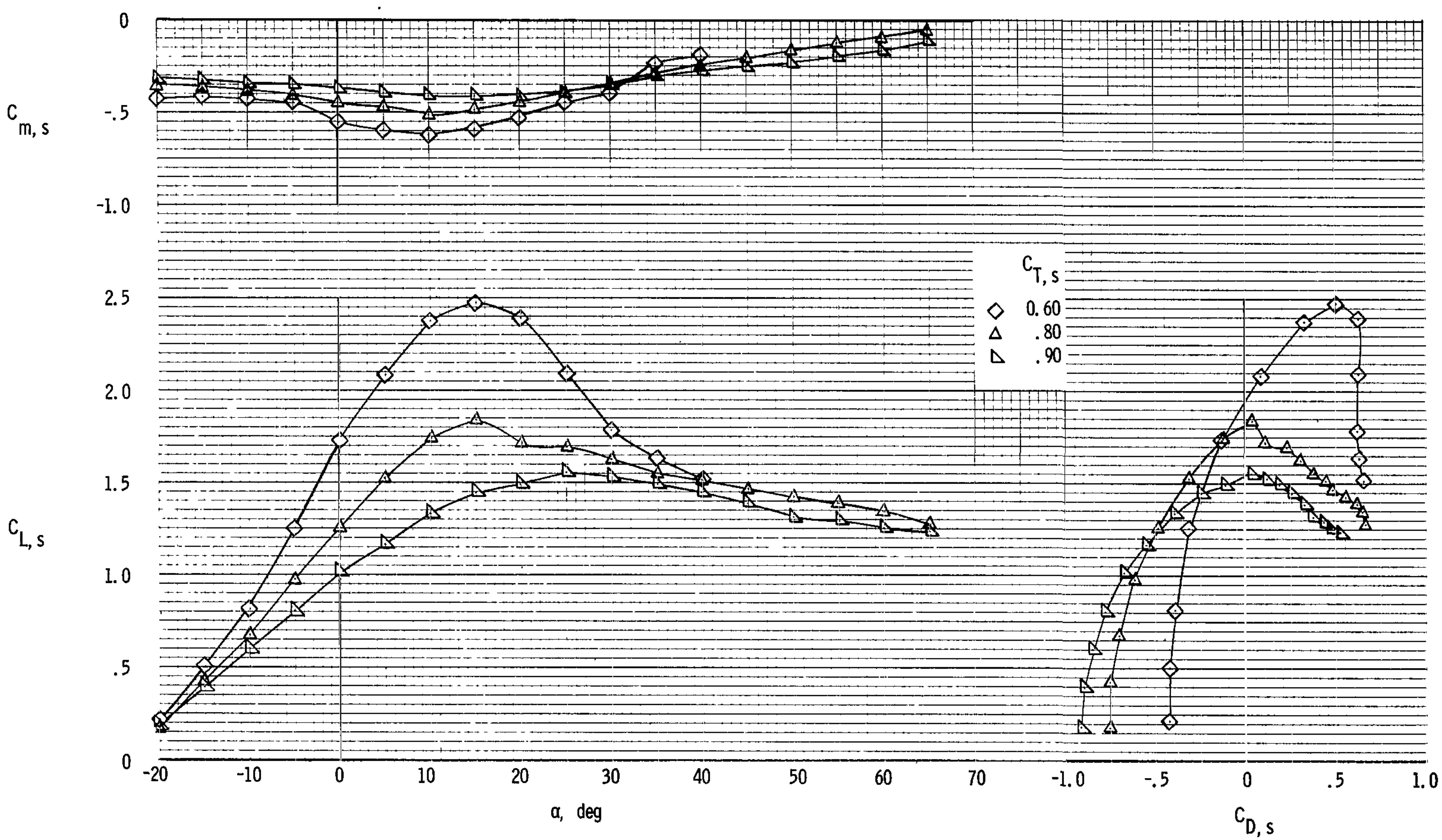

(a) Aerodynamic characteristics.

Figure 24.- Aerodynamic and flow characteristics of model with inboard section of slat deflected 10° (high position) and with trailing-edge flap deflected 70°. Up-at-tip rotation.

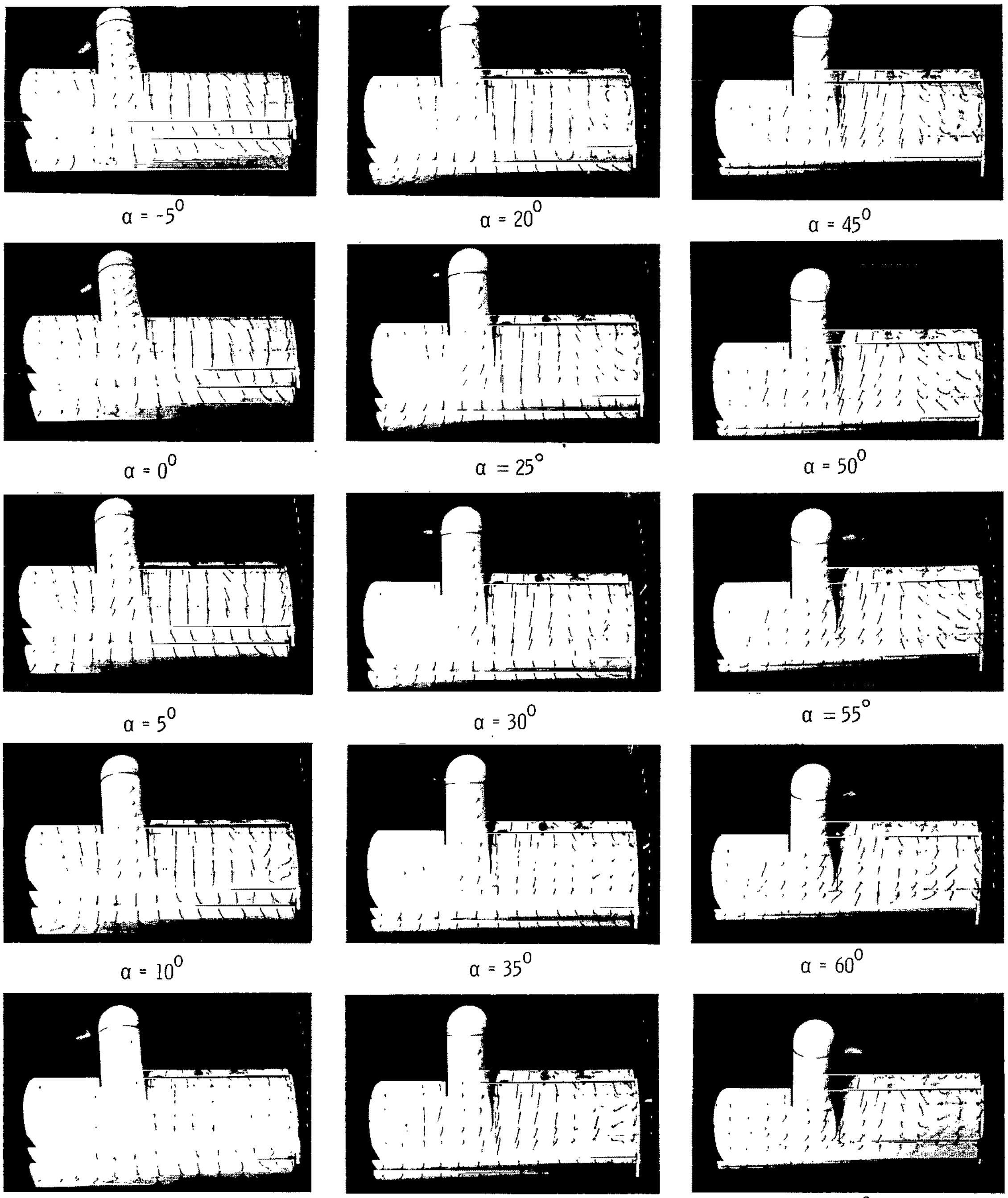

$\alpha = -5^0$ | $\alpha = 20^0$ | $\alpha = 45^0$

$\alpha = 0^0$ | $\alpha = 25^\circ$ | $\alpha = 50^0$

$\alpha = 5^0$ | $\alpha = 30^0$ | $\alpha = 55^\circ$

$\alpha = 10^0$ | $\alpha = 35^0$ | $\alpha = 60^0$

$\alpha = 15^0$ | $\alpha = 40^0$ | $\alpha = 65^0$

(b) Flow characteristics; $C_{T,s} = 0.90$. L-66-1087

Figure 24.- Continued.

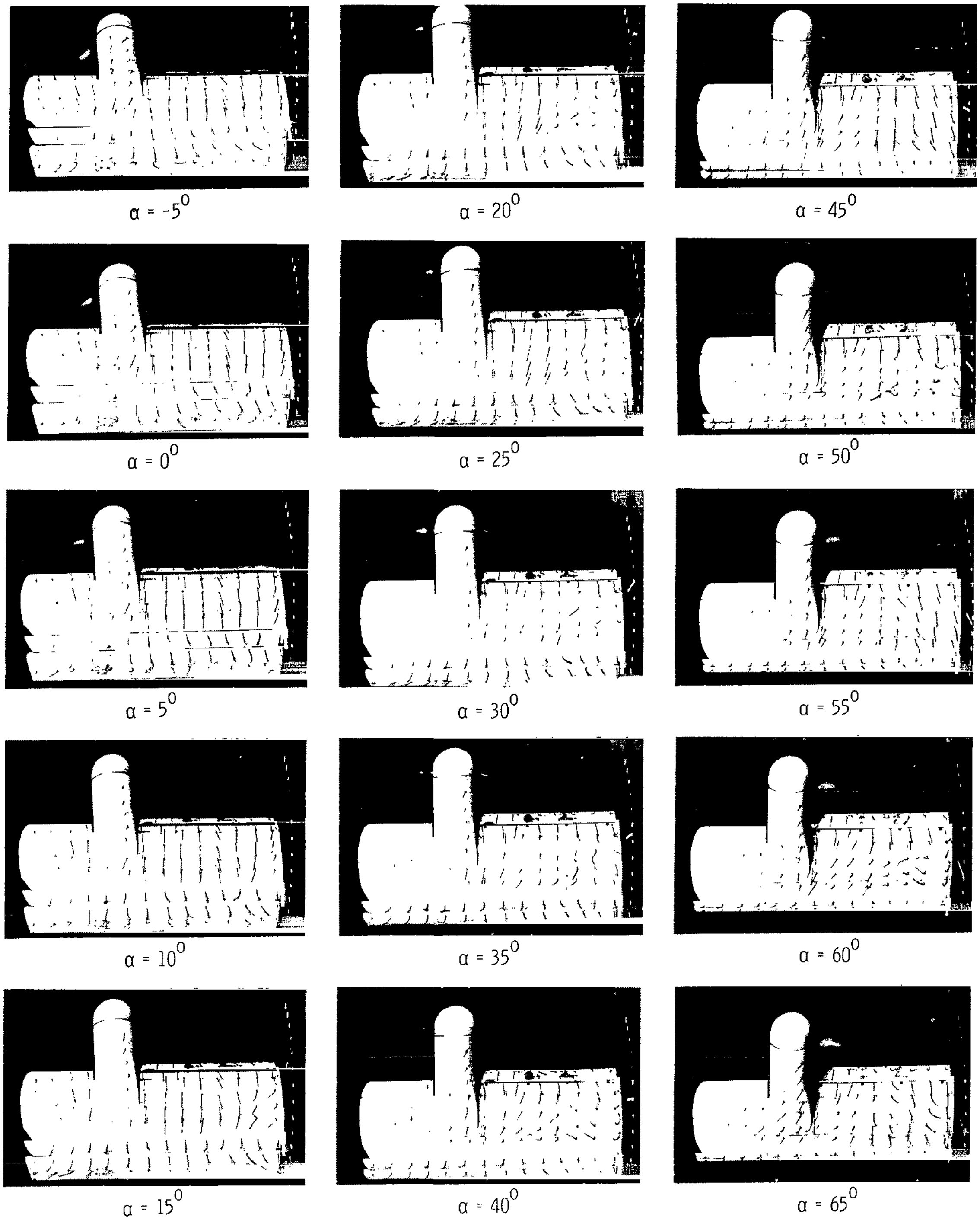

(c) Flow characteristics; $C_{T,s} = 0.80$. L-66-1088

Figure 24.- Continued.

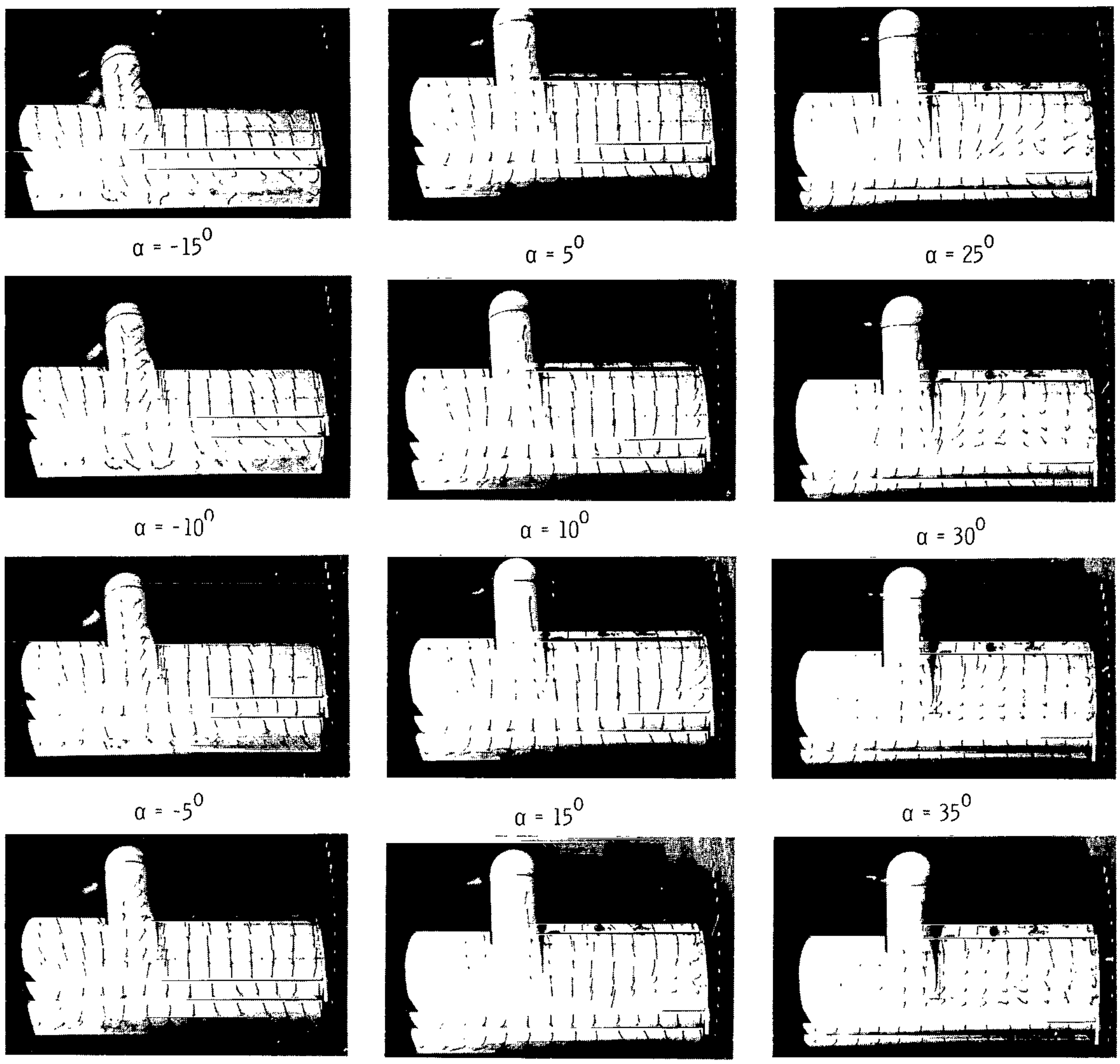

(d) Flow characteristics; $C_{T,s} = 0.60$. L-66-1089

Figure 24.- Concluded.

"The aeronautical and space activities of the United States shall be conducted so as to contribute . . . to the expansion of human knowledge of phenomena in the atmosphere and space. The Administration shall provide for the widest practicable and appropriate dissemination of information concerning its activities and the results thereof."

—NATIONAL AERONAUTICS AND SPACE ACT OF 1958

NASA SCIENTIFIC AND TECHNICAL PUBLICATIONS

TECHNICAL REPORTS: Scientific and technical information considered important, complete, and a lasting contribution to existing knowledge.

TECHNICAL NOTES: Information less broad in scope but nevertheless of importance as a contribution to existing knowledge.

TECHNICAL MEMORANDUMS: Information receiving limited distribution because of preliminary data, security classification, or other reasons.

CONTRACTOR REPORTS: Technical information generated in connection with a NASA contract or grant and released under NASA auspices.

TECHNICAL TRANSLATIONS: Information published in a foreign language considered to merit NASA distribution in English.

TECHNICAL REPRINTS: Information derived from NASA activities and initially published in the form of journal articles.

SPECIAL PUBLICATIONS: Information derived from or of value to NASA activities but not necessarily reporting the results of individual NASA-programmed scientific efforts. Publications include conference proceedings, monographs, data compilations, handbooks, sourcebooks, and special bibliographies.

Details on the availability of these publications may be obtained from:

SCIENTIFIC AND TECHNICAL INFORMATION DIVISION

NATIONAL AERONAUTICS AND SPACE ADMINISTRATION

Washington, D.C. 20546